

T.P.W. Vannecke

**Modelling of microbial populations
in biofilm reactors
for nitrogen removal from wastewater**



Promotor:

Prof. dr. ir. Eveline Volcke

Department of Biosystems Engineering

Faculty of Bioscience Engineering

Ghent University

Coupure links 653, 9000 Gent, Belgium

Eveline.Volcke@UGent.be

Examination committee (*: reading committee)

Prof. dr. ir. Guy Smagghe Chairman Ghent University, Belgium

Prof. dr. ir. Nico Boon Secretary Ghent University, Belgium

Prof. dr. ir. Eveline Volcke Promotor Ghent University, Belgium

Dr. ir. Jan Baetens* Ghent University, Belgium

Dr. Nicolas Bernet* INRA-LBE, France

Prof. dr. ir. Peter Goethals* Ghent University, Belgium

Dr. Julio Perez Canestro* Universtat Autònoma de
Barcelona, Spain
Delft University of
Technology, The
Netherlands

Dean:

Prof. dr. ir. Marc Van Meirvenne

Rector:

Prof. dr. Anne De Paepe

T.P.W. Vannecke

**Modelling of microbial populations
in biofilm reactors for nitrogen removal from
wastewater**

Thesis submitted in fulfillment of the requirements
for the degree of
Doctor (PhD) in Applied Biological Sciences

Dutch translation of the title:

Modelleren van microbiële populaties in biofilmreactoren voor stikstofverwijdering uit afvalwater

Please refer to this work as follows:

Vannecke T.P.W. (2015). Modelling of microbial populations in biofilm reactors for nitrogen removal from wastewater. PhD thesis, Faculty of Bioscience Engineering, Ghent University, Ghent, Belgium, pp. 213.

Thomas Vannecke is supported by the Research Foundation-Flanders (FWO) through a Ph.D. fellowship.

Cover: Picture taken in Scotland, Bridge of Orchy, by my brother Willem Vannecke. Biological nitrogen removal is of utmost importance to safeguard aquatic systems from negative human impacts such as eutrophication. Furthermore, I see my education and the PhD research as major stepping stones in my life, similar to the stepping stones bridging the river Abhainn Shira.

Printing: University Press, Zelzate

Copyright: 2015 Thomas P.W. Vannecke

ISBN: 978-90-5989-842-4

All rights reserved. No part of this thesis may be reproduced, stored in a retrieval system of any nature, or transmitted in any means, without permission of the author, or when appropriate, of the publishers of the publications.

Acknowledgements

Doing a PhD involves performing research but also developing yourself as a person. I think I can be proud of my work of the past four years. However, I would like to state clearly that my achievements would not have been possible without the help of many people.

I would like to start this section by expressing my gratitude towards the Research Foundation-Flanders (FWO) for the funding of my PhD research. Next, I would like to thank all the people who helped me since I started my PhD research back in 2011 – I really hope I do not forget someone.

First of all, I would like to thank my promotor Prof dr. ir. Eveline Volcke for her enthusiasm and dedication during the supervision of my PhD. Eveline, you learnt me many things, not only in the field of environmental constructions, wastewater engineering and mathematical modelling, but also all the skills a good researcher needs: writing scientific publications, presenting at conferences, project management and working efficiently. I thank you very much for all the opportunities you have given me by letting me follow courses on project management, efficient e-mails and even first aid and mindfulness. Furthermore, you were there on the more difficult moments during my PhD and you have convinced me to persist on these moments. During my PhD, I got to know more about myself, and life in general. My sincere thanks for playing such a tremendous role in all this.

This thesis was thoroughly assessed by the committee members. I would like to thank the committee members for their effort and suggestions. I also would like to thank the whole examination committee for the flexibility.

A very nice aspect of research is the collaboration with other people. I had the opportunity to work together with Jean-Philippe Steyer and Nicolas Bernet from the LBE-INRA in Narbonne, along with the complete staff (permanent scientists, engineers, technicians, support staff, PhD students and non-permanent scientists) of this wonderful lab. I was impressed by the close collaboration between engineers, microbiologists and modellers. I thank all of you, and Jean-Philippe and Nicolas in particular, very much for the support during my two short research stays and the very nice collaboration concerning

our research on the data of the experiments by O. Sanchez and D. Bougard. A special word of thanks also to Gaëlle Santa-Catalina for her help with the analysis of the molecular data.

Furthermore, I had the opportunity to work with, and especially learn from, very important people in the field of biotechnology engineering and mathematical modelling: George Ekama, Eberhard Morgenroth, Christian Picioreanu and George Wells. Thank you all for your patience with me and the knowledge and skills you have shared with me! I was lucky Mari Winkler stayed two years at our department as post-doc during my PhD. I am very happy I had the opportunity to meet this very motivated, enthusiastic and smart scientist. Mari, I have really a lot of respect for you and I thank you very much for your support and help with the correlation analysis, simulations and writing of Chapter 5. I wish you good luck with your further career! I also want to thank Nathalie Hubaux for the nice collaboration when we were preparing the joint contribution to WWTmod2014, a contribution finally resulting in a full paper in Water Science and Technology.

All the people of the Biosystems Engineering Department are very kind and had a substantial role in the finishing of this thesis. Without their support, I would have probably quit my PhD research before the end. Thank you Kris, Caroline and Luis L., my office mates, for the joyful chats, pep talks, laughs and also research related discussions! Quan, thank you for your help (for example by taking over the guidance of Dung) and the very interesting talks about aquaria and other stuff. Mingsheng, good luck with your research and the care of the reactors Celia has set up. Lucie, of course I wish you all the best for you and the baby. If everything goes well, we will become parents and PhD's at more or less the same time. I really hope we soon can drink a beer together on our 'achievements'. Thank you Celia for your down-to-earth perspective on science and life in general. Your enthusiasm was a great example for me. Luis "Don Corbala", thank you for the pep talks, your most welcome comments on my papers and your 'newsletter'. Both the scientific and less scientific discussions with you were great! I want also to express my thanks towards the other people of the department: Dane, Diego, Dieter,

Dongdong, Eddy, Fons, Frederik, Gerlinde, Güray, Inés, Jan, Janis, Jop, Lizet, Lut, Matthijs, Mehmet, Neil, Philippe, Ramadan, Rob, Salatul, Wolter, Xianghang and Zuo-Yi. Thank you all for the nice chats, the help you gave me and making my job as PhD student so agreeable! I look forward to see you back in the future, maybe some of you at Graspop Metal Meeting.

I also would like to thank the students I helped with their dissertation: Anamaria, Michael, Aleksandra, Dieter, Mohibul, Vero. I liked to guide all of you and I thank you for the nice collaboration, because I also learned a lot by working with you!

I also want to thank Koen Verschoore and Thomas Parmentier for their support when I considered to quit. They, along with many others, convinced me to persist and I am very thankful for that. Also Wim Jonckheere is acknowledged for his support during my PhD. For four years, we lunched together outside or in the Academic Club. We chatted about everything, mostly not related to work. Thank you so much for all these joyful chats, which made me relax during lunch time.

A special thanks goes to Anneke Devoogdt and David Dewulf and his team (IAM) to help me discover Cognitive Behavioral Therapy and Mindfulness.

Next, I would like to thank my parents, my brother Willem but also my parents- and sister-in-law. These people are among the most important people in my life. Without them, I would not have been able to complete my studies nor my PhD research. Due to their support, I could develop myself to the person I am now. Dank jullie wel papa, mama, Willem-Bob, Lieselotte, Tine en Jacques! Thank you Willem for the photo on the cover of my PhD thesis.

During the last four years, I also have met the girl of my life. Annelies, I love you with all my heart and I thank you so much for all your support. I really look forward to take care together with you for the child you are carrying right now. Liefje, bedankt voor alles, ik hou van je.

Ghent, November 2015

Thomas Vannecke

Table of Contents

ACKNOWLEDGEMENTS	V
TABLE OF CONTENTS	IX
LIST OF ABBREVIATIONS	XIII
LIST OF SYMBOLS	XV
SUMMARY	XIX
SAMENVATTING	XXV
1 INTRODUCTION	1
1.1 BIOLOGICAL NITROGEN REMOVAL.....	2
1.1.1 Nitrogen removal pathways.....	2
1.1.2 Biofilm reactors for nitrogen removal.....	4
1.2 THE NITRIFYING COMMUNITY	6
1.2.1 Microbial diversity.....	6
1.2.2 Ecological genomics and metagenomics.....	7
1.2.3 Microbial diversity in nitrifying systems	11
1.2.4 Composition of the microbial community.....	12
1.3 MODELLING MICROBIAL DIVERSITY	13
1.3.1 Model classification.....	14
1.3.2 Rationale behind the inclusion of diversity in models	15
1.3.3 Nitrifying models including diversity	17
1.3.4 Biofilm models in Aquasim.....	18
1.4 OVERALL OBJECTIVE	31
1.5 OUTLINE OF THE THESIS	32
2 FACTORS INFLUENCING MICROBIAL COMPETITION IN NITRIFYING BIOFILMS	35
2.1 ABSTRACT	36
2.2 PUBLISHED AS	36
2.3 INTRODUCTION	37
2.4 MATERIALS AND METHODS	39
2.4.1 Literature review on microbial characteristics of nitrifiers.....	39
2.4.2 Development of the multispecies biofilm model.....	40
2.5 RESULTS AND DISCUSSION.....	48
2.5.1 Literature review on microbial characteristics of nitrifiers.....	48
2.5.2 Scenario analysis	54
2.6 CONCLUSIONS	67
2.7 APPENDIX 2A: CONVERSION OF MICROBIAL CHARACTERISTICS TO 30 °C AND pH = 7.5	68
2.8 APPENDIX 2B: LITERATURE REVIEW ON MICROBIAL CHARACTERISTICS OF NITRIFIERS..	70

3 MODELLING THE INFLUENCE OF MICROBIAL DIVERSITY ON THE OVERALL REACTOR BEHAVIOUR	73
3.1 ABSTRACT	74
3.2 PUBLICATIONS ON WHICH THE CHAPTER IS BASED	74
3.3 INTRODUCTION	75
3.4 MATERIALS AND METHODS	76
3.4.1 <i>Modelling microbial diversity</i>	76
3.4.2 <i>Case study 1: Biofilm development</i>	82
3.4.3 <i>Case study 2: Functional redundancy</i>	82
3.5 RESULTS AND DISCUSSION	83
3.5.1 <i>Case study 1: Biofilm development</i>	83
3.5.2 <i>Case study 2: Functional redundancy</i>	88
3.6 CONCLUSIONS	93
3.7 APPENDIX 3A: MATLAB CODE FOR THE CONSTRUCTION OF A BIMODAL DISTRIBUTION ..	94
4 MODELLING AMMONIA-OXIDIZING POPULATION SHIFTS	95
4.1 ABSTRACT	96
4.2 PUBLISHED AS	96
4.3 INTRODUCTION	97
4.4 MATERIAL AND METHODS	99
4.4.1 <i>Experimental data</i>	99
4.4.2 <i>Reactor model</i>	100
4.4.3 <i>Simulation set-up</i>	106
4.4.4 <i>Definition of criteria to determine the competition outcome</i>	108
4.5 RESULTS AND DISCUSSION	109
4.5.1 <i>Steady state analysis – without endogenous respiration (Model 1)</i>	109
4.5.2 <i>Steady state analysis – endogenous respiration rate as a fraction of maximum growth rate (Model 2)</i>	113
4.5.3 <i>Simulation of experimental data (Model 3)</i>	115
4.6 CONCLUSIONS	116
5 INFLUENCE OF PROCESS DYNAMICS ON THE NITRIFYING COMMUNITY	117
5.1 ABSTRACT	118
5.2 SUBMITTED AS	118
5.3 INTRODUCTION	119
5.4 MATERIALS AND METHODS	120
5.4.1 <i>Experimental set-up and operational conditions</i>	120
5.4.2 <i>Microbiological and molecular methods</i>	122
5.4.3 <i>Correlation analysis</i>	125
5.4.4 <i>Modelling the dynamic reactor behaviour</i>	125
5.5 RESULTS AND DISCUSSION	134
5.5.1 <i>Correlation analysis</i>	134

5.5.2 <i>Modelling the dynamic reactor behaviour</i>	143
5.6 CONCLUSIONS	151
5.7 APPENDIX 5A: LITERATURE REVIEW ON FA AND FNA INHIBITION OF NITRIFIERS	153
6 CONCLUSIONS & PERSPECTIVES	155
6.1 MODELLING MICROBIAL DIVERSITY IN NITRIFYING BIOFILMS	156
6.1.1 <i>Rationale behind the inclusion of microbial diversity</i>	156
6.1.2 <i>Strategies to implement microbial diversity</i>	158
6.1.3 <i>Biological interpretation of the taxa</i>	161
6.1.4 <i>Determination of microbial parameters</i>	163
6.1.5 <i>Alternative approaches for the modelling of diversity</i>	166
6.2 INFLUENCE OF MICROBIAL DIVERSITY ON STEADY STATE AND DYNAMIC REACTOR BEHAVIOUR.....	169
6.3 FACTORS INFLUENCING MICROBIAL COMPETITION AND COEXISTENCE.....	172
6.3.1 <i>Biofilm characteristics</i>	172
6.3.2 <i>Microbial characteristics</i>	174
6.3.3 <i>Operational parameters and variables</i>	179
6.4 OUTLOOK	181
REFERENCES	185
CURRICULUM VITAE.....	207
PERSONAL PARTICULARS	208
BASIC EDUCATION.....	208
EXTRA TRAINING.....	208
EMPLOYMENT	209
RESEARCH STAYS ABROAD.....	209
PUBLICATIONS	210
<i>Papers in international journals with reading committee</i>	210
<i>Oral presentations at conferences</i>	210
<i>Other conference contributions</i>	211
<i>MSc theses</i>	212
<i>BSc thesis</i>	212
SUPERVISION OF THESIS STUDENTS	213

List of abbreviations

abbreviation	description
ATP	Adenosine TriPhosphate
amoA	Ammonia monooxygenase gene
ANAMMOX	Anaerobic AMMonium Oxidation
AOA	Ammonia-Oxidizing Archaea
AOB	Ammonia-Oxidizing Bacteria
CE-SSCP	Capillary Electrophoresis SSCP
COD	Chemical Oxygen Demand
CSTR	Continuous Stirred Tank Reactor
DAE	Differential Algebraic Equation
DEN	Denitrifying bacteria
DGGE	Denaturing Gradient Gel Electrophoresis
DNRA	Dissimilatory Nitrate Reduction to Ammonium
DNA	Desoxyribonucleic acid
DO	Dissolved Oxygen
HET	Heterotrophs
HRT	Hydraulic Retention Time
FA	Free Ammonia
FISH	Fluorescence In Situ Hybridization
FNA	Free Nitrous Acid
ITBR	Inverse Turbulent Bed Reactor
MABR	Membrane Aerated Biofilm Reactor
NLR	Nitrogen Loading Rate
NOB	Nitrite-Oxidizing Bacteria

abbreviation	description
NGS	Next Generation Sequencing
nxrA	Nitrite oxydoreductase gene
ODE	Ordinary Differential Equation
ODM	Organic Dry Matter
PCR	Polymerase Chain Reaction
PDE	Partial Differential Equation
qPCR	Quantative PCR
rRNA	ribosomal RNA
RNA	Ribonucleic acid
SOLiD	Sequencing by Oligo Ligation and Detection
SRT	Solids Retention Time
SS	Steady State
SSCP	Single Strand Conformation Polymorphism
TGGE	Temperature Gradient Gel Electrophoresis
TNH	Total Ammonium
TNO ₂	Total Nitrite
T-RFLP	Terminal restriction fragment length polymorphism

List of symbols

abbreviation	characterization	unit
A	Biofilm surface	m^2
b	Endogenous respiration rate	d^{-1}
C_i	Dissolved component i	$g.m^{-3}$
C_T	Cycle Threshold in qPCR	Number of cycles
d	Decay rate	d^{-1}
D_{C_i}	Diffusion coefficient of the dissolved component C_i	$m^2.d^{-1}$
D_{NH_4}	Diffusion coefficient of NH_4^+	$m^2.d^{-1}$
D_{NO_2}	Diffusion coefficient of NO_2^-	$m^2.d^{-1}$
D_{NO_3}	Diffusion coefficient of NO_3^-	$m^2.d^{-1}$
D_{O_2}	Diffusion coefficient of O_2	$m^2.d^{-1}$
D_{X_i}	Diffusion coefficient of particulate component X_i	$m^2.d^{-1}$
D_{SSCP}	Simpson diversity index of SSCP profile	-
d_p	Diameter particle	m
E	Efficiency of the model (Nash Sutcliffe criterion)	-
E_a	Activation energy	$kJ.(mol)^{-1}$
ϵ_X	Volume fraction of solid matrix	-
ϵ_{X_i}	Volume fraction of particulate component X_i	-
$\epsilon_{l,F}$	Liquid volume fraction of biofilm	-
$\epsilon_{l,B}$	Liquid volume fraction of bulk liquid	-
f_{X_I}	Inert fraction in biomass	$g\ COD.(g\ COD)^{-1}$
I_{L,C_i}	Flow of dissolved substances out of the biofilm	$g.d^{-1}$
I_{L,X_i}	Flow of solids out of the biofilm	$g\ COD.d^{-1}$

abbreviation	characterization	unit
I_{in,C_i}	Total input of substance C_i in the bulk volume	$g.d^{-1}$
I_{in,X_i}	Total input of substance X_i in the bulk volume	$g \text{ COD}.d^{-1}$
i_{NXB}	Nitrogen fraction in biomass	$g \text{ N}.(g \text{ COD})^{-1}$
i_{NXI}	Nitrogen fraction in particulate inert components	$g \text{ N}.(g \text{ COD})^{-1}$
k_{at}	Attachment coefficient	$m.d^{-1}$
k_{de}	Detachment coefficient	$m.d^{-1}$
K_{FA}	Affinity constant for free ammonia	$g \text{ FA-N}.m^{-3}$
K_{FNA}	Affinity constant for free nitrous acid	$g \text{ FNA-N}.m^{-3}$
$K_{I,FA}$	Inhibition constant for FA	$g \text{ FA-N}.m^{-3}$
$K_{I,FNA}$	Inhibition constant for FNA	$g \text{ FNA-N}.m^{-3}$
K_L	External mass transfer coefficient	$m.d^{-1}$
K_{NH}	Affinity constant for total ammonium	$g \text{ TNH-N}.m^{-3}$
K_{NO_2}	Affinity constant for nitrite	$g \text{ TNO}_2\text{-N}.m^{-3}$
K_{NO_3}	Affinity constant for nitrate	$g \text{ N}.m^{-3}$
K_{O_2}	Affinity constant for oxygen	$g \text{ O}_2.m^{-3}$
L_F	Biofilm thickness	m
L_{FSS}	Steady state biofilm thickness	m
m	Mass	g
M	Median	-
μ_{max}	Maximum growth rate	d^{-1}
η	Anoxic reduction factor	-
η_T	Viscosity of water at temperature T	$Pa.s$
n_p	Number of particles	-
Q_1	First quartile	-
Q_3	Third quartile	-
Q_{in}	Inflow rate	$m^3.d^{-1}$
ρ	Process rate (Growth, Decay or Endogenous Respiration)	$g \text{ COD}.m^{-3}.d^{-1}$
ρ_{X_i}	Density of particulate component X_i	$g \text{ COD}.m^{-3}$
r	Pearson correlation coefficient	-

abbreviation	characterization	unit
r_{Ci}	Conversion rate dissolved component i	$\text{g.m}^{-3}.\text{d}^{-1}$
r_{Xi}	Conversion rate particulate component i	$\text{g.m}^{-3}.\text{d}^{-1}$
θ	Biofilm porosity	-
S^*	Competition outcome criterion	g N.m^{-3}
S_{N2}	N_2 concentration	g N.m^{-3}
S_{NH}	Ammonium concentration	g N.m^{-3}
S_{NO2}	Nitrite concentration	g N.m^{-3}
S_{NO3}	Nitrate concentration	g N.m^{-3}
S_{O2}	Oxygen concentration (DO)	$\text{g O}_2.\text{m}^{-3}$
S_S	Soluble organic substrate	g COD.m^{-3}
u_{at}	Attachment velocity	m.d^{-1}
u_d	Detachment velocity	m.d^{-1}
u_F	Advective biofilm velocity	m.d^{-1}
$u_{F(LF)}$	Advective biofilm velocity at surface	m.d^{-1}
u_L	Velocity of interface layer between bio-film and bulk liquid	m.d^{-1}
V	Volume	m^3
χ^2	Sum of squares (calibration)	-
X_i	Particulate component i	g COD.m^{-3}
X_I	Inert particulate components	g COD.m^{-3}
X_S	Particulate organic substrate	g COD.m^{-3}
X_{eff}	Particulate components (effluent)	g COD.m^{-3}
Y	Yield coefficient	$\text{g COD}.\text{(g N)}^{-1}$
z	Spatial coordinate in Aquasim	m

Summary

This PhD research studied the interaction between microbial community structure, reactor behaviour and operational conditions in biofilm reactors for biological nitrogen removal from wastewater using mathematical modelling. Microbial diversity and competition were incorporated in 1-dimensional two-step nitrification biofilm models. The influence of microbial diversity on steady state and dynamic behaviour of nitrifying biofilms and biofilm reactors was investigated. Insight was gained on the influence of microbial characteristics and process conditions on microbial competition.

Chapter 1 provides some background on biological nitrogen removal, biofilms for nitrogen removal and the microbial diversity associated with the nitrifying community, besides the influence of environmental factors on the microbial community. Furthermore, an introduction was given on mathematical (biofilm) models and the rationale behind the incorporation of microbial diversity in nitrifying biofilm models was also addressed.

A large variety of microbial parameter values for nitrifying microorganisms has been reported in literature and was revised in **Chapter 2**. This variety mainly reflects the large biodiversity in nitrifying systems, even though part of it can be attributed to the variety of analysis methods applied. In this chapter, the microbial diversity of the nitrifying community was incorporated in a 1-dimensional, multispecies nitrifying biofilm model by taking into account the large variety of the maximum growth rate, substrate affinity and yield of nitrifiers reported in literature. This model, including the growth and decay of 60 species of ammonia-oxidizing bacteria (AOB) and 60 species of nitrite-oxidizing bacteria (NOB), was used to assess the influence of operational conditions and microbial characteristics on microbial competition based on steady state simulations. The 60 species per functional guild differed in maximum growth rate, affinity for electron donor and acceptor and yield and they were constructed based on species classes represented by 1 competitive advantage, 1 competitive disadvantage and 2 neutral characteristics. Operational conditions such as the nitrogen loading rate and the bulk liquid oxygen concentration were shown to influence both the bulk liquid composition as well as the microbial composition of the biofilm at steady state

through the prevailing concentration of substrates throughout the biofilm. Also the species present initially in the biofilm were shown to determine the steady state microbial biofilm composition and bulk liquid composition at steady state.

Considering oxygen and nitrogen limitation, a maximum of 3 dominant species in the nitrifying community coexisting at steady state, with two species of the same functional guild, i.e., performing the same function, was observed (**Chapter 2-4**). It was demonstrated that coexisting species of the same functional guild are typified by a trade-off between their maximum growth rate and their affinity for the most limiting nutrient (nitrogen or oxygen), according to the r-K selection theory. Furthermore, the simulated biomass distribution profiles in the biofilm were shown to reflect the ecological niches created by the diffusional substrate concentration gradients in the biofilms. Besides internal mass transfer limitation, also external mass transfer limitation, by determining the concentration of the limiting substrates in the biofilm, and endogenous respiration were shown to influence the microbial competition (**Chapter 4**).

In **Chapter 3**, a flat biofilm model considering the growth and endogenous respiration of 10 AOB and 10 NOB species was used in two case studies. Here, the species per functional type were constructed based on a bimodal distribution of the values for maximum growth rate, affinity constants and yield. In a first case study, the change of the microbial composition of a biofilm was followed over time until steady state was reached in terms of bulk liquid composition, biofilm thickness and microbial biofilm composition. It was demonstrated that a constant effluent composition not necessary reflects steady state conditions in terms of biofilm thickness and composition. In a second case study, the functional redundancy of the nitrifying community, i.e., the possibility of a changed nitrifying community to function equally as the original one, upon an increased nitrogen loading rate, was verified. Dynamic simulations with the 1-dimensional nitrifying biofilm model, including the competition between 10 AOB and 10 NOB, demonstrated that the coexistence of several species performing the same function assured an almost constant

process performance, i.e., conversion of most of the ammonium to nitrate, upon an increased nitrogen loading within a period of 8 months following the shift of the operational conditions. In Chapter 3, it was therefore concluded, based on the simulations, that increased complexity in biofilm models, concerning microbial diversity, is likely more useful when the focus is on understanding microbial competition and coexistence or biofilm composition, but under specific conditions, for example upon environmental or operational changes such as an increased nitrogen loading rate, these additional model features can be critically informative for bulk reactor behaviour prediction and general understanding.

An example of a case in which inclusion of microbial diversity in a biofilm model was informative for the bulk liquid composition and the process performance, is given in **Chapter 4**. Dynamic simulations were used to analyse an experimentally observed population shift between two genetically different ammonia-oxidizers, accompanied by a different nitrifying performance, in a biofilm reactor operated at different loading rates. A model including the competition between the two genetically different populations of ammonia-oxidizers, represented by two different sets of kinetic parameters, and nitrite-oxidizers was used. The dissolved oxygen concentration in the bulk liquid was identified as the key variable governing the experimentally observed population shift by the developed 1-dimensional biofilm model.

For engineers, it is interesting to gain insight in the effect of control strategies on microbial communities, on their turn influencing the process behaviour and/or its stability. **Chapter 5** assesses the influence of process dynamics on the microbial community in a biofilm reactor for wastewater treatment, which was controlled according to several strategies aiming at nitrite accumulation. The process dataset, combining conventional chemical and physical data with molecular information, was analysed through a correlation analysis and in a simulation study. During nitrate accumulation, an increased nitrogen loading rate (NLR) resulted in a drop of the bulk liquid oxygen concentration without resulting in nitrite accumulation. A biofilm model, considering the growth and decay of 1 AOB, 1 NOB and 1 heterotrophic guild, was able to reproduce the

bulk liquid nitrogen concentrations in two periods before and after this increased NLR. As the microbial parameters calibrated for AOB and NOB in both periods were different, it was concluded that the increased NLR governed an AOB and NOB population shift. It was assumed that each period was typified by 1 dominant AOB and probably several subdominant NOB populations. The control strategies for nitrite accumulation were mainly influencing the competition between AOB and NOB, instead of the microbial diversity of the nitrifying community.

Finally, **Chapter 7** offers some final considerations and conclusions on the modelling of microbial diversity in nitrifying biofilm reactors, the influence of microbial diversity on steady state and dynamic reactor behaviour and the factors influencing microbial diversity in nitrifying biofilms, next to some suggestions for future research.

Samenvatting

Dit doctoraatsonderzoek bestudeerde de interactie tussen de structuur van de microbiële gemeenschap, het reactorgedrag en de operationele condities in biofilmreactoren voor biologische stikstofverwijdering uit afvalwater, met behulp van wiskundige modellering. Microbiële diversiteit en competitie werden verwerkt in 1-dimensionale nitrificerende biofilmmodellen. De invloed van microbiële diversiteit op het *steady state* gedrag, d.i., wanneer de uitgangsvariabelen niet meer veranderen, en dynamische gedrag van nitrificerende biofilms en biofilmreactoren werd onderzocht. Inzicht werd verkregen over de invloed van microbiële eigenschappen en procescondities op microbiële competitie.

Hoofdstuk 1 geeft achtergrondinformatie over biologische stikstofverwijdering, biofilms voor stikstofverwijdering uit afvalwater en de microbiële diversiteit van de nitrificerende gemeenschap, naast de invloed van omgevingsfactoren op de microbiële gemeenschap. Daarnaast werd ook een inleiding gegeven over mathematische (biofilm) modellen en werd de grondgedachte achter de integratie van de microbiële diversiteit in nitrificerende biofilmmodellen aangehaald.

Een grote verscheidenheid aan microbiële parameterwaarden voor nitrificerende micro-organismen werd gerapporteerd in de literatuur (**Hoofdstuk 2**). De variatie is voornamelijk te wijten aan de grote biodiversiteit van nitrificerende systemen, hoewel een deel ervan ook kan worden toegeschreven aan de verschillende toegepaste analysemethoden. In dit hoofdstuk werd de microbiële diversiteit van de nitrificerende gemeenschap opgenomen in een 1-dimensionaal, nitrificerend biofilmmodel door rekening te houden met deze grote verscheidenheid van de maximale groeisnelheid, de substraataffiniteit en de celopbrengst (*yield*) van stikstofverwijderende organismen. Dit model, dat de groei en de transitie tot inerte componenten en organisch substraat (*decay*) van 60 soorten ammonia-oxiderende bacteriën (AOB) en 60 soorten nitriet oxiderende bacteriën (NOB) beschrijft, werd gebruikt om de invloed van operationele condities en microbiële eigenschappen op microbiële competitie na te gaan via *steady state* simulaties. De 60 soorten per functioneel type (AOB versus NOB) verschilden in maximale groeisnelheid, affiniteit voor elektron-

donor en -acceptor, en celopbrengst. Ze werden geconstrueerd door gebruik te maken van soortenklassen. Deze klassen werden voorgesteld door één competitief voordeel, één competitief nadeel en 2 neutrale kenmerken. Operationele condities zoals de stikstoflading en de zuurstofconcentratie in de reactor bleken zowel de effluentsamenstelling als de microbiële samenstelling van de biofilm bij *steady state* te beïnvloeden via de heersende substraatconcentratie in de biofilm. Ook de oorspronkelijke soortensamenstelling van de biofilm bleek de microbiële biofilmsamenstelling en de effluentsamenstelling bij *steady state* te beïnvloeden.

Bij zuurstof en stikstoflimitatie konden maximaal 3 dominante soorten, waarvan twee soorten die dezelfde functie uitvoeren, in de nitrificerende gemeenschap samenleven bij *steady state* (**Hoofdstuk 2-4**). Er werd aangetoond dat naast elkaar bestaande soorten van dezelfde functionele microbiële groep gekenmerkt worden door een compromis (*trade-off*) tussen hun maximale groeisnelheid en hun affiniteit voor het belangrijkste limiterende nutriënt (stikstof of zuurstof) volgens de r- en K-selectietheorie. Bovendien weerspiegelden de gesimuleerde biomassaprofielen in de biofilm de ecologische niches gecreëerd door substraatgradiënten. Naast interne massa-transferlimitatie, kunnen ook externe massatransferlimitatie, via de invloed op de concentratie van de limiterende substraten in de biofilm, en de oxidatie van aangelegde reservestoffen of endogene ademhaling (*endogenous respiration*) microbiële competitie beïnvloeden (**Hoofdstuk 4**).

In **Hoofdstuk 3** werd een vlakke biofilm, die de groei en endogene respiratie van 10 AOB soorten en 10 NOB soorten beschrijft, gebruikt in twee gevalstudies. Hier werden de 10 soorten per functioneel type (AOB versus NOB) voorgesteld door middel van een bimodale distributie voor de waarden van maximale groeisnelheid, affiniteit constanten en celopbrengst. In een eerste gevalstudie werd de verandering van de microbiële samenstelling van een biofilm gevolgd in de tijd tot er *steady state* werd bereikt op vlak van de effluentsamenstelling, biofilmdikte en biofilm soortensamenstelling. Er werd aangetoond dat een constant effluentsamenstelling niet noodzakelijk stabiele omstandigheden in de biofilm reflecteert. In een tweede gevalstudie werd de

functionele redundantie van de nitrificerende gemeenschap, d.i., de mogelijkheid van een veranderde nitrificerende gemeenschap om gelijkaardig te functioneren als de oorspronkelijke, bij een verhoogde stikstofbelasting gecontroleerd. Dynamische simulaties met het 1-dimensionaal biofilmmodel, waarin de competitie tussen 10 AOB en 10 NOB bacteriën was opgenomen, toonden aan dat de co-existentie van verschillende soorten met dezelfde functie een nagenoeg constante procesperformantie kunnen verzekeren. Zowel voor als 8 maanden na de verandering van de operationele condities was er immers een nagenoeg volledige omzetting van ammonium tot nitraat. In Hoofdstuk 3 werd er, op basis van de simulaties, geconcludeerd dat opname van microbiële diversiteit in biofilm modellen van praktisch nut is als de focus ligt op het begrijpen van microbiële competitie, co-existentie of de soortensamenstelling van de biofilm. Maar bij specifieke gevallen, bijvoorbeeld als er veranderingen optreden in de omgevings- of operationele factoren, kan bijkomende modelcomplexiteit ook van groot belang zijn voor het voorspellen en begrijpen van de effluent samenstelling.

Een voorbeeld van een geval waarin opname van microbiële diversiteit in een biofilmmodel informatief was voor het begrijpen van de procesperformantie en de effluentsamenstelling, wordt gegeven in **Hoofdstuk 4**. Dynamische simulaties werden gebruikt om een experimenteel waargenomen populatieverschuiving tussen twee genetisch verschillende ammonia-oxiderende bacteriën te analyseren. De populatieverschuiving werd waargenomen in een biofilmreactor werkend bij verschillende belastingen en ging gepaard met een verandering in het nitrificerende gedrag. Een model werd gebruikt waarin zowel de competitie tussen de twee genetisch verschillende populaties van ammonia-oxiderende bacteriën, voorgesteld door verschillende kinetische parameters, als de nitriet-oxiderende bacteriën waren opgenomen. De zuurstofconcentratie in de reactor werd met het model geïdentificeerd als de variabele die de experimenteel waargenomen populatieverschuiving heeft veroorzaakt.

Voor ingenieurs kan het interessant zijn om inzicht te verkrijgen in het effect van controlestrategieën op microbiële gemeenschappen, die op hun beurt het

procesgedrag en/of -stabiliteit beïnvloeden. In **Hoofdstuk 5** wordt de invloed van procesdynamica op de microbiële gemeenschap in een biofilmreactor voor waterzuivering, gecontroleerd op basis van verschillende controlestrategieën voor nitrietaccumulatie, onderzocht. De gebruikte dataset, die conventionele chemische en fysische data combineert met moleculaire informatie, werd geanalyseerd gebruik makend van een correlatieanalyse en in een simulatiestudie. Gedurende nitraataccumulatie veroorzaakte een verhoogde stikstoflading een verlaging van de zuurstofconcentratie in de reactor, zonder te resulteren in nitrietaccumulatie. Een biofilmmodel, die de groei en omzetting van biomassa in inerte componenten en organisch substraat van 1 ammonia-oxiderend, 1 nitriet oxiderend en 1 heterotroof type beschreef, kon de stikstofconcentraties in de reactor simuleren in twee perioden van reactoroperatie (voor en na de verhoogde stikstoflading). Aangezien de gekalibreerde microbiële parameters voor zowel de AOB als de NOB verschillend waren voor beide perioden, werd geconcludeerd dat de verhoogde stikstoflading een populatieshift heeft veroorzaakt. Er werd aangenomen dat elke periode gekenmerkt werd door 1 dominante AOB populatie en mogelijk verschillende subdominante NOB populaties. De controlestrategieën voor nitrietaccumulatie beïnvloedden vooral de competitie tussen de twee functionele types (AOB en NOB), in plaats van de microbiële diversiteit van de nitrificerende gemeenschap.

Tot slot biedt **Hoofdstuk 7** conclusies over het modelleren van microbiële diversiteit in nitrificerende biofilmreactoren, de invloed van microbiële diversiteit op *steady state* en dynamisch reactorgedrag en de factoren die van invloed zijn op de microbiële diversiteit in nitrificerende biofilms, naast een aantal suggesties voor toekomstig onderzoek.

1

Introduction

1.1 Biological nitrogen removal

Current wastewater treatment deals with (1) the removal of colloidal, suspended and floatable material from wastewater, (2) prevention of oxygen depletion and the production of malodorous gases in the environment, by confining microbial growth in the wastewater to a controlled system, (3) the removal of plant macronutrients phosphorus and nitrogen to prevent fish kills due to toxic ammonia and eutrophication of aquatic systems, thereby preventing algal blooms, and (4) the elimination of pathogenic organisms (Tchobanoglous *et al.* 2003; Madigan & Martinko 2006). In this thesis, the focus is on the biological nitrogen removal from wastewater.

1.1.1 Nitrogen removal pathways

Conventional biological nitrogen removal is a generally accepted pathway, resulting in the oxidation of ammonium to nitrite (nitritation) by the ammonia-oxidizing bacteria (AOB) and the oxidation of nitrite to nitrate (nitrification) by the nitrite-oxidizing bacteria (NOB) during nitrification. The produced nitrate is then reduced via nitrite to nitrogen gas during denitrification (Figure 1.1). It should be noted that, when nitrate in comparison to organic carbon is limiting, dissimilatory nitrate reduction to ammonium (DNRA) is assumed to occur (Cole & Brown 1980; Kraft *et al.* 2011), conserving nitrogen in the system (Tiedje *et al.* 1983).

Over the last 15 years, innovative processes have been developed that improve the sustainability of biological nitrogen removal from wastewater. Many of the newly developed processes rely on partial biological oxidation of ammonium to nitrite by the AOB, while further oxidation to nitrate by the NOB is prevented (Figure 1.1). The produced nitrite can be directly denitrified to nitrogen gas; the resulting process is denoted as partial nitrification - denitrification or shortcut nitrification - denitrification over nitrite. Another possibility lies in the conversion of only half of the ammonium to nitrite (partial nitritation), followed by the combination of ammonium and nitrite to nitrogen gas in a so-called anaerobic ammonium oxidation (anammox) reaction. These innovative processes result in significantly lower aeration

energy requirements, lowering or eliminating the need for external carbon dosage, while minimizing sludge production and CO₂-emission, in comparison with traditional nitrification-denitrification over nitrate (Turk & Mavinic 1986; Mulder *et al.* 1995; Verstraete & Philips 1998). To achieve nitrification-denitrification over nitrite, stable production of nitrite is necessary. Although nitrite is an intermediate, not or hardly formed in open-loop (uncontrolled) situations, nitrite accumulation can be achieved by selecting the desired microbial populations through adequate process operation control. In the case of nitrification, this comes down to the selection between two types or functional guilds of microorganisms: the ammonia-oxidizing bacteria (AOB) need to be favoured over the nitrite-oxidizing bacteria (NOB), by controlling pH (Anthonisen *et al.* 1976), temperature and sludge retention time (Hellinga *et al.* 1998) and/or the bulk liquid oxygen concentration (Bernet *et al.* 2001).

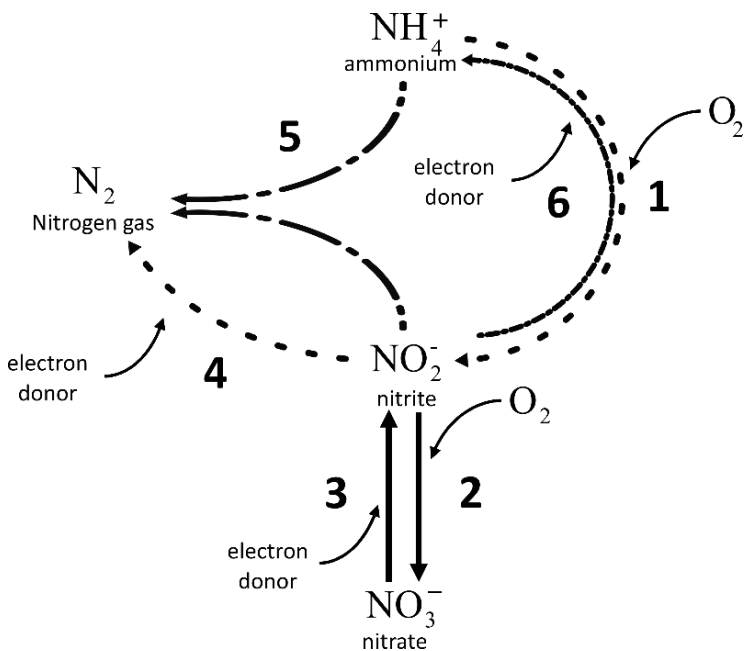


Figure 1.1 Simplified microbial nitrogen cycle depicting conventional biological nitrogen removal (1, 2, 3 and 4), nitrification – denitrification over nitrite (1 and 4), anammox following partial nitrification (1 and 5), besides dissimilatory nitrate reduction to ammonium (3 and 6).

It should be noted that in the overall nitrogen cycle also other processes occur. Nitrate is also reduced to nitrite and ammonia by usage of adenosine triphosphate (ATP, one of the main energy sources in all living cells) and reducing power during assimilatory nitrate reduction. Micro-organisms unable to reduce nitrate must find ammonia nitrogen in their environment as nitrogen source for incorporation in complex organic compounds (Lawrence 2005; Bertrand *et al.* 2011). During breakdown and mineralization of organic matter by both aerobic and anaerobic bacteria, ammonium is released in a process called ammonification (Kalf 2002). The process whereby atmospheric elemental nitrogen (dinitrogen, N₂) is reduced to ammonia and which is carried out by some free-living bacteria and cyanobacteria and by a few groups of bacteria in the symbiotic association with plants is called nitrogen fixation (Lawrence 2005; Bertrand *et al.* 2011).

1.1.2 Biofilm reactors for nitrogen removal

Biofilm reactors are particularly useful for the growth of slow growing microorganisms such as nitrifiers, as they are compact, allow high loading rates and they realize the dissociation of hydraulic and solids retention time (Nicolella *et al.* 2000). A biofilm can be defined as a structure of adhesive materials like extra-cellular polymers, enclosing colonies of microorganisms and cellular products (Lawrence 2005; Madigan & Martinko 2006), which either form spontaneously as large, dense granules (Lettinga *et al.* 1980; de Kreuk *et al.* 2005), grow attached on a static solid surface (Pynaert *et al.* 2003) or on a suspended carrier (Bernet *et al.* 2005; Bougard *et al.* 2006a). Several research groups have already used different types of biofilm reactors for establishing nitrification-denitrification over nitrite, e.g., Bougard *et al.* (2006a) and Bougard *et al.* (2006b) used an Inverse Turbulent Bed Reactor (ITBR) and Yilmaz *et al.* (2008) used granular sludge. Also biofilm reactors for partial nitrification in view of coupling with an anammox process were already described in literature, e.g., Gilbert *et al.* (2014) used a moving bed biofilm reactor and Lotti *et al.* (2014) used granules.

For two chapters of this thesis (Chapter 4 and Chapter 5), previously gathered experimental data from the Laboratory of Environmental Biotechnology

(LBE), a research unit of the French National Institute for Agricultural Research (INRA), were used. During experiments with nitrifying Inverse Turbulent Bed Reactors (ITBRs, Figure 1.2) conventional chemical and physical data were retrieved in combination with molecular information about microbial population dynamics (Bernet *et al.* 2004; Bougard *et al.* 2006a; Volcke *et al.* 2008). In ITBRs, floating particles, on which the biofilms grow during operation, are expanded by an upward current of gas (Buffiere *et al.* 2000). The reactor belongs to the category of inverse three-phase fluidized beds as the fluidization can be ensured by an upflow current of gas only, through the pseudo-fluidization mechanism (Buffière & Moletta 2000). Sánchez *et al.* (2005a) proved that this reactor type behaves like a two-phase reactor, with the liquid and solid phases behaving like a homogenous pseudo-fluid. According to Buffière and Moletta (1999), this kind of reactor enables in the field of biological wastewater treatment to (1) use the gas flow as only fluidizing agent, not requiring any extra energy cost in aerobic processes, (2) create a calming zone below the gas distributor acting as a settler to separate the sludge from the liquid and (3) control the biofilm thickness by friction effects.

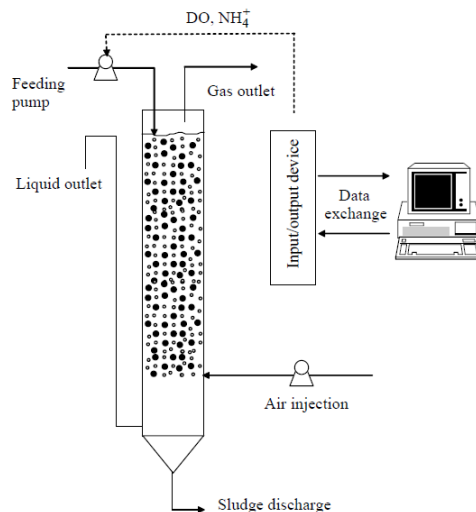


Figure 1.2 Inverse Turbulent Bed Reactor (ITBR). The black points represent biofilm covered low density spherical inert particles, kept afloat by an upward current of air (white bubbles). Picture taken from Bougard *et al.* (2006a).

1.2 The nitrifying community

In this thesis, the focus is on the microbial biodiversity in nitrifying biofilms. Key biological processes such as nitrification or nitrification do not result from the work of a single bacterial species but can be performed by a wide variety of organisms, each with their own characteristics and merits.

Table 1.1 Overview of possible functions in the nitrogen cycle executed by species from different genera. This list is not exhaustive. Table adapted from Tchobanoglous *et al.* (2003). The numbers of the functions correspond to the processes given in Figure 1.1. AOB: ammonia-oxidizing bacteria, AOA: ammonia-oxidizing archaea, NOB: nitrite-oxidizing bacteria, DEN: denitrifying bacteria, ANAMMOX: anaerobic ammonium oxidizing bacteria, DNRA: bacteria performing dissimilatory nitrite reduction to ammonium.

Function		Functional guild	Known genera (amongst others)
1	Nitrification	Nitrification: Aerobic oxidation of NH_4^+ to NO_2^-	AOB <i>Nitrosomonas</i> , <i>Nitrospira</i> , <i>Nitrosococcus</i>
			AOA <i>Nitrosopumilus</i>
2	Nitrification	Nitrification: Aerobic oxidation of NO_2^- to NO_3^-	NOB <i>Nitrobacter</i> , <i>Nitrospina</i> , <i>Nitrococcus</i> , <i>Nitrospira</i> , <i>Nitrotoga</i>
3	Denitrification	Anaerobic reduction of NO_3^- to NO_2^-	DEN <i>Acinetobacter</i> , <i>Agrobacterium</i> , <i>Bacillus</i> , <i>Corynebacterium</i> , <i>Flavobacterium</i> , <i>Pseudomonas</i> , <i>Rhizobium</i>
4		Anaerobic reduction of NO_2^- to N_2	
5	Anaerobic oxidation of NH_4^+ to N_2 with NO_2^- as electron acceptor		ANAMMOX <i>Kuenenia</i> , <i>Brocadia</i> , <i>Anammoxoglobus</i> , <i>Jettenia</i> , <i>Scalindua</i>
3+6	Anaerobic dissimilatory nitrate reduction to ammonium		DNRA <i>Escherichia</i> , <i>Desulfovibrio</i> , <i>Wolinella</i> , <i>Vibrio</i> , <i>Clostridium</i>

1.2.1 Microbial diversity

Biological diversity is, according to the United Nations Convention on Biological Diversity, the variability among living organisms from all sources, including terrestrial, marine and other aquatic ecosystems and the ecological complexes of which they are part (Lawrence 2005). This includes diversity within species (genes), between species and of ecosystems. Although difficult

to measure (Purvis & Hector 2000), diversity of a system can be represented by the total number of species (species richness), the relative abundance of each species (evenness) or a proportional statistic that combines both measures, such as the Shannon-Wiener index and the Simpson index (Hill 1973; Washington 1984; Stirling & Wilsey 2001; Huber *et al.* 2007). Ecological diversity measures can also be used with bacterial communities (Hill *et al.* 2003). Microbial diversity in the environment can be measured by various indices such as phylogenetic diversity, species diversity, genotype diversity, and gene diversity (Xu 2006). Above the species level, microbial diversity is commonly quantified based on evolutionary distances among observed taxonomic groups from a specific environment, e.g., the phylogenetic diversity based on the 16S ribosomal RNA subunit. Below the species level, microbial diversity is typically described using population genetic parameters such as gene diversity and genotype diversity. In Chapter 5, the Simpson diversity index (D_{SSCP}) was calculated from the fingerprinting profiles based on 16S rRNA and functional genes, determined based on capillary electrophoresis single strand conformational polymorphism (CE-SSCP). This diversity index, calculated as $D_{SSCP} = -\ln\sum(\text{peak areas})^2$ (Loisel *et al.* 2008), reflects the underlying diversity from the SSCP profile independently of sample size (Rosenzweig 1995).

1.2.2 Ecological genomics and metagenomics

In recent years, molecular techniques have been used for the characterization of nitrifying microbial communities and allowed the detection of a larger diversity of nitrifiers than expected based on conventional culture-based techniques (Bothe *et al.* 2000; Otawa *et al.* 2006).

A genome refers to the complete set of genes and chromosomes carried by an organism (Lawrence 2005). The term genomics is used to describe a specific discipline in genetics that deals with mapping, sequencing and analysing of genomes, besides functional analytical aspects such as whole genome RNA transcripts (transcriptomics), proteins (proteomics), and metabolites (metabolomics). Metagenomics, ecological genomics, community genomics or environmental genomics is the genomic analysis of microorganisms by

direct extraction, cloning and/or sequencing of DNA from an assemblage of microorganisms (Handelsman 2004; Riesenfeld *et al.* 2004; Streit & Schmitz 2004; Tringe & Rubin 2005; Xu 2006; Schmeisser *et al.* 2007). A brief overview of used techniques in ecological genomics is given in Table 1.2 and Table 1.3.

The demand for cheaper and faster sequencing methods has increased greatly and has driven the development of second-generation sequencing or next-generation sequencing (NGS) methods (Table 1.3). NGS platforms perform massively parallel sequencing, during which millions of fragments of DNA from a single sample are sequenced in unison. Massively parallel sequencing technology facilitates high-throughput sequencing, which allows an entire genome to be sequenced in less than one day (Grada & Weinbrecht 2013). The advent of next generation sequencing has allowed an explosion in sequencing of individual genomes, and started a revolution in metagenomic sequencing and analysis (Scholz *et al.* 2012).

Table 1.2 Overview of techniques used in microbial metagenomics to analyse the genomic composition of an assemblage of microorganisms. This list is not exhaustive. PCR, real-time PCR, DNA cloning and SSCP were used in the datasets described in Chapter 4 and 5.

Method	Full name/description	Reference (examples)
Bioinformatics	Post-processing of molecular data	Chen and Pachter (2005); (Hogeweg 2011)
DGGE/TGGE	Denaturing or Temperature Gradient Gel Electrophoresis	Muyzer (1999); Boon <i>et al.</i> (2002); Xiuheng <i>et al.</i> (2009)
DNA cloning systems	Isolation of multiple copies of specific genes in pure form, by moving the desired gene from a large, complex genome to a small, simple one (Madigan & Martinko 2006)	Rondon <i>et al.</i> (2000); Bernet <i>et al.</i> (2004); Bougard <i>et al.</i> (2006a)
FISH	Fluorescence In Situ Hybridization	Schramm <i>et al.</i> (1998); Terada <i>et al.</i> (2010); Lydmark <i>et al.</i> (2006); Almstrand <i>et al.</i> (2013)
Flow cytometry	Technique for counting and distinguishing different types of cells in a mixed cell population (Lawrence 2005)	Hammes <i>et al.</i> (2008); Wang <i>et al.</i> (2010); De Roy <i>et al.</i> (2012)
SSCP	Single Strand Conformational Polymorphism, separation is done for example by Capillary Electrophoresis	Bernet <i>et al.</i> (2004); Bougard <i>et al.</i> (2006a); Volcke <i>et al.</i> (2008)
Shotgun DNA sequencing	Sequencing of previously cloned small fragments of a genome in a random fashion followed by computational methods to reconstruct the entire genome (Madigan & Martinko 2006)	Chen and Pachter (2005); Eisen (2007)
T-RFLP	Terminal-Restriction Fragment Length Polymorphism	Osborn <i>et al.</i> (2000)
Microarray technology	Transcriptomic analysis of messenger RNA on supports (gene chips) on which genes or portions of genes are affixed and spatially arrayed in a known pattern (Madigan & Martinko 2006). A chip can contain spots of DNA segments corresponding to all of the genes in a genome (Griffiths <i>et al.</i> 2008)	Sebat <i>et al.</i> (2003); Gentry <i>et al.</i> (2006)
PCR and real-time PCR	Polymerase Chain Reaction, in which a gene or sequence of interest is amplified in a test tube rather than by cloning. Real-time PCR involves the use of fluorescent-labelled PCR primers. If real-time PCR is quantitative, it is denoted as qPCR (Lawrence 2005; Madigan & Martinko 2006; Griffiths <i>et al.</i> 2008)	Toze (1999); Boon <i>et al.</i> (2002)

Table 1.3 Overview of the next and third generation sequencing techniques used in microbial metagenomics to analyse the genomic composition of an assemblage of microorganisms (continuation of Table 1.2). This list is not exhaustive.

Method		Full name/description	Reference (examples)
Next generation sequencing	Illumina sequencing	Based on the concept of sequencing by synthesis to produce sequence reads of tens of millions of surface-amplified DNA fragments simultaneously (Mardis 2008)	Ye <i>et al.</i> (2012b); Wang <i>et al.</i> (2014)
	Ion Torrent	Light independent determination of sequence composition by measuring pH changes due to hydrogen ion liberation as nucleotides are incorporated during strand synthesis in picolitre wells (Whiteley <i>et al.</i> 2012)	Whiteley <i>et al.</i> (2012)
	Roche (454) GS FLX sequencer	This sequencer works on the principle of pyrosequencing, which uses the pyrophosphate molecule released on nucleotide incorporation by DNA polymerase to fuel a downstream set of reactions that ultimately produces light from the cleavage of oxyluciferin by luciferase (Mardis 2008)	Sanapareddy <i>et al.</i> (2009); Johnson <i>et al.</i> (2014); Wang <i>et al.</i> (2014)
	SOLiD	Sequencing by Oligo Ligation and Detection (Mardis 2008)	Kovács <i>et al.</i> (2013); Solli <i>et al.</i> (2014)
Third generation sequencing	MinION	New, portable single-molecule sequencer developed by Oxford Nanopore Technologies. It measures four inches in length and is powered from the USB 3.0 port of a laptop computer. The MinION™ measures the change in current resulting from DNA strands interacting with a charged protein nanopore. These measurements can then be used to deduce the underlying nucleotide sequence (Quick <i>et al.</i> 2014)	Bohmann <i>et al.</i> (2014)
	GridION	A high-throughput nanopore-based sequencer	Bohmann <i>et al.</i> (2014)

1.2.3 Microbial diversity in nitrifying systems

Species from three genera of AOB, i.e., *Nitrosomonas*, *Nitrosococcus* and *Nitrospira* are mostly reported to oxidize ammonia (Bothe *et al.* 2000). Furthermore, it should be noted that in nitrifying bioreactors, also ammonia-oxidizing archaea (AOA) can be widespread (Park *et al.* 2006; Brown *et al.* 2013). Erguder *et al.* (2009) proposed that the AOA might be important actors within the nitrogen cycle in low-nutrient, low-pH, and sulphide containing environments. In this thesis, only the ammonia-oxidizing bacteria are considered.

The guild of NOB comprises bacteria of at least five different genera: *Nitrobacter*, *Nitrospina*, *Nitrococcus*, *Nitrospira* and the recently discovered *Nitrotoga* (Kruse *et al.* 2013). As the ammonia-oxidizing bacteria, the nitrite-oxidizers are chemolithotrophic autotrophs. The NOB are able to use nitrite as a sole source of energy and carbon dioxide as the main source of carbon (Spieck & Bock 2005; Madigan & Martinko 2006). However, some strains are obligate litho-autotrophs that are also able to grow mixotrophically, defined in this context as the ability to simultaneously incorporate inorganic and organic carbon sources (Daims *et al.* 2001a). Furthermore, species of the genus *Nitrobacter* are also able to grow as chemo-organotrophs in anaerobic environments by using organic carbon as sole carbon and energy source, resulting in nitrate reduction (Freitag *et al.* 1987). It should be noted that in the models considered in this thesis, the nitrite-oxidizing bacteria are assumed to be obligate chemolithotrophic autotrophs, neglecting mixotrophic or heterotrophic growth of this functional guild.

In the nitrifying community, different microbial populations, cells of a particular bacterial species or strain (Madigan & Martinko 2006), carrying out the same metabolic reaction (ammonium oxidation or nitrite oxidation) and therefore belonging to the same functional type or guild (Simberloff & Dayan 1991; Wilson 1999), can be in competition for one or more common substrates such as ammonium, nitrite and oxygen. A higher species richness is expected in nitrifying biofilms than in nitrifying suspended cultures, as more niches, which is the particular set of resources and environmental conditions that an

individual species exploits (Prosser *et al.* 2007), are created by diffusional substrate concentration gradients (Costerton *et al.* 1994; Stewart 2003). In multi-species biofilm systems, this will lead to a biofilm with a layered structure, giving species with different ecophysiological characteristics the opportunity to survive (Nicoletta *et al.* 2000).

Indeed, using molecular techniques, the coexistence of two or more species of AOB or NOB in biofilms has been detected. Schramm *et al.* (1998) identified two genetically and morphologically different populations of NOB affiliated with the nitrite-oxidizer *Nitrospira moscoviensis* in bacterial aggregates from a fluidized bed reactor. Another example of the coexistence of two NOB species was given by Downing and Nerenberg (2008), who observed the coexistence of *Nitrobacter* spp. and *Nitrospira* spp. in a nitrifying membrane-aerated biofilm reactor. Also *Nitrosomonas oligotropha* was shown to coexist with other AOB species in this reactor type (Terada *et al.* 2010). Lydmark *et al.* (2006) found four AOB populations in a full-scale nitrifying trickling filter, of which two *Nitrosomonas oligotropha* populations dominated at all depths of the trickling filter. These two populations showed different distribution patterns within the biofilm, indicating different ecophysiological niches, even though they belong to the same AOB lineage. In a recent study the niche differentiation between two dominant *Nitrosomonas oligotropha* populations in pilot-scale moving bed biofilm reactors and trickling filters was confirmed experimentally based on their different reaction on changes in ammonium loading (Almstrand *et al.* 2013). Bernet *et al.* (2004) and Volcke *et al.* (2008) reported that upon the lowering of the ammonium loading rate in a heavily loaded inverse turbulent bed reactor, nitrate started to accumulate due to the presence of *Nitrospira*, and *Nitrosomonas sp.* started to grow at the expense of *N. europaea*. Gieseke *et al.* (2003) detected the coexistence of 3 different AOB populations next to NOB of the genera *Nitrobacter* and *Nitrospira* with heterogeneous distributions in a sequencing batch biofilm reactor.

1.2.4 Composition of the microbial community

Influent characteristics, changing environmental conditions, but also the design and the operation of the wastewater treatment systems can influence the

composition of the microbial community (Yuan & Blackall 2002), depending on the resistance, the resilience, i.e., the possibility to recover, and/or the functional redundancy of the microbial community, i.e., the possibility of the altered community to function equally as the original one (Allison & Martiny 2008). The composition of the microbial community can have important implications from an engineering perspective. For example, the coexistence of several species of one functional guild may influence the process stability. Siripong and Rittmann (2007) and Wittebolle *et al.* (2008) have shown that the coexistence of different species of 1 functional type can maintain the stability of the system for nitrification when operation conditions change, by providing functional redundancy. Maintaining microbial diversity in an Inverse Turbulent Bed Reactor (ITBR) for partial nitrification was shown to be of interest to recover complete nitrification and to increase the robustness of the process when facing disturbances (Bougard *et al.* 2006a). Ramirez *et al.* (2009) demonstrated for an anaerobic digestion reactor, that microbial composition may significantly affect the reactor behaviour and performance, e.g., when facing toxic loads.

1.3 Modelling microbial diversity

As more and more information is gathered through the metagenomic analysis of microbial ecosystems, the relations among the structure and functional stability of microbial communities, physicochemical parameters and the role of functional redundancy should be further investigated (Ramirez *et al.* 2009; Beneduce *et al.* 2014). As the microbial community structure can influence the reactor operation (Ramirez *et al.* 2009), the engineering of wastewater treatment systems would be improved if one could describe and control the associated microbial diversity (Yuan & Blackall 2002). Conceptual and predictive mathematical models, systematic attempts to translate the conceptual understanding of a real-world system into mathematical terms (Eberl *et al.* 2006), provide an adequate tool for understanding phenomena involved in biofilm processes, e.g., Wik and Breitholtz (1996) and Picioreanu *et al.* (1997). Extending these models in order to describe microbial community

information could greatly increase the understanding of ecosystems and possible ways to manipulate them (Nielsen *et al.* 2010), besides increasing the predictive power of process models (Hawkes & Keitt 2015). Mathematical models considering microbial diversity can (1) allow to test current ecological theories in a straightforward way, (2) be a valuable tool in the construction of microbial communities with desirable properties (synthetic ecology) by the identification of the key components that influence the stable coexistence of microorganisms (Escalante *et al.* 2015; Fredrickson 2015), (3) allow to develop control strategies for microbial population optimization, (4) allow the prediction of process performance based on microbial community data and (5) help to unravel if changes of the process performance can be linked to microbial community changes.

1.3.1 Model classification

Considering dynamic models with dependent variables such as time and/or space, a distinction should be made between two types of models (Velten 2009): phenomenological models, also called empirical models, statistical models, data-driven models or black box models, are constructed based on experimental data only. In contrast, in mechanistic models the model statements are based on a priori knowledge of the modelled system. When all necessary information about the modelled system is available, these models are also called white box models, although many mechanistic models are located somewhere between the extreme black and white box cases, and are denoted grey box models or semi-empirical models.

Mechanistic models using ordinary differential equations, i.e., ODE models, or a combination of ODE and algebraic equations, i.e., differential-algebraic equation (DAE) models, are restricted in the sense that they involve derivatives with respect to one variable only, which means that they describe the dynamical behaviour of the quantity of interest with respect to this one variable only, for example time (Velten 2009). In contrast to ODEs, partial differential equation (PDE) models involve derivatives with respect to at least two independent variables, and hence they can be used to describe the dynamics of

the quantities of interest with respect to several variables at the same time, for example space and time.

To model dynamic processes in biofilms, in which the spatial component is considered at least in 1 dimension, PDE models are involved. One-dimensional biofilm models are such models that assume that the variation of the state variables is restricted to a single direction perpendicular to the surface of the solid carrier. This is a valid simplification when vertical gradients are orders of magnitude higher than those in the directions parallel to the carrier surface (Wanner & Gujer 1986). Since this applies to most biofilm systems, dynamic multispecies 1-dimensional biofilm models are sufficient for the majority of practical purposes. Higher dimensional descriptions (2D or 3D), making the biofilm modelling much more complex, are needed only when the focus is on the modelling of biofilm structures with highly irregular surface (Picioreanu *et al.* 2004).

It should further be noted that the models in this study are non-linear biological models and are continuous, in contrast to discrete models such as cellular automata. Cellular automata are models that are characterized by a discrete lattice of cells, homogeneity, discrete states, local interactions and discrete dynamics (Ilachinski 2001).

1.3.2 Rationale behind the inclusion of diversity in models

Present models considering diversity and competition are generally used to find answers to fundamental ecological questions or to assess the impact of climate change on global biodiversity and ecosystem services. The focus is mainly on the biodiversity of plants and animals, although recently more and more mathematical approaches are being developed for simulating and understanding microbial community dynamics (Song *et al.* 2014).

The question of which forces shape predominantly ecological communities is a topic worthwhile investigation using mathematical models. One possibility to bridge two theories (Schilthuizen 2008), i.e., the niche theory (Hutchinson 1957; Holt 2009) attributing a central role to niche differences between species, and the neutral theory (Hubbell 2001), attributing a central role to

migration processes and demographic stochasticity, is to combine them in a common mathematical framework (Haegeman & Loreau 2011). Ofițeru *et al.* (2010) investigated the combined niche and neutral effects in the economically and environmentally important microbial communities of a wastewater treatment plant. When environmental factors were incorporated, more of the variance in the observations could be explained but immigration and random reproduction and deaths (neutral community assembly) remained the dominant driver in determining the relative abundance of the common taxa. Another example of using models for investigating current ecological theories is given by Kalmykov and Kalmykov (2013). An individual based cellular automata approach was used to verify and reformulate the competitive exclusion principle, postulating that species competing for the same limiting resource in one homogeneous habitat cannot coexist, contradicting with the observed biodiversity in reality. Furthermore, models including microbial diversity or even implementing metagenomics data could possibly be very helpful. The potential in identifying new questions, ways of thinking, concepts and theories which improve fundamental understanding and quantitative prediction of the activity and interactions of microorganisms in ecosystems, based on ecological metagenomics and transcriptomics, should be explored (Prosser 2015).

Understanding how species and ecosystems respond to climate change has become a major focus of ecology and conservation biology, in the view of global change, and models are being developed to study the importance of diversity for sustaining the ecosystem services, e.g. Nelson *et al.* (2009) and McMahan *et al.* (2011). It should be noted that, despite their importance to the functioning of ecosystems, microorganisms are rarely explicitly considered in individual ecosystem or global process models (Andr en & Balandreau 1999; Allison & Martiny 2008; Reed *et al.* 2014).

The focus of this study is on mechanistic models, although phenomenological models can be used for the prediction of reactor performance based on microbial community information derived from DNA fingerprinting (Seshan *et al.* 2014). However, these black-box mathematical methods cannot produce mechanistic models of complex dynamic systems, and thus cannot be used to

directly obtain clear mechanistic insights into dynamics of complex systems (Kalmykov & Kalmykov 2015). Also, statistical analysis of extensive microbial community data retrieved by metagenomics can be inadequate to make inferences on the biological relevance (Parks & Beiko 2010) and gene-centric metagenomic studies involving correlation-based approaches are unlikely to provide any major advances in understanding (Prosser 2015), as it can be very difficult to tear out causation from correlation.

In mechanistic models, microbial diversity and microbial competition are mostly neglected. Some models describing the dynamical reactor behaviour with respect to time and implementing the growth of different species performing the same function can be found for activated sludge systems (Wett *et al.* 2011), anaerobic digestion (Ramirez *et al.* 2009) and nitrifying biofilms using a 0-dimensional model (Volcke *et al.* 2008). A recent study used a 1-dimensional biofilm (PDE) multispecies biofilm model to demonstrate the influence of biomass detachment and microbial growth in the bulk liquid on the microbial community in a heterotrophic biofilm (Brockmann *et al.* 2013).

1.3.3 Nitrifying models including diversity

In this thesis, the focus is on the modelling of nitrifying biofilms. Regarding nitrification models, at the most a distinction is made between ammonia-oxidizers and nitrite-oxidizers in conventional models (see Sin *et al.* (2008), for an overview), assuming the same properties for all bacteria of each functional guild. Only a few nitrifying biofilm models including two or more species of the same functional guild (AOB or NOB) have been reported in literature. For example, a biofilm model including 1 type of AOB and 2 types of NOB was set up by Downing and Nerenberg (2008), to determine the importance of both nitrite and oxygen affinity in the selection of *Nitrospira* spp. over *Nitrobacter* spp. in a membrane-aerated biofilm reactor. However, to obtain a deeper understanding of the link between microbial coexistence and process stability, a larger number of species per type should be included in the model. Furthermore, until now, no mathematical models of nitrifying biofilms were developed including multiple species of both nitrifying functional guilds (nitrification and nitrification). Therefore, in this PhD research, focussing on

biological nitrogen removal in biofilm reactors, dynamic (time-varying) 1-dimensional (considering spatial gradients perpendicular to the carrier material) biofilm models, considering microbial diversity of the nitrifying community, will be constructed and implemented in the Aquasim software (Reichert 1994).

1.3.4 Biofilm models in Aquasim

1.3.4.1 General overview

The 1-dimensional two-step (nitrification and nitrification) nitrifying biofilm models in this study were implemented in Aquasim, a computer program designed for the identification and simulation of aquatic systems (Reichert 1994; Reichert 1998) and since 2013 freely available (<http://www.eawag.ch/de/abteilung/siam/software/>). The model output was processed and plots were made in Matlab (Mathworks).

The use of Aquasim offers a number of features that are advantageous for simulations (Eberl *et al.* 2006), such as: (1) variables and processes can readily be activated or inactivated, making it simple to evaluate different model formulations, (2) the biochemical and abiotic transformation reactions are automatically calculated for all compartments and phases of the system and (3) the substratum or carrier can be selected to be flat, spherical, or cylindrical, while Aquasim automatically adapts the mass balance equations accordingly.

Steady state, i.e. equilibrium (constant effluent composition, biofilm thickness, species composition and concentrations) simulations with the models developed in Aquasim (>5000 days) generally took less than 1 hour of simulation time, i.e., the time needed to complete a simulation.

1.3.4.2 The biofilm compartment

For biofilm modelling and simulation, Aquasim offers a biofilm reactor compartment consisting of three zones (Wanner & Morgenroth 2004): the bulk fluid, biofilm solid matrix and biofilm pore water. For all three zones, Aquasim calculates the development over time of microbial species and substrates, as well as the biofilm thickness. In the biofilm, spatial gradients perpendicular to

the substratum are calculated for microbial species and substrates, based on the number of grid points set by the user. The number of grid points is used to specify by how many discrete points the continuous z -axis, which is perpendicular to the carrier, is approximated. If the number of grid points is set to n , the depth of the biofilm is resolved into 2 boundary points and $n-2$ grid points located in the middle of $n-2$ cells of equal thickness. Two additional grid points are used to describe the boundary layer between the biofilm and the bulk fluid, resulting from external mass transfer limitation, and the bulk volume, which is completely mixed.

1.3.4.3 Equations for flat biofilms

The equations solved in the biofilm reactor compartment consist of a set of partial and ordinary integro-differential equations, which together with their boundary conditions, the equations for a completely mixed bulk fluid and a liquid boundary layer, have been implemented in Aquasim for the development of a one-dimensional mixed-culture biofilm model (Wanner & Gujer 1986; Wanner & Reichert 1996; Reichert & Wanner 1997; Reichert 1998). These equations are not visible from the Aquasim interface. In the following, a brief overview of these equations is given for flat biofilms (see Chapter 2 and 3), as presented by Reichert (1998). In Chapter 4 and Chapter 5, biofilms growing on spherical particles were considered. Equations in Aquasim for spherical particles biofilms take into account that the biofilm surface area is dependent on the spatial coordinate (z in Aquasim).

In order to formulate the 1-dimensional conservation laws, compartment-specific expressions for the 1-dimensional density $\hat{\mathbf{p}}$ (the amount of conserved quantity per unit compartment length), for the 1-dimensional flux $\hat{\mathbf{j}}$ (the amount of the conserved quantity transported per unit time) and for the 1-dimensional source term $\hat{\mathbf{r}}$ (the amount produced per unit compartment length and per unit time), must be derived (**Eq. 1.1**).

$$\frac{\partial \hat{\mathbf{p}}}{\partial t} + \frac{\partial \hat{\mathbf{j}}}{\partial z} = \hat{\mathbf{r}} \quad \text{Eq. 1.1}$$

The three zones distinguished in the biofilm reactor compartment are the solid matrix with volume fraction ε_X (index ‘M’), the pore volume with volume fraction θ , which is the biofilm porosity (index ‘P’) and the bulk volume (index ‘B’). It should be noted that $\varepsilon_X + \theta = 1$. The index F is used for the biofilm, when the distinction into solid matrix and pore volume is not relevant. The index L is used for the liquid boundary layer above the biofilm immediately adjacent to the biofilm surface. Particulate components are denoted with X and soluble components with C.

The spatial dimension perpendicular to the substratum is resolved by the space coordinate z , which is zero at the substratum or carrier and has an increasing value with increasing distance from the substratum up to the biofilm thickness, L_F .

The array of one-dimensional densities of these types of components is given in Eq. 1.2.

$$\hat{\rho} = \begin{pmatrix} AX_{M,i} \\ AX_{P,i} \\ A\varepsilon_{l,F}C_{P,i} \\ A\theta \end{pmatrix} \quad \text{Eq. 1.2}$$

The first component of Eq. 1.2 describes particulate species in the biofilm matrix, the second component describes the particulate species in the biofilm pore water, the third component describes the substances dissolved in the pore water of the biofilm and the last component describes the porosity of the biofilm.

The solid matrix is made up by n_X particulate components, of which the volume fractions ε_{Xi} and concentrations X_{Fi} are related through their respective densities ρ_{Xi} (Eq. 1.3). The same density has been assumed for all particulate components (both active biomass and inert particulate components).

$$\varepsilon_X = \sum_{i=1}^{n_X} \varepsilon_{Xi} = \sum_{i=1}^{n_X} \frac{X_{M,i}}{\rho_{Xi}} \quad \text{Eq. 1.3}$$

The liquid phase volume fraction ($\varepsilon_{l,F}$) is given by Eq. 1.4.

$$\varepsilon_{l,F} = \theta - \sum_{i=1}^{n_X} \frac{X_{P,i}}{\rho_{Xi}} \quad \text{Eq. 1.4}$$

The 1-dimensional fluxes of the substances with 1-dimensional densities as described by Eq. 1.2, are given by Eq. 1.5: the first component gives advective and diffusive flow of solids within the biofilm matrix, the second component the advection and diffusion of solids suspended in the pore volume, the third term the advection and diffusion of dissolved substances (Fick's law of diffusion) in the pore volume of the biofilm and fourth component the flow of free volume in the biofilm.

$$\hat{\mathbf{j}} = \begin{pmatrix} Au_F X_{M,i} - AD_{M,Xi} \frac{\partial X_{M,i}}{\partial z} \\ -(1-\theta)Au_F \frac{X_{P,i}}{\theta} - \theta AD_{P,Xi} \frac{\partial X_{P,i}}{\partial z} + A \sum_{k=1}^{n_X} \frac{D_{M,Xk}}{\rho_{Xk}} \frac{\partial X_{M,k}}{\partial z} \frac{X_{P,i}}{\theta} + A \sum_{k=1}^{n_X} \frac{D_{P,Xk}}{\rho_{Xk}} \frac{\partial X_{P,k}}{\partial z} \frac{X_{P,i}}{\theta} \\ -(1-\varepsilon_{l,F})Au_F C_{P,i} - \varepsilon_{l,F} AD_{P,Ci} \frac{\partial C_{P,i}}{\partial z} + \frac{\varepsilon_{l,F}}{\theta} A \sum_{k=1}^{n_X} \frac{D_{M,Xk}}{\rho_{Xk}} \frac{\partial X_{M,k}}{\partial z} C_{P,i} + \frac{\varepsilon_{l,F}}{\theta} A \sum_{k=1}^{n_X} \frac{D_{P,Xk}}{\rho_{Xk}} \frac{\partial X_{P,k}}{\partial z} C_{P,i} \\ \theta Au_F + A \sum_{k=1}^{n_X} \frac{D_{M,Xk}}{\rho_{Xk}} \frac{\partial X_{M,k}}{\partial z} \end{pmatrix} \quad \text{Eq. 1.5}$$

The advective velocity u_F is given by Eq. 1.6 when the porosity of a biofilm remains constant (as assumed in this thesis).

$$u_F = \frac{1}{A} \int_0^z \left(\frac{1}{1-\theta} \sum_{k=1}^{n_X} \frac{r_{M,Xk}}{\rho_{Xk}} \right) A dz' \quad \text{Eq. 1.6}$$

The set of biofilm equations are completed by the 1-dimensional source terms given in Eq. 1.7 with r transformation rates and $k_{de,vol,Xi}$ and $k_{at,vol,Xi}$ substance dependent volume detachment and attachment coefficients, respectively. The transformation rates can be calculated from the stoichiometric matrices and the corresponding reaction kinetics given for each model in the respective chapters (Chapter 2-5).

$$\hat{\mathbf{r}} = \begin{pmatrix} Ar_{M,Xi} - Ak_{de,vol,Xi} X_{M,i} + Ak_{at,vol,Xi} X_{P,i} \\ Ar_{P,Xi} + Ak_{de,vol,Xi} X_{M,i} - Ak_{at,vol,Xi} X_{P,i} \\ Ar_{Ci} \\ Ar_{\theta} \end{pmatrix} \quad \text{Eq. 1.7}$$

In this thesis, no suspended solids are considered in the biofilm pore volume ($X_{P,i} = 0 \text{ g COD.m}^{-3}$ and $D_{P,Xi} = 0 \text{ m}^2.\text{d}^{-1}$), an adequate choice to describe very dense biofilms with very small pores in which there is no relevant motion of suspended solids. As a result, the biofilm porosity θ , defined as the ratio

between the volume of the biofilm solid matrix to the total biofilm volume, equals the volume fraction of the biofilm liquid phase $\varepsilon_{l,F}$. The biofilm porosity has also been assumed constant, which means that a same fraction of free volume is produced as is of solid matrix volume. As a result, the solid matrix fraction of the biofilm (ε_X) remains constant at the value determined by the total initial concentrations of particulate components. Nevertheless, the individual concentrations of particulate components will change in time. Furthermore, a rigid biofilm was considered, which means that effective diffusive mass transport of particulate components in the biofilm was neglected ($D_{M,Xi} = 0 \text{ m}^2 \cdot \text{d}^{-1}$), which means that particulate components are displaced only by the expansion or shrinkage of the biofilm solid matrix. Finally, attachment of particulate components from the bulk liquid into the biofilm was also ignored ($u_{at} = 0 \text{ m} \cdot \text{d}^{-1}$ and $k_{at,surf,Xi} = 0 \text{ m} \cdot \text{d}^{-1}$). Considering these assumptions, the application of the general expression for differential conservation laws (Eq. 1.1) to the definitions given by the equations Eq. 1.2, Eq. 1.5 and Eq. 1.7, leads to the following set of differential equations.

The first equation (Eq. 1.8) describes the behaviour of the constituents of the biofilm solid matrix.

$$\frac{\partial X_{M,i}}{\partial t} = -u_F \frac{\partial X_{M,i}}{\partial z} + \left(r_{M,Xi} - \frac{X_{M,i}}{1 - \theta} \sum_{k=1}^{n_X} \frac{r_{M,Xk}}{\rho_{Xk}} \right) - k_{de,vol} X_{M,i} \quad \text{Eq. 1.8}$$

The second equation (Eq. 1.9) describes the behaviour of substances dissolved in the pore water.

$$\frac{\partial \varepsilon_{l,F}}{\partial t} C_{p,i} + \frac{\partial C_{p,i}}{\partial t} \varepsilon_{l,F} = (1 - \varepsilon_{l,F}) u_F \frac{\partial C_{p,i}}{\partial z} + \sum_{k=1}^{n_X} \frac{r_{M,Xk} \varepsilon_{l,F}}{\rho_{Xk} \theta} C_{p,i} + \frac{1}{A} \frac{\partial}{\partial z} \left(\varepsilon_{l,F} A D_{p,Ci} \frac{\partial C_{p,i}}{\partial z} \right) + r_{Ci} \quad \text{Eq. 1.9}$$

The next equations, describing the behaviour of solids suspended in the pore water of the biofilm and the changes of the porosity, respectively, can be ignored, as in this thesis no suspended solids are considered in the pore volume and the porosity is assumed constant.

The above mentioned equations must be combined with Eq. 1.10, which gives the temporal change of the biofilm thickness, L_F . In this equation u_L is the

velocity of the interface layer between biofilm and bulk volume and u_{de} the detachment velocity.

$$\frac{dL_F}{dt} = u_L = u_F(L_F) - u_{de} \quad \text{Eq. 1.10}$$

A global biofilm detachment (u_d) has been implemented in this thesis as a function of biofilm thickness and advective velocity at the biofilm surface ($u_{F,LF}$) using Eq. 1.11, in order to let the biofilm grow to the steady state thickness ($L_{F,ss}$) by setting the detachment rate equal to the biofilm growth at the surface ($u_{F,LF}$) when steady state is reached.

$$u_d = \begin{cases} \left(\frac{L_F}{L_{F,ss}}\right)^{10} \cdot u_{F,LF} & \text{if } u_{F,LF} > 0 \\ 0 & \text{if } u_{F,LF} < 0 \end{cases} \quad \text{Eq. 1.11}$$

In the case of a rigid biofilm matrix, no boundary condition is required for Eq. 1.8. at the substratum-biofilm interface. The boundary condition for Eq. 1.8 at the biofilm surface is determined by the attachment (neglected in this study) and the detachment processes.

$$(u_F - u_L)X_{M,i}(L_F) = (u_{de} - u_{at})X_{M,i}(L_F) \text{ for } u_{de} > u_{at} \quad \text{Eq. 1.12}$$

The boundary conditions for Eq. 1.9 that describes the behaviour of substances dissolved in the pore water of the biofilm are as follows. At the substratum-biofilm interface, the boundary condition is given as a continuity equation of the flow through the substratum (Eq. 1.13), with $I_{substr,Ci} = 0$, as an impermeable substratum was considered in this thesis.

$$-A\varepsilon_{l,F}D_{p,Ci} \frac{\partial C_{p,i}}{\partial z}(z=0) = I_{substr,Ci} \quad \text{Eq. 1.13}$$

The boundary condition at the biofilm surface is a continuity condition for the concentration in the bulk liquid Eq. 1.14, with $C_{L,i}$ the concentration of dissolved components of type i in the liquid boundary layer above the biofilm immediately adjacent to the biofilm surface.

$$C_{p,i}(L_F) = C_{L,i} \quad \text{Eq. 1.14}$$

The total flows of solids out of the biofilm (negative values for flows into the biofilm) are given by Eq. 1.15. This expression is the advective flow from the

solid matrix at $z = L_F$ and the last term is correcting for the movement of the biofilm surface.

$$I_{L,X_i} = Au_F X_{M,i} - Au_L X_{M,i}(L_F) \quad \text{Eq. 1.15}$$

The total flows of dissolved substances out of the biofilm (negative values for flows into the biofilm) are given by Eq. 1.16. This expression is the flow at $z = L_F$ plus a correction that considers the movement of the interface.

$$I_{L,C_i} = -(1 - \theta) \frac{\varepsilon_{L,F}}{\theta} Au_F C_{P,i}(L_F) - \varepsilon_{L,F} AD_{P,C_i} \frac{\partial C_{P,i}}{\partial z}(L_F) - Au_L \varepsilon_{L,F} C_{P,i}(L_F) \quad \text{Eq. 1.16}$$

The equations for the biofilm described so far are connected to the bulk volume of the biofilm reactor through a liquid boundary layer. In Aquasim the liquid boundary layer is only roughly described with the aid of mass transfer resistance (Wanner & Reichert 1996), for example for dissolved components by Eq. 1.17, with K_{L,C_i} , the diffusive resistance for the dissolved substance C_i and $C_{B,i}$, the bulk liquid concentration of the dissolved component i . In this thesis, external mass transfer limitation of the dissolved components is considered only in Chapter 4.

$$C_{L,i} - C_{B,i} = \frac{K_{L,C_i}}{A(L_F)} I_{L,C_i} \quad \text{Eq. 1.17}$$

The mass balance for particulate components in the bulk volume is given by Eq. 1.18, with V_B the bulk volume, and I_{in,X_i} , the total input of the substance described by the concentration X_i . The last term takes into account conversion in the bulk liquid.

$$\frac{d}{dt}(V_B X_{B,i}) = I_{in,X_i} - X_{B,i} Q_{ef} + I_{L,X_i} + V_B r_{X_i} \quad \text{Eq. 1.18}$$

The mass balance equation for dissolved substances in the bulk volume is given by Eq. 1.19, with $C_{B,i}$ the bulk liquid concentration of dissolved component i and $\varepsilon_{l,B}$ the liquid phase volume fraction in the bulk volume (the porosity is equal to unity in the bulk volume).

$$\frac{d}{dt}(V_B \varepsilon_{l,B} C_{B,i}) = I_{in,C_i} - \varepsilon_{l,B} C_{B,i} Q_{ef} + I_{L,C_i} + V_B r_{C_i} \quad \text{Eq. 1.19}$$

In this thesis, a confined reactor was considered, which has a constant total reactor volume V_R for the biofilm and the bulk water. The bulk volume is calculated by Eq. 1.20.

$$V_B = V_R - \int_0^{L_F} A(z') dz' \quad \text{Eq. 1.20}$$

When the bulk liquid oxygen concentration is to be set to a setpoint value (C_{B,O_2}^{SP}), which can be varied during a simulation, a process active in the bulk liquid given by Eq. 1.21 is implemented in Aquasim, with $K_{O_2} = 10^8$.

$$\frac{d(V_B \cdot C_{B,i})}{dt} = \dots K_{O_2} \cdot (C_{B,O_2}^{SP} - C_{B,O_2}) + \dots \quad \text{Eq. 1.21}$$

Aquasim is based on robust numerical algorithms that, for most situations, calculate steady state and dynamic solutions without the need to adjust the numerical parameters. The partial differential equations are converted by a finite-difference spatial discretization scheme (method of lines) to a system of algebraic and ordinary differential equations (Wanner & Gujer 1986; Wanner & Reichert 1996), the PDEs are thus discretized in space. For the time integration of this equation system (spatially discretized PDEs, ODEs and algebraic equations), the fully implicit integration algorithm of Gear (Gear 1971) is used, which was extended to differential algebraic systems and implemented by Petzold (DASSL, Petzold (1982)).

1.3.4.4 Kinetics for growth and production of inerts

The growth of the ammonia-oxidizing and nitrite-oxidizing bacteria were implemented in the biofilm model based on Koch *et al.* (2000b) and Hao *et al.* (2002b), using Monod-terms for the electron donor and acceptor, i.e., ammonium and oxygen for AOB and nitrite and oxygen for NOB. The Monod term (Monod 1949) is an empirical equation, similar to Michaelis-Menten equation for enzyme kinetics, and introduces the concept of a growth limiting substrate. When multiple substrates are rate limiting, the Monod equation is typically extended to include the effects of each substrate influencing the rate of microbial synthesis by using the multiplicative Monod expression (Bae & Rittmann 1996), see Eq. 1.22, with μ the actual growth rate (d^{-1}), μ_{\max} the

maximum growth rate (d^{-1}), S_1 and S_2 the two substrates, and K_{S1} and K_{S2} , the affinity constant or half saturation constant for S_1 and S_2 , respectively.

$$\mu = \mu_{max} \cdot \frac{S_1}{S_1 + K_{S1}} \cdot \frac{S_2}{S_2 + K_{S2}} \quad \text{Eq. 1.22}$$

To reflect the decreasing net biomass production with increasing solids retention time, and the formation of ‘inert’ particulate components (X_i), i.e., non or slowly degradable parts of decaying cells, two different mechanisms were applied in this thesis: endogenous respiration and decay. Endogenous respiration, a state in which microorganisms oxidize cellular storage compounds instead of organic matter from their environment (van Loosdrecht & Henze 1999) on oxygen, nitrite and nitrate, converting active biomass into inerts, was considered in Chapter 3 and Chapter 4 and was implemented based on Volcke *et al.* (2010). The growth of heterotrophs (Chapter 5), and decay of AOB, NOB (Chapter 2), besides heterotrophs (Chapter 5) was implemented following Mozumder *et al.* (2014). During biomass decay, living cells are converted to organic substrate (X_s) as well as a fraction of inert (X_i) material (van Loosdrecht & Henze 1999). Decay was assumed to generate soluble organic substrate (S_s) directly rather than producing particulate organic substrate (X_s), which is subsequently hydrolysed to S_s , it was thus assumed that the latter reaction is not rate-limiting. Although both endogenous respiration and decay result in the formation of a fraction of inert particulate components, decay of AOB and NOB over endogenous respiration was chosen in Chapter 2 because the number of equations needed for the implementation of decay of 60 species per functional type is more restricted compared to equations for endogenous respiration. In Chapter 5, decay of AOB, NOB and heterotrophs is implemented, because also heterotrophs, using the organic substrate (S_s) formed during decay, are modelled.

1.3.4.5 Inhibition

In Chapter 6, free ammonia (FA) and free nitrous acid (FNA) inhibition were modelled as in Jubany *et al.* (2009). The AOB inhibition by FA and NOB inhibition by FNA, which is substrate inhibition, a special form of uncompetitive inhibition (Bisswanger 2008) were described with a Haldane

model (Eq. 1.23, see Beltrame *et al.* (1980)). The Haldane term is essentially a combination of a Monod term and a inhibition term (Eq. 1.24 and Eq. 1.25). Inhibition of AOB by FNA and NOB inhibition by FA were described with a non-competitive model (Eq. 1.26).

$$\text{Haldane inhibition term: } \frac{S_1}{K_{S1} + S_1 + \frac{S_1^2}{K_I}} \quad \text{Eq. 1.23}$$

$$\frac{S_1}{K_{S1} + S_1} \cdot \frac{K_I}{K_I + S_1} = \frac{S_1}{K_{S1} + S_1} \cdot \frac{1}{1 + \frac{S_1}{K_I}} = \frac{S_1}{K_{S1} + S_1 + \frac{K_{S1} \cdot S_1}{K_I} + \frac{S_1^2}{K_I}} \quad \text{Eq. 1.24}$$

$$\frac{\frac{K_I}{K_I + K_{S1}} S_1}{\frac{K_I}{K_I + K_{S1}} \cdot K_{S1} + S_1 + \frac{S_1^2}{K_I + K_{S1}}} = \frac{\mu_H \cdot S_1}{K_{S1}^H + S_1 + \frac{S_1^2}{K_I^H}} \quad \text{Eq. 1.25}$$

In Eq. 1.23 - Eq. 1.25, S_1 is the concentration of the substrate/inhibitor, K_{S1} the affinity constant for the substrate/inhibitor, K_I the inhibition constant, and μ_H , K_{S1}^H , K_{IH}^H the conversion factors from non-competitive inhibition to Haldane inhibition.

$$\text{Non-competitive inhibition term: } \frac{S_1}{S_1 + K_{S1}} \cdot \frac{K_I}{K_I + S_2} \quad \text{Eq. 1.26}$$

In Eq. 1.26, S_1 is the concentration of the substrate, S_2 is the concentration of the inhibitor, K_{S1} the affinity constant for the substrate and K_I the inhibition constant.

1.3.4.6 Species representation

For Chapter 2, 3 and 4, nitrifying biofilm models were developed including microbial diversity, by using different kinetic parameter sets for different species of 1 guild. The different kinetic and stoichiometric parameter values, besides the equations for the process rates (growth and decay or endogenous respiration) have to be introduced in the Aquasim interface for each considered species separately. Three different methods of species representation were used in this thesis: the species classes method, the bimodal distribution method and parameter estimation based on experimental data.

In Chapter 2, the growth and decay of 60 AOB and 60 NOB species were implemented, while in Chapter 3, the growth and endogenous respiration of 10 AOB and 10 NOB species was considered in a nitrifying biofilm model. All species of the same functional guild considered in Chapter 2 and 3 differed in their maximum growth rate, affinity for the electron donor, i.e., ammonium for ammonia-oxidizing bacteria and nitrite for nitrite-oxidizing bacteria, affinity for electron acceptor (oxygen), and yield. The effect of these parameters on bulk liquid concentrations of ammonium, nitrite and nitrate and microbial competition outcome were verified. These parameters were chosen because they are related to intrinsic characteristics of ammonia-oxidizing and nitrite-oxidizing species, however should be carefully interpreted, as these parameters are not always the ones for which two-step nitrifying biofilm models implemented in Aquasim are the most sensitive, as shown by sensitivity analyses already performed in the past (Hao *et al.* 2002b; Brockmann & Morgenroth 2007; Brockmann *et al.* 2008; Brockmann & Morgenroth 2010).

In both Chapter 2 and 3, microbial diversity was added to nitrifying biofilm models without calibration to experimental data, but the way of implementing within-guild diversity was different. Two methods, i.e., the species classes and bimodal distribution method were developed in order to increase the chance of coexistence of different species of 1 functional guild at steady state, by assuming niche differentiation between different species of a guild instead of randomly assigning parameter values.

In Chapter 2, microbial diversity was implemented by constructing 12 species classes (Figure 1.3), with 1 competitive advantage, e.g., a high growth rate, 1 competitive disadvantage, e.g., a low oxygen affinity, and two neutral characteristics. For each species per species class, values were randomly taken from the ranges from the literature study described in Chapter 2: low values from the range between minimum and the first quartile, neutral values from the range between the first and third quartile and high values between the third quartile and the maximum. This approach was used to reflect trade-offs, and thus niche differentiation (Kneitel & Chase 2004) among species of the same functional guild by assuming that 1 competitive advantage comes at the cost

of 1 competitive disadvantage, as advantageous traits often have side effects (Futuyma 2005). Using the method of species classes, the minimum number of species that can be implemented in the model is 12, although more than 1 species per species class can be constructed randomly, as was done in Chapter 2 (5 species per species class).

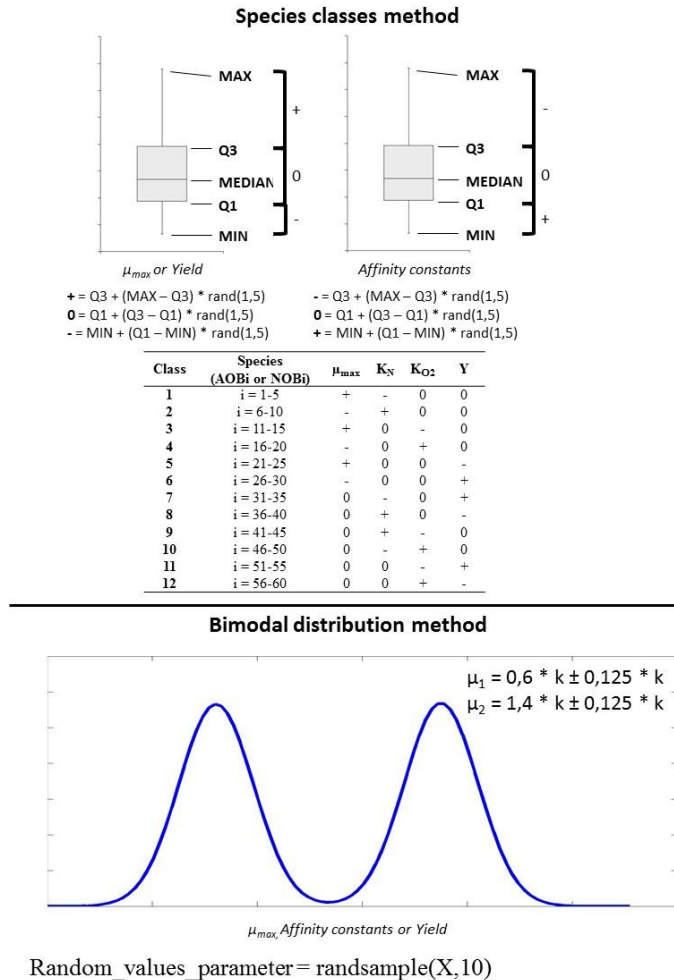


Figure 1.3 The two methods (species classes method and bimodal distribution method) used in this thesis for the construction of different species per functional type when no experimental data are available. Different values for the kinetic parameters μ_{max} , K_N (affinity for electron donor), K_{O_2} (affinity for electron acceptor) and yield were assigned to the different species of a type. Note that a high affinity (+) corresponds to a low affinity constant. k is the average or median value of the interval considered for a specific microbial parameter.

For the model used in Chapter 3, the ranges of values for maximum growth rate, affinities for nitrogen and oxygen and yield were also based on the literature review described in Chapter 2. However, for each microbial parameter, a normal bimodal distribution was now constructed (Figure 1.3) as in Ramirez *et al.* (2009), who based this distribution on a curve fitting process using experimental data. The eight bimodal distributions were each typified by two means ($\mu_1 = 0.6 \cdot k$; $\mu_2 = 1.4 \cdot k$) and standard deviations of $\sigma_{1,2} = 0.125 \cdot k$, with k the average value of the range of the corresponding parameter reported in literature, as revised in Chapter 2. The desired number of species can then be constructed by randomly picking values from each bimodal distribution.

In Chapter 4, a model was used implementing the growth of 2 AOB and 1 NOB species. The microbial parameters were taken from Volcke *et al.* (2008), who calibrated a 0-dimensional biofilm model with the same 2 AOB and 1 NOB species to experimental data. In Chapter 5, the microbial parameters of AOB and NOB guild were calibrated to experimental data on the bulk liquid composition.

1.3.4.7 Model calibration and parameter estimation

In Chapter 5, a biofilm model considering the growth and decay of 1 AOB, 1 NOB and 1 heterotroph was calibrated to experimental data using Aquasim. In Aquasim, the optimization objective function is to minimize the sum of the squares of the weighted difference between actual measurements and simulated results within the constraints of parameter ranges (Reichert *et al.* 1995; Reichert 1998; Swayne *et al.* 2010), see Eq. 1.27.

$$\chi^2(p) = \sum_{i=1}^n \left(\frac{y_{meas,i} - y_i(p)}{\sigma_{meas,i}} \right)^2 \quad \text{Eq. 1.27}$$

In Eq. 1.27, $y_{meas,i}$ is the i -th measurement, $y_i(p)$ the calculated value of the model variable corresponding to the i -th measurement and evaluated at the time and location of this measurement, $\sigma_{meas,i}$ the standard deviation defined globally for all measurements listed under the same variable, p (p_1, \dots, p_m) are the model parameters, and n the number of data points. The sum extends over all the data points of all variables specified as fit targets. Simultaneous

comparisons of data for measurements corresponding to different variables are possible (Reichert 1998).

Aquasim performs a minimization of the sum of the least squares with the constraints ($p_{\min,i} \leq p_i \leq p_{\max,i}$) where $p_{\min,i}$ and $p_{\max,i}$ are the minimum and maximum possible values of the parameter p_i whose value is subject to optimisation (Montràs Boet 2009). The secant algorithm (Ralston & Jennrich 1978) combined with the active set technique (Gill *et al.* 1981) was selected to perform the numerical minimisation of the function object (Eq. 1.27). A maximum number of iterations equal to 200 was set to keep the computational time reasonable.

1.4 Overall objective

The overall goal of this PhD research is to study the interaction between microbial community structure, process performance and operational conditions in biofilm reactors for biological nitrogen removal from wastewater.

The main objectives and at the same time most innovative aspects of this research project are:

- The incorporation of microbial diversity and competition in 1-dimensional biofilm models. A higher number of species per functional guild than in previously reported biofilm models will be considered and microbial diversity of both the ammonia-oxidizing and nitrite-oxidizing guild will be investigated at the same time.
- Investigation of the influence of microbial diversity on steady state and dynamic behaviour of nitrifying biofilms and biofilm reactors. The importance of microbial diversity, more specific functional redundancy, for the stability of reactor performance will be studied. Possible unnoticed changes in the microbial community will be explored.
- Gain insight in the influence of process conditions and microbial characteristics on microbial competition. The factors shaping the

microbial community and determining the competition outcome will be investigated with special attention for the reasons of coexistence of different species of the same functional guild in biofilms.

1.5 Outline of the thesis

An extensive literature study on the microbial parameter values is reported in **Chapter 2**. The variety of the values of maximum growth rate, affinity for electron donor and acceptor, besides yield for nitrifying microorganisms reported in literature is revised. Steady state simulations with a biofilm model including the growth and decay of 60 AOB species and 60 NOB species, taking into account the large variety of microbial parameter values observed in literature, are performed. The factors shaping the nitrifying community, in terms of operation conditions and microbial characteristics, will be investigated. The 60 species of each functional guild are constructed based on the species classes method.

The critical question of which purposes justify the inclusion of microbial diversity in biofilm models is addressed in **Chapter 3**. In a first case study, the change of a nitrifying community in a biofilm is followed over time until the bulk liquid as well as the microbial community are at steady state, using a biofilm model including the growth and endogenous respiration of 10 AOB and 10 NOB species. The diversity is implemented in the model using the bimodal distribution method. In a second case study, dynamic simulations will be performed with this biofilm model, to verify the functional redundancy of a nitrifying community, i.e., the possibility of a changed nitrifying community to function equally as the original one, upon an increased nitrogen loading rate.

In contrast to Chapter 2 and 3, Chapter 4 and 5 are based on mathematical modelling of experimental data. For **Chapter 4**, the data of Bernet *et al.* (2004) and Volcke *et al.* (2008) are used, who observed a population shift from *Nitrosomonas europaea* to *Nitrosomonas* sp., besides the shift from nitrite to nitrate accumulation, upon a lowering of the nitrogen loading rate in an Inverse Turbulent Bed Reactor (ITBR). Using the data set combining conventional chemical and physical data and molecular information, the reactor behaviour

of the ITBR, both in terms of nitrifying performance and on the scale of the microbial community, operated at varying loading rate, will be described with a biofilm model including the growth and endogenous respiration of 2 AOB and 1 NOB. Microbial parameter values were taken from the calibrated 0-dimensional model of Volcke *et al.* (2008). Furthermore, the applicability of the 1-dimensional biofilm model will be compared with this 0-dimensional biofilm model and a steady state analysis will be performed to verify the influence of microbial growth and endogenous respiration parameters as well as external mass transfer limitation on microbial competition.

For **Chapter 5**, data from Bougard (2004) and Bougard *et al.* (2006a), besides new molecular data, will be used to verify the effect of process dynamics on microbial competition based on a correlation analysis and in a simulation study. A biofilm model considering the growth and decay of 1 AOB, 1 NOB and 1 heterotroph, including free ammonia and free nitrous acid inhibition of the AOB and NOB, will be calibrated using the experimental data of the process dynamics.

Chapter 6 offers some final considerations and conclusions, besides discussing future perspectives.

In Table 1.4, the differences between Chapter 2-5 are further elaborated.

Table 1.4 Overview of the differences between the chapters of this thesis. SS: steady state, DYN: dynamic, ER: endogenous respiration.

Chapter	Type of simulations	Microbial community	Species construction	Processes included	FA and FNA inhibition	Boundary layer	Experimental data	Topic
2	SS	60 AOB 60 NOB	Species classes method	Growth Decay	-	-	-	<ul style="list-style-type: none"> Literature study on microbial parameter values Analysis of factors influencing microbial competition
3	SS + DYN	10 AOB 10 NOB	Bimodal distribution method	Growth ER	-	-	-	<ul style="list-style-type: none"> Case study 1: The change of the nitrifying community in time and its effect on reactor behaviour Case study 2: Investigation of functional redundancy upon an increased nitrogen loading rate
4	SS + DYN	2 AOB 1 NOB	Calibration (Volcke <i>et al.</i> 2008)	Growth ER	-	✓	Volcke <i>et al.</i> (2008)	<ul style="list-style-type: none"> Simulation of an experimental observed AOB population shift Comparison of 0- and 1-dimensional biofilm models Analysis of the effect of microbial growth and endogenous respiration parameters besides mass transfer limitation on microbial competition
5	DYN	1 AOB (calibrated) 1 NOB (calibrated) 1 HET	Calibration	Growth Decay	✓	-	Bougard (2004) Bougard <i>et al.</i> (2006a)	<ul style="list-style-type: none"> Influence of process dynamics on microbial community

2

Factors influencing microbial competition in nitrifying biofilms

2.1 Abstract

A large variety of microbial parameter values for nitrifying microorganisms has been reported in literature and was revised in this chapter. Part of the variety was attributed to the variety of analysis methods applied; it also reflects the large biodiversity in nitrifying systems. This diversity is mostly neglected in conventional nitrifying biofilm models. In this contribution, a 1-dimensional, multispecies nitrifying biofilm model was set up, taking into account the large variety of the maximum growth rate, the substrate affinity and the yield of nitrifiers reported in literature. Microbial diversity was implemented in the model by considering 60 species of ammonia-oxidizing bacteria (AOB) and 60 species of nitrite-oxidizing bacteria (NOB). A steady state analysis showed that operational conditions such as the nitrogen loading rate and the bulk liquid oxygen concentration influence both the bulk liquid output as well as the microbial composition of the biofilm through the prevailing concentration of substrates throughout the biofilm. Considering two limiting resources (nitrogen and oxygen), the coexistence of two species of the same functional guild (AOB or NOB) was possible at steady state. Their spatial distribution in the biofilm could be explained using the r- and K-selection theory.

2.2 Published as

Vannecke, T.P.W. & Volcke, E.I.P. (2015). Modelling microbial competition in nitrifying biofilm reactors. *Biotechnology and Bioengineering*, 112(12), 2550-2561. DOI: 10.1002/bit.25680.

2.3 Introduction

Biological nitrogen removal from wastewater can be considered a proven technology and has been widely implemented. During nitrification, which is the key reaction in biological nitrogen removal processes, ammonia-oxidizing bacteria (AOB) convert ammonia to nitrite, which is further oxidized to nitrate by nitrite-oxidizing bacteria (NOB).

In recent years, molecular techniques have been used for the characterization of nitrifying microbial communities and allowed the detection of a larger diversity of nitrifiers than expected based on conventional culture-based techniques (Bothe *et al.* 2000; Otawa *et al.* 2006). With molecular techniques, the coexistence of two or more species of AOB or NOB in biofilms has been detected. Schramm *et al.* (1998) identified two genetically and morphologically different populations of NOB affiliated with the nitrite-oxidizer *Nitrospira moscoviensis* in bacterial aggregates from a fluidized bed reactor. Another example of the coexistence of two NOB species was given by Downing and Nerenberg (2008), who observed the coexistence of *Nitrobacter* spp. and *Nitrospira* spp. in a nitrifying membrane-aerated biofilm reactor. Also *Nitrosomonas oligotropha* was shown to coexist with other AOB species in this reactor type (Terada *et al.* 2010). Lydmark *et al.* (2006) found four AOB populations in a full-scale nitrifying trickling filter, of which two *Nitrosomonas oligotropha* populations dominated at all depths of the trickling filter. These two populations showed different distribution patterns within the biofilm, indicating different ecophysiological niches, even though they belong to the same AOB lineage. In a recent study the niche differentiation between two dominant *Nitrosomonas oligotropha* populations in pilot-scale moving bed biofilm reactors and trickling filters was confirmed experimentally based on their different reaction on changes in ammonium loading (Almstrand *et al.* 2013). Bernet *et al.* (2004) and Volcke *et al.* (2008) reported that upon the lowering of the ammonium loading rate in a heavily loaded Inverse Turbulent Bed reactor (ITBR), nitrate started to accumulate due to the presence of *Nitrospira*, and *Nitrosomonas* sp. started to grow at the expense of *N. europaea*. Gieseke *et al.* (2003) detected the coexistence of 3 different AOB

populations next to NOB of the genera *Nitrobacter* and *Nitrospira* with heterogeneous distributions in a sequencing batch biofilm reactor.

The coexistence of several species of one functional guild can maintain the stability of the system for nitrification when operational conditions change (Siripong & Rittmann 2007; Wittebolle *et al.* 2008). Maintaining microbial diversity in an ITBR for partial nitrification was shown to be of interest to recover complete nitrification and to increase the robustness of the process when facing disturbances (Bougard *et al.* 2006a). Ramirez *et al.* (2009) demonstrated for an anaerobic digestion reactor, that microbial composition may significantly affect the reactor behaviour and process performance, e.g., when facing toxic loads. As the microbial community structure can influence the reactor operation (Ramirez *et al.* 2009), the engineering of wastewater treatment systems would be improved if one could describe and control the associated microbial diversity (Yuan & Blackall 2002). Also, the relations among the structure and functional stability of nitrifying communities, physicochemical parameters and the role of functional redundancy need to be further investigated (Beneduce *et al.* 2014). Mathematical models including molecular diversity are a useful tool in this respect.

However, in present nitrifying biofilm models, there is mostly only a distinction between the functional guilds, i.e., ammonium oxidation by AOB and nitrite oxidation by NOB. Conceptual and predictive mathematical models describing microbial diversity should be developed to obtain a deeper understanding of ecosystems and possible ways to manipulate them (Nielsen *et al.* 2010). Recently, mathematical models have been developed including microbial diversity, e.g., a recent study used a multi-species biofilm model to demonstrate the influence of biomass detachment and microbial growth in the bulk liquid on the microbial community in a heterotrophic biofilm (Brockmann *et al.* 2013). A few nitrifying biofilm models including two or more species of the same functional guild (AOB or NOB) have been presented. A biofilm model including 1 type of AOB and 2 types of NOB was set up by Downing and Nerenberg (2008), to determine the importance of both nitrite and oxygen affinity in the selection of *Nitrospira* spp. over *Nitrobacter* spp. in a

membrane-aerated biofilm reactor. The observed microbial population shifts upon the lowering of the loading rate in an inverse turbulent bed reactor were successfully described considering the growth of 2 types of AOB and 1 type of NOB in 0-dimensional (neglecting spatial variations) and 1-dimensional (considering vertical gradients perpendicular to the surface) biofilm models, by Volcke *et al.* (2008) and Vannecke *et al.* (2014), as presented in Chapter 4, respectively. However, to obtain a deeper understanding of the link between microbial coexistence and process stability, a larger number of species per type should be included in the model. Furthermore, until now, no mathematical models of nitrifying biofilms were developed including multiple species of both nitrifying functional guilds (nitrification and denitrification).

In order to intertwine the factors influencing microbial competition and coexistence in nitrifying biofilms, a 1-dimensional two-step nitrification biofilm model including the growth and decay of 60 species of AOB and 60 species of NOB was set up in this study. Microbial diversity in nitrifying biofilms was implemented in the model based on an extensive literature study on the reported range of parameter values for the maximum growth rate, substrate affinity and yield of nitrifiers. The developed multispecies model was used to investigate the influence on the community structure of both the operational conditions, in terms of bulk liquid oxygen concentration and ammonium loading rate, and the considered microbial characteristics. Furthermore, aspects of the local biofilm environment and microbial characteristics were related to the spatial organization of the coexisting nitrifier populations under typical process conditions.

2.4 Materials and methods

2.4.1 Literature review on microbial characteristics of nitrifiers

The parameter values reported in literature for the maximum growth rate (μ_{\max}^{AOB} and μ_{\max}^{NOB}), the affinity constants for the electron donor ($K_{\text{NH}}^{\text{AOB}}$ and $K_{\text{NO}_2}^{\text{NOB}}$) and electron acceptor ($K_{\text{O}_2}^{\text{AOB}}$ and $K_{\text{O}_2}^{\text{NOB}}$), besides yield (Y_{AOB} and Y_{NOB}) of AOB and NOB were reviewed.

A subdivision was made based on the growth type, i.e., suspended versus attached, and based on the way the parameter values were retrieved. As the determination of microbial parameters on pure (axenic) cultures or enriched cultures are limited, these reports were combined with studies using mixed cultures. Reported parameters determined using batch experiments and/or respirometry or based on model calibration with experimental data were preferred. However, parameter values from older literature were taken up as well, in case they were frequently used in mathematical models.

The reported parameter values for AOB and NOB were converted to be valid at a temperature of 30 °C and a pH of 7.5 based on the equations detailed in the Appendix 2A (Table A.2.1).

The reported values for each investigated microbial parameter were summarized graphically as boxplots, plotting the minimum value, the first quartile (Q1), the median (M), the third quartile (Q3), and the maximum value of the observed ranges. The median was chosen above the mean to describe the range of microbial parameters, as it reduces the importance of outliers. Statistical analysis of the results was performed with SPSS Statistics for Windows, Version 20 (2011, IBM Corp., Armonk, NY, USA), using non-parametric tests due to the relatively low number and/or non-normal distribution of parameter values found for some microbial characteristics. Two or more unpaired groups, e.g., maximum growth rates for AOB growing suspended versus attached, were compared with the Mann-Whitney U test, which was developed for this purpose (Landau & Everitt 2004). The significance level was set at $p=0.05$.

2.4.2 Development of the multispecies biofilm model

2.4.2.1 Two-step nitrification biofilm model

A 1-dimensional two-step nitrification biofilm model, including biomass variations perpendicular to the substratum on which the considered microorganisms grow, was implemented in the Aquasim software (Reichert 1994). The model described growth and decay of 60 AOB and 60 NOB species. To simulate the production of organic materials during biomass decay, the

death-regeneration concept was used, which comprises the transition of living cells to substrate (X_S) as well as a fraction of inert (X_I) material (van Loosdrecht & Henze 1999). Decay is assumed to generate soluble organic substrate (S_S) directly rather than producing particulate organic substrate (X_S), which is subsequently hydrolysed to S_S - it is thus assumed that the latter reaction is not rate-limiting.

To simplify the interpretation of the results, external mass transfer limitation was not considered. Also the inhibition of AOB and NOB by NH_3 and HNO_2 was neglected. Considering the variety of inhibition constants for NH_3 and HNO_2 of different AOB and NOB species or populations would greatly increase the complexity of the model. As the influent did not contain organic carbon and heterotrophic growth on biomass decay products can be neglected (Mozumder *et al.* 2014), heterotrophic growth was neglected as well in this study.

The overall model stoichiometry of the model used in this chapter are given in Table 2.1. The corresponding kinetics and parameters are given in Table 2.2 and Table 2.3, respectively. More information on the conversion of the parameter values to a temperature of 30 °C and a pH of 7.5 is given in Appendix 2A.

An autotrophic, flat biofilm with an initial thickness of $1 \cdot 10^{-6}$ m and a typical steady state thickness of $350 \cdot 10^{-6}$ m (Gieseke *et al.* 2003) was considered in a reactor of 0.001 m³. The number of grid points was set to 100 to ensure adequate resolution of predicted substrate and biomass gradients over the depth of the biofilm even at biofilm thicknesses of $350 \cdot 10^{-6}$ m. The biofilm was assumed to be rigid, meaning that particulate components are displaced only by the expansion or shrinkage of the biofilm solid matrix. The biofilm porosity was assumed constant at 80%.

Table 2.1 Stoichiometric matrix describing the growth and decay of 60 ammonia-oxidizing species (AOBi) and 60 nitrite-oxidizing species (NOBi), $i = 1 - 60$.

A_{ij}	i component \rightarrow j process \downarrow	S_i [g COD.m ⁻³]	S_{NH} [g N.m ⁻³]	S_{NO_2} [g N.m ⁻³]	S_{NO_3} [g N.m ⁻³]	S_{O_2} [g O ₂ .m ⁻³]	X_{AOBi} [g COD. m ⁻³]	X_{NOBi} [g COD. m ⁻³]	X_i [g COD. m ⁻³]
	<i>Growth</i>								
	1. growth of X_{AOBi}		$-1/Y_{AOBi} \cdot i_{NXB}$	$1/Y_{AOBi}$		$1-3.43/Y_{AOBi}$	1		
	2. growth of X_{NOBi}		$-i_{NXB}$	$-1/Y_{NOBi}$	$1/Y_{NOBi}$	$1-1.14/Y_{NOBi}$		1	
	<i>Decay</i>								
	3. decay of X_{AOBi}	$1-f_i$	$i_{NXB} \cdot f_i \cdot i_{NXI} \cdot (1-f_i) \cdot i_{NSS}$				-1		f_i
	4. decay of X_{NOBi}	$1-f_i$	$i_{NXB} \cdot f_i \cdot i_{NXI} \cdot (1-f_i) \cdot i_{NSS}$					-1	f_i
Composition matrix									
	g COD/unit comp	1	0	-3.43	-4.57	-1	1	1	1
	g N/unit comp	i_{NSS}	1	1	1	0	i_{NXB}	i_{NXI}	i_{NXI}

Table 2.2 Reaction kinetics for growth and decay corresponding to the processes from Table 2.1 with AOBi the ammonia-oxidizing species, NOBi the nitrite-oxidizing species and $i = 1 - 60$.

j process ↓	
1. growth of X_{AOBi}	$\rho_{G,AOBi} = \mu_{max}^{AOBi} \cdot \frac{S_{O_2}}{K_{O_2}^{AOBi} + S_{O_2}} \cdot \frac{S_{NH}}{K_{NH}^{AOBi} + S_{NH}} \cdot X_{AOBi}$
2. growth of X_{NOBi}	$\rho_{G,NOBi} = \mu_{max}^{NOBi} \cdot \frac{S_{O_2}}{K_{O_2}^{NOBi} + S_{O_2}} \cdot \frac{S_{NO_2}}{K_{NO_2}^{NOBi} + S_{NO_2}} \cdot \frac{S_{NH}}{K_{NH}^{NOBi} + S_{NH}} \cdot X_{NOBi}$
3. decay of X_{AOBi}	$\rho_{D,AOBi} = d_{AOBi} \cdot X_{AOBi}$
4. decay of X_{NOBi}	$\rho_{D,NOBi} = d_{NOBi} \cdot X_{NOBi}$

Table 2.3 Stoichiometric, kinetic and mass transfer parameter values of the multispecies biofilm model with AOBi the ammonia-oxidizing species, NOBi the nitrite-oxidizing species and $i = 1 - 60$.

Parameter	Description	Value	Unit	Reference
<i>Stoichiometric parameters</i>				
i_{NXB}	Nitrogen fraction in biomass	0.07	g N.(g COD) ⁻¹	Mozumder <i>et al.</i> (2014)
i_{NXI}	Nitrogen fraction in inerts	0.07	g N.(g COD) ⁻¹	Mozumder <i>et al.</i> (2014)
i_{NSS}	Nitrogen fraction in soluble organic substrate	0.03	g N.(g COD) ⁻¹	ASM3 (Henze <i>et al.</i> 2000)
f_{XI}	Fraction of inert COD generated in biomass decay	0.08	g COD.(g COD) ⁻¹	ASM2 (Henze <i>et al.</i> 2000)
Y_{AOBi}	Yield coefficient of AOBi	0.09 – 0.41	g COD.(g N) ⁻¹	See Table 2.5
Y_{NOBi}	Yield coefficient of NOBi	0.02 – 0.20	g COD.(g N) ⁻¹	See Table 2.5
<i>Kinetic parameters (pH 7.5 and T=30 °C)</i>				
d^{AOBi}	Decay rate of AOBi	0.017 – 0.17	d ⁻¹	Set to 0.05 μ_{max}^{AOBi}
d^{NOBi}	Decay rate of NOBi	0.012 – 0.18	d ⁻¹	Set to 0.05 μ_{max}^{NOBi}
K_{NH}^{AOBi}	Affinity of AOBi for ammonium	0.07 – 51.30	g TNH-N.m ⁻³	See Table 2.5
$K_{O_2}^{AOBi}$	Affinity of AOBi for oxygen	0.07 – 3.00	g O ₂ .m ⁻³	See Table 2.5
$K_{NO_2}^{NOBi}$	Affinity of NOBi for nitrite	0.05 – 38.69	g TNO ₂ -N.m ⁻³	See Table 2.5
$K_{O_2}^{NOBi}$	Affinity of NOBi for oxygen	0.04 – 4.01	g O ₂ .m ⁻³	See Table 2.5
K_{NH}^{NOBi}	Affinity of NOBi for ammonium (nitrogen source)	0.02	g TNH-N.m ⁻³	Mozumder <i>et al.</i> (2014)
μ_{max}^{AOBi}	Maximum growth rate AOBi	0.33 – 3.40	d ⁻¹	See Table 2.5
μ_{max}^{NOBi}	Maximum growth rate NOBi	0.24 – 3.54	d ⁻¹	See Table 2.5
<i>Mass transfer parameters</i>				
D_{NH_4}	Diffusion coefficient NH ₄	1.6e-4	m ² .d ⁻¹	Picioreanu <i>et al.</i> (1997)
D_{NO_2}	Diffusion coefficient NO ₂	1.5e-4	m ² .d ⁻¹	Picioreanu <i>et al.</i> (1997)
D_{NO_3}	Diffusion coefficient NO ₃	1.5e-4	m ² .d ⁻¹	Picioreanu <i>et al.</i> (1997)
D_{O_2}	Diffusion coefficient O ₂	1.7e-4	m ² .d ⁻¹	Picioreanu <i>et al.</i> (1997)
D_{SS}	Diffusion coefficient S _S	1.0e-4	m ² .d ⁻¹	Hao and van Loosdrecht (2004)

The effect of nitrogen loading rate (NLR) and bulk liquid oxygen concentration (DO) on the effluent composition and the microbial composition of the biofilm were verified in the current chapter, as these disturbance variables were assumed to play an important role based on previous experimental observations and simulation results (Bernet *et al.* 2004; Volcke *et al.* 2008; Vannecke *et al.* 2014). Constant bulk liquid oxygen concentrations between 0.4 and 2 g O₂.m⁻³, corresponding with the range of dissolved oxygen needed for optimal nitrification at high solids retention time (Stenstrom & Poduska 1980), were considered. The biofilm reactor was considered to be fed with synthetic wastewater containing exclusively 320 g TNH-N.m⁻³ but no carbon source nor any microorganisms. In order to obtain nitrogen loading rates between 120 and 5300 g N.m⁻³.d⁻¹, similar to the ones used by Bougard *et al.* (2006a), the influent flow rate was varied from $Q_{in} = 0.375 \cdot 10^{-3} \text{ m}^3 \cdot \text{d}^{-1}$ to $Q_{in} = 0.0166 \text{ m}^3 \cdot \text{d}^{-1}$. The temperature of the reactor was assumed to be constant at 30 °C and the pH at 7.5.

The total biomass in the biofilm at steady state was 20.60 g COD, which corresponds to 15450 g VSS.(m³ reactor)⁻¹. Considering a biofilm porosity of 80%, the density of autotrophic (X_{AOB} and X_{NOB}) and particulate inert materials (X_I) in the biofilm was set to 70000/0.2 g VSS.m⁻³ (Picioreanu *et al.* 1997; Volcke *et al.* 2010) which corresponds to 93333/0.2 g COD.m⁻³ = 466665 g COD.m⁻³ (for a typical conversion factor of 0.75 g VSS.(g COD)⁻¹, see Henze *et al.* (2000)). An initial active biomass fractioning of 75% AOB and 25% NOB was assumed, according to the number of electrons exchanged by the oxidation of NH₄⁺ to NO₂⁻ and from NO₂⁻ to NO₃⁻, respectively. In order to verify which species would become dominant without favouring one of the species, all species per type (AOB and NOB) had an equal initial concentration (ammonia-oxidizing bacteria: $466665 \text{ g COD} \cdot \text{m}^{-3} \cdot (0.2 \cdot 0.75) / 60 = 1167 \text{ g COD} \cdot \text{m}^{-3}$ and nitrite-oxidizing bacteria: $466665 \text{ g COD} \cdot \text{m}^{-3} \cdot (0.2 \cdot 0.25) / 60 = 389 \text{ g COD} \cdot \text{m}^{-3}$). Although for non-linear models, as the ones used in this thesis, the initial conditions can influence the steady state outcome, the influence of the initial concentrations of the species was verified not to

influence the steady state competition outcome, based on preliminary simulations with different realistic (non-uniform) initial species distributions.

2.4.2.2 *Species representation*

The 60 species of each type (AOB or NOB) differed in the parameter values for their maximum growth rate, affinity for the electron donor, affinity for oxygen and yield. These were the microbial characteristics of which the effect on microbial competition was tested.

Each species was assumed to possess 1 competitive advantage (high growth rate, high affinity or high yield), 1 competitive disadvantage (low growth rate, low affinity or low yield) and 2 average characteristics, resulting in 12 species classes (Table 2.4). This approach was used to reflect trade-offs, and thus niche differentiation (Kneitel & Chase 2004) among species of the same functional guild by assuming that 1 competitive advantage comes at the cost of 1 competitive disadvantage, as advantageous traits often have side effects (Futuyma 2005). To construct 5 species per species class, parameter values for maximum growth rate, affinity for substrates and yield, were randomly selected, using the *rand* function in Matlab (Mathworks), from three ranges obtained from the literature review of this contribution: (1) values between the minimum and Q1 of the reported range were considered as low, (2) the values between Q1 and Q3 as neutral and (3) the values between Q3 and the maximum as high. Note that a high affinity corresponds with a low affinity constant. The *rand* function can be used to generate uniformly distributed random numbers with an accuracy of $1 \cdot 10^{-4}$ in the interval (0-1). Therefore, in this thesis Eq. 2.1 was used to generate random numbers for microbial parameters between the intervals for high, neutral and low values. The resulting numbers were rounded to two decimal digits to the right of the decimal point.

$$\begin{aligned}
 \text{HIGH} &= \text{Q3} + (\text{MAX} - \text{Q3}) * \text{rand}(1,5) \\
 \text{NEUTRAL} &= \text{Q1} + (\text{Q3} - \text{Q1}) * \text{rand}(1,5) \\
 \text{LOW} &= \text{MIN} + (\text{Q1} - \text{MIN}) * \text{rand}(1,5)
 \end{aligned}
 \tag{Eq. 2.1}$$

Table 2.4 Representation of the 12 species classes modelled in the multispecies model. Each species has 1 competitive advantage (+), 1 competitive disadvantage (-) and two average characteristics (0). Note that a high affinity (+) corresponds with a low affinity constant. For each species class, 5 species were randomly constructed per type.

Class	Species (AOBi or NOBi)	μ_{\max}	K_N	K_{O_2}	Y
1	i = 1-5	+	-	0	0
2	i = 6-10	-	+	0	0
3	i = 11-15	+	0	-	0
4	i = 16-20	-	0	+	0
5	i = 21-25	+	0	0	-
6	i = 26-30	-	0	0	+
7	i = 31-35	0	-	0	+
8	i = 36-40	0	+	0	-
9	i = 41-45	0	+	-	0
10	i = 46-50	0	-	+	0
11	i = 51-55	0	0	-	+
12	i = 56-60	0	0	+	-

It should be noted that testing such a high number of parameter values (60 per functional guild) for maximum growth rate, affinity for electron acceptor and donor and yield can be seen as a kind of sensitivity analysis, as it allows one to verify which parameters are mainly influencing bulk liquid nitrogen concentrations and microbial competition outcome.

Table 2.5 Characteristics all AOB and NOB species considered. The species surviving at steady state in the discussed simulations are indicated in bold. The characteristics of the corresponding classes are given in Table 2.4.

Species classes	Species number	AOB				NOB			
		μ_{AOB} d ⁻¹	K_{AOB} g N.m ⁻³	K_{AOB}^{NO} g O ₂ .m ⁻³	Y_{AOB} g COD.(g N) ⁻¹	μ_{NOB} d ⁻¹	K_{NOB} g N.m ⁻³	K_{NOB}^{NO} g O ₂ .m ⁻³	Y_{NOB} g COD.(g N) ⁻¹
1	1	3.12	36.94	0.66	0.21	2.86	30.32	0.65	0.17
	2	2.47	43.38	0.55	0.20	3.11	20.29	0.73	0.17
	3	2.07	51.15	0.34	0.21	3.03	25.71	0.37	0.21
	4	2.81	50.08	0.51	0.19	2.14	31.71	0.31	0.15
	5	3.27	36.17	0.52	0.17	3.14	29.62	0.36	0.19
2	6	0.90	0.38	0.77	0.18	0.43	0.11	0.37	0.21
	7	0.62	0.76	0.30	0.20	0.84	0.73	0.75	0.15
	8	0.47	1.27	0.27	0.18	0.43	1.24	0.62	0.19
	9	0.57	0.13	0.41	0.18	0.64	1.32	0.77	0.20
	10	0.76	1.58	0.56	0.18	0.94	0.66	0.48	0.16
3	11	2.99	6.06	2.78	0.17	3.30	7.29	2.43	0.16
	12	1.98	7.98	2.34	0.16	3.06	5.49	2.46	0.20
	13	3.11	12.98	1.62	0.21	3.15	7.01	1.65	0.19
	14	2.17	4.57	2.41	0.17	2.79	11.66	1.74	0.16
	15	2.65	6.43	2.90	0.20	3.10	15.85	2.90	0.18
4	16	0.71	15.58	0.10	0.18	0.57	16.04	0.12	0.18
	17	0.56	17.02	0.10	0.18	0.70	7.73	0.14	0.20
	18	0.87	9.01	0.13	0.17	0.82	9.02	0.22	0.17
	19	0.81	7.38	0.22	0.15	0.39	11.45	0.17	0.19
	20	0.61	11.87	0.15	0.16	0.83	13.65	0.24	0.19
5	21	2.09	1.69	0.24	0.12	3.35	17.13	0.58	0.11
	22	2.63	2.19	0.64	0.09	2.08	16.78	0.38	0.12
	23	1.97	5.23	0.43	0.09	2.68	9.17	0.49	0.11
	24	3.28	9.45	0.67	0.10	2.71	15.03	0.70	0.14
	25	2.89	3.84	0.48	0.13	2.09	4.21	0.35	0.15
6	26	0.48	5.44	0.49	0.33	0.43	18.29	0.78	0.34
	27	0.84	5.54	0.59	0.30	0.47	12.67	0.55	0.39
	28	0.85	10.84	0.74	0.39	0.76	16.37	0.75	0.25
	29	0.92	14.69	0.33	0.29	0.56	8.54	0.64	0.29
	30	0.63	7.61	0.63	0.25	0.92	12.47	0.51	0.41
7	31	1.59	23.11	0.30	0.25	1.35	26.19	0.65	0.32
	32	1.58	41.06	0.46	0.30	1.61	39.98	0.60	0.22
	33	1.27	48.35	0.73	0.40	1.86	20.91	0.53	0.35
	34	1.76	38.64	0.54	0.23	1.96	27.72	0.38	0.31
	35	1.96	48.05	0.44	0.30	1.61	27.93	0.77	0.22
8	36	1.81	1.64	0.35	0.14	1.85	0.24	0.72	0.10
	37	0.98	0.27	0.65	0.13	1.28	0.13	0.48	0.15
	38	1.65	0.44	0.43	0.13	1.17	1.06	0.66	0.14
	39	1.94	0.11	0.47	0.14	1.06	0.98	0.57	0.09
	40	1.23	1.04	0.33	0.09	1.26	1.61	0.67	0.12
9	41	1.91	0.72	1.00	0.20	1.27	1.26	2.45	0.19
	42	1.45	0.69	1.50	0.17	1.58	0.88	1.60	0.20
	43	1.71	1.05	2.49	0.15	1.17	0.39	2.87	0.15
	44	1.70	0.34	1.31	0.19	1.53	0.75	0.83	0.16
	45	1.79	0.37	2.43	0.16	1.56	0.34	2.62	0.18
10	46	1.09	23.85	0.22	0.19	1.92	38.28	0.09	0.19
	47	1.56	33.64	0.17	0.20	1.75	33.35	0.15	0.18
	48	1.20	38.87	0.17	0.20	1.40	19.91	0.15	0.19
	49	1.27	49.09	0.22	0.17	1.28	35.48	0.16	0.19
	50	1.35	45.93	0.08	0.17	1.00	32.03	0.21	0.16
11	51	1.47	6.16	2.44	0.32	1.84	2.84	2.50	0.32
	52	1.27	13.30	1.99	0.22	0.95	11.60	2.81	0.35
	53	1.79	5.66	1.54	0.36	1.24	12.56	2.52	0.40
	54	1.77	9.47	2.63	0.33	1.12	12.80	1.44	0.30
	55	1.51	8.24	2.01	0.38	1.88	16.45	1.13	0.23
12	56	1.95	5.22	0.16	0.15	1.00	17.85	0.08	0.14
	57	1.89	5.42	0.24	0.14	1.58	10.56	0.21	0.14
	58	1.36	7.24	0.20	0.11	1.75	17.97	0.16	0.11
	59	0.94	3.31	0.24	0.12	1.65	2.93	0.19	0.10
	60	1.49	14.45	0.11	0.11	1.29	5.21	0.11	0.11

Recent records on the experimental determination of the decay rate of AOB and NOB species in biofilm reactors are limited, e.g., Ye *et al.* (2012a) investigated the decay of AOB and NOB in a two-stage moving bed biofilm reactor. In the current study, the decay rate of each species was considered to be 5% of its corresponding maximum growth rate, similar as Mozumder *et al.* (2014). As a consequence, the assumed higher turnover rate of microbial r-strategists versus K-strategists (Andrews & Harris 1986) was also reflected in this model.

2.4.2.3 Scenario analysis

To investigate the influence of operational conditions on microbial competition, simulations were run at different values for the bulk liquid oxygen concentration (DO) and nitrogen loading rate (NLR). For each individual simulation, the DO and NLR were kept constant.

Steady state simulations were performed in order to allow straightforward analysis of the effect of operational conditions and microbial characteristics on microbial competition and coexistence. The simulations were performed long enough (100000 days) to ensure steady state conditions in the bulk liquid (in terms of effluent composition) and in the biofilm (in terms of microbial community composition). These simulations took generally less than 1 hour of simulation time. Although the steady state effluent composition was reached within a few days, in some cases the steady state microbial community composition was only reached after about 25000 days.

2.5 Results and discussion

2.5.1 Literature review on microbial characteristics of nitrifiers

A wide range of parameter values for maximum growth rate, affinity and yield was found in literature. The boxplots of the considered microbial characteristics are represented in Figure 2.1 (AOB) and Figure 2.2 (NOB) and the raw data are available in Appendix 2B (Table A.2.2: AOB and Table A.2.3: NOB).

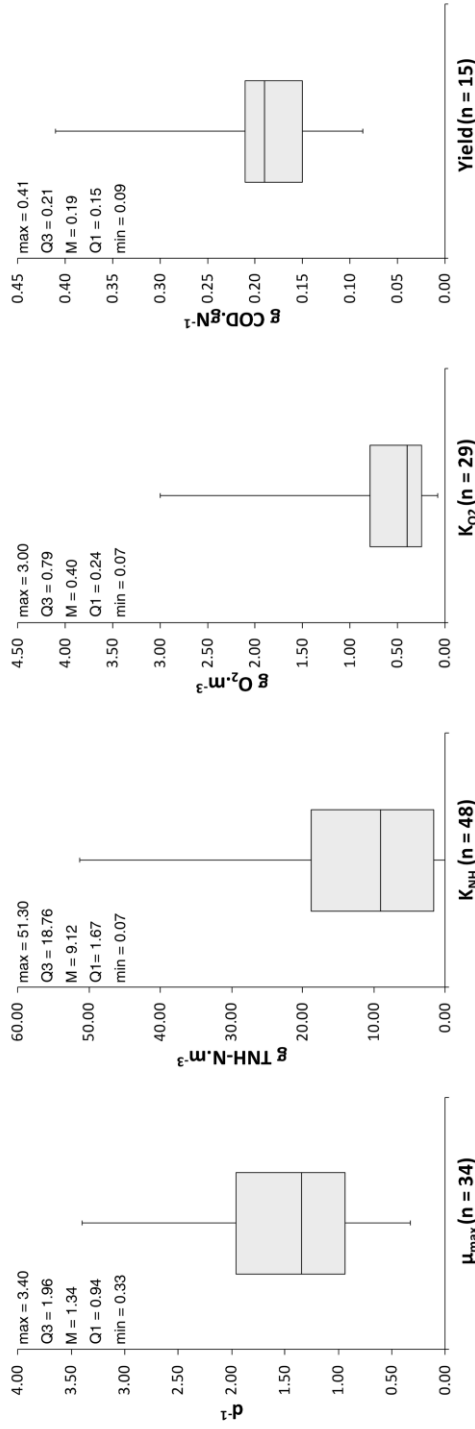


Figure 2.1 Boxplots representing the ranges for the maximum growth rate (A , μ_{max}), affinity for ammonium (B , K_{NH_4}), affinity for oxygen (C , K_{O_2}) and yield (D), for ammonia-oxidizing bacteria (AOB) at 30 °C and pH 7.5 found in literature. Max = maximum value found in literature, Q3= third quartile, M = median, Q1= first quartile and min = minimum value.

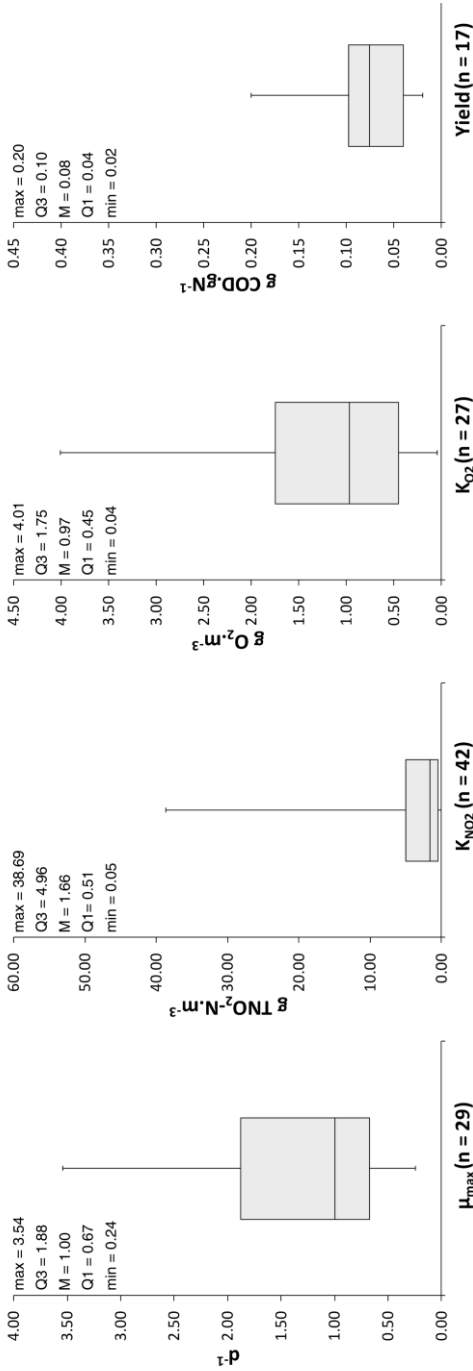


Figure 2.2 Boxplots representing the ranges for the maximum growth rate (A, μ_{max}), affinity for nitrite (B, K_{NO_2}), affinity for oxygen (C, K_{O_2}) and yield (D), for nitrite-oxidizing bacteria (NOB) at 30 °C and pH 7.5 found in literature. Max = maximum value found in literature, Q3= third quartile, M = median, Q1= first quartile and min = minimum value.

Microbial parameters cited in literature are mostly determined on suspended growth systems. No statistical differences were found between parameters for suspended and attached growth, possibly due to the low number of parameter values valid for attached systems available in literature. Although the lack of a significant difference could also indicate that there is no selection for specialized species growing in biofilms versus flocs, this is not expected as a clear differentiation in microbial ecology between suspended and attached bacteria was observed by Park *et al.* (2015) using molecular data.

In this thesis, apparent affinity constants were used. This is also the case for modelling of activated sludge processes. Diffusion has a larger impact on the process (the apparent affinity constant increases and thus the apparent affinity of an organism for its substrate decreases) when biomass density of the flocs increases. However, in biofilm modelling, diffusion is included separately in the equations used. The kinetic parameters that should be selected for biofilms are therefore the “true” coefficients corresponding to the kinetics of suspended cells (Pérez *et al.* 2005). In other words, the used apparent affinity constants in this thesis could be lumping different resistances to substrate transport and conversion (Arnaldos *et al.* 2015). The relative magnitude of each of these resistances will depend on the type of system under study. Furthermore, when using apparent affinity constants, it is very difficult to distinguish transport and biology related factors influencing the process. For example, Manser *et al.* (2005) reported lower affinity constants for flocs in membrane bioreactors compared to flocs of conventional activated sludge systems as the flocs in the former are generally smaller than in the latter. In contrast, other studies have claimed that membrane bioreactors select for bacterial groups with low half-saturation indices (K-strategists) as compared to conventional activated sludge systems due to the high solids retention times (and thus low substrate levels) commonly employed in these types of systems (Munz *et al.* 2010).

However, the differences between the values of the affinity constants for suspended and attached growth found in literature during the current study (Table A.2.2 and Table A.2.3) are small as the determination of affinity constants on pure (axenic) cultures of suspended cells is limited, and the range

of affinity constants found in literature (Figure 2.1 and Figure 2.2) was very large. Furthermore, currently, affinity constants for flocs and biofilms are mostly determined in a similar way, as biofilms are typically crushed for the determination of parameters (Riefler & Smets 2003), resulting in pseudo-suspended growth (flocs), and respirometry on biofilm particles should minimize the effect of external mass transfer (Carvalho *et al.* 2002; Carrera *et al.* 2004).

As no significant difference was found between the parameter values for suspended and attached growth, data from publications on both growth types were combined in the boxplots. As apparent affinity constants were used, the affinity constants were possibly too high (affinity of the organisms estimated too low) in the simulation study, mainly affecting the bulk liquid concentrations of oxygen, ammonium, nitrite and nitrate.

No significant difference was found between the maximum growth rate or the affinity for oxygen of AOB and NOB. Apparently, the large range of observed values for each microbial parameter prevents statistically sound conclusions. However, some interesting trends could be observed from the median of the observed ranges (reducing the influence of outliers): (1) AOB tend to have a higher maximum growth rate than NOB at 30 °C ($\mu_{max}^{AOB} = 1.34 \text{ d}^{-1}$ and $\mu_{max}^{NOB} = 1.00 \text{ d}^{-1}$), and (2) AOB tend to have a higher oxygen affinity than NOB ($K_{O_2}^{AOB} = 0.40 \text{ g O}_2 \cdot \text{m}^{-3}$ and $K_{O_2}^{NOB} = 0.97 \text{ g O}_2 \cdot \text{m}^{-3}$ at 30 °C). This is in line with common knowledge, applied to achieve nitrite accumulation for innovative nitrogen removal by outcompeting the NOB at high temperature, e.g., in the SHARON process (Hellinga *et al.* 1998), or low oxygen concentration, e.g., as elaborated by Bernet *et al.* (2001).

The affinity for the electron donor (ammonium for AOB and nitrite for NOB) was found to be significantly ($p < 0.05$) lower for AOB than for NOB ($K_{NH}^{AOB} = 9.12 \text{ g TNH} \cdot \text{m}^{-3}$ and $K_{NO_2}^{NOB} = 1.66 \text{ g TNO}_2 \cdot \text{m}^{-3}$). This allows NOB to grow deeper in the biofilm than AOB, where they are dependent on the nitrite produced by the AOB. The median yield coefficient of AOB was about two

times larger than the one for NOB ($Y_{AOB} = 0.19 \text{ g COD.g N}^{-1}$ and $Y_{NOB} = 0.08 \text{ g COD.g N}^{-1}$), as theoretically expected (Winkler *et al.* 2012).

The large variety in parameter values observed in literature could be a consequence of the different conditions under which the parameters are determined and the large number of different analysis techniques used. A large range of different techniques is used for the determination of maximum growth rate and yield (Blackburne *et al.* 2007a) and substrate affinity constants (Riefler *et al.* 1998; Carvallo *et al.* 2002; Guisasola *et al.* 2005), whether or not combined with the calibration of a mathematical model (Munz *et al.* 2012). For aerobic systems, many of the applied methods for determination of kinetic parameters are based on the indirect determination of the substrate uptake profile by the associated oxygen uptake profile (Riefler *et al.* 1998). However, the operational conditions for parameter determination, for example reactor configuration, pH and temperature can differ substantially. Some incentives were given to standardize the determination of parameters, e.g., Spanjers and Vanrolleghem (1995) and Vanrolleghem *et al.* (1999). In order to make the comparison of parameter values more straightforward and to attribute observed parameter value differences to the applied determination techniques versus the intrinsic microbial characteristics, the use of these standardized analysis techniques is advised.

Furthermore, also a large microbial diversity of the nitrifying community gives rise to a large variety of parameter values. The use of different mixed-culture inocula (Terada *et al.* 2010) versus pure cultures (Hunik *et al.* 1992, 1993; Hunik *et al.* 1994) can have a major influence on the microbial species composition of the investigated system and thus the resulting parameter values. Determination of parameter values in combination with culture-independent molecular techniques such as denaturing gradient gel electrophoresis (DGGE) and terminal restriction fragment length polymorphism (T-RFLP) on PCR (polymerase chain reaction) amplified target genes, besides real-time PCR and fluorescence in situ hybridization (FISH), could allow the association of the determined parameter values with specific species. If parameter values differ for the same species, operational conditions may have influenced the microbial

characteristics, e.g., one similar microbial community was acclimated to new operational conditions (Kim 2013) or different strains of a species had different metabolic characteristics (Lydmark *et al.* 2006). The interaction between modellers and microbiologists is therefore encouraged in order to keep track of microbial diversity in mathematical modelling, allowing for example model-based population optimisation (Yuan & Blackall 2002).

2.5.2 Scenario analysis

2.5.2.1 Influence of operational conditions

The percentage of influent total ammonium converted to ammonium, nitrite, nitrate and biomass (organic) nitrogen depends on the combination of bulk liquid oxygen concentration and nitrogen loading rate (Figure 2.3). When the oxygen limitation is severe and consequently the oxygen penetration is very low, ammonium and nitrite are not completely converted and are present in the effluent, up to maximum 205 g N.m^{-3} (64% of incoming nitrogen) and 57.6 g N.m^{-3} (18% of incoming nitrogen), respectively, for a DO of $0.4 \text{ g O}_2.\text{m}^{-3}$ and a NLR of $5300 \text{ g N.m}^{-3}.\text{d}^{-1}$. However, when nitrogen is the main limiting substrate, more than 99% of the incoming ammonium is converted to nitrate. As apparent affinity constants were used in a biofilm model, considering diffusion with separate equations, it is possible that affinity was estimated too low and the bulk liquid nitrogen concentrations were therefore not estimated correctly. However, as the focus in this chapter is on the influence of operational conditions and microbial characteristics on steady state competition outcome, the exact prediction of bulk liquid concentrations was not deemed necessary.

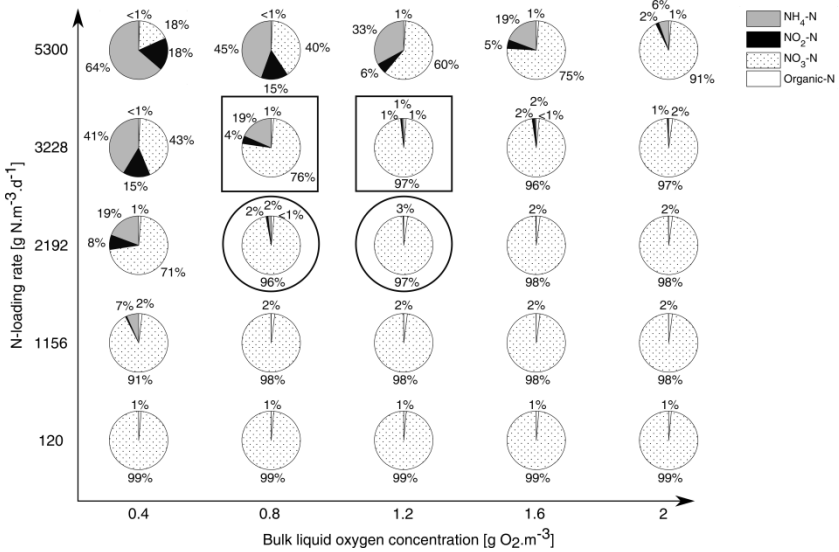


Figure 2.3 Steady state bulk liquid composition in terms of bulk oxygen concentration and nitrogen loading rate, represented as the percentage of incoming total ammonium ($320 \text{ g TNH-N.m}^{-3}$) converted to ammonium ($\text{NH}_4^+\text{-N}$), nitrite ($\text{NO}_2^-\text{-N}$), nitrate ($\text{NO}_3^-\text{-N}$) or organic nitrogen in biomass (Organic-N). The simulations discussed in the section on the influence of operational conditions and on coexistence are marked with a circle and a square, respectively. It should be noted that in the upper left corner of the graph mainly oxygen is limiting, while in the lower right corner mainly nitrogen is limiting.

In all simulations, the active layer was located within maximum $150 \cdot 10^{-6} \text{ m}$ of the surface of the biofilm, on top of a thick layer of inert particulates originating from biomass decay. The steady state microbial composition of the active layer (Figure 2.4) could differ significantly even if the bulk liquid output was very similar. For example, when a NLR of $2192 \text{ g N.m}^{-3}.\text{d}^{-1}$ was combined with a DO of 0.8 or $1.2 \text{ g O}_2.\text{m}^{-3}$, at least 96% of the incoming ammonium was converted to nitrate, although the steady state microbial composition in the biofilm was totally different in these simulations, i.e., AOB56 and NOB60 versus AOB39 and NOB6, respectively. For a DO of $0.8 \text{ g O}_2.\text{m}^{-3}$, the biofilm was typified by an oxygen limited nitrifying community having a high affinity for oxygen ($K_{\text{O}_2}^{\text{AOB56}} = 0.16 \text{ g O}_2.\text{m}^{-3}$ and $K_{\text{O}_2}^{\text{NOB60}} = 0.11 \text{ g O}_2.\text{m}^{-3}$, Table 2.6) while for a DO of $1.2 \text{ g O}_2.\text{m}^{-3}$, the nitrifying community was nitrogen limited and characterized by a high affinity for nitrogen ($K_{\text{NH}}^{\text{AOB39}} = 0.11 \text{ g N.m}^{-3}$ and $K_{\text{NO}_2}^{\text{NOB6}} = 0.11 \text{ g N.m}^{-3}$, Table 2.6). This shows the importance of the affinity

for the limiting nutrient(s) on the steady state microbial composition of the biofilm. It is also clear that the operational conditions affect the microbial composition by influencing the limiting nutrient concentration in the biofilm. The selection for a slow growing AOB (K-strategist, *Nitrosospira* spp.) and for a fast growing AOB (r-strategist, *Nitrosomonas* spp.), based on the prevailing concentrations of ammonia in the reactor, was experimentally demonstrated by Terada *et al.* (2013).

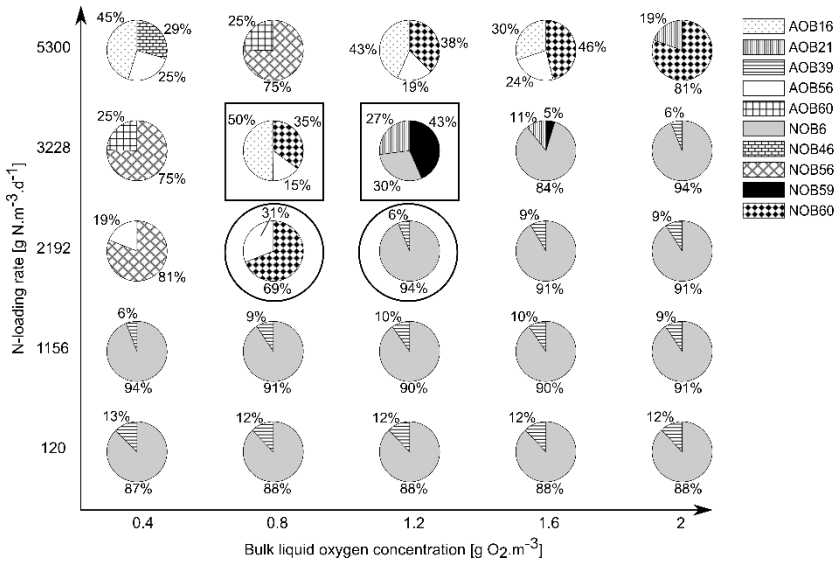


Figure 2.4 Steady state microbial composition of the biofilm in terms of bulk oxygen concentration and nitrogen loading rate, represented as the percentage of the active biomass made up by the species constituting a fraction higher than 0.01%. The simulations discussed in the section on the influence of operational conditions and on coexistence are marked with a circle and a square, respectively. It should be noted that in the upper left corner of the graph mainly oxygen is limiting, while in the lower right corner mainly nitrogen is limiting.

Table 2.6 Maximum growth rate (μ_{\max}), affinity for electron donor (K_N) and affinity for electron acceptor (K_{O_2}) for the species surviving at steady state (Figure 2.4), besides the range of bulk liquid oxygen:ammonium ratios at which a species survives in the biofilm at steady state and its main strategy. The highest maximum growth rate and lowest affinity constants observed per functional type are underlined.

		Range $O_2:NH_4^+$ ratio	μ_{\max} (d^{-1})	K_N ($g\ N.m^{-3}$)	K_{O_2} ($g\ O_2.m^{-3}$)	Strategy
AOB	AOB16	0.002 - 0.026	0.71	15.58	<u>0.10</u>	K-strategist for oxygen
	AOB21	0.113 - 0.457	<u>2.09</u>	1.69	0.24	r-strategist
	AOB39	0.019 - 151.63	1.94	<u>0.11</u>	0.47	K-strategist for nitrogen with rather high growth rate (generalist)
	AOB56	0.002 - 0.141	1.95	5.22	0.16	K-strategist for oxygen with rather high growth rate (generalist)
	AOB60	0.003 - 0.006	1.49	14.45	0.11	K-strategist for oxygen
NOB	NOB6	0.019 - 151.63	0.43	<u>0.11</u>	0.37	K-strategist for nitrogen
	NOB46	0.002	<u>1.92</u>	38.28	0.09	K-strategist for oxygen with high growth rate (generalist)
	NOB56	0.002-0.006	1.00	17.85	<u>0.08</u>	K-strategist for oxygen
	NOB59	0.457 - 0.678	1.65	2.93	0.19	r-strategist
	NOB60	0.011 - 0.141	1.29	5.21	0.11	K-strategist for oxygen with rather high growth rate (generalist)

As can be seen from Table 2.6, the species surviving at steady state are able to survive due to the value for their maximum growth rate and/or affinity constant for the main limiting substrate, as determined by the ratio of bulk liquid oxygen:ammonium concentrations. Oxygen limitation occurs if the $O_2:NH_4^+$ ratio is smaller than 0.15, and nitrogen limitation occurs if the ratio is higher than 0.15. For both types, two extremes of specificity, defined as a measure for the unevenness with which a taxon occurs in different habitats in a spatial setting (Hawkes & Keitt 2015; Mariadassou *et al.* 2015), could be distinguished, i.e., taxa found with equal abundances in many habitats (generalists) and taxa always and only found in one habitat (specialists). A species dominant at steady state was either a specialist with 1 strong competitive advantage or a generalist, found in a broad range of $O_2:NH_4^+$ ratios. The specialists in this study were either r-strategists with a high growth rate but low affinity or K-strategists with a low growth rate but high affinity

for the most limiting substrate. The generalists have a rather high growth rate besides a high affinity for the limiting substrate. However, these strategies should be carefully interpreted and only considered on a case by case basis. A generalist with a rather high affinity for oxygen can be for example denoted as an r-strategist and coexist with a K-strategist with a lower growth rate but higher affinity for oxygen when oxygen is limiting, as is observed for AOB16 (K-strategist) and AOB56 (r-strategist/generalist), see in the example given below in Section 2.5.2.2. It should also be noted that NOB46 has a high growth rate ($\mu_{\max}^{\text{NOB46}} = 1.92 \text{ d}^{-1}$) and high affinity for oxygen ($K_{\text{O}_2}^{\text{NOB46}} = 0.09 \text{ g O}_2\cdot\text{m}^{-3}$), but a very low affinity for nitrite ($K_{\text{NO}_2}^{\text{NOB46}} = 38.28 \text{ g N}\cdot\text{m}^{-3}$). Therefore, this species, although being a generalist concerning oxygen, can only survive if the nitrite concentration is high enough ($\text{NLR} = 5300 \text{ g N}\cdot\text{m}^{-3}\cdot\text{d}^{-1}$).

2.5.2.2 *Coexistence of species from the same functional guild at steady state*

In some of the investigated scenarios, two AOB (Scenario A) or two NOB (Scenario B) were able to coexist in a biofilm at steady state.

A constant DO and NLR of $0.8 \text{ g O}_2\cdot\text{m}^{-3}$ and $3228 \text{ g N}\cdot\text{m}^{-3}\cdot\text{d}^{-1}$ (Scenario A) resulted in only partial conversion (80%) of the incoming ammonium (Figure 2.3) to nitrite (4%) and nitrate (76%) and the coexistence of three nitrifying species at steady state, i.e., AOB16, AOB56 and NOB60 (Figure 2.4). The active layer was situated within $40\cdot 10^{-6} \text{ m}$ from the biofilm surface (Figure 2.5A). The oxygen concentration in the biofilm (Figure 2.5D) dropped from $0.8 \text{ g O}_2\cdot\text{m}^{-3}$ (bulk DO) to $0.01 \text{ g O}_2\cdot\text{m}^{-3}$ within about $30\cdot 10^{-6} \text{ m}$ from the biofilm surface. The ammonium concentration (Figure 2.5B: $59 \text{ g N}\cdot\text{m}^{-3}$) and nitrite concentration (Figure 2.5C: $13 \text{ g N}\cdot\text{m}^{-3}$) were in the active layer clearly higher than the corresponding affinity constants of the surviving species (Table 2.6) and only a negligible nitrogen concentration gradient was observed. Therefore, the community was mainly oxygen limited, resulting in only partial conversion of the incoming ammonium (Figure 2.3). Consequently, all selected species had a relatively high affinity for oxygen ($K_{\text{O}_2}^{\text{AOB16}} = 0.10$

$\text{g O}_2\cdot\text{m}^{-3}$, $K_{\text{O}_2}^{\text{AOB56}} = 0.16 \text{ g O}_2\cdot\text{m}^{-3}$ and $K_{\text{O}_2}^{\text{NOB60}} = 0.11 \text{ g O}_2\cdot\text{m}^{-3}$, Table 2.6). AOB16 and AOB56 belonged to a different species class, AOB16 being a K-strategist with a higher affinity for oxygen and a lower growth rate than r-strategist AOB56 ($\mu_{\text{max}}^{\text{AOB16}} = 0.71 \text{ d}^{-1}$ and $\mu_{\text{max}}^{\text{AOB56}} = 1.95 \text{ d}^{-1}$, Table 2.6). The r-strategist AOB56 is located at the outside of the biofilm, while the K-strategist AOB16 is located underneath (Figure 2.5A), forming two distinct zones along the oxygen concentration gradient (Figure 2.5D). It should be noted that AOB16 is still able to grow up to $40 \cdot 10^{-6} \text{ m}$ from the surface at a small fraction of its maximum growth rate, due to its low affinity constant for oxygen and the fact that the oxygen concentration in these regions is very low, but non-zero ($>0.0067 \text{ g O}_2\cdot\text{m}^{-3}$). In the regions below, decay becomes more and more important and the formation of inerts pushes the active zone upwards.

Lydmark *et al.* (2006) observed a similar vertical distribution of two genetically different *Nitrosomonas oligotropha* populations, with the K-strategist more or less equally distributed over the complete active layer, while the r-strategist was only present at the surface of the biofilm.

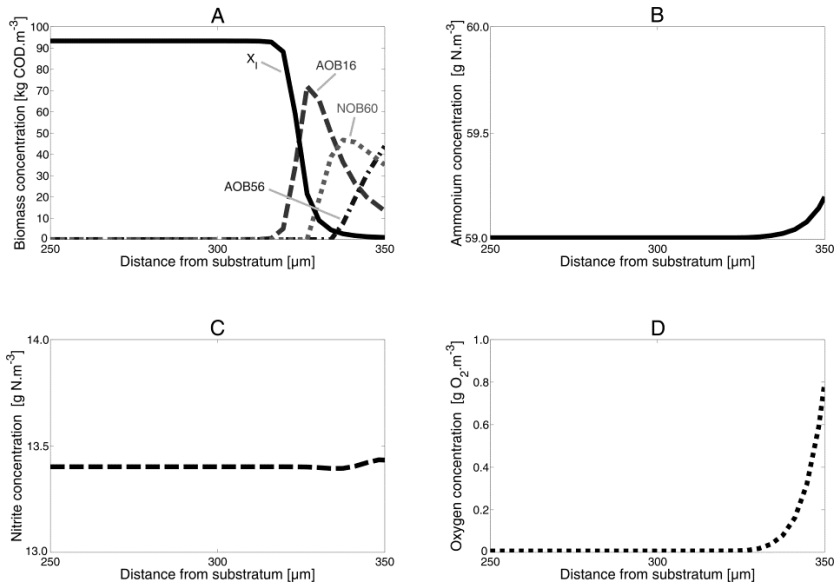


Figure 2.5 Steady state biomass (A; X_1 = inert particulate components) and the corresponding concentration profiles of the substrates (ammonium: B, nitrite: C and oxygen: D) in the active biofilm layer (upper 100 μm) for the simulation with a nitrogen loading rate of $3228 \text{ g N}\cdot\text{m}^{-3}\cdot\text{d}^{-1}$ and a bulk liquid oxygen concentration of $0.8 \text{ g O}_2\cdot\text{m}^{-3}$ (Scenario A).

For a constant DO and NLR of $1.2 \text{ g O}_2\cdot\text{m}^{-3}$ and $3228 \text{ g N}\cdot\text{m}^{-3}\cdot\text{d}^{-1}$ (Scenario B), 97% on the incoming ammonium was converted to nitrate (Figure 2.3) and two NOB coexisted at steady state, namely NOB6 and NOB59 (Figure 2.4). The active layer was situated within $70\cdot 10^{-6} \text{ m}$ from the biofilm surface (Figure 2.6A). The oxygen concentration (Figure 2.6D) dropped from $1.2 \text{ g O}_2\cdot\text{m}^{-3}$ (bulk DO) to $0.02 \text{ g O}_2\cdot\text{m}^{-3}$ within about $60\cdot 10^{-6} \text{ m}$ of the biofilm surface. Although the oxygen penetration depth delimited the active layer, the biofilm concentration of nitrite (Figure 2.6C: 2.96 to $2.80 \text{ g N}\cdot\text{m}^{-3}$) was close to the affinity constant of NOB59 ($K_{\text{NO}_2}^{\text{NOB59}} = 2.93 \text{ g N}\cdot\text{m}^{-3}$, Table 2.6), indicating that nitrite was limiting for this species. Also the affinity constant for ammonium of the only surviving AOB, AOB21 ($K_{\text{NH}}^{\text{AOB21}} = 1.69 \text{ g N}\cdot\text{m}^{-3}$, Table 2.6) was close to the ammonium concentration prevailing in the biofilm (Figure 2.6B: 2.62 to $2.37 \text{ g N}\cdot\text{m}^{-3}$). Furthermore, the nitrogen concentration showed a somewhat steeper slope compared to scenario A. Another indication for nitrogen limitation instead of oxygen limitation is the 97% conversion of the

incoming ammonium to nitrate (Figure 2.3). Considering nitrite as the main limiting substrate, the spatial distribution of the two coexisting NOB of Scenario B (Figure 2.6A) follows the r-K selection theory: NOB6, the K-strategist with a high affinity for nitrogen but low growth rate ($K_{\text{NO}_2}^{\text{NOB6}} = 0.11 \text{ g N.m}^{-3}$ and $\mu_{\text{max}}^{\text{NOB6}} = 0.43 \text{ d}^{-1}$, Table 2.6), lives beneath the r-strategist NOB59 with a low affinity for nitrite but a high growth rate ($K_{\text{NO}_2}^{\text{NOB59}} = 2.93 \text{ g N.m}^{-3}$ and $\mu_{\text{max}}^{\text{NOB59}} = 1.65 \text{ d}^{-1}$, Table 2.6). It should be noted that NOB6 is still able to grow up to $70 \cdot 10^{-6} \text{ m}$ from the surface at a small fraction of its maximum growth rate, due the fact that the oxygen concentration ($>0.02 \text{ g O}_2.\text{m}^{-3}$) and nitrite concentration ($>2.79 \text{ g N.m}^{-3}$) in these regions are low, but non-zero.

Schramm *et al.* (1998) described a similar spatial distribution for a nitrogen limited fluidized bed reactor at a temperature of $30 \text{ }^\circ\text{C}$. Two genetically different populations coexisted, with a K-strategist distantly related to *Nitrospira moscoviensis* also occurring deep in the biofilm and a second smaller population of an r-strategist closely related to *Nitrospira moscoviensis*, surviving only at the surface of the biofilm. The r-strategist and the K-strategist observed in Scenario B could also belong to different genera of NOB, for example *Nitrobacter* sp. versus *Nitrospira* sp., respectively, as observed by Downing and Nerenberg (2008).

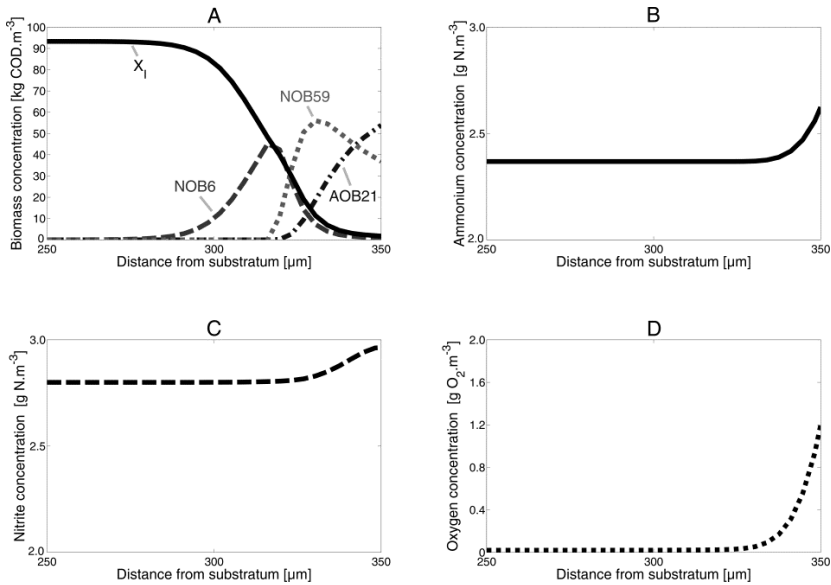


Figure 2.6 Steady state biomass (A; X_1 = inert particulate components) and the corresponding concentration profiles of the substrates (ammonium: B, nitrite: C and oxygen: D) in the active biofilm layer (upper 100 μm) for the simulation with a nitrogen loading rate of 3228 g N.m⁻³.d⁻¹ and a bulk liquid oxygen concentration of 1.2 g O₂.m⁻³ (Scenario B).

The influence of the initial community composition on the steady state bulk liquid composition and microbial composition of the biofilm was examined for both scenarios, firstly by replacing the whole functional guild (AOB or NOB) by one of the two coexisting species of the corresponding scenario and secondly by removing one of the coexisting species of the corresponding scenario from the whole functional guild (Table 2.7). For Scenario A, the initial removal of 1 of the dominant AOB (AOB16 or AOB56) or the replacement of the whole AOB community by 1 of the dominant AOB drastically changed the steady state effluent composition, besides the steady state microbial composition. For example, when AOB16 was the only AOB in the AOB community, about 39% of the incoming ammonium remained unconverted in the effluent, compared to 19% when the initial AOB community was made up of 60 species. For Scenario B, an initial NOB community of 60 species resulted in complete conversion of the incoming ammonium to nitrate, while an initial NOB community made up solely of NOB6 resulted in a substantial nitrite

accumulation (55% of the incoming ammonium). These observations confirm the suggestion of Terada *et al.* (2010), that the AOB and NOB population compositions of the inoculum may determine the dominant species in the biofilm, which in turn affects the nitrification performance. The inoculum effect on the AOB communities of parallel sequential batch reactors was also demonstrated experimentally by Wittebolle *et al.* (2009). However, it should be noted that this observation holds only for systems operated with synthetic wastewater lacking microorganisms in the feed, as the system under study. The result may be different for reactors operated with real wastewater, where microorganisms are continuously fed to the reactor and microorganisms from the bulk liquid could attach to the biofilm.

Table 2.7 Influence of initial community composition on the steady state effluent composition in terms of percentage of incoming total ammonium (320 g TNH-N.m⁻³) converted to ammonium (NH₄⁺-N), nitrite (NO₂⁻-N), nitrate (NO₃⁻-N) or organic nitrogen (Organic-N) and on the steady state microbial biofilm composition as the percentage of the active biomass made up by the species constituting a fraction higher than 0.01% for both Scenario A (oxygen limitation) and Scenario B (nitrogen limitation).

SCENARIO A (OXYGEN LIMITATION)					
initial → composition	60 AOB 60 NOB	AOB16 60 NOB	AOB56 60 NOB	59 AOB (no AOB16) 60 NOB	59 AOB (no AOB56) 60 NOB
Bulk liquid composition (%)					
NH ₄ ⁺ -N	18.5	38.6	15.8	18.6	14.1
NO ₂ ⁻ -N	4.2	5.7	7.7	10.2	5.4
NO ₃ ⁻ -N	75.9	54.7	75.0	70.1	79.4
Org-N	1.4	1.1	1.5	1.2	1.2
Microbial composition of the biofilm (%)					
AOB16	50.0	82.3			-
AOB56	15.0		18.5	-	
AOB60	-			22.3	40.2
NOB56	-	-	81.5	77.7	-
NOB60	35.0	17.7	-	-	59.8
SCENARIO B (NITROGEN LIMITATION)					
Bulk liquid composition (%)					
initial → composition	60 AOB 60 NOB	60 AOB NOB6	60 AOB NOB59	60 AOB 59 NOB (no NOB6)	60 AOB 59 NOB (no NOB59)
NH ₄ ⁺ -N	0.8	0.7	0.4	0.4	1.3
NO ₂ ⁻ -N	0.9	54.6	0.7	0.7	0.9
NO ₃ ⁻ -N	96.9	43.3	97.4	97.4	96.4
Org-N	1.4	1.3	1.5	1.5	1.4
Microbial composition of the biofilm (%)					
AOB9	-	-	-	-	-
AOB21	27.0	12.6	-	-	18.1
AOB39	-	-	31.4	31.4	-
NOB6	29.6	87.4			-
NOB59	43.4		68.6	68.6	
NOB60	-			-	81.9

2.5.2.3 Outlook

In this chapter, the incorporation of microbial diversity in mathematical models was proven useful to analyse microbial competition in biofilms and interpret observed spatial distributions of coexisting species. Using the developed mathematical model reflecting the growth and decay of 60 AOB and 60 NOB, considering oxygen and nitrogen limitation, a maximum of 3 dominant species in the nitrifying community, with two species performing the same function (ammonium oxidation or nitrite oxidation) coexisting at steady state was observed. This contrasts with the behaviour of continuous cultures of microorganisms competing for 1 limiting nutrient, in which only 1 species is able to survive at steady state (Hsu *et al.* 1977; Hsu 1980). Similarly, when describing microbial competition in biofilms using 0-dimensional models, only 1 species will survive at steady state (Volcke *et al.* 2008).

While the current contribution focuses on steady state behaviour, it is clear that there is an even higher chance of coexistence of species of the same functional guild during dynamic reactor operation. Gieseke *et al.* (2003) detected the coexistence of 3 different AOB populations next to NOB of the genera *Nitrobacter* and *Nitrospira* with heterogeneous distributions in a sequencing batch biofilm reactor (SBBR). They concluded that the spatial heterogeneity resulted from the continuously changing microenvironments during the SBBR cycle.

The one-dimensional model developed in this study assumes that the variation of the state variables is restricted to a single direction perpendicular to the surface of the solid carrier. When modelling biofilm structures with highly irregular surface, it is expected that the substrate concentration gradients will differ spatially due to different biofilm thicknesses. Therefore, a higher steady state microbial diversity is expected when considering 2- or 3-dimensional biofilm models instead of a 1-dimensional one. A higher steady state diversity is also expected when taking into account inhibition by free ammonia (FA) or nitric acid (FNA) and/or a different affinity for additional limiting nutrients (besides oxygen and nitrogen) such as carbon dioxide. Furthermore, also predation by eukaryotic microorganisms is expected to shape the microbial

community in biofilms (Saur *et al.* 2014), e.g., selective predation pressure can favour or suppress particular bacterial species (Pernthaler 2005).

As the use of 60 species per type can be seen as an inherent sensitivity analysis for the varied microbial parameters, i.e., maximum growth rate, affinity for electron donor and acceptor and yield, it can be concluded that maximum growth rate and affinity for the main limiting nutrient, in this study oxygen or nitrogen, are very important for the steady state bulk liquid concentration and competition outcome. Even species from the same species class (for example AOB56 and AOB60: class 12) were able to coexist in a biofilm, as long as they differed in their strategy: here AOB56 is an r-strategist with a higher growth rate ($\mu_{\max}^{\text{AOB56}} = 1.95 \text{ d}^{-1}$) and AOB60 was a K-strategist for oxygen ($K_{\text{O}_2}^{\text{AOB60}} = 0.11 \text{ g O}_2 \cdot \text{m}^{-3}$). In contrast, yield was shown not to be important for the competition outcome and small changes of yield within the reported range (Figure 2.1 and Figure 2.2) did not influence the substrate removal nor the competition outcome or biomass concentration gradients. This indicates that in the considered model, kinetic parameters were more important than stoichiometric ones for the steady state results. In this study, this is most likely due to the fact that the ranges of considered values for maximum growth rate and affinity constants were larger than the ones considered for yield (Figure 2.1 and Figure 2.2), resulting from the fact that yield is determined mainly on the basis of the energy yielded from catabolic reactions. Also Hsu *et al.* (1977), who developed a mathematical model based on Monod kinetics, for one substrate and n competing species concluded that the species will survive whose affinity constant is smallest in comparison with its intrinsic rate of natural increase and that it is irrelevant how efficiently the species convert the nutrient into cell growth (yield). However, in reality, due to the trade-off between growth rate and yield (Pfeiffer & Bonhoeffer 2002), species with a high yield but lower growth rate, using their resources economically, could promote altruism in spatially structured environments, such as biofilms (Kreft 2004). This indicates that yield besides kinetic parameters as growth rate could indeed play an important role in biofilm competition, for example when yet another limiting substrate for the autotrophs, carbon dioxide (Guisasola *et al.*

2007), their carbon source for biomass production, would be considered in mathematical models.

2.6 Conclusions

The large variety of microbial parameter values for nitrifiers reported in literature reflects the large biodiversity in microbial systems, even though part of it can also be explained by the variety in determination techniques. The use of standardized determination methods is recommended to exclude the latter.

The interaction between modellers and microbiologists is greatly encouraged in order to keep track of microbial diversity in mathematical modelling.

The presented 1-dimensional biofilm multispecies model was able to simulate steady state microbial coexistence of species performing the same function (ammonium oxidation or nitrite oxidation) and is a useful tool in the interpretation of microbial competition and of the observed spatial distributions of coexisting species.

The steady state microbial composition of the biofilm could differ significantly even if the effluent composition was very similar. It was shown that the nitrogen loading rate and the bulk liquid oxygen concentration influence both the macroscopic output as well as the microbial composition of the biofilm by influencing the concentration of the limiting nutrients in the biofilm. Besides, the steady state reactor performance and microbial distribution was also influenced by the initial community composition.

Considering two limiting resources (nitrogen and oxygen), the steady state coexistence of maximum two species of the same functional group (two AOB or two NOB) in the nitrifying community was observed. Their spatial distribution in the biofilm could be explained using the r- and K-selection theory.

2.7 Appendix 2A: Conversion of microbial characteristics to 30 °C and pH = 7.5

Published maximum growth rates of AOB and NOB were converted to a rate at 30 °C using Eq. 2A.1 and Eq. 2A.2 with $E_a^{AOB} = 68 \text{ kJ.mol}^{-1}$; $E_a^{NOB} = 44 \text{ kJ.mol}^{-1}$ and $R = 8.31 \text{ J. (mol.K)}^{-1}$.

$$\mu_{\max}^{AOB}(T) = \mu_{\max}^{AOB}(T_{\text{ref}}) \cdot \exp\left(\frac{E_a^{AOB} \cdot (T - T_{\text{ref}})}{R \cdot T \cdot T_{\text{ref}}}\right) \quad \text{Eq. 2A.1}$$

$$\mu_{\max}^{NOB}(T) = \mu_{\max}^{NOB}(T_{\text{ref}}) \cdot \exp\left(\frac{E_a^{NOB} \cdot (T - T_{\text{ref}})}{R \cdot T \cdot T_{\text{ref}}}\right) \quad \text{Eq. 2A.2}$$

All affinity constants for ammonium (AOB) and the affinity constants for nitrite (NOB) were converted to g TNH-N.m^{-3} and $\text{g TNO}_2\text{-N.m}^{-3}$, respectively, unless the published affinity constant was expressed as g N.m^{-3} . Affinity constants for nitrogen expressed as $\text{g NH}_3\text{-N.m}^{-3}$ or $\text{g NH}_4^+\text{-N.m}^{-3}$ (AOB) and as $\text{g HNO}_2\text{-N.m}^{-3}$ or $\text{g NO}_2^-\text{-N.m}^{-3}$ (NOB) were converted to g TNH-N.m^{-3} and $\text{g TNO}_2\text{-N.m}^{-3}$, respectively (Table A.2.1).

Yield coefficients expressed in $\text{g organic dry matter.(g N)}^{-1}$ or g odm.(g N)^{-1} were converted to yield coefficients expressed as g COD.(g N)^{-1} by using the conversion factor of $1.3659 \text{ g COD.g odm}^{-1}$, based on the typical biomass composition $\text{CH}_{1.8}\text{O}_{0.5}\text{N}_{0.2}$.

Table A.2.1 Equations to express affinity constants for ammonium (AOB) and nitrite (NOB) in units of TNH-N.m^{-3} and $\text{TNO}_2\text{-N.m}^{-3}$, respectively, with $\text{pKa}(\text{NH}_4) = -\log\left(e^{\left(\frac{-6344}{273.15+T}\right)}\right)$ and $\text{pKa}(\text{HNO}_2) = -\log\left(e^{\left(\frac{-2300}{273.15+T}\right)}\right)$ calculated for $T = 30^\circ\text{C}$ and $\text{pH} = 7.5$ following Anthonisen et al. (1976).

Input: $\frac{K^{AOB}}{K^{NH}}$ expressed as \rightarrow	Units		
	$\text{g NH}_3\text{.m}^{-3}$	$\text{g NH}_3\text{-N.m}^{-3}$	$\text{g NH}_4^+\text{.m}^{-3}$
Output: $\frac{K^{AOB}}{K^{NH}}$ expressed as (TNH-N.m^{-3})	$[\text{NH}_3] \cdot \frac{14}{17} \cdot (1 + 10^{(\text{pKa}(\text{NH}_4) - \text{pH})})$	$[\text{NH}_3] \cdot (1 + 10^{(\text{pKa}(\text{NH}_4) - \text{pH})})$	$[\text{NH}_4^+] \cdot \frac{14}{18} \cdot (1 + 10^{(\text{pH} - \text{pKa}(\text{NH}_4)})})$
Input: $\frac{K^{NOB}}{K^{NO2}}$ expressed as \rightarrow	Units		
Output: $\frac{K^{NOB}}{K^{NO2}}$ expressed as ($\text{TNO}_2\text{-N.m}^{-3}$)	$\text{g NO}_2\text{.m}^{-3}$	$\text{g NO}_2\text{-N.m}^{-3}$	$\text{g HNO}_2\text{-N.m}^{-3}$
	$[\text{NO}_2] \cdot \frac{14}{46} \cdot (1 + 10^{(\text{pKa}(\text{HNO}_2) - \text{pH})})$	$[\text{NO}_2] \cdot (1 + 10^{(\text{pKa}(\text{HNO}_2) - \text{pH})})$	$[\text{HNO}_2] \cdot \frac{14}{47} \cdot (1 + 10^{(\text{pH} - \text{pKa}(\text{HNO}_2)})})$

2.8 Appendix 2B: Literature review on microbial characteristics of nitrifiers

The results of the literature review on the microbial characteristics of AOB and NOB are summarized in Table A.2.2 and Table A.2.2, respectively.

Table A.2.2 Values of the maximum growth rate (μ_{\max}^{AOB} , average: 1.49 ± 0.76), affinity for ammonium ($K_{\text{NH}}^{\text{AOB}}$, average: 12.31 ± 12.55), affinity for oxygen ($K_{\text{O}_2}^{\text{AOB}}$, average: 0.61 ± 0.61) and yield (Y_{AOB} , average: 0.20 ± 0.09) for ammonia-oxidizers (AOB) at 30 °C and pH 7.5 found in literature. Growth type: S = suspended growth and A = attached growth. Publication type: E = experimental determination, C = calibration of model based on experimental results and L = other literature values.

	μ_{\max}^{AOB} d^{-1}	$K_{\text{NH}}^{\text{AOB}}$ $\text{g TNH-N}\cdot\text{m}^{-3}$	$K_{\text{O}_2}^{\text{AOB}}$ $\text{g O}_2\cdot\text{m}^{-3}$	Y_{AOB} $\text{g COD}\cdot(\text{g N})^{-1}$	Growth type	Publication type	Publication
1	0.93			0.19	S	E	Blackburne <i>et al.</i> (2007a)
2		28.39	1.45	0.14	S	E	Brouwer (1995)
3	0.97	11.28			S	E/C	Carrera <i>et al.</i> (2004)
4	0.34	28.72			A	E/C	Carrera <i>et al.</i> (2004)
5		11.28			A	E	Carvalho <i>et al.</i> (2002)
6		11.93	0.99		S	E	Ciudad <i>et al.</i> (2006)
7	1.00	0.92	0.24	0.41	A	L	Downing and Nerenberg (2008)
8	3.40	9.33		0.21	A	E/C	Fang <i>et al.</i> (2009)
9		0.72		0.41	S	C	Gee <i>et al.</i> (1990)
10	1.08				S	E	Glover (1985)
11	0.84				S	E	Glover (1985)
12			0.74		S	E	Guisasola <i>et al.</i> (2005)
13	2.01				A	L	Hao <i>et al.</i> (2002a)
14		18.29			S	E	Hellinga <i>et al.</i> (1999)
15	1.37	17.95	0.16	0.16	A	L	Hunik <i>et al.</i> (1994)
16		19.21			S	E	Hunik <i>et al.</i> (1992)
17	0.58	0.72	0.25	0.15	S	L	Jones <i>et al.</i> (2007)
18	1.90	7.86	0.74	0.18	S	E	Jubany <i>et al.</i> (2008)
19		11.13			S	E	Jubany (2007)
20	2.34				S	C	Kaelin <i>et al.</i> (2009)
21	1.26	1.03	0.5		S	L	Kampschreur <i>et al.</i> (2007)
22	0.84	3.74		0.086	S	E	Keen and Prosser (1987)
23	2.51	35.90	1	0.21	A	L	Koch <i>et al.</i> (2000a)
24		23.06	0.18		S	E	Laanbroek and Gerards (1993)
25	1.2		0.43		A	E	Lackner <i>et al.</i> (2010)
26			0.68		A	E	Lackner <i>et al.</i> (2010)
27	1.36	18.61		0.15	S	E	Lochtman (1995)
28		6.15			S	E	Lopez-Fiuza <i>et al.</i> (2002)
29		0.13	0.18		S	E	Manser <i>et al.</i> (2005)
30		0.14	0.79		S	E	Manser <i>et al.</i> (2005)
31				0.21	S	L	Manser <i>et al.</i> (2006)
32		5.13	1		S	C	Moussa <i>et al.</i> (2005)
33			3		S	C	Moussa <i>et al.</i> (2005)
34	3.08				S	E/C	Munz <i>et al.</i> (2011a)
35	1.32				S	C	Munz <i>et al.</i> (2011b)
36	1.79	1.92			S	C	Munz <i>et al.</i> (2012)
37	1.95		0.3		S	E	Nowak <i>et al.</i> (1995)
38	1.96	19.88			S	C	Pambrun <i>et al.</i> (2006)
39	2.04	0.065			S	E	Poduska and Andrews (1975)
40		42.15	0.334		S	E	Rongsayamanont <i>et al.</i> (2010)
41		11.09	0.325		S	E	Rongsayamanont <i>et al.</i> (2010)
42		51.30			A	E	Rongsayamanont <i>et al.</i> (2010)
43		14.99			A	E	Rongsayamanont <i>et al.</i> (2010)
44			1.66		S	E	Sánchez <i>et al.</i> (2001)
45		0.26			A	E	Sánchez <i>et al.</i> (2003)
46		4.37			S	E	Sánchez <i>et al.</i> (2005b)
47		0.57			A	E	Schramm <i>et al.</i> (1999)
48	1.26				S	E	Shaw <i>et al.</i> (2006)
49	0.33	1.68		0.19	S	C	Sheintuch <i>et al.</i> (1995)
50		2.71			A	C	Shi and Tao (2013)
51		1.62	0.20		S	E	Sliekers <i>et al.</i> (2005)
52		8.90	0.074		S	E	Sliekers <i>et al.</i> (2005)
53		16.15			S	E	Suzuki <i>et al.</i> (1974)
54	0.92	29.65	0.17		S	E	Terada <i>et al.</i> (2013)
55	0.42	3.56	0.10		S	E	Terada <i>et al.</i> (2013)
56		14.32			S	E	Vadivelu <i>et al.</i> (2006a)
57	1.03				S	E	Vadivelu <i>et al.</i> (2006c)
58	0.65	29.82	0.94		S	E	Van Hulle <i>et al.</i> (2007)
59	2.51	3.30	0.40		S	L	Wett and Rauch (2003)
60	1.93	1.11	0.30	0.20	S	L	Wiesmann (1994)
61		28.23			S	E/L	Wiesmann (1994)
62	1.91	1.03	0.4	0.15	A	L	Wik and Breitholtz (1996)
63	2.02	27.84	0.24		S	C	Wyffels <i>et al.</i> (2004)
64	1.46	2.87			S	E	Yoshioka <i>et al.</i> (1982)

Table A.2.2 Values of the maximum growth rate (μ_{\max}^{NOB} , average: 1.23 ± 0.79), affinity for nitrite ($K_{\text{NO}_2}^{\text{NOB}}$, average: 3.64 ± 6.25), affinity for oxygen ($K_{\text{O}_2}^{\text{NOB}}$, average: 1.24 ± 1.13) and yield (Y_{AOB} , average: 0.08 ± 0.05) for nitrite-oxidizers (NOB) at 30 °C and pH 7.5 found in literature. Growth type: S = suspended growth and A = attached growth. Publication type: E = experimental determination, C = calibration of model based on experimental results and L = other literature values.

	μ_{\max}^{NOB} d^{-1}	$K_{\text{NO}_2}^{\text{NOB}}$ $\text{g TN O}_2\text{-N.m}^{-3}$	$K_{\text{O}_2}^{\text{NOB}}$ $\text{g O}_2\text{-m}^{-3}$	Y_{NOB} $\text{g COD} \cdot (\text{g N})^{-1}$	Growth type	Publication type	Publication
1	0.90			0.098	S	E	Blackburne <i>et al.</i> (2007a)
2		1	0.54	0.20	S	E	Blackburne <i>et al.</i> (2007b)
3		1.25	0.43		S	E	Blackburne <i>et al.</i> (2007b)
4	0.24	1.60			S	E/C	Carrera <i>et al.</i> (2004)
5	0.24	4.10			A	E/C	Carrera <i>et al.</i> (2004)
6		4.10			A	E	Carvallo <i>et al.</i> (2002)
7		3.53	1.40		S	E	Ciudad <i>et al.</i> (2006)
8	0.60	2.80		0.020	S	E	Copp and Murphy (1995)
9	0.50	0.39	0.51	0.11	A	C/L	Downing and Nerenberg (2008)
10	0.45	0.27	0.4		A	C	Downing and Nerenberg (2008)
11	3.54	4.85		0.05	A	E/C	Fang <i>et al.</i> (2009)
12		1.00		0.11	S	C	Gee <i>et al.</i> (1990)
13	1.44				S	E	Glover (1985)
14			1.75		S	E	Guisasola <i>et al.</i> (2005)
15	1.43				A	L	Hao <i>et al.</i> (2002a)
16	0.86	5.04	0.54	0.057	A	L	Hunik <i>et al.</i> (1994)
17		5.55			S	E	Hunik <i>et al.</i> (1993)
18	0.53	0.05	0.50	0.09	S	L	Jones <i>et al.</i> (2007)
19	0.72	12.60		0.08	S	C	Jubany <i>et al.</i> (2005)
20	1.37	1.91	1.75	0.08	S	E	Jubany <i>et al.</i> (2008)
21		38.69			S	E	Jubany (2007)
22	1.31				S	C	Kaelin <i>et al.</i> (2009)
23	1.02	3.00	1.00		S	L	Kampschreur <i>et al.</i> (2007)
24	0.94	2.80		0.076	S	E	Keen and Prosser (1987)
25	2.36	5.00	0.20	0.03	A	L	Koch <i>et al.</i> (2000a)
26		5.42	2.65		S	E	Laanbroek and Gerards (1993)
27	1.00		4.01		A	C	Lackner <i>et al.</i> (2010)
28			1.78		A	C	Lackner <i>et al.</i> (2010)
29	0.79			0.04	S	E	Lochtman (1995)
30		1.7			S	E	Lopez-Fiuzza <i>et al.</i> (2002)
31		0.17	0.13		S	E	Manser <i>et al.</i> (2005)
32		0.28	0.47		S	E	Manser <i>et al.</i> (2005)
33				0.03	S	L	Manser <i>et al.</i> (2006)
34		2	1		S	C	Moussa <i>et al.</i> (2005)
35	2.01				S	E/C	Munz <i>et al.</i> (2011a)
36	1.88		0.6		S	E	Nowak <i>et al.</i> (1995)
37	0.67	1.62			S	C	Pambrun <i>et al.</i> (2006)
38	2.18	0.16			S	E	Poduska and Andrews (1975)
39		9.59	0.357		S	E	Rongsayamanont <i>et al.</i> (2010)
40		5.66	0.967		S	E	Rongsayamanont <i>et al.</i> (2010)
41		8.82	3.53		A	E	Rongsayamanont <i>et al.</i> (2010)
42		6.45	3.38		A	E	Rongsayamanont <i>et al.</i> (2010)
43			3		S	E	Sanchez <i>et al.</i> (2001)
44		1.60			A	E	Sánchez <i>et al.</i> (2003)
45		0.14			A	E	Schramm <i>et al.</i> (1999)
46	0.26	0.52		0.15	S	C	Sheintuch <i>et al.</i> (1995)
47		5.11			A	C	Shi and Tao (2013)
48		0.21	0.042		S	E	Sliekers <i>et al.</i> (2005)
49	0.77	1.49			S	E	Vadivelu <i>et al.</i> (2006b)
50	2.40	0.30	1.00		S	L	Wett and Rauch (2003)
51	1.96	0.51	1.10	0.057	S	E/L	Wiesmann (1994)
52		0.63			S	E	Wiesmann (1994)
53	1.89	0.80	0.40	0.04	A	L	Wik and Breitholtz (1996)
54	1.47	0.21			S	E	Yoshioka <i>et al.</i> (1982)

3

Modelling the influence of microbial diversity on the overall reactor behaviour

3.1 Abstract

A model describing a given system should be as simple as possible – but not simpler. The appropriate level of complexity depends both on the type of system and on the intended use of the model. This chapter addresses the critical question of which purposes justify increased complexity of biofilm (reactor) models. The additional model feature compared to conventional models considered is the inclusion of microbial diversity, distinguishing between different species performing the same function. With a multispecies model considering interspecies diversity, by implementing the growth and endogenous respiration of 10 ammonia-oxidizing and 10 nitrite-oxidizing species, it was demonstrated that a given reactor performance in terms of bulk liquid concentrations does not necessarily reflect microbial steady state conditions. In a second case study, the functional redundancy of the nitrifying community, i.e., the possibility of a changed nitrifying community to function equally as the original one, upon an increased nitrogen loading rate, was verified. It was concluded that increased complexity in biofilm models, concerning microbial diversity, is likely more useful when the focus is on understanding microbial competition and coexistence, but under specific conditions, these additional model features can be critically informative for bulk reactor behaviour prediction and general understanding.

3.2 Publications on which the chapter is based

Vannecke, T.P.W., Wells, G., Hubaux, N., Morgenroth, E. & Volcke, E.I.P. (2015). Considering microbial and aggregate heterogeneity in biofilm reactor models: How far do we need to go? *Water Science and Technology*, 72(10), 1692-1699. DOI: 10.2166/wst.2015.389.

Vannecke, T.P.W. & Volcke, E.I.P. (2014). Modelling microbial community dynamics in a nitrifying biofilm: effect of the nitrogen loading rate. *Communications in Agricultural and Applied Biological Sciences* 79, 21–26. In: 19th National symposium on Applied Biological Sciences, Proceedings, Gembloux, Belgium, 7 February 2014.

3.3 Introduction

Mathematical biofilm (reactor) models are excellent tools for predicting overall process performance as well as for understanding underlying phenomena such as microbial interactions, segregation, or competition. Deciding which features to include in biofilm (reactor) models is a critical component of model structure selection. Eberl *et al.* (2006) emphasize the value of identifying model features that can be omitted without decreasing the utility of the model for its intended purpose, as summarized in their “golden rule” of modelling: “a model should be as simple as possible, and only as complex as needed.” In essence, decreasing model complexity via simplifying assumptions can greatly ease computational requirements and interpretation of model outputs. The level of complexity to include in a model depends in large part on its intended use, but determining this level is not always straightforward.

One example of the utility of increasing biofilm model complexity in certain circumstances is the use of multidimensional (2D, 3D) simulations instead of the simpler, and more common, 1-dimensional biofilm models. Even within numerical 1-dimensional biofilm models, a range of complexity exists. In this contribution, the focus is on numerical 1-dimensional biofilm models with stratification of biomass, multiple substrates, and multiple functional guilds. A common simplifying assumption in such biofilm models is to neglect microbial diversity and resulting internal microbial competition within function guilds. However, experimental observations have demonstrated diverse assemblages of microbial populations within individual functional guilds in, for example, nitrifying biofilm reactors, where several genetically different populations of ammonia-oxidizers (Schramm *et al.* 2000; Bernet *et al.* 2004; Lydmark *et al.* 2006; Volcke *et al.* 2008; Terada *et al.* 2010; Almstrand *et al.* 2013) or nitrite-oxidizers (Schramm *et al.* 1998; Schramm *et al.* 2000; Downing & Nerenberg 2008) coexisted in the biofilm.

Moreover, and of critical importance to this chapter, diversity within functional guilds has been proposed to influence process performance and stability

(Wittebolle *et al.* 2005; Siripong & Rittmann 2007; Wittebolle *et al.* 2008; Ramirez *et al.* 2009). Indeed, mathematical models including microbial community information have proven useful in investigating the link between the microbial community and the process performance, e.g., Chapter 2 (Vannecke & Volcke 2015) and Chapter 4 (Vannecke *et al.* 2014).

In this chapter, the focus is on the critical question of what modelling questions justify an increase in complexity in biofilm (reactor) models. The discussion is based on two examples with increased complexity that provide new insights on microbial competition and its effect on the overall reactor behaviour. The two examples deal with 1) the influence of microbial diversity on biofilm development and microbial population dynamics in a nitrifying biofilm, and 2) the modelling of functional redundancy in a nitrifying biofilm upon an increased nitrogen loading rate.

3.4 Materials and methods

3.4.1 Modelling microbial diversity

To model microbial competition in a flat nitrifying biofilm, a two-step nitrification biofilm model including the growth and endogenous respiration, a state in which microorganisms oxidize cellular storage compounds instead of organic matter from their environment (van Loosdrecht & Henze 1999), of 10 ammonia-oxidizing bacteria (AOB) and 10 nitrite-oxidizing species (NOB) was set up and implemented in Aquasim (Reichert 1994).

The grid point number was set to 20, allowing capture of the required level of detail and at the same time keeping a reasonable computation time. Temperature and pH were kept constant at 30 °C and pH = 7.5, respectively. The general stoichiometric matrix (Table 3.1) and reaction kinetics (Table 3.2) were based on the model described in Chapter 4 (Vannecke *et al.* 2014). The corresponding parameter values are given in Table 3.3.

Table 3.1 Stoichiometric matrix with AOBi the ammonia-oxidizing species and NOBi the nitrite-oxidizing species with $i = 1 - 10$. ER: endogenous respiration.

A_{ij}	i component \rightarrow j process \downarrow	S_{NH} [g N.m ⁻³]	S_{NO_2} [g N.m ⁻³]	S_{NO_3} [g N.m ⁻³]	S_{O_2} [g O ₂ .m ⁻³]	S_{N_2} [g N.m ⁻³]	X_{AOBi} [g COD.m ⁻³]	X_{NOBi} [g COD.m ⁻³]	X_i [g COD.m ⁻³]
<i>Growth</i>									
1.	growth AOBi	$-1/Y_{AOBi} - i_{NXB}$	$1/Y_{AOBi}$		$1-3.43/Y_{AOBi}$		1		
2.	growth NOBi	$-i_{NXB}$	$-1/Y_{NOBi}$	$1/Y_{NOBi}$	$1-1.14/Y_{NOBi}$			1	
<i>Endogenous respiration (ER)</i>									
3.	aerobic ER AOBi	$i_{NXB} - i_{NXI} \cdot f_{XI}$			$-(1-f_{XI})$		-1		f_{XI}
4.	anoxic (NO ₂) ER AOBi	$i_{NXB} - i_{NXI} \cdot f_{XI}$	$-(1-f_{XI})/1.71$			$(1-f_{XI})/1.71$	-1		f_{XI}
5.	anoxic (NO ₃) ER AOBi	$i_{NXB} - i_{NXI} \cdot f_{XI}$		$-(1-f_{XI})/2.86$		$(1-f_{XI})/2.86$	-1		f_{XI}
6.	aerobic ER NOBi	$i_{NXB} - i_{NXI} \cdot f_{XI}$			$-(1-f_{XI})$			-1	f_{XI}
7.	anoxic (NO ₂) ER NOBi	$i_{NXB} - i_{NXI} \cdot f_{XI}$	$-(1-f_{XI})/1.71$			$(1-f_{XI})/1.71$		-1	f_{XI}
8.	anoxic (NO ₃) ER NOBi	$i_{NXB} - i_{NXI} \cdot f_{XI}$		$-(1-f_{XI})/2.86$		$(1-f_{XI})/2.86$		-1	f_{XI}
composition matrix									
g COD/unit comp		0	-3.43	-4.57	-1	-1.71	1	1	1
g N/unit comp		1	1	1	0	1	i_{NXB}	i_{NXB}	i_{NXI}

Table 3.2 Reaction kinetics corresponding to the processes from Table 3.1 with AOBi the ammonia-oxidizing species and NOBi the nitrite-oxidizing species with $i = 1 - 10$. ER: endogenous respiration.

j process ↓	
1. Growth AOBi	$\rho_{G,AOBi} = \mu_{\max}^{AOBi} \cdot \frac{S_{O_2}}{K_{O_2}^{AOBi} + S_{O_2}} \cdot \frac{S_{NH}}{K_{NH}^{AOBi} + S_{NH}} \cdot X_{AOBi}$
2. Growth NOBi	$\rho_{G,NOBi} = \mu_{\max}^{NOBi} \cdot \frac{S_{O_2}}{K_{O_2}^{NOBi} + S_{O_2}} \cdot \frac{S_{NO_2}}{K_{NO_2}^{NOBi} + S_{NO_2}} \cdot X_{NOBi}$
3. Aerobic ER AOBi	$\rho_{ER,AOBi,O_2} = b^{AOBi} \cdot \frac{S_{O_2}}{K_{O_2}^{AOBi} + S_{O_2}} \cdot X_{AOBi}$
4. Anoxic (NO_2^-) ER AOBi	$\rho_{ER,AOBi,NO_2} = b^{AOBi} \cdot \eta \cdot \frac{K_{O_2}^{AOBi}}{K_{O_2}^{AOBi} + S_{O_2}} \cdot \frac{S_{NO_2}}{K_{NO_2} + S_{NO_2}} \cdot \frac{S_{NO_2}}{S_{NO_2} + S_{NO_3}} \cdot X_{AOBi}$
5. Anoxic (NO_3^-) ER AOBi	$\rho_{ER,AOBi,NO_3} = b^{AOBi} \cdot \eta \cdot \frac{K_{O_2}^{AOBi}}{K_{O_2}^{AOBi} + S_{O_2}} \cdot \frac{S_{NO_3}}{K_{NO_3} + S_{NO_3}} \cdot \frac{S_{NO_3}}{S_{NO_2} + S_{NO_3}} \cdot X_{AOBi}$
6. Aerobic ER NOBi	$\rho_{ER,NOBi,O_2} = b^{NOBi} \cdot \frac{S_{O_2}}{K_{O_2}^{NOBi} + S_{O_2}} \cdot X_{NOBi}$
7. Anoxic (NO_2^-) ER NOBi	$\rho_{ER,NOBi,NO_2} = b^{NOBi} \cdot \eta \cdot \frac{K_{O_2}^{NOBi}}{K_{O_2}^{NOBi} + S_{O_2}} \cdot \frac{S_{NO_2}}{K_{NO_2} + S_{NO_2}} \cdot \frac{S_{NO_2}}{S_{NO_2} + S_{NO_3}} \cdot X_{NOBi}$
8. Anoxic (NO_3^-) ER NOBi	$\rho_{ER,NOBi,NO_3} = b^{NOBi} \cdot \eta \cdot \frac{K_{O_2}^{NOBi}}{K_{O_2}^{NOBi} + S_{O_2}} \cdot \frac{S_{NO_3}}{K_{NO_3} + S_{NO_3}} \cdot \frac{S_{NO_3}}{S_{NO_2} + S_{NO_3}} \cdot X_{NOBi}$

Table 3.3 Stoichiometric, kinetic and mass transfer parameter values with AOBi the ammonia-oxidizing species, NOBi the nitrite-oxidizing species and $i = 1-10$. ER: Endogenous Respiration.

Parameter	Description	Value	Unit	Reference
<i>Stoichiometric parameters</i>				
i_{NXB}	Nitrogen fraction in biomass	0.086	$\text{g N} \cdot (\text{g COD})^{-1}$	ASM1 (Henze <i>et al.</i> 2000)
i_{NXI}	Nitrogen fraction in inerts	0.06	$\text{g N} \cdot (\text{g COD})^{-1}$	ASM1 (Henze <i>et al.</i> 2000)
f_{XI}	Inert fraction in biomass	0.20	$\text{g COD} \cdot (\text{g COD})^{-1}$	ASM3 (Henze <i>et al.</i> 2000)
Y_{AOBi}	Yield coefficient of AOBi		$\text{g COD} \cdot (\text{g N})^{-1}$	See Table 3.4
Y_{NOBi}	Yield coefficient of NOBi		$\text{g COD} \cdot (\text{g N})^{-1}$	See Table 3.4
<i>Kinetic parameters (pH 7.5 and $T=30$ °C)</i>				
b_{AOBi}	ER rate of AOBi	$0.05 \cdot \mu_{\max}^{AOBi}$	d^{-1}	Assumed
b_{NOBi}	ER rate of NOBi	$0.05 \cdot \mu_{\max}^{NOBi}$	d^{-1}	Assumed
K_{NH}^{AOBi}	Affinity of AOBi for ammonium	0.25	$\text{g N} \cdot \text{m}^{-3}$	Table 3.4
$K_{O_2}^{AOBi}$	Affinity of AOBi for oxygen	0.3	$\text{g O}_2 \cdot \text{m}^{-3}$	Table 3.4
$K_{NO_2}^{NOBi}$	Affinity of NOBi for nitrite	1.6	$\text{g N} \cdot \text{m}^{-3}$	Table 3.4
$K_{O_2}^{NOBi}$	Affinity of NOBi for oxygen	2.2	$\text{g O}_2 \cdot \text{m}^{-3}$	Table 3.4
K_{NO_3}	Affinity for nitrate of ER	1	$\text{g N} \cdot \text{m}^{-3}$	de Kreuk <i>et al.</i> (2007)
K_{NO_2}	Affinity for nitrite of ER	1	$\text{g N} \cdot \text{m}^{-3}$	Assumed equal to K_{NO_3}
η	Anoxic reduction factor	0.5	-	Koch <i>et al.</i> (2000b)
μ_{\max}^{AOBi}	Maximum growth rate AOBi		d^{-1}	See Table 3.4
μ_{\max}^{NOBi}	Maximum growth rate NOBi		d^{-1}	See Table 3.4
<i>Mass transfer parameters</i>				
D_{NH_4}	Diffusion coefficient NH_4	$1.6 \cdot 10^{-4}$	$\text{m}^2 \cdot \text{d}^{-1}$	Picioreanu <i>et al.</i> (1997)
D_{NO_2}	Diffusion coefficient NO_2	$1.5 \cdot 10^{-4}$	$\text{m}^2 \cdot \text{d}^{-1}$	Picioreanu <i>et al.</i> (1997)
D_{NO_3}	Diffusion coefficient NO_3	$1.5 \cdot 10^{-4}$	$\text{m}^2 \cdot \text{d}^{-1}$	Picioreanu <i>et al.</i> (1997)
D_{O_2}	Diffusion coefficient O_2	$1.7 \cdot 10^{-4}$	$\text{m}^2 \cdot \text{d}^{-1}$	Picioreanu <i>et al.</i> (1997)

Possible ranges of values for maximum growth rate (μ_{\max}), yield (Y), affinity for the electron donor ($K_{\text{NH}}^{\text{AOB}}$ and $K_{\text{NO}_2}^{\text{NOB}}$) and the affinity for the electron acceptor (K_{O_2}) were determined based on the extensive literature review described in Chapter 2 (Vannecke & Volcke 2015). For each microbial parameter, a normal bimodal distribution was constructed in Matlab based on experimental findings of Ramirez *et al.* (2009), see Appendix 3A for the Matlab code. The eight bimodal distributions were each typified by two means ($\mu_1 = 0.6 \cdot k$; $\mu_2 = 1.4 \cdot k$) and standard deviations of $\sigma_{1,2} = 0.125 \cdot k$, with k the average value of the range of values found in literature for the corresponding parameter. It should be noted that using this strategy, the constructed bimodal distributions depend on the order of magnitude of the respective average parameter value (k), in other words, parameters with a smaller average value such as yield will differ less between different constructed species than the parameter values such as the maximum growth rate and the affinity constants with a larger average value. However, as shown in Chapter 2, the maximum growth rate and affinity constants are the most important parameters that should differ enough in order to determine the competition outcome. Furthermore, a stoichiometric relationship exists between the amount of electron donor removed and biomass yield, therefore, yield should not differ too much between different species of 1 functional type.

Ten species per type were then constructed by picking 10 random numbers from each bimodal distribution using the Matlab function *randsample*, which gives similarly to the *rand* function uniformly distributed random numbers with an accuracy of $1 \cdot 10^{-4}$ from a defined distribution. Parameter values were rounded to two digits to the right of the decimal point and the ones taken up in the final model are given in Table 3.4. The endogenous respiration rate for each species was assumed to be 5% of its corresponding maximum growth rate. The biomass density, including active and inert particulate components and considering a biofilm porosity of 80% was set to $93333/0.2 \text{ g COD.m}^{-3} = 466665 \text{ g COD.m}^{-3}$ (Picioreanu *et al.* 1997; Volcke *et al.* 2010). The initial concentration of each AOB and NOB species was equal for all species of the same type (AOB: $7000 \text{ g COD.m}^{-3}$ and NOB: $2333 \text{ g COD.m}^{-3}$). As

heterotrophic growth on biomass decay products can be neglected (Mozumder *et al.* 2014), and the influent did not contain an organic carbon source, heterotrophic growth was not considered in this model. To simplify the interpretation of the results, inhibition of AOB and NOB by NH_3 and HNO_2 as well as external mass transfer limitation, was neglected.

Table 3.4. Microbial parameters characterizing the AOB and NOB species in the multispecies nitrification biofilm model.

	μ_{\max}^{AOB} [d ⁻¹]	$K_{\text{NH}}^{\text{AOB}}$ [g N.m ⁻³]	$K_{\text{O}_2}^{\text{AOB}}$ [g O ₂ .m ⁻³]	Y^{AOB} [$\frac{\text{g COD}}{\text{g N}}$]
AOB1	1.10	2.84	0.95	0.23
AOB2	2.41	6.51	0.37	0.11
AOB3	1.91	12.97	0.35	0.07
AOB4	0.79	4.82	0.47	0.08
AOB5	2.08	10.54	0.33	0.24
AOB6	2.22	5.96	0.36	0.10
AOB7	0.71	4.62	0.82	0.25
AOB8	1.77	4.71	0.83	0.21
AOB9	0.59	12.10	0.91	0.08
AOB10	0.68	12.27	0.27	0.13
	μ_{\max}^{NOB} [d ⁻¹]	$K_{\text{NO}_2}^{\text{NOB}}$ [g N.m ⁻³]	$K_{\text{O}_2}^{\text{NOB}}$ [g O ₂ .m ⁻³]	Y^{NOB} [$\frac{\text{g COD}}{\text{g N}}$]
NOB1	1.77	4.31	0.99	0.10
NOB2	0.74	1.91	1.69	0.11
NOB3	0.74	4.45	0.84	0.10
NOB4	0.87	3.84	0.66	0.09
NOB5	0.66	1.98	1.75	0.04
NOB6	1.67	2.73	1.58	0.09
NOB7	0.71	5.07	0.67	0.04
NOB8	0.50	5.16	0.99	0.08
NOB9	1.54	4.45	2.05	0.06
NOB10	0.63	4.26	0.73	0.10

3.4.2 Case study 1: Biofilm development

In Case study 1, the development of a biofilm was followed in time until the bulk liquid concentrations of ammonium, nitrite and nitrate, besides the microbial populations were at steady state. Therefore, simulations were run during a sufficient period of time (5000 days) to ensure overall steady state reactor conditions. These simulations took generally less than 30 minutes of simulation time. The influent contained only ammonium (250 g N.m^{-3}), resulting in a nitrogen loading rate of $900 \text{ g N.m}^{-3}.\text{d}^{-1}$. The total biomass in the reactor was assumed to be 100 g COD.m^{-3} . The initial biofilm thickness was $1 \cdot 10^{-6} \text{ m}$. At the steady state biofilm thickness of $1 \cdot 10^{-3} \text{ m}$, it was assumed that the biofilm growth rate and the detachment rate kept each other in balance. The initial concentration of ammonium in the bulk liquid was set equal to the influent ammonium concentration (250 g N.m^{-3}) while the initial concentrations of nitrite and nitrate were negligible (1 g N.m^{-3}). The bulk liquid oxygen concentration was kept constant at $3 \text{ g O}_2.\text{m}^{-3}$ during the simulations.

3.4.3 Case study 2: Functional redundancy

In Case study 2, the effect of a changed nitrogen loading rate on both the bulk liquid composition and the nitrifying community in a flat nitrifying biofilm were investigated. A total period of 3 years was simulated and the nitrogen loading rate was increased after 1 year from $1325 \text{ g N.m}^{-3}.\text{d}^{-1}$ ($Q_{\text{in}} = 0.0053 \text{ m}^3.\text{d}^{-1}$) to $1800 \text{ g N.m}^{-3}.\text{d}^{-1}$ ($Q_{\text{in}} = 0.0072 \text{ m}^3.\text{d}^{-1}$). This operation shift was assumed to be accompanied by a drop of the bulk liquid oxygen concentration from 2 to $0.5 \text{ g O}_2.\text{m}^{-3}$. The total biomass in the reactor was assumed to be 10 g COD.m^{-3} . The initial and steady state biofilm thickness were assumed to be $100 \cdot 10^{-6} \text{ m}$. The initial concentration of ammonium in the bulk liquid was set equal to the influent ammonium concentration (250 g N.m^{-3}) while the initial concentrations of nitrite and nitrate were negligible (1 g N.m^{-3}).

3.5 Results and discussion

3.5.1 Case study 1: Biofilm development

Using the two-step nitrification biofilm model implementing the growth and endogenous respiration of 10 AOB and 10 NOB species, it was observed that the reactor behaviour, in terms of nitrifying performance, was already at steady state within 10 days after start-up (Figure 3.1A). At first, nitrite accumulated to a maximum concentration of $185 \text{ g NO}_2\text{-N.m}^{-3}$ on day 1, but was completely converted after four days. At steady state, ammonium was almost completely converted to nitrate, resulting in a nitrate effluent concentration of $241 \text{ g NO}_3\text{-N.m}^{-3}$.

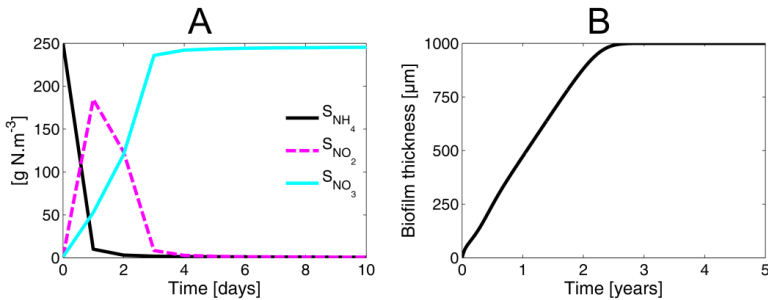


Figure 3.1 Bulk liquid concentration of nitrogen components (A) and the biofilm thickness (B) in function of time. Note the different scale and units (days versus years) of the x-axis in both figures.

In contrast to the overall reactor performance (effluent composition), the steady state biofilm thickness of 1 mm was only reached after about 2.5 years (Figure 3.1B), indicating that constant reactor performance does not necessarily imply that the steady state biofilm thickness is already reached. The biofilm thickness increased linearly due to the formation of active biomass by microbial growth and the formation of inert particulate components by endogenous respiration. Inert particulate components made up more than 90% of the total particulate mass in the biofilm at steady state.

The steady state conditions of the microbial community were only reached after 140 months (Table 3.5). A major microbial community shift was even observed after 100 months of operation. Initially, all AOB species made up

7.5% and all NOB species 2.5% of the total particulate matter mass (100 g COD) in the biofilm. Due to microbial competition, the initial fraction of each species changed in time to its steady state value.

In the AOB community, species AOB1 became dominant. In the NOB community, NOB6 remained dominant for 90 months (7.5 years). However, after 60 months, species NOB2, which was virtually absent in the biofilm for 40 months, reappeared in the biofilm. This species became dominant after 100 months and remained the dominant NOB species at steady state. At steady state, 3 dominant species coexisted in the biofilm: AOB1, NOB6 and NOB2. All the non-dominant species could be considered absent and not contributing to the microbial conversions. However, it is assumed that when the operation conditions change, these species could re-emerge when the new conditions are favourable for them, as their concentrations were negligible, but non-zero.

The AOB:NOB decreased from 3.3 at month 30, when the biofilm thickness reached steady state, to 1.38 at month 140. Both for marine (Foesel *et al.* 2008) and freshwater systems (Schramm *et al.* 1999; Gieseke *et al.* 2001; Altmann *et al.* 2003), dominance of the NOB over AOB has been observed. Foesel *et al.* (2008) concluded that the numerical dominance of various *Nitrospira* spp. over AOB might be a general characteristic of ammonium-limited systems, although the abundance of *Nitrospira* spp. was observed by Gieseke *et al.* (2001) to be 30 times higher than the abundance of the AOB in the upper $1 \cdot 10^{-4}$ m of an oxygen limited biofilm. Therefore, possibly other mechanisms play a role in the dominance of NOB over AOB. An elevated NOB:AOB ratio in aerobic granular sludge was observed by Winkler *et al.* (2012) and attributed by Winkler *et al.* (2015) to the nitrite-loop pathway, i.e., the availability of additional nitrite for the NOB from partial denitrification (nitrite-loop). However, in the model of this chapter, no denitrification was included. Therefore, it is assumed that the elevated NOB:AOB ratio at steady state was due to (1) the lower endogenous respiration of nitrite-oxidizers on oxygen due to the lower oxygen availability in deeper layers of the biofilm, where the NOB live, (2) the lower endogenous respiration rate of NOB compared to AOB because it is defined as a fraction (5%) of the maximum growth rate, which is

lower for the NOB at 30 °C and (2) the higher detachment of AOB species dominant at the surface, as the surface detachment is equal to the growth rate of the biofilm at the surface. In the aerobic regions, oxygen is the main electron acceptor for endogenous respiration, as endogenous respiration on nitrite and nitrate is inhibited by oxygen (Table 3.2). As the nitrite-oxidizers live in a zone with a lower oxygen concentration than the ammonia-oxidizers, their endogenous respiration rate is assumed to be lower, due to the considered Monod term for oxygen ($\frac{S_{O_2}}{S_{O_2}+K_{O_2}}$), resulting in an elevated NOB:AOB ratio. Although endogenous respiration using oxygen as electron acceptor can be considered here as the main reason for the elevated NOB:AOB ratio, also the higher detachment of the AOB and the higher turn-over of the AOB, are important, as in Chapter 2, where decay is considered instead of endogenous respiration, an elevated NOB:AOB ratio was also observed for some of the simulations.

The steady state substrate and biomass concentration gradients are displayed in Figure 3.2. One could note that the number of species coexisting at steady state might be influenced by the number of grid points, an effect which may be more pronounced as more species are taken up in the model. This was not investigated in detail; the number of grid points applied in this study was found sufficient to capture the required level of detail concerning microbial coexistence at steady state.

Table 3.5 Evolution of the percentage of the total particulate matter (100 g COD) made up by each species in the biofilm through time. Percentages of individual AOB and NOB species are visualized by color codes from 0% (white) to 25% (black). At steady state (> 140 months), three species coexisted: AOB1, NOB2 and NOB6.

Time (months) → Fraction (%) ↓	0	10	20	30	40	50	60	70	80	90	100	110	120	130	140
AOB1	7.5	24.63	13.98	7.83	5.55	5.52	5.51	5.51	5.50	5.48	5.40	5.31	5.26	5.25	5.25
AOB2	7.5	0.002	0	0	0	0	0	0	0	0	0	0	0	0	0
AOB3	7.5	0	0	0	0	0	0	0	0	0	0	0	0	0	0
AOB4	7.5	0.002	0	0	0	0	0	0	0	0	0	0	0	0	0
AOB5	7.5	0	0	0	0	0	0	0	0	0	0	0	0	0	0
AOB6	7.5	0.029	0	0	0	0	0	0	0	0	0	0	0	0	0
AOB7	7.5	0.002	0	0	0	0	0	0	0	0	0	0	0	0	0
AOB8	7.5	0.069	0	0	0	0	0	0	0	0	0	0	0	0	0
AOB9	7.5	0	0	0	0	0	0	0	0	0	0	0	0	0	0
AOB10	7.5	0	0	0	0	0	0	0	0	0	0	0	0	0	0
Total AOB	75	24.73	13.98	7.82	5.55	5.52	5.51	5.51	5.50	5.48	5.40	5.31	5.26	5.25	5.25
NOB1	2.5	0.003	0	0	0	0	0	0	0	0	0	0	0	0	0
NOB2	2.5	0.10	0.002	0	0	0	0.007	0.042	0.17	0.63	1.60	2.69	3.25	3.44	3.49
NOB3	2.5	0.001	0	0	0	0	0	0	0	0	0	0	0	0	0
NOB4	2.5	0.005	0	0	0	0	0	0	0	0	0	0	0	0	0
NOB5	2.5	0.037	0	0	0	0	0	0.001	0.001	0	0	0	0	0	0
NOB6	2.5	7.06	3.90	2.35	1.85	1.84	1.83	1.82	1.77	1.59	1.19	0.70	0.43	0.34	0.31
NOB7	2.5	0.001	0	0	0	0	0	0	0	0	0	0	0	0	0
NOB8	2.5	0.001	0	0	0	0	0	0	0	0	0	0	0	0	0
NOB9	2.5	0	0	0	0	0	0	0	0	0	0	0	0	0	0
NOB10	2.5	0.002	0	0	0	0	0	0	0	0	0	0	0	0	0
Total NOB	25	7.22	3.90	2.35	1.85	1.84	1.84	1.86	1.94	2.22	2.79	3.38	3.68	3.77	3.80
Total XI	0	68.05	82.12	89.82	92.61	92.64	92.64	92.63	92.55	92.30	91.80	91.31	91.06	90.98	90.96
Ratio AOB:NOB	3.00	3.43	3.58	3.33	3.00	3.00	2.99	2.96	2.84	2.47	1.94	1.57	1.43	1.39	1.38

In this study, ammonium and nitrite were limiting, as the concentrations of these substrates prevailing in the biofilm, $0.28 \text{ g NH}_4^+\text{-N.m}^{-3}$ and $0.26 \text{ g NO}_2^-\text{-N.m}^{-3}$ respectively, were much lower than the affinity constants considered (Figure 3.2A-B). Indeed, species with a rather high affinity for ammonium (AOB1: $K_{\text{NH}}^{\text{AOB1}} = 2.84 \text{ g NH}_4^+\text{-N.m}^{-3}$) and nitrite (NOB2: $K_{\text{NO}_2}^{\text{NOB2}} = 1.91 \text{ g NO}_2^-\text{-N.m}^{-3}$ and NOB6: $K_{\text{NO}_2}^{\text{NOB6}} = 2.73 \text{ g NO}_2^-\text{-N.m}^{-3}$) were selected for. Oxygen was not as limiting, since its concentration (Figure 3.2C) prevailing in the biofilm was much closer to the considered oxygen affinity constants.

From the biomass concentration profile (Figure 3.2D), it is observed that at steady state, NOB6 was present in a small concentration at the surface of the biofilm while NOB2 had the highest concentration $83 \cdot 10^{-6} \text{ m}$ below the surface of the biofilm. The coexistence of two genetically and morphologically different populations of NOB with different distribution patterns in a biofilm was observed experimentally by Schramm *et al.* (1998). When coexistence of species performing the same function is observed, a distinction is typically made between slow growing species with a high substrate affinity (K-strategists) and fast growing species with a low substrate affinity (r-strategists). The r- and K-selection strategy (Andrews & Harris 1986) could explain experimentally observed population shifts and microbial coexistence in nitrifying biofilms, e.g., by Schramm *et al.* (2000) and Almstrand *et al.* (2013). In the NOB community considered in this study, NOB6 was an r-strategist with a relatively high growth rate ($\mu_{\text{max}}^{\text{NOB6}} = 1.67 \text{ d}^{-1}$) and NOB2 was a K-strategist with a relatively high affinity for nitrite, corresponding with a low affinity constant ($K_{\text{NO}_2}^{\text{NOB2}} = 1.91 \text{ g NO}_2^-\text{-N.m}^{-3}$). The r-strategist NOB6 was able to survive close to the surface due to the higher substrate concentrations prevailing there, in combination with its high maximum growth rate. As a K-strategist, NOB2 was able to cope with the limiting substrate concentrations deeper in the biofilm.

Considering the development of the NOB community in time, it was observed that the r-strategist NOB6 was able to cope rapidly with the prevailing conditions and grew at a high rate due to its relatively high maximum growth rate. After 100 months, the slow growing K-strategist NOB2 became dominant

over NOB6 due to its higher affinity for nitrite. It can thus be concluded that the r- and K-selection strategy not only can be used here to explain the steady state microbial distribution profile but also the development of the microbial community composition over time.

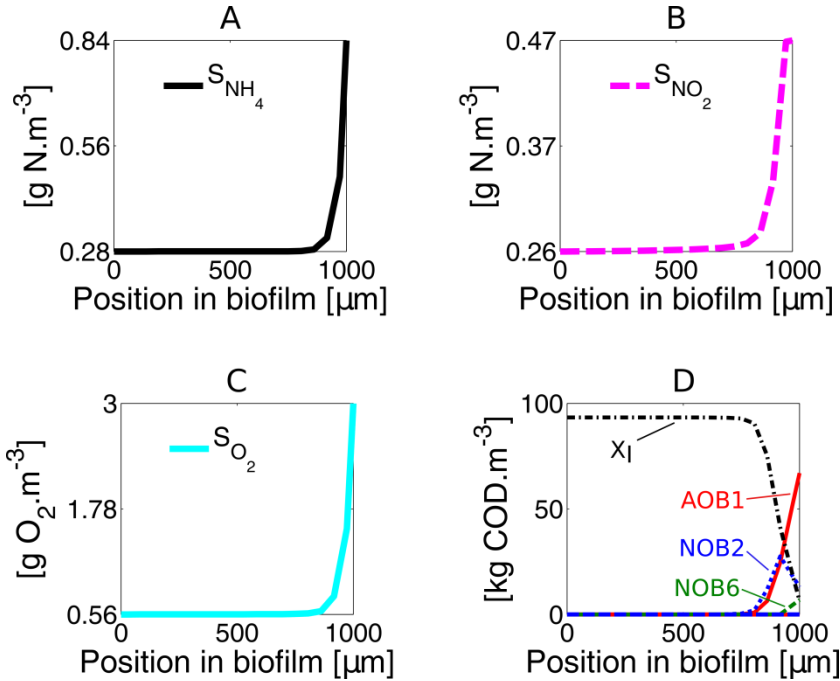


Figure 3.2. Steady state concentration profiles for ammonium (A), nitrite (B), oxygen (C) and particulate matter (D; X_I = inert particulate components) in function of the position of the biofilm (0 μm = bottom, 1000 μm = surface of the biofilm). Note the different scale of the y-axis of the substrate concentration profiles.

3.5.2 Case study 2: Functional redundancy

Simulations were performed to determine the effect of a changing nitrogen loading on the process performance, considering both the ammonium elimination efficiency and the possible nitrite accumulation as well as changes in the microbial community. The effect of the operation shift after 365 days on the effluent composition is given in Figure 3.3. In phase I, an effluent nitrate concentration of 242 $g\ N.m^{-3}$ and an ammonium elimination efficiency of 99.8% were observed. After the operation shift, the ammonium elimination efficiency suddenly dropped for a period of 1 month, reaching a minimum of

82.6% after 6 days. However, significant nitrite accumulation (up to 140 g N.m^{-3}) was observed 8 months after the operation shift. The latter was attributed to the lower average affinity for oxygen of the NOB compared to the AOB. After this period, by providing functional redundancy, the presence of different species of 1 functional type allowed the process performance to return almost completely to its original state, with an effluent nitrate concentration of 238 g N.m^{-3} and a total ammonium elimination efficiency of 99%.

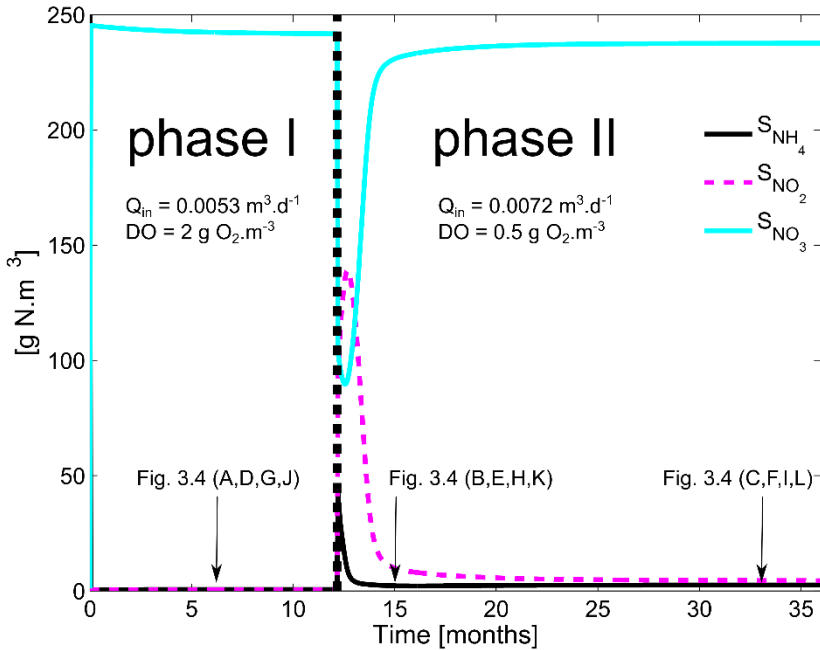


Figure 3.3 Bulk liquid concentration of nitrogen components in function of time. The dashed line at 12 months denotes the operation shift. Arrows indicate sample times for biomass and concentration profiles (Figure 3.4).

The operation shift also had a clear effect on the composition of the microbial community. The evolution in time of the particulate species is given in Table 3.6. During phase I, AOB1, NOB2 and NOB5 were the dominant species, each making up more than 4% of the total particulate mass in the biofilm. Just after the operation shift, 4 species were dominant: AOB1, AOB6, NOB2 and NOB4. Finally, two species survived: AOB6 and NOB4. In phase I, AOB (about 35%) were relatively more dominant than NOB (about 20%). In phase II the fraction of NOB was similar as in phase I while the AOB fraction decreased to about

7%. The fraction of inert particles (X_I) increased from about 40% in phase I to 70% in phase II. The AOB:NOB ratio also decreased during this simulation, similar to the observation made for Case study 1. Here the fractions of AOB and NOB are relatively higher, as the fraction of inert biomass (X_I) is smaller.

Table 3.6 Evolution of the fraction (%) of the total particulate matter (10 g COD) made up by each species in the biofilm through time. Fractions of individual AOB and NOB species are visualized by colour codes from 0% (white) to 37% (black).

Time [months] →	0	3	6	9	12	15	18	21	24	27	30	33	36
Fraction (%) ↓	<i>Phase I</i>					<i>Phase II</i>							
	NH ₄ limitation					O ₂ limitation							
AOB1	7.5	18.4	29.2	34.4	36.7	13.9	2.9	0.9	0.3	0.1	0.1	0.0	0.0
AOB2	7.5	0.6	0.0	0.0	0.0	0.3	0.2	0.1	0.1	0.0	0.0	0.0	0.0
AOB3	7.5	0.1	0.0	0.0	0.0	0.0	0.0	0.0	0.0	0.0	0.0	0.0	0.0
AOB4	7.5	4.5	2.9	1.6	0.8	0.5	0.2	0.1	0.1	0.1	0.1	0.1	0.0
AOB5	7.5	0.1	0.0	0.0	0.0	0.0	0.0	0.0	0.0	0.0	0.0	0.0	0.0
AOB6	7.5	1.4	0.2	0.0	0.0	8.4	8.5	7.5	7.2	7.1	7.0	7.0	7.0
AOB7	7.5	3.8	1.9	0.8	0.3	0.1	0.0	0.0	0.0	0.0	0.0	0.0	0.0
AOB8	7.5	2.4	0.6	0.1	0.0	0.0	0.0	0.0	0.0	0.0	0.0	0.0	0.0
AOB9	7.5	1.6	0.3	0.1	0.0	0.0	0.0	0.0	0.0	0.0	0.0	0.0	0.0
AOB10	7.5	1.2	0.2	0.0	0.0	0.0	0.0	0.0	0.0	0.0	0.0	0.0	0.0
Total AOB	75.0	34.1	35.4	37.0	37.8	23.3	11.8	8.6	7.7	7.3	7.2	7.1	7.0
NOB1	2.5	1.0	0.2	0.1	0.0	1.5	1.0	0.3	0.1	0.0	0.0	0.0	0.0
NOB2	2.5	5.6	7.7	10.3	12.9	4.2	1.3	0.5	0.3	0.1	0.1	0.0	0.0
NOB3	2.5	1.5	0.7	0.4	0.2	0.1	0.1	0.1	0.0	0.0	0.0	0.0	0.0
NOB4	2.5	2.6	2.2	1.9	1.5	12.1	18.5	20.5	21.6	22.3	22.8	23.2	23.5
NOB5	2.5	4.3	4.8	5.3	5.5	1.8	0.6	0.3	0.1	0.1	0.0	0.0	0.0
NOB6	2.5	4.1	2.7	1.8	1.2	1.2	0.2	0.0	0.0	0.0	0.0	0.0	0.0
NOB7	2.5	1.3	0.6	0.3	0.1	0.2	0.1	0.1	0.1	0.1	0.1	0.1	0.0
NOB8	2.5	1.3	0.6	0.2	0.1	0.1	0.0	0.0	0.0	0.0	0.0	0.0	0.0
NOB9	2.5	0.3	0.0	0.0	0.0	0.0	0.0	0.0	0.0	0.0	0.0	0.0	0.0
NOB10	2.5	1.8	1.1	0.7	0.4	0.4	0.3	0.2	0.2	0.2	0.1	0.1	0.1
Total NOB	25.0	24.0	20.7	20.9	21.8	21.5	22.2	22.0	22.4	22.8	23.1	23.4	23.6
Total XI	0.0	42.0	43.9	42.1	40.4	55.2	66.0	69.3	69.9	69.9	69.7	69.5	69.3
Ratio AOB:NOB	3.00	1.42	1.71	1.77	1.73	1.08	0.53	0.39	0.34	0.32	0.31	0.30	0.30

A clear advantage of using 1-dimensional biofilm models is the possibility to investigate the biomass distribution profiles in the biofilm. Biofilm profiles were plotted after 6 months (phase I), 15 months (i.e., 3 months after the operation shift) and 33 months (phase II) of operation (Figure 3.4A-C) and compared with the ammonium (Figure 3.4D-F), nitrite (Figure 3.4G-I) and oxygen (Figure 3.4J-L) substrate concentration profiles in the biofilm.

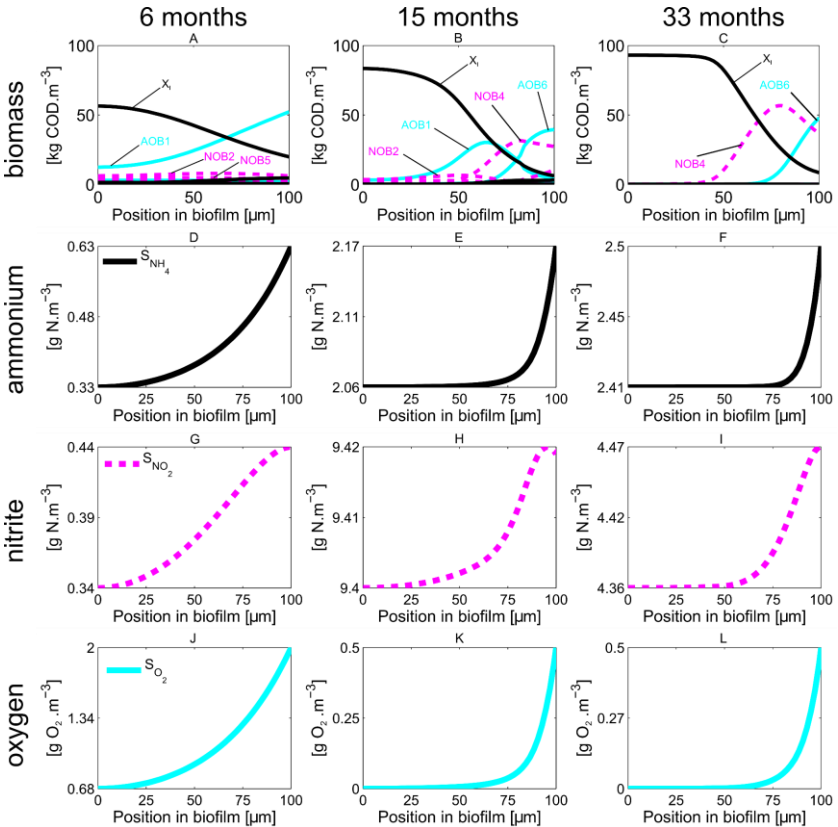


Figure 3.4 Biomass concentration profiles (A, B, C) and concentration profiles of ammonium (D, E, F), nitrite (G, H, I) and oxygen (J, K, L) in function of the position in the biofilm (0 μm = bottom, 100 μm = surface of biofilm). Profiles at 6 months (A, D, G, J), 15 months (B, E, H, K) and 33 months (C, F, I, L) after start-up of the simulation are given. Only species with a fraction higher than 4% and the inert particulate components (X_i) are indicated on the biomass concentration profiles. Mind the different scale of the y-axis of the substrate concentration profiles.

During phase I, the concentration of ammonium (Figure 3.4D) and nitrite (Figure 3.4G), was much lower than the lowest affinity constants for these substrates considered in this study, indicating that these substrates were

relatively more limiting than oxygen. The dominant species of this phase, AOB1, NOB2 and NOB5 (Figure 3.4A) were characterized by a high affinity for their nitrogen source ($K_{\text{NH}}^{\text{AOB1}} = 2.84 \text{ g N} \cdot \text{m}^{-3}$, $K_{\text{NO}_2}^{\text{NOB2}} = 1.91 \text{ g N} \cdot \text{m}^{-3}$ and $K_{\text{NO}_2}^{\text{NOB5}} = 1.98 \text{ g N} \cdot \text{m}^{-3}$). The prevalence of NOB2 over NOB5 at the end of phase I was due to its higher growth rate and slightly higher affinities for electron donor and acceptor. In phase I, the concentration of AOB1 was the highest at the outside of the biofilm, while NOB2 and NOB5 showed a relatively constant concentration through the whole biofilm, as they were dependent on the nitrite, produced by the AOB, for their growth. In all phases, the oxygen concentration showed a clear gradient (Figure 3.4J-L) through the biofilm, but oxygen limitation determined the competition outcome particularly in phase II, as at almost all depths, the oxygen concentration was considerably lower than the lowest affinity constants for oxygen considered in this study.

Ammonium (Figure 3.4F) was more limiting than oxygen only for the dominant AOB species in phase II (AOB6) within $14 \cdot 10^{-6} \text{ m}$ from the surface of the biofilm, where the oxygen concentration was still higher than $0.13 \text{ g O}_2 \cdot \text{m}^{-3}$. The new species (AOB6 and NOB4) becoming dominant three months after the operation shift and growing at the expense of the remaining populations of AOB1 and NOB2 (Figure 3.4B) were typified by a relatively high affinity for oxygen ($K_{\text{O}_2}^{\text{AOB6}} = 0.36 \text{ g O}_2 \cdot \text{m}^{-3}$ and $K_{\text{O}_2}^{\text{NOB4}} = 0.66 \text{ g O}_2 \cdot \text{m}^{-3}$). At that time, also other NOB species such as NOB1 ($K_{\text{O}_2}^{\text{NOB1}} = 0.99 \text{ g O}_2 \cdot \text{m}^{-3}$) were present in the biofilm, albeit in smaller fractions (< 4%). Both NOB1 and NOB4 were typified by a rather high affinity for oxygen, but NOB1 had a higher growth rate and a lower affinity for nitrite ($K_{\text{NO}_2}^{\text{NOB1}} = 4.31 \text{ g N} \cdot \text{m}^{-3}$ and $K_{\text{NO}_2}^{\text{NOB4}} = 3.84 \text{ g N} \cdot \text{m}^{-3}$) than NOB4. Therefore, NOB1 was able to respond rapidly on the changing conditions after the operation shift. However, it was outcompeted by NOB4 once the bulk liquid concentration of nitrite dropped down 8 months after the operation shift. About 2 years after the operation shift, only two species remained in the biofilm: AOB6 and NOB4, both having a high affinity for oxygen. In phase II, a typical nitrifying biofilm could be observed (Figure 3.4C) with inert particulate components (X_i), NOB4 and

AOB6 having the highest concentration at the bottom, in the middle and at the surface of the biofilm, respectively.

3.6 Conclusions

Two case studies were highlighted in which additional model complexity was included beyond the conventional formulation for numerical 1-dimensional biofilm models. In case study 1, it was demonstrated, using a biofilm model including the growth of several species performing the same function, that a constant reactor behaviour, in terms of bulk liquid concentrations of ammonium, nitrite and nitrate, may be hiding major microbial community shifts. In case study 2, it was shown that the coexistence of several species performing the same function assured an almost complete conversion of ammonium to nitrate and a total ammonium elimination efficiency of 99% upon an increased nitrogen loading within a period of 8 months following the operation shift, by providing functional redundancy. Nitrifying biofilm models including microbial diversity can furthermore be used to investigate experimentally observed, major microbial population shifts resulting in a different nitrifying performance, see Chapter 4 (Vannecke *et al.* 2014).

The additional model complexity considered in this study had a substantial impact on bulk liquid outputs in some specific conditions, and on the spatial distribution of dissolved and particulate components under all conditions. It is likely a general rule that increased complexity concerning microbial diversity will be more useful when the focus is on understanding microbial competition and coexistence. When the focus is on substrate removal rates, and optimal bulk conditions, this complexity is clearly not always necessary. However, under some conditions, for example upon environmental or operational changes such as an increased nitrogen loading rate, such additional model features can be critically informative for bulk reactor behaviour prediction or understanding.

3.7 Appendix 3A: Matlab code for the construction of a bimodal distribution

```

clear all
close all
clc

%%%%%% Characteristics of the bimodal distribution %%%%%%%
q = [0.5 0.5];
m = [k*0.6 5*1.4];      %% With k the average or median of the interval of
                        %% parameter values considered
s = [k*0.125 k*0.125];
distrib = struct('mu', m, 'sigma', s, 'weight', q);
nb = 1e006;

%% Construction of two scaled and translated gaussians
X = randn(nb,length(q)).*repmat(s,nb,1)+repmat(m,nb,1);

%% Selection of one gaussian or the other
rsel = rand(nb,1);
idx1 = (repmat(rsel,1,length(q))>repmat(cumsum(q),nb,1));
idx2 = (repmat(rsel,1,length(q))<repmat(cumsum(q),nb,1));
idx1(:,2:end) = idx1(:,1:end-1).*idx2(:,2:end);
idx1(:,1) = idx2(:,1);
X = sum(X.*idx1,2);

%% Plot result
Numbers=ksdensity(X);
[y,x]=ksdensity(X);
figure(1);
plot(x,y,'linewidth',2)
Title('Bimodal distribution of microbial parameter')

%% Pick 10 random numbers
Random_values_parameter = randsample(X,10);

```

4

Modelling ammonia-oxidizing population shifts

4.1 Abstract

The dynamic reactor behaviour of a nitrifying inverse turbulent bed reactor, operated at varying loading rate, was described with a 1-dimensional two-step nitrification biofilm model. In contrast with conventional biofilm models, this model includes the competition between two genetically different populations of ammonia-oxidizers (AOB), besides nitrite-oxidizers (NOB). Previously gathered experimental evidence showed that different loading rates in the reactor resulted in a change in the composition of the AOB community, besides a different nitrifying performance. The dissolved oxygen concentration in the bulk liquid was put forward as the key variable governing the experimentally observed shift from *Nitrosomonas europaea* (AOB1) to *Nitrosomonas* sp. (AOB2), which was confirmed by the developed 1-dimensional biofilm model. Both steady state and dynamic analysis showed that the influence of microbial growth and endogenous respiration parameters as well as external mass transfer limitation have a clear effect on the competition dynamics.

4.2 Published as

Vannecke, T.P.W., Bernet, N., Steyer, J.-P. & Volcke, E.I.P. (2014). Modelling ammonium oxidizing population shifts in a biofilm reactor. *Water Science and Technology*, 69(1), 208-215. DOI: 10.2166/wst.2013.701.

4.3 Introduction

Biological nitrogen removal from wastewater can be considered as a proven technology and has been widely implemented. The most common pathway is the combination of two sequential processes: autotrophic nitrification and heterotrophic denitrification. During nitrification, ammonia-oxidizing bacteria (AOB) convert ammonia to nitrite, which is further oxidized to nitrate by nitrite-oxidizing bacteria (NOB).

While in the conventional treatment systems bacteria are grown in flocs which are more prone to washout events, biofilm reactors display distinct advantages for the cultivation of slow growing nitrifiers, due to their specific biomass retention characteristics (Nicoletta *et al.* 2000). Within biofilms, diffusional substrate concentration gradients result in a growth rate gradient. In multi-species biofilm systems, this will lead to a biofilm with a layered structure, giving species with different ecophysiological characteristics the opportunity to survive. Besides different functional types as AOB or NOB, also different species of the same functional type can coexist. Schramm *et al.* (1998) identified in bacterial aggregates from a fluidized bed two genetically and morphologically different populations of NOB affiliated with the nitrite oxidizer *Nitrospira moscoviensis*. Another example of the coexistence of two NOB species is given by Downing and Nerenberg (2008). In a nitrifying, membrane-aerated biofilm reactor (MABR), they observed a shift in NOB species with decreasing oxygen concentrations. Also different types of AOB have been reported to coexist in this reactor type (Terada *et al.* 2010). Lydmark *et al.* (2006) found in a full-scale nitrifying trickling filter four AOB populations, of which two *Nitrosomonas oligotropha* populations dominated at all depths. These two populations showed different distribution patterns within the biofilm, indicating different ecophysiological niches, even though they belong to the same AOB lineage. In a recent study the niche differentiation between two dominant *Nitrosomonas oligotropha* populations in pilotscale moving bed biofilm reactors and trickling filters was confirmed experimentally based on their different reaction on changes in ammonium loading (Almstrand *et al.* 2013). Bernet *et al.* (2004) reported that, for a nitrifying Inverse

Turbulent Bed Reactor (ITBR), the amount of carrier material affects the reactor behaviour, not only in terms of the bulk liquid composition, but also in terms of the biofilm composition (different AOB types). Different solid hold-ups of the reactors resulted in different liquid volumes, leading to different hydraulic retention times (HRT) and consequently different ammonium loading rates. Upon lowering the ammonium loading rate in the most heavily loaded reactor by lowering its feeding rate, nitrate started to accumulate due to the presence of *Nitrospira*. Furthermore, nitrate accumulation was accompanied by the appearance of a different ammonia-oxidizer population, *Nitrosomonas sp.* (AOB2), growing at the expense of *N. europaea* (AOB1) (Volcke *et al.* 2008). It was postulated that this population shift was due to a selection pressure driven by the different dissolved oxygen concentration in both reactors after the change in ammonium loading rate.

Models provide an adequate tool for understanding phenomena involved in biofilm processes, e.g., Wik and Breitholtz (1996) and Picioreanu *et al.* (1997). However, present mathematical models mostly neglect microbial diversity. Conceptual and predictive mathematical models describing microbial community information should be developed to obtain a deeper understanding of ecosystems and possible ways to manipulate them (Nielsen *et al.* 2010). From an engineering perspective, it is of interest to include microbial community structure information in mathematical models. Extending an activated sludge model using two AOB populations (Wett *et al.* 2011) and the Anaerobic Digestion Model No. 1 to describe microbial diversity within functional groups (Ramirez *et al.* 2009) allowed a more accurate prediction of nitrification and aerobic digestion, respectively, upon changing process conditions. A recent study showed the influence of biomass detachment and microbial growth in the bulk liquid on the microbial community distribution in a heterotrophic biofilm using a multi-species biofilm model (Brockmann *et al.* 2013). The biofilm was discretized into 50 layers to ensure adequate resolution of predicted substrate and biomass gradients over the depth of the biofilm even at biofilm thicknesses as high as $1 \cdot 10^{-3}$ m.

In present nitrifying biofilm models, there is mostly only a distinction between ammonia-oxidizers and nitrite-oxidizers. Nevertheless, a biofilm model including 1 type of AOB and 2 types of NOB was set up by Downing and Nerenberg (2008), to determine the importance of both nitrite and oxygen affinity in the selection of *Nitrospira* spp. over *Nitrobacter* spp. in a MABR. Volcke *et al.* (2008) successfully described the observed microbial population shifts upon the lowering of the loading rate in an ITBR reactor through a 0-dimensional (neglecting spatial variations) nitrification model considering the growth of 2 types of AOB and 1 type of NOB. Even though this simplified model was useful in predicting the simulation outcome, it clearly neglects substrate gradients and biomass distribution profiles within the biofilm. To overcome this limitation, in this contribution a 1-dimensional biofilm model was developed as an alternative to describe the experimental data of Volcke *et al.* (2008). As the biofilm structures under study were not characterized by a highly irregular surface, higher dimensional descriptions (2D or 3D, see e.g., Picioreanu *et al.* (2004)), making the biofilm modelling much more complex, were judged unnecessary. The advantages of this 1-dimensional model compared to the 0-dimensional model for accurately describing the experimental data of Volcke *et al.* (2008), in terms of the nitrifying performance of the ITBR as well as the underlying microbial dynamics, were evaluated. Particular attention was paid to the influence of microbial growth and endogenous respiration parameters as well as external mass transfer limitation on the competition outcome, through both steady state and dynamic analysis.

4.4 Material and methods

4.4.1 Experimental data

In the ITBR ($V_{\text{reactor}} = 1.35 \cdot 10^{-3} \text{ m}^3$), biomass was grown on low density inert particles ($d_p = 147 \cdot 10^{-6} \text{ m}$) which are fluidized by an upward current of gas (Bernet *et al.* 2004). The solid hold-up ratio, i.e., the ratio of static to expanded bed height, of the ITBR considered in this study was 0.3. The porosity of the bed was 0.41, which resulted in an active reactor volume fixed at $1.11 \cdot 10^{-3} \text{ m}^3$.

The total amount of particulate material (viable biomass and inerts) was 10 g COD, corresponding to a biofilm thickness of $9.6 \cdot 10^{-6}$ m, if a uniform distribution of all the biomass is considered over the bed. The synthetic influent was supplied at a constant flow rate of $0.0072 \text{ m}^3 \cdot \text{d}^{-1}$ and contained 250 g $\text{NH}_4^+ \cdot \text{N} \cdot \text{m}^{-3}$ as ammonium sulphate. After 4 months, the ammonium loading rate of the reactor was lowered from $1622 \text{ g NH}_4^+ \cdot \text{N} \cdot \text{m}^{-3} \cdot \text{d}^{-1}$ to $1164 \text{ g NH}_4^+ \cdot \text{N} \cdot \text{m}^{-3} \cdot \text{d}^{-1}$, by decreasing the influent flow rate to $0.0053 \text{ m}^3 \cdot \text{d}^{-1}$ and thus increasing the HRT (from 3.66 h to 5 h). Oxygen measurements were occasionally performed (no on-line measurements) but it has been verified that the initial oxygen level in the reactor was limiting ($<1 \text{ g O}_2 \cdot \text{m}^{-3}$) for nitrite oxidation and that this was no longer the case after lowering the influent flow rate. After lowering the influent flow rate, the dissolved oxygen concentration of the bulk liquid was observed to be sufficiently high to allow complete nitrite oxidation by *Nitrospira* (NOB). The operation shift was further characterised by the growth of *Nitrosomonas* sp. (AOB2) at the expense of *Nitrosomonas europaea* (AOB1). Temperature was maintained at 30 °C by a water jacket and pH was controlled at 7.5 by base addition. The airflow rate was kept constant at $0.72 \text{ m}^3 \cdot \text{d}^{-1}$. A detailed description of the reactor set-up and operation, besides the analytical and microbiological methods applied, is given by Bernet *et al.* (2004) and Volcke *et al.* (2008).

4.4.2 Reactor model

A 1-dimensional two-step nitrification biofilm model, including the competition between two different species of AOB, besides NOB, was implemented in the Aquasim software (Reichert 1994). As during the experiments nitrite or nitrate accumulated, and the ammonium was oxidized for at least 95% (Volcke *et al.* 2008), free ammonia inhibition will have been low. The highest nitrite concentration observed, $225 \text{ g NO}_2 \cdot \text{N} \cdot \text{m}^{-3}$, corresponds in combination with a pH of 7.5 and a temperature of 30 °C to a FNA concentration of $0.014 \text{ g HNO}_2 \cdot \text{N} \cdot \text{m}^{-3}$. This makes also FNA inhibition very unlikely for both AOB and NOB (see Chapter 5 for a literature study on inhibition constants). Furthermore, if a difference in inhibition would have been the reason for the population shift, *Nitrosomonas europaea* (AOB1)

would have been the species acclimated to a higher free ammonia and/or free nitrous acid concentration and would have probably remained dominant when the inhibiting conditions were relaxed by lowering the nitrogen loading rate. Therefore, as Volcke *et al.* (2008) was able to simulate the observed population shift by means of a 0-dimensional biofilm model implementing the growth of 2 AOB, an r-strategist and a K-strategist concerning oxygen, it was assumed that the increase of the bulk liquid oxygen concentration after the lowering of the nitrogen loading rate was the reason for the population shift. In this chapter, *Nitrosomonas europaea* (AOB1) is represented as a K-strategist, with a relatively low growth rate but a high affinity for oxygen and *Nitrosomonas* sp. (AOB2) as an r-strategist, with a relatively high growth rate and low affinity for oxygen, according to the r- and K-selection theory (Andrews & Harris 1986). The parameter values from the calibrated 0-dimensional biofilm model of Volcke *et al.* (2008) were applied. Growth of AOB and NOB was described based on Hao *et al.* (2002b). Inhibition of AOB and NOB by NH_3 and HNO_2 was not considered to simplify interpretation of the results. As the influent did not contain organic carbon, heterotrophic growth was neglected as well. This was shown to be a valid assumption for co-diffusion systems (Lackner *et al.* 2008). Mozumder *et al.* (2014) also reported that heterotrophic growth on biomass decay products could be neglected. To describe biomass decay, endogenous respiration, a state in which microorganisms oxidize cellular storage compounds instead of organic matter from their environment (van Loosdrecht & Henze 1999), was implemented in the model, considering oxygen, nitrite and nitrate as possible electron acceptors. The overall model stoichiometry, kinetics and the corresponding parameter values for the 1-dimensional biofilm model are summarized in Table 4.1, Table 4.2 and Table 4.3, respectively. Note that the parameter values were based on those from the calibrated and validated model of Volcke *et al.* (2008). A detailed sensitivity analysis was beyond the scope of this study.

Table 4.1 Stoichiometric matrix. AOBi denotes AOB1 or AOB2.

A_{ij}	i component \rightarrow j process \downarrow	S_{NH} [g N.m ⁻³]	S_{NO_2} [g N.m ⁻³]	S_{NO_3} [g N.m ⁻³]	S_{O_2} [g O ₂ .m ⁻³]	S_{N_2} [g N.m ⁻³]	X_{AOBi} [g COD.m ⁻³]	X_{NOB} [g COD.m ⁻³]	X_i [g COD.m ⁻³]
<i>Growth</i>									
1.	growth AOBi	$-1/Y_{AOBi} - i_{NXB}$	$1/Y_{AOBi}$		$1-3.43/Y_{AOBi}$		1		
2.	growth NOB	$-i_{NXB}$	$-1/Y_{NOB}$	$1/Y_{NOB}$	$1-1.14/Y_{NOB}$			1	
<i>Endogenous respiration</i>									
3.	aerobic end. resp. AOBi	$i_{NXB} - i_{NXi} \cdot f_{Xi}$			$-(1-f_{Xi})$		-1		f_{Xi}
4.	anoxic (NO ₂) end. resp. AOBi	$i_{NXB} - i_{NXi} \cdot f_{Xi}$	$-(1-f_{Xi})/1.71$			$(1-f_{Xi})/1.71$	-1		f_{Xi}
5.	anoxic (NO ₃) end. resp. AOBi	$i_{NXB} - i_{NXi} \cdot f_{Xi}$		$-(1-f_{Xi})/2.86$		$(1-f_{Xi})/2.86$	-1		f_{Xi}
6.	aerobic end. resp. NOB	$i_{NXB} - i_{NXi} \cdot f_{Xi}$			$-(1-f_{Xi})$			-1	f_{Xi}
7.	anoxic (NO ₂) end. resp. NOB	$i_{NXB} - i_{NXi} \cdot f_{Xi}$	$-(1-f_{Xi})/1.71$			$(1-f_{Xi})/1.71$		-1	f_{Xi}
8.	anoxic (NO ₃) end. resp. NOB	$i_{NXB} - i_{NXi} \cdot f_{Xi}$		$-(1-f_{Xi})/2.86$		$(1-f_{Xi})/2.86$		-1	f_{Xi}
composition matrix									
	g COD/unit comp	0	-3.43	-4.57	-1	-1.71	1	1	1
	g N/unit comp	1	1	1	0	1	i_{NXB}	i_{NOB}	i_{NXi}

Table 4.2 Reaction kinetics corresponding to the processes from Table 4.1. AOBi: AOB1 or AOB2. ER: endogenous respiration.

j process ↓	
1. Growth AOBi	$\rho_{G,AOBi} = \mu_{max}^{AOBi} \cdot \frac{S_{O_2}}{K_{O_2}^{AOBi} + S_{O_2}} \cdot \frac{S_{NH}}{K_{NH}^{AOBi} + S_{NH}} \cdot X_{AOBi}$
2. Growth NOB	$\rho_{G,NOB} = \mu_{max}^{NOB} \cdot \frac{S_{O_2}}{K_{O_2}^{NOB} + S_{O_2}} \cdot \frac{S_{NO_2}}{K_{NO_2}^{NOB} + S_{NO_2}} \cdot X_{NOB}$
3. Aerobic ER AOBi	$\rho_{ER,AOBi,O_2} = b^{AOBi} \cdot \frac{S_{O_2}}{K_{O_2}^{AOBi} + S_{O_2}} \cdot X_{AOBi}$
4. Anoxic (NO ₂) ER AOBi	$\rho_{ER,AOBi,NO_2} = b^{AOBi} \cdot \eta \cdot \frac{K_{O_2}^{AOBi}}{K_{O_2}^{AOBi} + S_{O_2}} \cdot \frac{S_{NO_2}}{K_{NO_2} + S_{NO_2}} \cdot \frac{S_{NO_2}}{S_{NO_2} + S_{NO_3}} \cdot X_{AOBi}$
5. Anoxic (NO ₃ ⁻) ER AOBi	$\rho_{ER,AOBi,NO_3} = b^{AOBi} \cdot \eta \cdot \frac{K_{O_2}^{AOBi}}{K_{O_2}^{AOBi} + S_{O_2}} \cdot \frac{S_{NO_3}}{K_{NO_3} + S_{NO_3}} \cdot \frac{S_{NO_3}}{S_{NO_2} + S_{NO_3}} \cdot X_{AOBi}$
6. Aerobic ER NOB	$\rho_{ER,NOB,O_2} = b^{NOB} \cdot \frac{S_{O_2}}{K_{O_2}^{NOB} + S_{O_2}} \cdot X_{NOB}$
7. Anoxic (NO ₂) ER NOB	$\rho_{ER,NOB,NO_2} = b^{NOB} \cdot \eta \cdot \frac{K_{O_2}^{NOB}}{K_{O_2}^{NOB} + S_{O_2}} \cdot \frac{S_{NO_2}}{K_{NO_2} + S_{NO_2}} \cdot \frac{S_{NO_2}}{S_{NO_2} + S_{NO_3}} \cdot X_{NOB}$
8. Anoxic (NO ₃ ⁻) ER NOB	$\rho_{ER,NOB,NO_3} = b^{NOB} \cdot \eta \cdot \frac{K_{O_2}^{NOB}}{K_{O_2}^{NOB} + S_{O_2}} \cdot \frac{S_{NO_3}}{K_{NO_3} + S_{NO_3}} \cdot \frac{S_{NO_3}}{S_{NO_2} + S_{NO_3}} \cdot X_{NOB}$

Table 4.3 Stoichiometric, kinetic and mass transfer parameter values. ER: endogenous respiration.

Parameter	Description	Value	Unit	Reference
<i>Stoichiometric parameters</i>				
i_{NXB}	Nitrogen fraction in biomass	0.086	g N.(g COD) ⁻¹	ASM1 (Henze <i>et al.</i> 2000)
i_{NXI}	Nitrogen fraction in inerts	0.06	g N.(g COD) ⁻¹	ASM1 (Henze <i>et al.</i> 2000)
f_{XI}	Inert fraction in biomass	0.20	g COD.(g COD) ⁻¹	ASM3 (Henze <i>et al.</i> 2000)
Y_{AOB1}	Yield coefficient of AOB1	0.20	g COD.(g N) ⁻¹	Wiesmann (1994) ⁽¹⁾
Y_{AOB2}	Yield coefficient of AOB2	= Y_{AOB1}	g COD.(g N) ⁻¹	Volcke <i>et al.</i> (2008)
Y_{NOB}	Yield coefficient of NOB	0.057	g COD.(g N) ⁻¹	Wiesmann (1994) ⁽¹⁾
<i>Kinetic parameters (pH 7.5 and T=30 °C)</i>				
b_{AOB1}	ER rate of AOB1	0.068 or 0.1	d ⁻¹	Set to 0.05 $\mu_{max}^{AOB1} / 0.1 \text{ d}^{-1}$
b_{AOB2}	ER rate of AOB2	0.121 or 0.1	d ⁻¹	Set to 0.05 $\mu_{max}^{AOB2} / 0.1 \text{ d}^{-1}$
b_{NOB}	ER rate of NOB	0.040	d ⁻¹	Set to 0.05 μ_{max}^{NOB}
K_{NH}^{AOB1}	Affinity of AOB1 for ammonium	0.25	g N.m ⁻³	Sánchez <i>et al.</i> (2003)
K_{NH}^{AOB2}	Affinity of AOB2 for ammonium	= K_{NH}^{AOB1}	g N.m ⁻³	Volcke <i>et al.</i> (2008)
$K_{O_2}^{AOB1}$	Affinity of AOB1 for oxygen	0.3	g O ₂ .m ⁻³	Wiesmann (1994)
$K_{O_2}^{AOB2}$	Affinity of AOB2 for oxygen	1	g O ₂ .m ⁻³	Volcke <i>et al.</i> (2008)
$K_{NO_2}^{NOB}$	Affinity of NOB for nitrite	1.6	g N.m ⁻³	Sánchez <i>et al.</i> (2003)
$K_{O_2}^{NOB}$	Affinity of NOB for oxygen	2.2	g O ₂ .m ⁻³	Hao <i>et al.</i> (2002b)
K_{NO_3}	Affinity for nitrate of ER	1	g N.m ⁻³	de Kreuk <i>et al.</i> (2007)
K_{NO_2}	Affinity for nitrite of ER	1	g N.m ⁻³	Assumed equal to K_{NO_3}
η	Anoxic reduction factor	0.5	-	Koch <i>et al.</i> (2000b)
μ_{max}^{AOB1}	Maximum growth rate AOB1	1.36	d ⁻¹	Hellinga <i>et al.</i> (1999) ⁽²⁾
μ_{max}^{AOB2}	Maximum growth rate AOB2	2.42	d ⁻¹	Volcke <i>et al.</i> (2008)
μ_{max}^{NOB}	Maximum growth rate NOB	0.79	d ⁻¹	Hellinga <i>et al.</i> (1999) ⁽²⁾
<i>Mass transfer parameters</i>				
D_{NH_4}	Diffusion coefficient NH ₄	1.6e-4	m ² .d ⁻¹	Picioreanu <i>et al.</i> (1997)
D_{NO_2}	Diffusion coefficient NO ₂	1.5e-4	m ² .d ⁻¹	Picioreanu <i>et al.</i> (1997)
D_{NO_3}	Diffusion coefficient NO ₃	1.5e-4	m ² .d ⁻¹	Picioreanu <i>et al.</i> (1997)
D_{O_2}	Diffusion coefficient O ₂	1.7e-4	m ² .d ⁻¹	Picioreanu <i>et al.</i> (1997)
K_L	External mass transfer coefficient of NH ₄ ⁺ , NO ₂ , NO ₃ and O ₂	0.91	m.d ⁻¹	Bernet <i>et al.</i> (2005)

⁽¹⁾ Yield coefficients expressed in grams organic dry matter (ODM) per gram nitrogen were converted to grams chemical oxygen demand (COD) per gram nitrogen using a typical biomass composition of CH_{1.8}O_{0.5}N_{0.2}, corresponding to 1.3659 g COD.g⁻¹ ODM.

⁽²⁾ The maximum growth rate was converted to be valid for a temperature of 30 °C based on values given in Hellinga *et al.* (1999) at 35 °C through Eq. 4.1 and Eq. 4.2:

$$\mu_{max}^{AOB}(T) = \mu_{max}^{AOB}(T_{ref}) \cdot \exp\left(\frac{E_a^{AOB} \cdot (T - T_{ref})}{R \cdot T \cdot T_{ref}}\right) \quad \text{Eq. 4.1}$$

$$\mu_{max}^{NOB}(T) = \mu_{max}^{NOB}(T_{ref}) \cdot \exp\left(\frac{E_a^{NOB} \cdot (T - T_{ref})}{R \cdot T \cdot T_{ref}}\right) \quad \text{Eq. 4.2}$$

with $E_a^{AOB} = 68 \text{ kJ} \cdot (\text{mol})^{-1}$; $E_a^{NOB} = 44 \text{ kJ} \cdot (\text{mol})^{-1}$ (Hao *et al.* 2002a); $R = 8.31 \text{ J} \cdot (\text{mol} \cdot \text{K})^{-1}$.

The 1-dimensional model developed in this study assumes that the variation of the state variables is restricted to a single direction perpendicular to the surface of the solid carrier. This is a valid simplification when vertical gradients are orders of magnitude higher than those in the directions parallel to the carrier surface (Wanner & Gujer 1986). Since this applies to most biofilm systems, dynamic multispecies 1-dimensional biofilm models are sufficient for the majority of practical purposes. As the modelling of biofilm structures with highly irregular surface was not the focus of this study, higher dimensional descriptions (2D or 3D), making the biofilm modelling much more complex, were judged unnecessary. The biofilm, which is autotrophic, was assumed to be quite dense with very small pores, in which no relevant motion of suspended solids takes place. The biofilm was moreover assumed to be rigid, meaning that particulate components are displaced only by the expansion or shrinkage of the biofilm solid matrix. In addition, the biofilm porosity has been assumed constant ($\theta = 0.8$) and the biomass density (viable biomass and inerts) in the biofilm was set to $93333/0.2 \text{ g COD.m}^{-3} = 466665 \text{ g COD.m}^{-3}$ (Picioreanu *et al.* 1997; Volcke *et al.* 2010). An initial active biomass fractioning of 75% AOB and 25% NOB was assumed, according to the number of electrons exchanged by the oxidation of NH_4^+ to NO_2^- and from NO_2^- to NO_3^- , respectively.

As the reactor type was considered confined, biofilm growth on the spherical particles was associated with a decrease in bulk liquid volume, to $1 \cdot 10^{-3} \text{ m}^3$ following Eq. 4.5, with n_{sp} the number of particles, r_{sp} the radius of 1 particle and $L_F(t)$ the biofilm thickness at time t .

$$V_{bulk}(t) = V_{reactor} - n_{sp} \cdot \frac{4}{3} \cdot \pi \cdot (r_{sp} + L_F(t))^3 \quad \text{Eq. 4.3}$$

The biofilm growth has been limited by detachment. The equilibrium biofilm thickness ($L_{F_{SS}}$) was set at $9.6 \cdot 10^{-6} \text{ m}$, corresponding with the experimentally determined total particulate matter mass of 10 g COD . It was assumed that all the biomass was distributed evenly over all the particles present in the reactor. The reactor temperature ($30 \text{ }^\circ\text{C}$) and pH (7.5) were assumed constant. The oxygen level in the bulk liquid was controlled to a fixed value. Constant bulk

liquid oxygen concentrations within a range of 0-7 g O₂.m⁻³ were considered for steady state simulation. For the dynamic simulations, the bulk liquid oxygen concentration was assumed to be 0.5 g O₂.m⁻³ before the reduction in ammonium loading rate and 2 g O₂.m⁻³ after. During the experiments, the measured oxygen concentration was checked to be in accordance with these values, although the exact values were not recorded on-line. The bulk liquid was assumed to be homogenous (Sánchez *et al.* 2005a). At first, external mass transfer limitation has been neglected to allow straightforward evaluation of the simulation results. Next, a boundary layer, resulting from external mass transfer limitation, was considered in this 1-dimensional model, using an external mass transfer coefficient of 0.91 m.d⁻¹ (Bernet *et al.* 2005).

The initial concentration of ammonium in the bulk liquid has been assumed to be equal to the influent concentration (250 g NH₄⁺-N.m⁻³). Negligible amounts of nitrite and nitrate (1 g N.m⁻³ each) were assumed to be present in the bulk liquid initially, to avoid numerical errors arising from zero concentrations in the kinetic expressions for endogenous respiration on nitrite and nitrate.

4.4.3 Simulation set-up

The simulation set-up is summarised in Table 4.4. Firstly, steady state simulations were performed to assess the influence of microbial growth and endogenous respiration parameters on microbial competition dynamics. All steady state simulations have been performed over several years of operation to ensure that steady state conditions were achieved. These simulations took generally less than 1 hour of simulation time. In a first series of steady state simulations (Model 1), endogenous respiration was neglected to allow direct comparison with the 0-dimensional model. Secondly, the endogenous respiration rate of AOB1, AOB2 and NOB was defined as 5% of the maximum growth rate of the species (Model 2). The resulting values for the respiration rates ($b^{AOB1} = 0.068 \text{ d}^{-1}$, $b^{AOB2} = 0.121 \text{ d}^{-1}$; $b^{NOB} = 0.040 \text{ d}^{-1}$) are in the same range as those considered by Hao *et al.* (2002b).

To be able to describe the experimental data from Volcke *et al.* (2008), some modifications of the model were necessary (Model 3). The endogenous

respiration rate of both AOBs was set equal to 0.1 d^{-1} , while keeping the endogenous respiration rate of NOB at $b^{\text{NOB}} = 0.040 \text{ d}^{-1}$. External mass transfer was also included. Firstly, some steady state simulations were performed with Model 3. The influent flow rate amounted to $Q_{\text{in}} = 0.0072 \text{ m}^3 \cdot \text{d}^{-1}$. Next, dynamic simulations were run for 123 days, preceded by a start-up period of 23 days, at a loading rate of $Q_{\text{in}} = 0.0072 \text{ m}^3 \cdot \text{d}^{-1}$, and followed by a decrease in loading rate (63 days, $Q_{\text{in}} = 0.0053 \text{ m}^3 \cdot \text{d}^{-1}$), according to the experimental conditions.

Using the available experimental data of Volcke *et al.* (2008), Model 3 was validated. The model accuracy of Model 3 was verified by calculating the Nash Sutcliffe criterion (model efficiency E, see Nash and Sutcliffe (1970)) as given in Eq. 4.4, with y_i^m the i^{th} observed value, y_i the corresponding calculated value and \bar{y}_m the mean value of the observations.

$$E = 1 - \frac{\sum_{i=1}^n (y_i^m - y_i)^2}{\sum_{i=1}^n (y_i^m - \bar{y}_m)^2} \quad \text{Eq. 4.4}$$

If the model efficiency is lower than zero, the observed mean is a better predictor than the model, therefore, the model efficiency should be preferably larger than 0 with a maximum of 1 (perfect fit between simulation and observations).

Table 4.4 Overview of the simulation set-up in terms of parameter values (b: decay rate; K_L : external mass transfer coefficient) and type of simulations (SS: steady state; D: dynamic) performed.

	b (d⁻¹)	K_L (m.d⁻¹)	SS	D	Comments
Model 1	$b_{AOB1} = 0$ $b_{AOB2} = 0$ $b_{NOB} = 0$	-	✓	-	Based on 0-dimensional model (Volcke <i>et al.</i> 2008)
Model 2	$b_{AOB1} = 0.068$ $b_{AOB2} = 0.121$ $b_{NOB} = 0.040$	-	✓	-	Endogenous respiration rate is 5% of maximum growth rate
Model 3	$b_{AOB1} = 0.1$ $b_{AOB2} = 0.1$ $b_{NOB} = 0.040$	0.91	✓	✓	Model used for reproduction of experimental data

4.4.4 Definition of criteria to determine the competition outcome

For 0-dimensional models, straightforward criteria for the outcome of microbial competition can be defined and applied to AOB based on Eq. 4.5 (Volcke *et al.* 2008):

$$S^{*AOBi} = K_{NH}^{AOBi} \cdot \frac{1}{\mu_{max}^{AOBi} \cdot S_{O2} / (K_{O2}^{AOBi} + S_{O2}) \cdot SRT^{-1}} \text{ for } i = 1, 2 \quad \text{Eq. 4.5}$$

The species with the smallest non-zero value of S^{*AOBi} will win the competition, while the other species will be washed out of the reactor. In this study, it was examined whether this criterion can also be applied to determine the competition outcome of 1-dimensional models. For the calculation of S^{*AOBi} with Eq. 4.5, the solid retention time (SRT) needs to be known. The definition of SRT in biofilms is ambiguous. Either an overall SRT for all species in the biofilm can be used, or a species-specific SRT. The overall SRT was calculated as the ratio between the biofilm thickness, L_F (m) and the detachment rate, u_d (m.d⁻¹) based on Eq. 4.6.

$$SRT_{overall} = \frac{L_F}{u_d} \quad \text{Eq. 4.6}$$

The SRT of an individual species depends on its position in the biofilm and was calculated using Eq. 4.7.

$$\text{SRT}_{\text{AOBi}} = \frac{m_{\text{AOBi}}^{\text{tot}}}{Q_{\text{in}} \cdot X_{\text{AOBi}}^{\text{eff}}} = \frac{m_{\text{AOBi}}^{\text{particle}} \cdot n_p}{Q_{\text{in}} \cdot X_{\text{AOBi}}^{\text{eff}}} \text{ for } i = 1, 2 \quad \text{Eq. 4.7}$$

In Eq. 4.7, $m_{\text{AOBi}}^{\text{tot}}$ represents total biomass of AOBi (g COD) in the reactor, $m_{\text{AOBi}}^{\text{particle}}$ total biomass of AOBi (g COD) on 1 particle, n_p total number of spherical particles, Q_{in} flow rate ($\text{m}^3 \cdot \text{d}^{-1}$) and $X_{\text{AOBi}}^{\text{eff}}$ biomass concentration (g COD. m^{-3}) present in the effluent due to detachment.

The criteria to determine the competition outcome, as obtained by steady state simulations, were applied to the 1-dimensional biofilm model in which both endogenous respiration and external mass transfer were neglected (Model 1). Firstly, the $S^{*\text{AOBi}}$ was determined using the overall SRT (Eq. 4.6). Next, the $S^{*\text{AOBi}}$ was also determined using the mean SRT of each AOB separately (Eq. 4.7).

4.5 Results and discussion

4.5.1 Steady state analysis – without endogenous respiration

(Model 1)

To compare the 1-dimensional model with the 0-dimensional model, both endogenous respiration and external mass transfer were neglected in Model 1. For bulk liquid oxygen concentrations higher than $0.1 \text{ g O}_2 \cdot \text{m}^{-3}$, 98% of the influent ammonium was converted (Figure 4.1A). Nitrite accumulated in the reactor for bulk liquid oxygen concentrations lower than $0.2 \text{ g O}_2 \cdot \text{m}^{-3}$. For higher oxygen concentrations, almost all ammonium was converted to nitrate, nitrite accumulation being very low (less than 1.5% of the influent ammonium).

With respect to the AOB population, a microbial population shift occurred around a bulk liquid oxygen concentration of $0.62 \text{ g O}_2 \cdot \text{m}^{-3}$ (Figure 4.1B). For bulk liquid oxygen concentrations lower than $0.616 \text{ g O}_2 \cdot \text{m}^{-3}$, K-strategist AOB1 won the competition, and for bulk liquid oxygen concentrations higher than $0.622 \text{ g O}_2 \cdot \text{m}^{-3}$, r-strategist AOB2 completely outcompeted AOB1. In the

very narrow oxygen concentration range between these values, AOB1 and AOB2 coexisted at steady state (detail plot in Figure 4.1B). It is important to stress that coexistence of AOB1 and AOB2 was not obtained with the 0-dimensional model of Volcke *et al.* (2008). In general, coexistence of species performing the same function cannot be obtained with 0-dimensional models. On the other hand, the oxygen concentration at which the population shift between AOB1 and AOB2 occurred was about the same ($0.6 \text{ g O}_2\cdot\text{m}^{-3}$) as for the 0-dimensional model. This could have been expected, since the considered biofilm was very thin ($9.6\cdot 10^{-6} \text{ m}$) and the same microbial parameters were used in both studies.

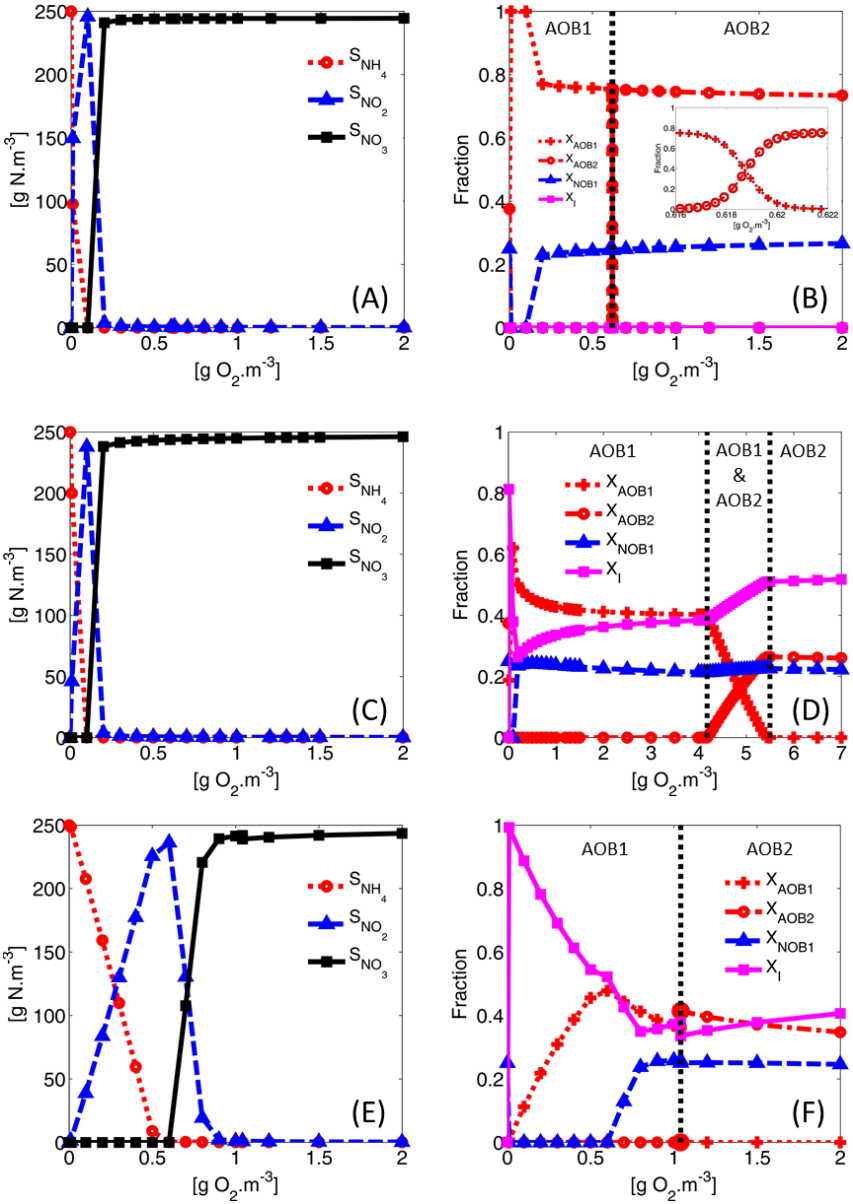


Figure 4.1 Influence of dissolved oxygen concentration in the bulk liquid on steady state bulk liquid concentrations of nitrogen components (left) and on steady state biomass and particulate fractions (X_I = inert particulate components) in the biofilm (right). Simulation results are plotted for the model without endogenous respiration (top, A-B), defining endogenous respiration rate as $0.05\ \mu_{max}$ (middle, C-D) and defining $b^{AOB1} = b^{AOB2} = 0.1\ d^{-1}$ with inclusion of a boundary layer (bottom, E-F). Note the different scale of the x-axis for Figure 4.1D.

It is important to note that the microbial population shift was not reflected in the reactor performance. It seems that, at high oxygen concentrations, AOB2 took over completely the function of AOB1, converting ammonium to nitrite at the same rate. This is in agreement with the observations of Siripong and Rittmann (2007) and Wittebolle *et al.* (2008), based on the diversity data of nitrifying bacterial communities. They concluded that by providing functional redundancy, coexistence of different species of 1 functional type can maintain the stability of the system for nitrification when operation conditions change.

Subsequently, the criterion given by Eq. 4.5 was applied to determine the competition outcome. The overall SRT (Eq. 4.6) amounted to 25 days for oxygen concentrations higher than $0.2 \text{ g O}_2 \cdot \text{m}^{-3}$. The calculated S^{*AOBi} (Eq. 4.5) of the AOBs predicted which species was dominant (smallest nonzero value of S^{*AOBi}) in a same way as the simulation results for Model 1 (Figure 4.1B). Furthermore, the bulk liquid oxygen concentration at which the ‘competition switch’ occurred was predicted correctly. However, coexistence of both AOB (Figure 4.1B) could not be predicted. In general, coexistence can never be predicted with a criterion as given by Eq. 4.5, considering 1-dimensional biofilm models, since one S^{*AOBi} will always be smaller than the other, implying one species is dominant and the other one is washed out the biofilm.

Next, the criterion for the outcome of interspecies competition (Eq. 4.5) was applied based on the mean SRT for each AOB separately (Eq. 4.7). In the oxygen concentration range in which a species was dominant, its SRT was about 21 days. However, the concentration of the outcompeted species in the biofilm was near zero and the effluent concentration of the outcompeted species was consequently very low ($<1 \cdot 10^{-30} \text{ g COD} \cdot \text{m}^{-3}$). Therefore, as in Eq. 4.7 the effluent concentration of the species is in the denominator, the SRT of the outcompeted species increased to very large numbers. This implied that the value of S^{*AOBi} was the smallest for the outcompeted species (Eq. 4.5), as the SRT is in the denominator, leading to a wrong prediction of the competition outcome. Furthermore, it should be noted that the simulations with the 1-dimensional model first need to be performed to calculate the SRT regardless

of the SRT value applied. It can thus be concluded that the criteria are not very useful to be used in combination with 1-dimensional models.

4.5.2 Steady state analysis – endogenous respiration rate as a fraction of maximum growth rate (Model 2)

Taking into account the endogenous respiration at a rate equal to 5% of the maximum growth rate, the steady state effluent composition did not show large differences with the case in which endogenous respiration was neglected (Figure 4.1C versus A). However, the microbial population shift occurred at a higher oxygen concentration and coexistence was observed in a larger range of oxygen concentrations ($4.18 - 5.5 \text{ g O}_2\cdot\text{m}^{-3}$) considering endogenous respiration (Figure 4.1D versus B). Besides, AOB1 outcompetes AOB2 up to higher oxygen concentrations compared to the case in which endogenous respiration was not considered (up to about $5 \text{ g O}_2\cdot\text{m}^{-3}$). The reason for this lies in the fact that the endogenous respiration rate of the species with the lowest growth rate (AOB1) has a significantly lower absolute value than the species with the highest growth rate ($b^{\text{AOB1}} = 0.068 \text{ d}^{-1}$ versus $b^{\text{AOB2}} = 0.121 \text{ d}^{-1}$), which provides an additional competitive advantage for AOB1, on top of its high affinity for oxygen. After adjusting the endogenous respiration of both AOBs to $b^{\text{AOB1}} = b^{\text{AOB2}} = 0.1 \text{ d}^{-1}$ (data not shown), coexistence of both AOBs at an oxygen concentration of $0.36 \text{ g O}_2\cdot\text{m}^{-3}$ was observed at steady state in a small range comparable to the simulation series in which no endogenous respiration was considered.

A clear advantage of using 1-dimensional biofilm models instead of 0-dimensional ones is the possibility to study both biomass and substrate concentration profiles in the biofilm. Figure 4.2 displays the biomass profiles and substrate profiles at steady state for a bulk liquid oxygen concentration of $4.84 \text{ g O}_2\cdot\text{m}^{-3}$. This bulk liquid oxygen concentration was chosen because it corresponds with the coexistence of AOB1 and AOB2 in about equal fractions (making up 17% and 15% of the particulate matter, respectively, see Figure 4.1D). However, due to the thin steady state thickness, biomass and substrate concentration gradients were as good as lacking in this case. The biofilm

thickness considered in the model ($9.6 \cdot 10^{-6}$ m) is lower than the large ball-shaped clusters formed by *Nitrosomonas* cells of more than $10 \cdot 10^{-6}$ m diameter (Schramm *et al.* 1996; Okabe *et al.* 2004). Furthermore, up to 70% of the flocs in an activated sludge process can be in the range of $2 \cdot 10^{-6}$ m to $16 \cdot 10^{-6}$ m (Li & Ganczarczyk 1991), corresponding to the thin steady state thickness of the biofilm observed in the ITBR under study. This is the main reason why a 0-dimensional biofilm model was also able to simulate the experimental data (Volcke *et al.* 2008). When such flat substrate and biomass profiles are observed (Figure 4.2) and when internal mass transfer limitation (diffusion) is thus negligible, choosing a simple and straightforward 0-dimensional model, as proposed by Volcke *et al.* (2008), is advisable. An advantage of the latter models is that they allow straightforward prediction of the competition outcome (Volcke *et al.* 2008). However, the added value of applying 1-dimensional models will become larger for thicker biofilms, showing more pronounced concentration gradients and thus comprising more ecological niches.

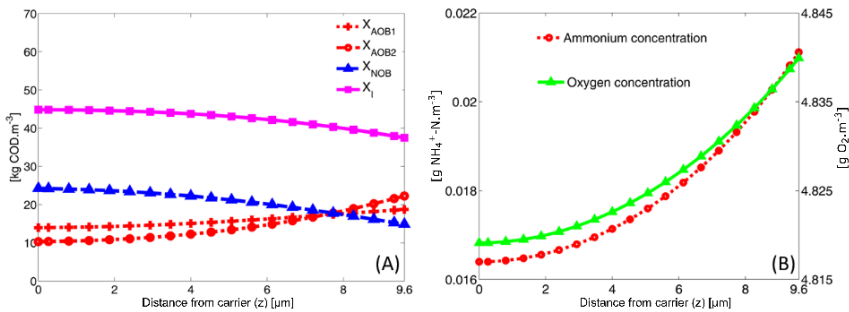


Figure 4.2 Steady state concentration profile of particulate matter (left, X_I = particulate inert components) and the substrates of the AOB (right) in the biofilm for a bulk liquid oxygen concentration of $4.84 \text{ g O}_2.\text{m}^{-3}$. Simulation results for a model with endogenous respiration as a fraction of maximum growth rate.

4.5.3 Simulation of experimental data (Model 3)

The insights gained from the steady state analysis were used to describe the experimental data of Bernet *et al.* (2004) and Volcke *et al.* (2008). Using Model 2, dynamic simulation of the observed microbial population shift from AOB1 to AOB2 was not possible, as the chosen endogenous respiration rate resulted in a clear competitive advantage for AOB1 (Figure 4.1D). Therefore, the endogenous respiration rate of AOB1 and AOB2 was changed to a fixed value of 0.1 d^{-1} , resulting in the dominance of AOB2 for dissolved oxygen concentrations higher than $1.04 \text{ g O}_2\cdot\text{m}^{-3}$ at steady state (Figure 4.1F).

However, the resulting model still did not reflect the observed reactor behaviour, namely nitrite accumulation before the operation shift. This was remedied by considering external mass transfer ($K_L = 0.91 \text{ m}\cdot\text{d}^{-1}$ from Bernet *et al.* (2005)). Steady state analysis of the resulting model (Figure 4.1E) showed that nitrite accumulation took place up to oxygen concentrations of $1 \text{ g O}_2\cdot\text{m}^{-3}$ and nitrate was formed only if the oxygen concentration was larger than $0.6 \text{ g O}_2\cdot\text{m}^{-3}$.

When Model 3 was used for dynamic simulations, the dynamic simulation results showed a good resemblance ($E_{\text{NO}_2} = 0.53$; $E_{\text{NO}_3} = 0.44$; $E_{\text{AOB2:AOB1}} = 0.90$) with the available experimental data (Figure 4.3), as all calculated model efficiencies (Nash Sutcliffe criterion) were well above zero. The model efficiency for the ratio of AOB2:AOB1 was even close to 1. The results supported the hypothesis that the higher oxygen concentration in phase II allowed complete nitrite oxidation to nitrate (Figure 4.3A) and gave AOB2 the possibility to grow at the expense of AOB1 (Figure 4.3B). The difference in maximum growth rate and affinity for oxygen of the two AOBs thus explained the population shift after lowering the loading rate in the ITBR observed during the experiments.

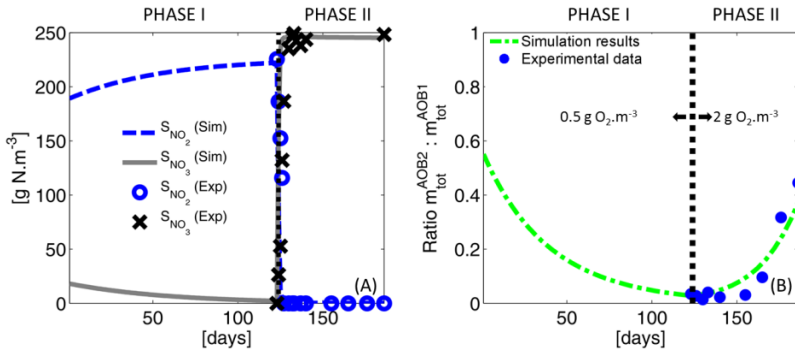


Figure 4.3 Dynamic simulation results, using a 1-dimensional model with endogenous respiration ($b_{AOB1} = b_{AOB2} = 0.1 \text{ d}^{-1}$) and a boundary layer. The nitrite and nitrate bulk liquid concentrations (left) and microbial community dynamics (ratio of AOB2 over AOB1, right) of the ITBR are given in function of time. The vertical line denotes the operation shift at day 124.

4.6 Conclusions

Microbial competition in a nitrifying biofilm (ITBR) reactor, operated at a varying loading rate, was described through a 1-dimensional nitrification biofilm model, which includes the competition between two genetically different populations of ammonia-oxidizing bacteria (AOB) and one population of nitrite-oxidizing bacteria (NOB).

Microbial competition between different types of AOB is affected by the endogenous respiration rate, while external mass transfer limitations affect the competition between AOB and NOB and thus the reactor behaviour in terms of nitrite and/or nitrate production.

Straightforward criteria for the competition outcome predicted by 0-dimensional models (neglecting spatial variations) are not applicable to 1-dimensional biofilm models.

5

Influence of process dynamics on the nitrifying community

5.1 Abstract

For engineers, it is interesting to gain insight in the effect of control strategies on microbial communities, on their turn influencing the process behaviour and/or its stability. This chapter assesses the influence of process dynamics on the microbial community in a biofilm reactor for wastewater treatment, which was controlled according to several strategies aiming at nitrite accumulation. The process dataset, combining conventional chemical and physical data with molecular information, was analysed through a correlation analysis and in a simulation study. During nitrate (NO_3^-) accumulation, an increased nitrogen loading rate (NLR) resulted in a drop of the bulk liquid oxygen concentration without resulting in nitrite accumulation (NO_2^-). A biofilm model was able to reproduce the bulk liquid nitrogen concentrations in two periods before and after this increased NLR. As the microbial parameters calibrated for the ammonia-oxidizing bacteria (AOB) and nitrite-oxidizing bacteria (NOB) in both periods were different, it was concluded that the increased NLR governed an AOB and NOB population shift. Based on the available molecular data, it was assumed that each period was typified by 1 dominant AOB and probably several subdominant NOB populations. The control strategies for nitrite accumulation influenced the bulk liquid composition by controlling the competition between AOB and NOB.

5.2 Submitted as

Vannecke, T.P.W., Bernet, N., Winkler, M.K.H., Santa-Catalina, G., J.-P. Steyer & Volcke, E.I.P. (Submitted). Influence of process dynamics on the microbial diversity in a nitrifying biofilm reactor. *Biotechnology and Bioengineering*.

5.3 Introduction

The microbial community composition in a reactor does not only influence its performance, but also its stability (Siripong & Rittmann 2007; Wittebolle *et al.* 2008; Ramirez *et al.* 2009). Indeed, more diverse systems imply a greater pool of physiological and genetic traits, which provide them with the capacity to interchange and sustain functions under varying environmental conditions (Bellucci *et al.* 2015). From an engineering point of view, it is interesting to correlate microbial shifts to system performance (Winkler *et al.* 2013). Moreover, the engineering of wastewater treatment systems would be greatly improved if one also could control the associated microbial diversity (Yuan & Blackall 2002). To achieve this goal, it is required to gain insight in the effect of control strategies on the microbial communities which on their turn influence the process behaviour and/or its stability.

Techniques for biological nitrogen removal from wastewater based on ammonium oxidation to nitrite (nitritation) while preventing further oxidation to nitrate results in significant cost savings over conventional nitrification-denitrification over nitrite (Turk & Mavinic 1986; Verstraete & Philips 1998; Peng & Zhu 2006). Various control strategies have been proposed to promote nitrite accumulation, by favouring the ammonia-oxidizing bacteria (AOB) and inhibiting the nitrite-oxidizing bacteria (NOB): (1) pH control causing inhibition by free ammonia (FA) and free nitrous acid (FNA) of NOB, which is stronger than for AOB (Anthonisen *et al.* 1976), (2) temperature control in combination with short sludge retention times to washout NOB (Lochtman 1995), as at elevated temperatures, AOB have a higher growth rate than NOB (Wiesmann 1994), and (3) control of the dissolved oxygen (DO) concentration (Garrido *et al.* 1997; Bernet *et al.* 2001), as NOB have a lower affinity for oxygen and are hence more sensitive to DO limitation than AOB (Jayamohan *et al.* 1988). Moreover, biofilm reactors display distinct advantages for the cultivation of the slow growing nitrifiers, due to their specific biomass retention characteristics (Nicolella *et al.* 2000; Ras *et al.* 2011; Xu *et al.* 2015).

In this contribution, the influence of process dynamics on the microbial diversity in a nitrifying biofilm reactor, subjected to different control strategies for nitrite accumulation, is investigated. A unique data set combining both conventional chemical and physical data with molecular information for the nitrification process, and including both new and previously gathered experimental data (Bougard *et al.* 2006a), is analysed. Through a correlation analysis and a simulation study insight is gained on the influence of the process dynamics and the control strategies on the microbial diversity and competition in a nitrifying biofilm reactor. Furthermore, the hypothesis that an observed population shift between *Nitrosomonas halophila* and *Nitrosomonas europaea*, before the control strategies for nitrite accumulation were implemented, was induced by an increased nitrogen loading rate, was tested.

5.4 Materials and methods

5.4.1 Experimental set-up and operational conditions

Bougard *et al.* (2006a) investigated the impact of two control strategies to obtain nitrite accumulation (nitrification) in an inverse turbulent bed reactor or ITBR (Buffiere *et al.* 2000): (1) high temperature (35 °C) control, in order to increase the free ammonia (FA) concentration and (2) adjustment of the nitrogen loading rate (NLR) through fuzzy-logic control of the liquid flow (Q_{in}) rate, in order to keep both bulk liquid oxygen concentration (DO) as well the effluent concentration of ammonium low. It should be noted that the objective of the latter control strategy was not an exact regulation of oxygen and/or ammonia concentration around a precise set point, but to stimulate the microbial activity while achieving the control design objectives (Bougard *et al.* 2006a). Four membership functions were defined on the oxygen, three for the ammonia concentration and six membership functions were set on the liquid feed flow (Figure 5.1).

Membership functions	Fuzzy-logic rules
	<ol style="list-style-type: none"> 1. If (O₂ is VL) and (NH₄ is S) then (ΔQ_{in} is +++) 2. If (O₂ is VL) and (NH₄ is M) then (ΔQ_{in} is ++) 3. If (O₂ is VL) and (NH₄ is L) then (ΔQ_{in} is -) 4. If (O₂ is L) and (NH₄ is S) then (ΔQ_{in} is ++)
	<ol style="list-style-type: none"> 5. If (O₂ is L) and (NH₄ is S) then (ΔQ_{in} is ++) 6. If (O₂ is L) and (NH₄ is L) then (ΔQ_{in} is -) 7. If (O₂ is M) and (NH₄ is S) then (ΔQ_{in} is +) 8. If (O₂ is M) and (NH₄ is M) then (ΔQ_{in} is n) 9. If (O₂ is M) and (NH₄ is L) then (ΔQ_{in} is -)
	<ol style="list-style-type: none"> 10. If (O₂ is S) and (NH₄ is S) then (ΔQ_{in} is n) 11. If (O₂ is S) and (NH₄ is M) then (ΔQ_{in} is -) 12. If (O₂ is S) and (NH₄ is L) then (ΔQ_{in} is --)
<p>S: small, M: medium, L: large, VL: very large +++: very high increase, ++: high increase, +: increase, n: neutral, -: decrease, --: strong decrease O₂ and NH₄: bulk liquid ammonium and oxygen concentration, ΔQ_{in}: change of inflow rate</p>	

Figure 5.1 Membership functions and fuzzy-logic rules of the fuzzy-logic control of the inflow rate (Q_{in}) to adjust the nitrogen loading rate used by Bougard *et al.* (2006a). Figure based on Bougard (2004).

Both control strategies led to nitrite accumulation, but the fuzzy logic controller of the inflow rate adjusting the NLR did not affect the composition of the microbial community, while temperature control did. Besides, a major shift in the nitrifying community of the biofilm reactor took place during nitrate (NO_3^-) accumulation in the period before the control strategies for nitrite accumulation were implemented: *Nitrosomonas halophila* (AOB1) was completely replaced in the biofilm by *Nitrosomonas europaea* (AOB2) (Bougard *et al.* 2006a).

The reactor was filled for 20% of its active volume with solid biocarriers, on which the biomass grew, kept afloat by an upward current of air. The aeration

was fixed at a flowrate of $2.88 \text{ m}^3 \cdot \text{d}^{-1}$. The reactor temperature was maintained at $30 \text{ }^\circ\text{C}$ or $35 \text{ }^\circ\text{C}$ and the pH around 7.2.

The experiment ran for 592 days. During continuous operation mode, the reactor was fed with synthetic wastewater, containing around $2000 \text{ g TNH} \cdot \text{m}^{-3}$ and $2.82 \cdot 10^3 \text{ g Viandox} \cdot \text{m}^{-3}$ or $583 \text{ g COD} \cdot \text{m}^{-3}$ as a carbon source (meat juice), using a conversion factor of $0.207 \text{ g COD} \cdot (\text{g Viandox})^{-1}$ (Bougard 2004). Viandox is composed of components difficult to degrade and was added to the synthetic wastewater to simulate reject water of anaerobic digesters.

During reactor operation, the nitrogen loading rate (NLR) and the influent ammonium concentration, as well as the bulk liquid ammonium, nitrite and nitrate concentrations were monitored about every two days. Reactor temperature, pH and bulk liquid oxygen concentration (DO) were monitored online, every two minutes.

Further details on the experimental set-up, operational conditions and analytical methods can be found in Bougard *et al.* (2006a) and Bougard *et al.* (2006b).

5.4.2 Microbiological and molecular methods

Molecular information on the bacterial community and ammonia-oxidizing guild published by Bougard *et al.* (2006a), based on Polymerase Chain Reaction – Single Strand Conformational Polymorphism (PCR-SSCP) combined with the cloning-sequencing technique, were complemented with new, unpublished data on the quantity and microbial diversity of the total bacterial and nitrifying community, based on quantitative PCR (qPCR) and Capillary Electrophoresis-Single Strand Conformation Polymorphism (CE-SSCP), respectively. Samples ($n=30$) were taken over the experimental period of 592 days during reactor operation. Preparation and storage of the samples, besides DNA extraction was done as reported in Braun *et al.* (2015).

5.4.2.1 qPCR of the nitrifying community

The quantity of total Bacteria, AOB and NOB was measured in samples of $5 \text{ }\mu\text{L}$ diluted DNA taken from the nitrifying ITBR using qPCR-analysis. For the

qPCR-analysis of the total bacterial community, the V3 variable region of 16S rRNA genes was amplified from total genomic DNA with the bacterial primers taken from Braun *et al.* (2015). For the AOB, the gene coding for the enzyme ammonia monooxygenase (*amoA*), the functional gene for oxidation of ammonia to nitrite, was amplified using the forward primer from Kowalchuk *et al.* (1997), the reverse primer from Hermansson and Lindgren (2001) and the probe from Graham *et al.* (2007). For the NOB, the gene coding for the enzyme nitrite oxidoreductase (*nxrA*), the functional gene for oxidation of nitrite to nitrate, was amplified using the primers from Wertz *et al.* (2008). The fluorophores used were Yakima Yellow, FAM and SybrGreen for the total community, the AOB and the NOB, respectively.

For the total bacterial community, AOB and NOB, two C_T -values (cycle threshold), defined as the number of cycles required for the fluorescent signal to cross the threshold, were obtained per sample. C_T -levels are inversely proportional to the amount of target nucleic acid in the sample. A standard curve, corresponding to the used fluorophore (Table 5.1), was generated at each assay, using dilutions of PCR products from known environmental clones (Braun *et al.* 2015). The amount of total bacterial, AOB and NOB DNA was then calculated based on the standard equation following Eq. 5.1, and was used to calculate the fraction of AOB and NOB in the total bacterial community.

$$\log_{10}(\text{amount}) = \frac{(C_t - Y_{\text{intercept}})}{\text{slope}} \quad \text{Eq. 5.1}$$

Although a small fraction of heterotrophs, possessing multiple (>3) gene copies of the 16S rRNA gene could be present, we can assume that due to the low C:N ratio of the influent (0.3) and the low biodegradability of the C-source (Viandox) the biofilm was mainly composed of nitrifiers, as the growth of heterotrophs on decay products can be neglected (Mozumder *et al.* 2014). Nitrifiers possess 1 copy of the 16S rRNA gene (Stoddard *et al.* 2015). As the focus was mainly on the relative fractions of AOB and NOB in the biofilm, the correction for gene copy number was not deemed necessary, because both

amoA (Norton *et al.* 2002) and nxrA (Poly *et al.* 2008; Lückner *et al.* 2010) can be present in equal (2-3) amounts of gene copies per cell.

Table 5.1 Standard curve parameters for the qPCR-analysis.

	Total bacterial community	AOB	NOB
Fluorophore	Yakima Yellow	FAM	SybrGreen
Slope	-3.342	-3.369	-3.310
Y-intercept	42.93	43.16	35.27
Efficiency	0.99	0.98	1.00
R²	0.970	0.998	0.993

5.4.2.2 CE-SSCP of the nitrifying community

The total bacterial community in the biofilm was monitored by CE-SSCP as described by Braun *et al.* (2015). For specific CE-SSCP of the AOB of the β -subdivision, the total genomic DNA was first amplified with a PCR using specific primers (forward primers CTO189fA/B, CTO189fC and reverse CTO654R) taken from Kowalchuk *et al.* (1997). Next, the V3 variable region of 16S rRNA genes was amplified from the PCR product using the same procedure as for the total bacterial community. For the specific CE-SSCP of the NOB, nitrite oxydoreductase (nxrA) was amplified (Wertz *et al.* 2008). The same primers as in Wertz *et al.* (2008) were used with an additional fluorophore (6-FAM) at the 3' end of the reverse primer.

The obtained SSCP profiles, with the number of peaks corresponding to the number of detected bacterial species/strains, were analysed statistically using the StatFingerprints package in R (Michelland *et al.* 2009; Braun *et al.* 2015). The Simpson diversity index (D_{SSCP}) was calculated for each fingerprinting profile as $D_{SSCP} = -\ln \sum (\text{peak areas})^2$ (Loisel *et al.* 2008). This diversity index reflects the underlying diversity from the SSCP profile independently of sample size (Rosenzweig 1995): a low and high D_{SSCP} depicts a low and high diversity, respectively.

5.4.3 Correlation analysis

To analyse the large amount of data on the process dynamics and the effect on the microbial dynamics, a correlation analysis was performed in IBM SPSS statistics 22 (Armonk, New York, U.S.). The correlation was expressed using the Pearson product-moment correlation coefficient r ; $r = 1$ indicates total positive correlation, $r = 0$ no correlation, and $r = -1$ total negative correlation. Only correlations with a p -value smaller than 0.05 were considered significant. The correlation analysis of the physical and chemical data was based on 291 datapoints (290 for DO); the correlation analysis of the microbial community was based on 28 datapoints, as for 2 samples on which molecular data were retrieved, the corresponding physical and chemical data were unavailable.

5.4.4 Modelling the dynamic reactor behaviour

5.4.4.1 Reactor model

A 1-dimensional two-step nitrification biofilm model, including biomass variations perpendicular to the carrier on which the considered microorganisms grow, was set up to describe the experimental set-up of Bougard *et al.* (2006a) and was implemented in the Aquasim software (Reichert 1994). The model describing growth and decay of the AOB, NOB and heterotrophs is based on the model developed by Mozumder *et al.* (2014). The difference lies in the fact that anammox was not included and only 1 state variable is used to describe heterotrophic biomass while the model of Mozumder *et al.* (2014) distinguishes 3 state variables for heterotrophic biomass, based on the type of electron acceptor used. The model of Mozumder *et al.* (2014) was extended with inhibition of AOB and NOB by FA and FNA (Jubany *et al.* 2009), temperature dependency of growth and decay rates (Henze *et al.* 2000; Hao *et al.* 2002a), temperature dependency of diffusion (Bernet *et al.* 2005) and temperature and pH dependency of the FA:TNH and FNA:TNO₂ fractions (Anthonisen *et al.* 1976).

The overall model stoichiometry and kinetics, besides the corresponding parameter values of the developed biofilm model are given in Table 5.2, Table 5.3 and Table 5.4, respectively.

Table 5.2 Stoichiometric matrix describing the growth and decay of AOB, NOB and heterotrophs. Adapted from Mozumder *et al.* (2014). AOBi: AOB population Period A or Period B (Approach 1-2) / AOB population A and B (Approach 3); NOBi: NOB population Period A or Period B (Approach 1-2) / NOB population A and B (Approach 3)

A_{ij}	i component \rightarrow j process \downarrow	S_S [g COD.m ⁻³]	S_{NH} [g N.m ⁻³]	S_{NO_2} [g N.m ⁻³]	S_{NO_3} [g N.m ⁻³]	S_{O_2} [g O ₂ .m ⁻³]	S_{N_2} [g N.m ⁻³]	X_{AOBi} [g COD.m ⁻³]	X_{NOBi} [g COD.m ⁻³]	X_H [g COD.m ⁻³]	X_i [g COD.m ⁻³]
<i>growth</i>											
1.	growth of X_{AOBi}		$-1/Y_{AOBi} - INXB$	$1/Y_{AOBi}$		$1 - 3.43/Y_{AOBi}$		1			
2.	growth of X_{NOBi}		$-INXB$	$-1/Y_{NOBi}$	$1/Y_{NOBi}$	$1 - 1.14/Y_{NOBi}$			1		
3.	aerobic growth of heterotrophs	$-1/Y_H$	$-INXB + 1/Y_H - INSS$			$1 - 1/Y_H$				1	
4.	anoxic (on NO ₂) growth of heterotrophs	$1/Y_{H,NO_2}$	$-INXB + 1/Y_H - INSS$	$-\left(\frac{1 - Y_{H,NO_2}}{1.71 \cdot Y_{H,NO_2}} \right)$			$\frac{1 - Y_{H,NO_2}}{1.71 \cdot Y_{H,NO_2}}$			1	
5.	anoxic (on NO ₃) growth of heterotrophs	$1/Y_{H,NO_3}$	$-INXB + 1/Y_H - INSS$	$\frac{1 - Y_{H,NO_3}}{1.14 \cdot Y_{H,NO_3}}$	$-\left(\frac{1 - Y_{H,NO_3}}{1.14 \cdot Y_{H,NO_3}} \right)$					1	
<i>decay</i>											
6.	decay of X_{AOBi}	$1 - f_i$	$INXB \cdot f_i - INXR \cdot (1 - f_i) - INSS$					-1			f_i
7.	decay of X_{NOBi}	$1 - f_i$	$INXB \cdot f_i - INXR \cdot (1 - f_i) - INSS$						-1		f_i
8.	decay of X_H	$1 - f_i$	$INXB \cdot f_i - INXR \cdot (1 - f_i) - INSS$							-1	f_i
composition matrix											
g COD/unit comp		1	0	-3.43	-4.57	-1	-1.71	1	1	1	1
g N/unit comp		i_{NSS}	1	1	1	0	1	i_{NXB}	i_{NNB}	i_{NXH}	i_{NXI}

Table 5.3 Reaction kinetics for growth and decay corresponding to the processes from Table 5.2. Adapted from Mozumder *et al.* (2014). FA and FNA inhibition were included for AOB and NOB following Jubany *et al.* (2009). AOBi: AOB population Period A or Period B (Approach 1-2) / AOB population A and B (Approach 3); NOBi: NOB population Period A or Period B (Approach 1-2) / NOB population A and B (Approach 3)

j process ↓	
1. growth of AOBi	$\rho_{G,AOBi} = \mu_{max}^{AOBi} \cdot \frac{S_{O_2}}{K_{O_2}^{AOBi} + S_{O_2}} \cdot \frac{K_{I,FNA}^{AOBi}}{K_{I,FNA}^{AOBi} + S_{FNA}} \cdot \frac{S_{FA}}{K_{FA}^{AOBi} + S_{FA} + S_{FA}^2/K_{I,FA}^{AOBi}} \cdot X_{AOBi}$
2. growth of NOBi	$\rho_{G,NOBi} = \mu_{max}^{NOBi} \cdot \frac{S_{O_2}}{K_{O_2}^{NOBi} + S_{O_2}} \cdot \frac{K_{I,FA}^{NOBi}}{K_{I,FA}^{NOBi} + S_{FA}} \cdot \frac{S_{FNA}}{K_{FNA}^{NOBi} + S_{FNA} + S_{FNA}^2/K_{I,FNA}^{NOBi}} \cdot \frac{S_{TNH}}{K_{TNH}^{NOBi} + S_{TNH}} \cdot X_{NOBi}$
3. growth of aerobic heterotrophs	$\rho_{G,H,O_2} = \mu_{max}^H \cdot \frac{S_S}{K_S^H + S_S} \cdot \frac{S_{O_2}}{K_{O_2}^H + S_{O_2}} \cdot \frac{S_{TNH}}{K_{TNH}^H + S_{TNH}} \cdot X_H$
4. anoxic growth (on NO ₂ ⁻) of heterotrophs	$\rho_{G,H,NO_2} = \mu_{max}^H \cdot \eta_{NO_2} \cdot \frac{K_{NO_2}^H}{K_{O_2}^H + S_{O_2}} \cdot \frac{S_{NO_2}}{K_{NO_2}^H + S_{NO_2}} \cdot \frac{S_{NO_2}}{S_{NO_2} + S_{NO_3}} \cdot \frac{S_S}{K_S^H + S_S} \cdot \frac{S_{TNH}}{K_{TNH}^H + S_{TNH}} \cdot X_H$
5. anoxic growth (on NO ₃ ⁻) of heterotrophs	$\rho_{G,H,NO_3} = \mu_{max}^H \cdot \eta_{NO_3} \cdot \frac{K_{NO_2}^H}{K_{O_2}^H + S_{O_2}} \cdot \frac{S_{NO_3}}{K_{NO_3}^H + S_{NO_3}} \cdot \frac{S_{NO_3}}{S_{NO_2} + S_{NO_3}} \cdot \frac{S_S}{K_S^H + S_S} \cdot \frac{S_{TNH}}{K_{TNH}^H + S_{TNH}} \cdot X_H$
6. decay of AOBi	$\rho_{D,AOBi} = d_{AOBi} \cdot X_{AOBi}$
7. decay of NOBi	$\rho_{D,NOBi} = d_{NOBi} \cdot X_{NOBi}$
8. decay of heterotrophs	$\rho_{D,H} = d_H \cdot X_H$

It should be noted that AOB inhibition by FA and NOB inhibition by FNA (substrate inhibition, i.e., a special form of uncompetitive inhibition (Bisswanger 2008)) were described with a Haldane model (Beltrame *et al.* 1980) while AOB inhibition by FNA and NOB inhibition by FA were described with a non-competitive model. The Haldane model is essentially the combination of a Monod term and a non-competitive inhibition term.

Table 5.4 Biofilm characteristics and stoichiometric, kinetic and mass transfer parameter values of the multispecies biofilm model valid for 30 °C and pH 7.5; note that temperature and pH dependency were included in the model. HET: heterotrophs.

Parameter	Value	Unit	Comments
<i>Biofilm characteristics</i>			
Autotrophic biomass (viable + inert) concentration	80000	g COD.m ⁻³	van Benthum <i>et al.</i> (1995) ⁽¹⁾
Heterotrophic biomass (viable + inert) concentration	26667	g COD.m ⁻³	van Benthum <i>et al.</i> (1995) ⁽¹⁾
LF _{SS}	Steady state biofilm thickness	20e-006	m Calculated
<i>Stoichiometric parameters</i>			
Y _{AOBi}	Yield (AOBi)	0.19	g COD.(g N) ⁻¹ Median value in Figure 2.1
Y _{NOBi}	Yield (NOBi)	0.08	g COD.(g N) ⁻¹ Median value in Figure 2.2
Y _H	Yield of HET on O ₂	0.67	g COD.(g COD) ⁻¹ Henze <i>et al.</i> (2000)
Y _{H,NO2}	Yield of HET on NO ₂ ⁻	0.53	g COD.(g COD) ⁻¹ Muller <i>et al.</i> (2003)
Y _{H,NO3}	Yield of HET on NO ₃ ⁻	0.53	g COD.(g COD) ⁻¹ Muller <i>et al.</i> (2003)
i _{NXB}	Biomass nitrogen fraction	0.07	g N.(g COD) ⁻¹ Mozumder <i>et al.</i> (2014)
i _{NXI}	Inert nitrogen fraction	0.07	g N.(g COD) ⁻¹ Mozumder <i>et al.</i> (2014)
i _{NSS}	Organic substrate nitrogen fraction	0.03	g N.(g COD) ⁻¹ Henze <i>et al.</i> (2000)
f _i	Inert fraction in biomass	0.08	g COD.(g COD) ⁻¹ Henze <i>et al.</i> (2000)
<i>Kinetic (at 30 °C and pH 7.5)</i>			
μ _{max} ^{AOBi}	Maximum growth rate (AOBi)	0.65 / 0.71	d ⁻¹ This study ⁽²⁾
μ _{max} ^{NOBi}	Maximum growth rate (NOBi)	1.43 / 0.30	d ⁻¹ This study ⁽²⁾
μ _{max} ^{HET}	Maximum growth rate HET	12	d ⁻¹ Henze <i>et al.</i> (2000) ⁽³⁾
K _{FA} ^{AOBi}	Affinity of AOBi for FA	1.25 / 1.29	g FA-N.m ⁻³ This study ⁽⁴⁾
K _{FNA} ^{NOBi}	Affinity of NOBi for FNA	0.0015 / 0.0024	g FNA-N.m ⁻³ This study ⁽⁴⁾
K _{TNH} ^{NOBi}	Affinity of NOBi for ammonium (nitrogen source)	0.02	g TNH-N.m ⁻³ Mozumder <i>et al.</i> (2014)
K _{TNO2} ^H	Affinity of HET for total nitrite	0.3	g N.m ⁻³ Alpkvist <i>et al.</i> (2006)
K _{NO3} ^H	Affinity of HET for total nitrate	0.3	g N.m ⁻³ Alpkvist <i>et al.</i> (2006)
K _{O2} ^{AOBi}	Affinity of AOBi for O ₂	0.078 / 0.71	g O ₂ .m ⁻³ This study
K _{O2} ^{NOBi}	Affinity of NOBi for O ₂	0.049 / 0.06	g O ₂ .m ⁻³ This study
K _{TNH} ^H	Affinity of HET for ammonium (nitrogen source)	0.02	g TNH-N.m ⁻³ Mozumder <i>et al.</i> (2014)
K _{O2} ^H	Affinity of HET for O ₂	0.2	g O ₂ .m ⁻³ Henze <i>et al.</i> (2000)
K _S ^H	Affinity of HET for organic substrate	20	g COD.m ⁻³ Henze <i>et al.</i> (2000)
K _{I,FA} ^{AOBi}	FA inhibition (AOBi)	490.51 / 489.05	g FA-N.m ⁻³ This study ⁽⁴⁾
K _{I,FA} ^{NOBi}	FA inhibition (NOBi)	12.93 / 10.06	g FA-N.m ⁻³ This study ⁽⁴⁾
K _{I,FNA} ^{AOBi}	FNA inhibition (AOBi)	0.42 / 0.21	g FNA-N.m ⁻³ This study ⁽⁴⁾
K _{I,FNA} ^{NOBi}	FNA inhibition (NOBi)	0.27 / 0.13	g FNA-N.m ⁻³ This study ⁽⁴⁾
d ^{AOBi}	Decay rate (AOBi)	0.073 / 0.061	d ⁻¹ This study ⁽⁴⁾
d ^{NOBi}	Decay rate (NOBi)	0.13 / 0.051	d ⁻¹ This study ⁽⁴⁾
d ^H	Decay rate (HET)	0.6	d ⁻¹ Defined as 0.05 · μ _{max} ^{HET}
η _{NO2} →η _{NO3}	Anoxic reduction factor	0.8	- Henze <i>et al.</i> (2000)
<i>Mass transfer parameters</i>			
D _{NH4}	Diffusion coefficient NH ₄ ⁺	1.60x10 ⁻⁴	m ² .d ⁻¹ Bernet <i>et al.</i> (2005) ⁽⁵⁾
D _{NO2}	Diffusion coefficient NO ₂ ⁻	1.61x10 ⁻⁴	m ² .d ⁻¹ Bernet <i>et al.</i> (2005) ⁽⁵⁾
D _{NO3}	Diffusion coefficient NO ₃ ⁻	1.79x10 ⁻⁴	m ² .d ⁻¹ Bernet <i>et al.</i> (2005) ⁽⁵⁾
D _{O2}	Diffusion coefficient O ₂	1.52x10 ⁻⁴	m ² .d ⁻¹ Bernet <i>et al.</i> (2005) ⁽⁵⁾
D _{N2}	Diffusion coefficient N ₂	2.2x10 ⁻⁴	m ² .d ⁻¹ Williamson and McCarty (1976)
D _S	Diffusion coefficient organic substrate	1x10 ⁻⁴	m ² .d ⁻¹ Hao and van Loosdrecht

⁽¹⁾ Calculated from a autotrophic and heterotrophic biomass concentration of 60000 g VSS.m⁻³ and 20000 g VSS.m⁻³ van Benthum *et al.* (1995), respectively, using a conversion factor of 0.75 g VSS.(g COD)⁻¹ (Henze *et al.* 2000).

⁽²⁾ Temperature dependency of the maximum growth rate of AOB and NOB was modelled using and Eq. 5.2 and Eq. 5.3, respectively, with $E_a^{AOB} = 68 \text{ kJ.mol}^{-1}$; $E_a^{NOB} = 44 \text{ kJ.mol}^{-1}$ and $R = 8.31 \text{ J.(mol.K)}^{-1}$ (Hao *et al.* 2002a).

$$\mu_{\max}^{AOB}(T) = \mu_{\max}^{AOB}(T_{ref}) \cdot \exp\left(\frac{E_a^{AOB} \cdot (T - T_{ref})}{R \cdot T \cdot T_{ref}}\right) \quad \text{Eq. 5.2}$$

$$\mu_{\max}^{NOB}(T) = \mu_{\max}^{NOB}(T_{ref}) \cdot \exp\left(\frac{E_a^{NOB} \cdot (T - T_{ref})}{R \cdot T \cdot T_{ref}}\right) \quad \text{Eq. 5.3}$$

⁽³⁾ The temperature dependency of the maximum growth rate of heterotrophs was implemented using the temperature relationship of ASM3 (Henze *et al.* 2000), as described by Eq. 5.4.

$$\mu_{\max}^{HET}(T) = \mu_{\max}^{HET}(T_{ref}) \cdot \exp(0.0693(T - T_{ref})) \quad \text{Eq. 5.4}$$

⁽⁴⁾ The fraction of FA:TNH and the fraction of FNA:TNO₂ are dependent on pH and temperature and were calculated for a certain combination of reactor temperature and pH using Eq. 5.5 and Eq. 5.6, respectively, taken from Anthonisen *et al.* (1976).

$$\frac{FA}{TNH} = \frac{1}{1 + 10^{pK_{aNH_4} - pH}}, \text{ with } pK_{aNH_4} = -\log(\exp^{-\frac{6344}{T(K)}}) \quad \text{Eq. 5.5}$$

$$\frac{FNA}{TNO_2} = \frac{1}{1 + 10^{pH - pK_{aNO_2}}}, \text{ with } pK_{aNO_2} = -\log(\exp^{-\frac{2300}{T(K)}}) \quad \text{Eq. 5.6}$$

⁽⁵⁾ Diffusion of ammonium, nitrite, nitrate and oxygen (m².d⁻¹) and its temperature dependency were modelled as described by Bernet *et al.* (2005). The temperature dependency of oxygen diffusion was calculated using Eq. 5.7 (Wijffels *et al.* 1995) and the temperature dependency of ammonium, nitrite and nitrate diffusion was calculated using Eq. 5.8 (Hunik *et al.* 1994).

$$D_{O_2} = 0.85 \cdot 1.91 \cdot 10^{-6} \cdot e^{-\frac{17200}{R \cdot T}} \cdot 86400 \quad \text{Eq. 5.7}$$

$$D_n = fd_n \cdot Dw_n \cdot \frac{\eta_{25}}{\eta_T} \cdot \frac{T}{298.15} \quad \text{Eq. 5.8}$$

In Eq. 5.8, Dw_n stands for the diffusion coefficients of ammonium, nitrite or nitrate in water, i.e., $D_{NH_4} = 1.69e-004 \text{ m}^2.d^{-1}$, $D_{NO_2} = 1.65e-004 \text{ m}^2.d^{-1}$ and $D_{NO_3} = 1.64e-004 \text{ m}^2.d^{-1}$, taken from Flora *et al.* (1999), fd_n for 0.835 (ammonium), 0.86 (nitrite) or 0.96 (nitrate), taken from Williamson and McCarty (1976) and η_{25} and η_T the viscosity of water at 25°C and at temperature T.

The model in the current contribution describes biofilm growth on spherical particles with a radius of $73.5 \cdot 10^{-6}$ m in an ITBR ($V = 2.84 \cdot 10^{-3}$ m³). The total number of particles ($2 \cdot 10^8$ particles) was calculated based on the total volume of particles ($5.68 \cdot 10^{-4}$ m³) in the reactor and the volume of 1 particle ($1.7 \cdot 10^{-12}$ m³). During the experiments about 80% ($1.6 \cdot 10^8$) of the particles were occupied (Bougard 2004). The total amount of biomass of 17 g VSS or 23 g COD, using a conversion factor of $0.75 \text{ g VSS} \cdot (\text{g COD})^{-1}$ (Henze *et al.* 2000), was assumed to be divided homogeneously over the colonized particles, resulting in a steady state thickness of $LF_{SS} = 20 \cdot 10^{-6}$ m. It was assumed that steady state thickness had already been reached at the start of the simulations, as the experiment was preceded by a start-up period of 22 days.

The biofilm was assumed to be rigid, meaning that particulate components are displaced only by the expansion or shrinkage of the biofilm solid matrix. The biofilm porosity was assumed constant at 80%. An initial active biomass fractioning at the start of Period I of the heterotrophs was set as 0.01%. The remaining active biomass was assumed to be made up by 75% AOB and 25% NOB, according to the number of electrons exchanged by the oxidation of NH_4^+ to NO_2^- and from NO_2^- to NO_3^- , respectively.

The flow rate, influent ammonium and COD concentration, the temperature of the reactor, pH, and DO were implemented in the model, using the offline and online monitored data. So, rather than implementing the control strategies as such, the variation of both the controlled, i.e. temperature for temperature control, and liquid flow rate (Q_{in}) for the controller adjusting the NLR, and the manipulated variables (controller output) was considered. For temperature control, the controller output is related to all variables for which temperature dependency is implemented in the model, i.e., the ratio of free ammonia (FA) and total ammonium, the ratio of nitrous acid (FNA) and total nitrite, diffusivity of ammonium, nitrite, nitrate and oxygen, besides the growth and decay rates of the microorganisms. For fuzzy-logic control of the inflow rate, the controller output is the bulk liquid ammonium and oxygen concentration corresponding to the NLR.

5.4.4.2 Model calibration

As the focus of this contribution is on the effect of process dynamics on the nitrifying community, no sensitivity analysis was performed but instead it was verified by trial and error whether the simplest model possible was able to simulate the overall reactor behaviour (nitrite versus nitrate accumulation, besides residual ammonium concentration) when only selected microbial parameters were calibrated. The selection of microbial parameters was based on the results of Chapter 2 (importance of maximum growth rate and affinity for electron donor and acceptor) and Chapter 4 (importance of endogenous respiration, in Chapter 5 replaced by decay).

First, only the microbial parameters of AOB known to have an important effect on bulk liquid composition, i.e., maximum growth rate and affinity for ammonium and oxygen, see Chapter 2 and previously performed sensitivity analyses (Brockmann & Morgenroth 2007; Brockmann *et al.* 2008; Brockmann & Morgenroth 2010; Brockmann *et al.* 2013), were calibrated to the experimentally recorded bulk liquid concentrations of total ammonium (TNH), total nitrite (TNO₂) and nitrate (NO₃⁻). By checking the fit of the simulation results with the observed overall process performance, it was found that besides the calibration of these microbial parameters for the AOB, these parameters also needed to be calibrated for the NOB guild. Also FA and FNA inhibition of AOB and NOB needed to be implemented in the model and the decay rate and inhibition constants for FA and FNA of both the AOB and the NOB guild needed to be calibrated.

The values for decay rate, maximum growth rate, the affinity constants and inhibition constants of both the AOB and NOB were estimated using Aquasim by minimizing the sum of the squares of the weighted deviations (χ^2) between the measurements and the simulation results of the bulk liquid ammonium, nitrite and nitrate concentrations (Reichert *et al.* 1995). The sum (χ^2) extends over all the data points of all variables specified as fit targets (TNH, TNO₂ and NO₃⁻), which were given equal weights ($\chi^2_{\text{tot}} = \chi^2_{\text{TNH}} + \chi^2_{\text{TNO}_2} + \chi^2_{\text{NO}_3}$).

The sum was minimized numerically using the secant algorithm (Ralston & Jennrich 1978) and the maximum number of interactions was set at 200, in order to keep the computational time reasonable. The initial bulk liquid and biofilm concentrations of dissolved substances were assumed to be 0.01 g N.m⁻³ and the initial biomass concentrations in the biofilm were calculated from the biomass (viable + inerts) density, considering a volume fraction of 0.01 of heterotrophs, 0.1425 of AOB and 0.0475 NOB. The biofilm thickness was assumed to be at steady state and the concentration of particulate inert components in the biofilm was assumed to be 0 g COD.m⁻³. When the whole period of reactor operation was calibrated in two separate periods, the initial values of the biofilm thickness, the dissolved (bulk and biofilm) and particulate (biofilm) components of the second period were the last simulation values of the previous period.

The parameter space or constraints concerning the microbial characteristics of AOB and NOB were based on the minimum and maximum values of the range reported in literature. The minimum and maximum values of the ranges for maximum growth rate and affinity constants were taken from Chapter 2 (see Vannecke and Volcke (2015)). The minimum and maximum values for decay rates were based on the ranges for maximum growth rate (Chapter 2) by defining the decay rate as 5% of the value for maximum growth rate. A review of inhibition constant values reported in literature was given in this chapter, providing the constraints for the parameter values of the inhibition constants. The starting (uncalibrated) value of all considered microbial parameters was the median value of the corresponding range.

For each simulation, the model accuracy was verified by calculating the Nash-Sutcliffe criterion (model efficiency E, see Nash and Sutcliffe (1970)) as given in Eq. 5.9, with y_i^m the i^{th} observed value, y_i the corresponding calculated value and \bar{y}_m the mean value of the observations.

$$E = 1 - \frac{\sum_{i=1}^n (y_i^m - y_i)^2}{\sum_{i=1}^n (y_i^m - \bar{y}_m)^2} \quad \text{Eq. 5.9}$$

Model efficiencies for the fit with bulk liquid concentrations of TNH (E_{TNH}), TNO₂ (E_{TNO_2}) and nitrate (E_{NO_3}) were calculated. If the model efficiency is

lower than zero, the observed mean is a better predictor than the model, therefore, the model efficiency should be preferably larger than 0 with a maximum of 1 (perfect fit between simulation and observations).

5.4.4.3 Simulation set-up

As the inclusion of diversity within functional guilds is only necessary when the reactor behaviour is clearly influenced by changes in the microbial community, see Chapter 3 (Vannecke *et al.* 2015), it was attempted to simulate the dynamics of the bulk liquid observed by Bougard *et al.* (2006a) with the simplest model possible. Therefore, the model described above considering the growth of 1 AOB population, 1 NOB population and 1 heterotrophic population was used for three different simulations (Table 5.5). Firstly, this model neglecting diversity, was calibrated over the whole experimental period. As the simulation results of Approach 1 were not in correspondence with the overall reactor behaviour, it was decided to calibrate the model over two separate periods: Period A (day 0 – 100) and Period B (day 100 – 592), distinguished by the dominance of *Nitrosomonas halophila* and *Nitrosomonas europaea*, respectively (Bougard *et al.* 2006a). As the simulation results of Approach 2 better reflected the overall behaviour, the calibrated microbial parameters of both periods were used to construct two AOB and two NOB species. The growth and decay of these species were implemented simultaneously in a model, hereby considering within-guild diversity. This model was used in Approach 3, to try to reflect the overall reactor behaviour of the whole experimental period.

Table 5.5 Overview of the simulation set-up. In Approach 3, the two AOB and NOB populations are based on the calibrated values for period A and B from Approach 2.

Approach	Period calibrated (days)	Nitrifying community (calibrated)
1	0-592	1 AOB + 1 NOB
2	Period A: 0-100 Period B: 100-592	1 AOB + 1 NOB
3	0-592	2 AOB + 2 NOB

5.5 Results and discussion

5.5.1 Correlation analysis

5.5.1.1 Chemical and physical data

During operation, four periods could be distinguished (Table 5.6). Period I (day 0 - 113) was typified with a temperature of 30°C and nitrate accumulation, period II (day 114 - 230) with temperature control to 35°C and nitrite accumulation, period III (day 231 - 491) with a temperature of 30°C and recovery to full nitrification by lowering the NLR and period IV (day 492-592) with a temperature of 30°C and fuzzy-logic control of the inflow rate with resulting nitrite accumulation. The reactor was brought back to full nitrification in period III to allow to test the ability of the fuzzy-logic controller to achieve partial nitrification in the next experimental period.

Table 5.6 Periods distinguished during continuous operation (592 days) of the nitrifying reactor (Bougard et al. 2006a). NLR: nitrogen loading rate and Q_{in} : liquid flow rate.

Period	Days	Dominant AOB	Temperature (°C)	Control strategies	Process performance
I	0-50	<i>N. halophila</i>	30	-	NO_3^- accumulation
	51-113	<i>N. halophila</i> <i>N. europaea</i>			
II	114-230	<i>N. europaea</i>	30 → 35	Temperature control	NO_2^- accumulation
III	231-491	<i>N. europaea</i>	30	Lowering Q_{in}	Shift from NO_2^- to NO_3^- accumulation
IV	492-592	<i>N. europaea</i>	30	Fuzzy-logic control of Q_{in} for adjusting NLR	NO_2^- accumulation

An overview of the operational conditions during reactor operation is given in Figure 5.2.

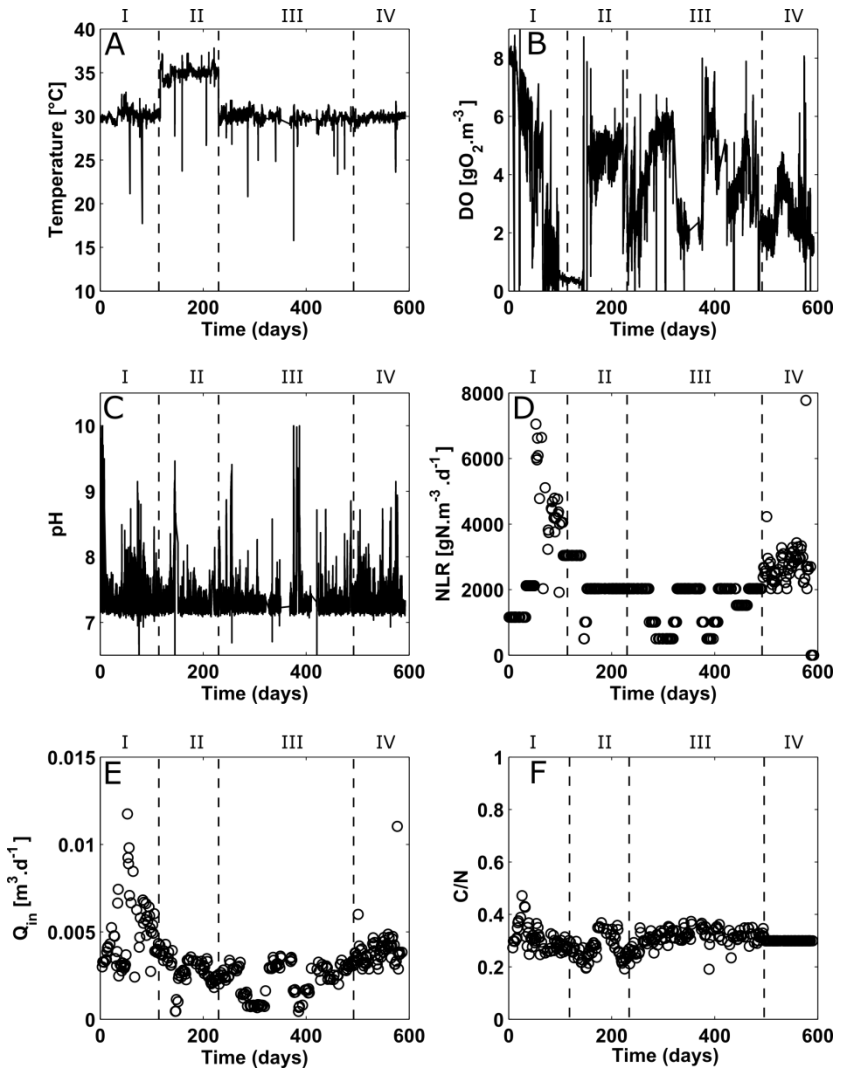


Figure 5.2 Overview of the operational conditions during reactor operation (Bougard et al. 2006a). (A) temperature, (B) bulk liquid oxygen concentration (DO), (C) pH, (D) nitrogen loading rate (NLR), (E) flow rate Q_{in} and (F) C/N-ratio. Temperature, DO and pH were monitored online every 2 minutes, the other variables were measured offline every 2 days. The roman numbers denote the different periods distinguished (Table 5.6).

Figure 5.3 displays the bulk liquid total ammonium (TNH), total nitrite (TNO₂) and nitrate concentrations (Figure 5.3A) and the corresponding bulk liquid FA and FNA concentrations (Figure 5.3B), calculated from the total ammonium and total nitrite concentrations, considering the reactor temperature and pH (Anthonisen *et al.* 1976). Table 5.7 summarizes the results of the correlation analysis of the physical and chemical data.

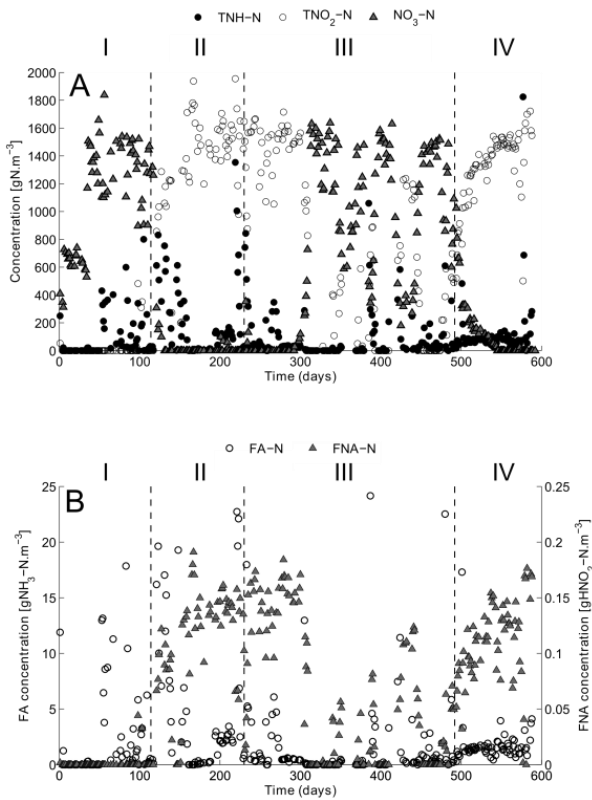


Figure 5.3 Bulk liquid concentrations of total ammonium (TNH), total nitrite (TNO₂) and nitrate during the experiment (plot A), taken from Bougard *et al.* (2006a) and the corresponding free ammonia (FA) and free nitrous acid (FNA) concentrations (plot B), calculated based on reactor temperature and pH (Anthonisen *et al.* 1976). The roman numbers denote the different periods of the experiment (Table 5.6). Note the different scales of the y-axes in plot B.

The strongest significant correlation observed for temperature, was the negative correlation with nitrate ($r = -0.39$, $p < 0.05$, Table 5.7), confirming the lower production of nitrate at higher temperature, which was the basis for the temperature control strategy applied in Period II (Table 5.7).

The oxygen concentration in the bulk liquid was negatively correlated with the total ammonium in the bulk liquid ($r = -0.21$, $p < 0.05$, Table 5.7) and with the nitrogen loading rate ($r = -0.45$, $p < 0.05$, Table 5.7). An increasing NLR and bulk liquid concentration of total ammonium thus result in a decreasing bulk liquid oxygen concentration for the prevailing fixed aeration flow rate, due to the increasing biological activity and oxygen consumption of the nitrifiers.

The FA concentration increased ($r = 0.74$, $p < 0.05$) and the FNA concentration decreased ($r = -0.29$, $p < 0.05$) with increasing pH (Table 5.7), following the expected patterns (Anthonisen *et al.* 1976). The strong correlation indicates that small deviations from the pH set-point (see Figure 5.2) could have large effects on the FA and FNA concentration. The concentrations of FA and FNA observed in the bulk liquid were equal to or even higher than the median value of the reported FA inhibition constants for NOB and FNA inhibition constants for AOB and NOB (Figure 5.4), indicating possible inhibition of the NOB by FA and the AOB and NOB by FNA.

Overall, from the correlation analysis of the physical and chemical data, it can be concluded that temperature, DO and nitrogen loading rate, besides pH had a large influence on the bulk liquid concentration of the different nitrogen compounds and thus constituted suitable control handles for process operation.

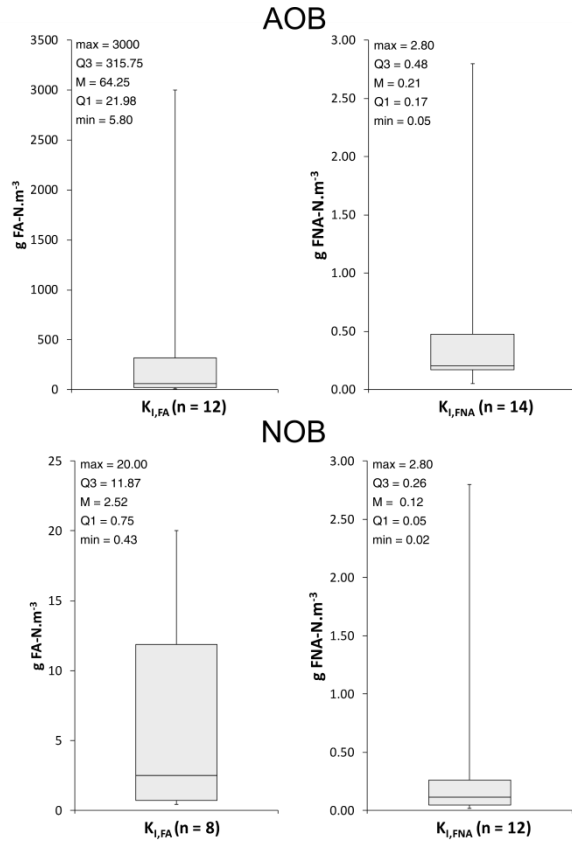


Figure 5.4 Boxplots representing the reported ranges for inhibition constants for FA ($K_{I,FA}$, left) and FNA ($K_{I,FNA}$, right) of AOB (top) and NOB (bottom) found in literature. Max = maximum value found in literature, Q3= third quartile, M = median, Q1= first quartile and min = minimum value. The raw data of the literature review can be found in Appendix 5A. It should be noted that FA inhibition of AOB and FNA inhibition of NOB is generally described by a Haldane term, while FNA inhibition of AOB and FA inhibition of NOB is described with a non-competitive inhibition term.

5.5.1.2 Microbial community information

The fraction of AOB and NOB in the biofilm (qPCR) and the diversity of the total and nitrifying community (CE-SSCP) are summarised in Figure 5.5A and Figure 5.5B, respectively. In Table 5.8, the correlation analysis considering the microbial community related to the physical and chemical data is given.

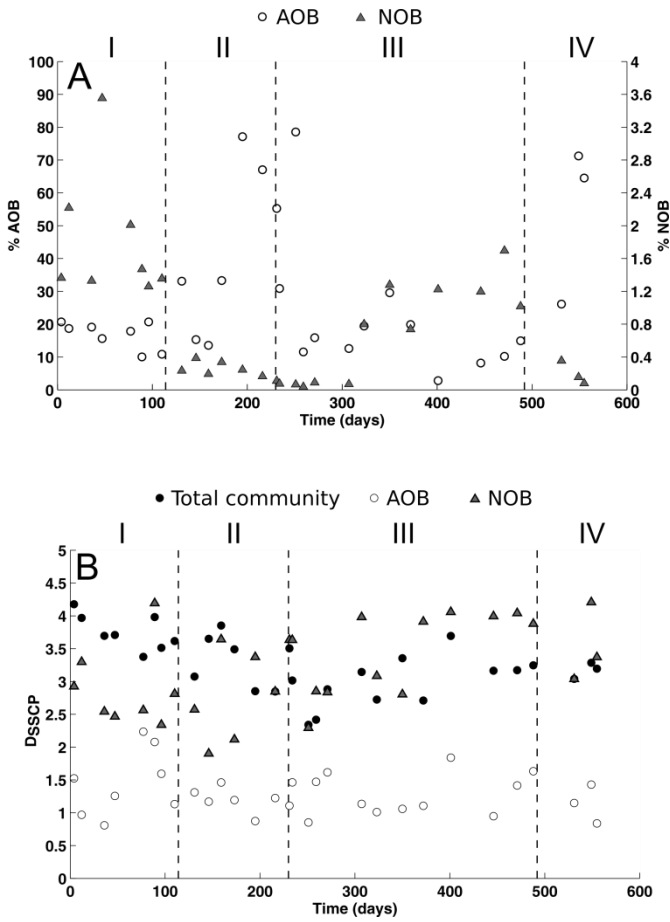


Figure 5.5 Information on the microbial composition of the biofilm: (A) the percentage of AOB and NOB in the microbial community ($n=30$), based on qPCR-analysis and (B) the diversity of the microbial community ($n=30$), analysed using CE-SSCP and expressed as the negative logarithm of the Simpson index, D_{SSCP} . The roman numbers denote the different periods distinguished (Table 5.6). Note the difference scales of the y-axes in plot A.

Table 5.8 Correlation matrix between data on the process conditions and the microbial community (n=28). Correlation coefficient r and p-value are given. Bold values refer to significant correlations (p-value<0.05).

	Fraction AOB (%)	Fraction NOB (%)	Diversity total community (D')	AOB diversity (D')	NOB diversity (D')
TNH (g TNH-N.m ⁻³)	0.07 (0.71)	-0.34 (0.07)	-0.12 (0.53)	0.1 (0.6)	-0.16 (0.39)
TNO ₂ (g TNO ₂ -N.m ⁻³)	0.63 (p<0.01)	-0.78 (p<0.01)	-0.45 (0.01)	-0.22 (0.24)	0.04 (0.83)
NO ₃ (g NO ₃ -N.m ⁻³)	-0.57 (p<0.01)	0.72 (p<0.01)	0.24 (0.19)	0.27 (0.16)	0.2 (0.29)
FA (g NH ₃ -N.m ⁻³)	-0.07 (0.7)	-0.2 (0.3)	0.07 (0.72)	-0.01 (0.96)	-0.27 (0.14)
FNA (g HNO ₂ -N.m ⁻³)	0.64 (p<0.01)	-0.73 (p<0.01)	-0.48 (0.01)	-0.26 (0.16)	-0.02 (0.91)
Temperature (°C)	0.28 (0.13)	-0.34 (0.07)	0.06 (0.77)	-0.14 (0.45)	-0.36 (0.05)
DO (g O ₂ .m ⁻³)	0.04 (0.85)	-0.02 (0.9)	0.13 (0.48)	-0.29 (0.11)	0.18 (0.34)
pH	-0.09 (0.64)	-0.1 (0.6)	0.2 (0.3)	0.13 (0.49)	-0.27 (0.15)
NLR (g N.m ⁻³ .d ⁻¹)	0.14 (0.45)	0.1 (0.59)	0.07 (0.71)	0.42 (0.02)	-0.02 (0.93)
C/N-ratio (g COD.g N ⁻¹)	-0.19 (0.31)	0.3 (0.1)	0.33 (0.07)	-0.06 (0.76)	0.22 (0.25)
Fraction AOB (%)		-0.47 (0.01)	-0.39 (0.04)	-0.41 (0.02)	-0.09 (0.65)
Fraction NOB (%)			0.53 (p<0.01)	0.22 (0.25)	-0.07 (0.71)
Diversity total community (D _{SSCP})				0.28 (0.14)	0.03 (0.88)
AOB diversity (D _{SSCP})					0.18 (0.35)
NOB diversity (D _{SSCP})					

The fraction of AOB was positively correlated ($r = 0.63$, $p < 0.05$) with the total nitrite concentrations and the fraction of NOB was correlated negatively ($r = -0.78$, $p < 0.05$) with the nitrite concentration and positively ($r = 0.72$, $p < 0.05$) with the nitrate concentration (Table 5.8). This indicates that the qPCR analysis based on the *amoA* and *nrxA* genes correctly targeted the AOB and the NOB, respectively.

The overall fraction of AOB ($28 \pm 21.86\%$) was higher than the fraction of NOB ($0.84 \pm 0.82\%$) in the biofilm (Figure 5.5A), as expected from the yield differences in AOB and NOB (Winkler *et al.* 2012).

Logically, the fraction of NOB decreased in the periods of nitrite accumulation (Table 5.6), reaching a minimum of 0.04% during period III (Figure 5.5A). This low biomass content explains why it took so long before the system could reach again complete conversion of ammonium to nitrate in period III (Table 5.6). The nitrogen loading rate had to be reduced several times (Figure 5.2) to

relax the inhibitory conditions and oxygen limitation, in order to allow NOB growth in the biofilm and get the system back to full nitrification, which was necessary to test an alternative control for nitrite accumulation in Period IV. Elawwad *et al.* (2013) shows that NOB are indeed more sensitive than AOB to starvation and require longer periods for complete recovery.

Although diversity was calculated from SSCP profiles and only strong tendencies can be significant, some trends were visible (Figure 5.5B). The diversity of the total community was maximal at day 4 ($D_{SSCP} = 4.18$), declined to its minimum ($D_{SSCP} = 2.34$) during Period III (Figure 5.5B) and was negatively correlated with total nitrite ($r = -0.45$, $p < 0.05$) and FNA ($r = -0.48$, $p < 0.05$) concentrations, which shows total diversity decreased when nitrite accumulated. The diversity of the total community ($D_{SSCP} = 3.29 \pm 0.45$) resembled the diversity of the NOB ($D_{SSCP} = 3.17 \pm 0.66$), while the AOB diversity ($D_{SSCP} = 1.30 \pm 0.35$) was clearly lower (Figure 5.5B). The fraction of AOB and NOB were indeed negatively ($r = -0.39$, $p < 0.05$) and positively ($r = 0.53$, $p < 0.05$) correlated with the total diversity, respectively (Table 5.8). These observations indicate that the NOB diversity was higher than the AOB diversity.

The highest AOB diversity ($D_{SSCP} \approx 2$) was observed in period I around day 77 (Figure 5.5B), which corresponds with the coexistence of *Nitrosomonas halophila* and *Nitrosomonas europaea* in the biofilm reported by Bougard *et al.* (2006a). When *Nitrosomonas europaea* was the only AOB in the biofilm from day 100, the D_{SSCP} value declined to 1.

The NOB diversity reached its lowest value ($D_{SSCP} = 1.90$) during Period II (Figure 5.5B), when the reactor was submitted to temperature control (Table 5.6). Surprisingly, high NOB diversity (up to $D_{SSCP} = 4.21$) was observed during Period IV, when fuzzy-logic control of the inflow rate was used to adjust the NLR (Table 5.6). This could confirm the conclusion of Bougard *et al.* (2006a) that, although both control strategies resulted in nitrite accumulation, the fuzzy-logic controller of the inflow rate in Period IV maintained the microbial diversity better than temperature control. It was indeed an objective to design the controller of Period IV, adjusting the NLR,

(1) good enough to accumulate steadily nitrite within the reactor but (2) bad enough to maintain the microbial diversity (Bougard *et al.* 2006a). The maintenance of overall microbial diversity is important to ensure reactor performance and process stability on the long term, e.g., when facing disturbances (Daims *et al.* 2001b; Egli *et al.* 2003; Ramirez *et al.* 2009) or when the decision is taken to go back to complete nitrification after nitrite accumulation (Bougard *et al.* 2006a).

5.5.2 Modelling the dynamic reactor behaviour

5.5.2.1 Approach 1: Conventional model (1 AOB and 1 NOB) for whole period

Preliminary simulations had shown that, in order to be able to reflect the overall dynamic reactor behaviour, i.e., nitrite or nitrate accumulation besides residual ammonium bulk liquid concentration, the microbial parameters of both AOB and NOB needed to be calibrated. Furthermore, based on the literature study on FA and FNA inhibition of AOB and NOB, it was concluded that the observed FA and FNA concentrations were high enough to be possibly inhibiting for both AOB and NOB. Therefore, FA and FNA inhibition were added to the model following Jubany *et al.* (2009). Therefore, by minimizing the sum of the squares of the weighted difference (χ^2) between experimental measurements and simulation results of bulk liquid total ammonium (TNH), total nitrite (TNO₂) and nitrate concentration, the maximum growth rate, decay rate, affinity for electron donor and acceptor and inhibition constants for FA and FNA inhibition were estimated for AOB and NOB.

First, it was attempted to simulate the macroscale dynamics (Approach 1) by calibrating a single AOB and a single NOB population, each characterized by lumped parameter values reflecting the mean behaviour of their functional guild, as is common practice in nitrification process models. Even for the best possible fit (χ^2_{tot} : 2197; χ^2_{TNH} : 1291; $\chi^2_{\text{TNO}_2}$: 419; $\chi^2_{\text{NO}_3}$: 487, see Figure 5.6), the overall dynamics were not simulated correctly: nitrite accumulated during the simulation of Period III (Table 5.6), while in this period the system was brought back from nitrite to nitrate accumulation by lowering the NLR (Table

5.6). Furthermore, the model efficiencies considering total ammonium ($E_{\text{TNH}} = -2.98$), total nitrite ($E_{\text{TNO}_2} = -0.29$) and nitrate ($E_{\text{NO}_3} = -0.50$) were all below zero. In conclusion, it was not possible to simulate the whole experimental period with a single AOB and a single NOB population. This indicates that one or more significant population shifts had taken place during the whole experimental period.

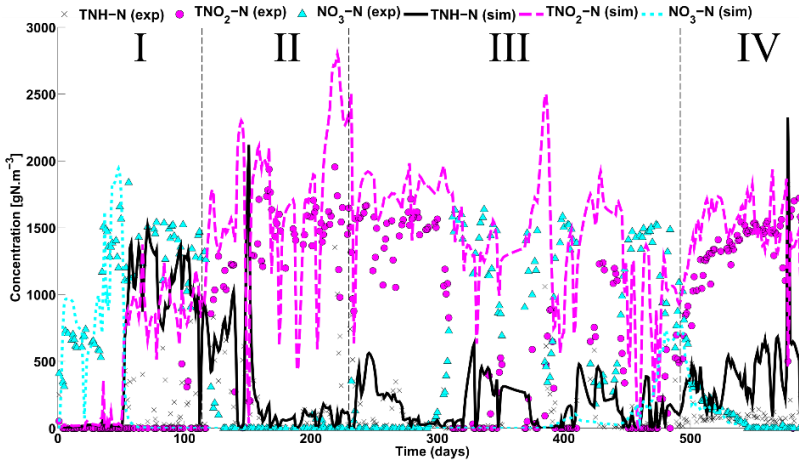


Figure 5.6 Simulation of the bulk output of the reactor using the calibrated 1-dimensional biofilm model considering the growth and decay of 1 AOB and 1 NOB population (Approach 1), besides heterotrophs. Exp: experimental data and sim: simulated data. The roman numbers denote the different periods distinguished (Table 5.6).

5.5.2.2 Approach 2: Conventional model (1 AOB and 1 NOB) distinguishing two periods

As it was not possible to simulate the whole experimental period with a single AOB and a single NOB population, it was decided to split up the experimental dataset into the two periods i.e. Period A (0 – 100 days) and Period B (100 – 592 days), shown by Bougard *et al.* (2006a) to be dominated by two different AOB species: *Nitrosomonas halophila* and *Nitrosomonas europaea*, respectively. The model was then calibrated individually for these periods and the relative changes of the parameter values over these two periods were verified.

The process performance ($\chi^2_{\text{tot}} = 1334$) was better reflected when the model was calibrated for Period A ($\chi^2_{\text{tot}_A}$: 254; χ^2_{TNH} : 63; $\chi^2_{\text{TNO}_2}$: 109; $\chi^2_{\text{NO}_3}$: 82) and Period B ($\chi^2_{\text{tot}_B}$: 1080; χ^2_{TNH} : 693; $\chi^2_{\text{TNO}_2}$: 168; $\chi^2_{\text{NO}_3}$: 219) separately (Approach 2, Figure 5.7). Although the Nash Sutcliffe criterion was negative for total ammonium ($E_{\text{TNH}} = -0.11$), total nitrite ($E_{\text{TNO}_2} = -0.91$) and nitrate ($E_{\text{NO}_3} = -0.43$) in Period A and for total ammonium ($E_{\text{TNH}} = -1.61$) in Period B, the model efficiencies obtained were generally larger than in Simulation 1. Moreover, the model efficiencies for total nitrite ($E_{\text{TNO}_2} = 0.37$) and nitrate in Period B ($E_{\text{NO}_3} = 0.18$) were higher than zero. Even now, the model efficiencies (Nash Sutcliffe criterion) were quite low, due to the large variability of the dataset. However, using Approach 2, the model was shown to reflect the overall reactor behaviour better, also by visual inspection (Figure 5.7). This led to the conclusion that, in order to be able to reflect the experimental observations, the model had to be calibrated during two periods: Period A (0-100 days) and Period B (100-592 days). These periods were based on the AOB population shift observed by Bougard *et al.* (2006a): in Period A, *Nitrosomonas halophila* was a dominant AOB, while in Period B, this species was completely replaced by *Nitrosomonas europaea*. The CE-SSCP data described in this study indicated that the AOB diversity was indeed highest when both AOB coexisted around day 50.

The calibrated microbial parameters of both AOB and NOB were different for both periods (Table 5.9). This indicates that besides the AOB shift, also

changes in the NOB guild were taking place around day 100. Although identification of the dominant bacterial peaks of the SSCP profiles using the cloning-sequencing technique revealed no NOB nor a NOB shift (Bougard *et al.* 2006a), it is possible that besides the visible AOB shift, also undetected microbial community changes were occurring in the NOB guild.

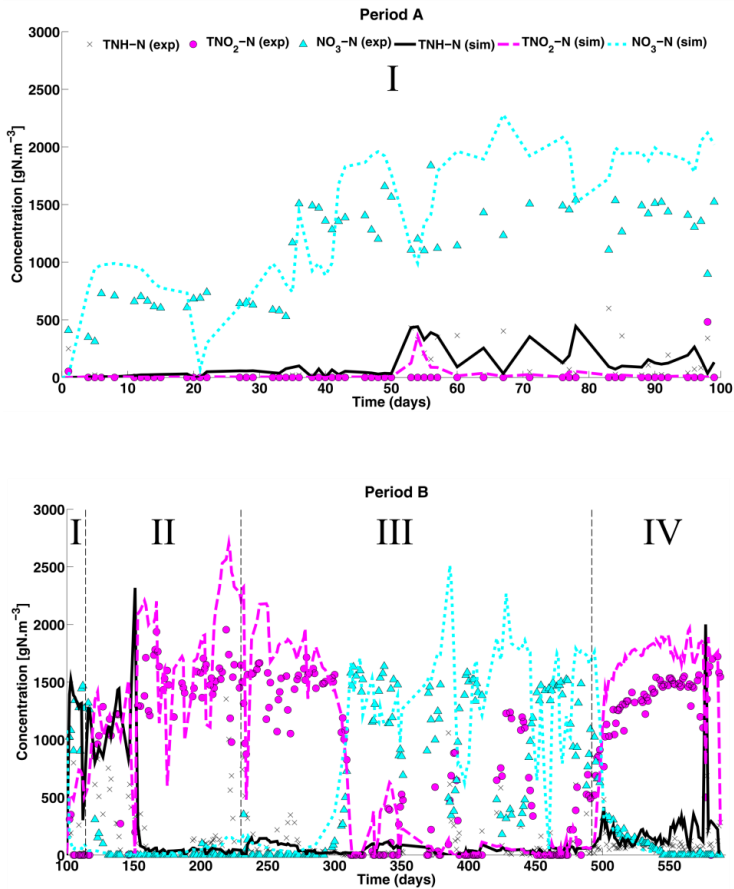


Figure 5.7 Simulation of bulk output of the reactor of Period A (top) and Period B (bottom) using the calibrated 1-dimensional biofilm model (exp: experimental data and sim: simulated data). The roman numbers denote the different periods distinguished (Table 5.6).

Table 5.9 Constraints and calibrated microbial parameters values for AOB and NOB at 30 °C and pH 7.5 when two periods were calibrated, i.e., Period A: day 0-100 and Period B: day 100-592 (Approach 2). The calibrated values should be carefully interpreted, as the uncertainty of the estimated values was not verified.

		Starting (median) value	Minimum value	Maximum value	Calibrated value Period A	Calibrated value Period B
$K_{I,FA}^{AOB}$	g FA-N.m ⁻³	64.25	5.80	3000	490.51	489.05
$K_{I,FA}^{NOB}$	g FA-N.m ⁻³	2.52	0.43	20	12.93	10.06
$K_{I,FNA}^{AOB}$	g FNA-N.m ⁻³	0.21	0.05	2.80	0.42	0.21
$K_{I,FNA}^{NOB}$	g FNA-N.m ⁻³	0.12	0.02	2.80	0.27	0.13
K_{FA}^{AOB}	g FA-N.m ⁻³	0.23	0.0018	1.29	1.25	1.29
K_{FNA}^{NOB}	g FNA-N.m ⁻³	1.04e-004	3.12e-006	2.41e-003	0.0015	0.0024
$K_{O_2}^{AOB}$	g O ₂ .m ⁻³	0.40	0.07	3	0.078	0.71
$K_{O_2}^{NOB}$	g O ₂ .m ⁻³	0.97	0.04	4.01	0.049	0.06
μ_{max}^{AOB}	d ⁻¹	1.34	0.33	3.40	0.65	0.71
μ_{max}^{NOB}	d ⁻¹	1	0.24	3.54	1.43	0.30
b_{AOB}	d ⁻¹	0.067	0.017	0.17	0.073	0.061
b_{NOB}	d ⁻¹	0.05	0.012	0.18	0.13	0.051

The oxygen affinity constant of AOB differed clearly between Period A and Period B (Table 5.9). In Period A, the AOB guild is typified by a high affinity for oxygen ($K_{O_2}^{AOB} = 0.078 \text{ g O}_2\cdot\text{m}^{-3}$) but a low maximum growth rate ($\mu_{\max}^{AOB} = 0.65 \text{ d}^{-1}$) and in Period B by a low affinity for oxygen ($K_{O_2}^{AOB} = 0.71 \text{ g O}_2\cdot\text{m}^{-3}$) but a higher maximum growth rate ($\mu_{\max}^{AOB} = 0.71 \text{ d}^{-1}$). This indicates that the drop of DO concentrations to very low values (between $0.3 - 0.7 \text{ g O}_2\cdot\text{m}^{-3}$) at the end of period I (Table 5.6), following an increase of the NLR (Figure 5.2), was governing the observed AOB population shift from *Nitrosomonas halophila* to *Nitrosomonas europaea*, following the K- and r-strategy concerning oxygen (Andrews & Harris 1986), respectively. The observed diversity of AOB (Figure 5.5B) was very low and declined even more after *Nitrosomonas halophila* was washed out of the biofilm. It can thus be concluded that the calibrated microbial parameters for the AOB probably correspond with the observed species, i.e. *Nitrosomonas halophila*, dominant during the most of Period A and *Nitrosomonas europaea*, dominant during Period B.

Also the NOB community changed between the two periods. As for the AOB, the oxygen affinity of the NOB decreased from Period A ($K_{O_2}^{NOB} = 0.049 \text{ g O}_2\cdot\text{m}^{-3}$) to Period B ($K_{O_2}^{NOB} = 0.06 \text{ g O}_2\cdot\text{m}^{-3}$), further identifying the drop of bulk liquid oxygen concentrations following an NLR increase in Period I (Table 5.6) as the main reason for the population shift. However, for the NOB, the maximum growth rate decreased from $\mu_{\max}^{NOB} = 1.43 \text{ d}^{-1}$ in Period A to $\mu_{\max}^{NOB} = 0.30 \text{ d}^{-1}$ in Period B, in contrast to the maximum growth rate of the AOB. Furthermore, in Period A, the NOB guild was typified by a high growth rate (1.43 d^{-1}) and a high affinity for oxygen ($0.049 \text{ g O}_2\cdot\text{m}^{-3}$). However, this does not exclude that several subdominant species of NOB, both r-strategists (high growth rate) and K-strategists (high oxygen affinity) were present in very low concentrations. The coexistence of several subdominant NOB species was judged likely as a high diversity of NOB was expected based on the similarity of the NOB and total bacterial community diversity revealed by the CE-SSCP analysis of the current contribution (Figure 5.5B) and the decrease of the total bacterial community diversity when NOB were washed out during nitrite

accumulation (Table 5.8). Furthermore, the coexistence of different NOB species was already observed in biofilms (Schramm *et al.* 1998; Gieseke *et al.* 2003; Downing & Nerenberg 2008). Therefore, it can be concluded that the calibrated microbial parameters for Period A and Period B probably represent lumped parameters for different NOB populations and represent two different NOB guilds rather than two different NOB species.

The possibility to simulate the bulk output of the reactor in Period B (Figure 5.7B), using a model considering the growth of 1 AOB and 1 NOB, indicates that in this case no diversity needed to be included in the model to explain the bulk liquid nitrogen concentrations and that the implemented control strategies for nitrite accumulation, i.e., temperature control and fuzzy-logic control of the liquid flow rate to adjust the NLR, were influencing the microbial community mainly on the level of guilds (AOB and NOB), as shown by the qPCR analysis. This indicates that, although changes in microbial diversity or population shifts in Period B were possible, e.g., low NOB diversity during temperature control and higher NOB diversity during fuzzy-logic control of the inflow rate, as indicated by the CE-SSCP analysis, these changes did not influence the reactor behaviour instantaneously. The extension of biofilm models with within-guild diversity is only necessary when the reactor behaviour is clearly influenced by changes in the microbial community, see Chapter 3 (Vannecke *et al.* 2015). However, these unnoticed changes in microbial composition and diversity of the (nitrifying) community may have important effects on the reactor performance and process stability on the long term, e.g., when facing disturbances (Daims *et al.* 2001b; Egli *et al.* 2003; Ramirez *et al.* 2009) or when the decision is taken to go back to complete nitrification after nitrite accumulation (Bougard *et al.* 2006a).

For both periods, no concentration profiles could be observed in the biofilm. The steady state biofilm thickness was indeed very small, reducing the effect of internal mass transfer limitation, similar to the observations in Chapter 4 for the same biofilm reactor type. Although CE-SSCP indicates a rather high NOB diversity, this diversity will probably not have resulted from the presence of different niches in the biofilm due to diffusional substrate gradients. Therefore,

the assumption of a uniform distribution of all biomass over 80% of all the particles is unlikely to be true: some particles will be covered with a very thin biofilm while others are covered with a thicker biofilm, allowing different species to occupy different niches.

5.5.2.3 *Approach 3: Model including within-guild diversity (2 AOB and 2 NOB) for whole period*

As Period A and Period B could be described individually by a single AOB and a single NOB species (see Table 5.9 for their characteristics), these two AOB and two NOB populations were integrated in one model to simulate the bulk output of the reactor of the whole experimental period (592 days).

It was not possible to calibrate the model including 2 AOB and 2 NOB populations, besides 1 heterotrophic population, to describe bulk liquid concentrations of ammonium, nitrite and nitrate over the complete experimental period (Approach 3, Figure 5.8). The model predicted nitrate accumulation for the whole experimental period, therefore, the overall fit of the simulation results for bulk liquid nitrogen concentrations was very low ($\chi^2_{\text{tot}} = 3204$). Also the model efficiencies for total ammonium ($E_{\text{TNH}} = -0.44$), total nitrite ($E_{\text{TNO}_2} = -1.26$) and especially for nitrate ($E_{\text{NO}_3} = -5.19$) were shown to be lower than zero.

The AOB and NOB species of Period A remained dominant during Period B, while the AOB and NOB species of Period B should become dominant after 100 days. The species of Period B were not able to survive the severe drop in DO starting around day 50, due to their lower affinity for oxygen than the species from Period A. In the real system, the species of Period B could have invaded the system by attachment from the bulk liquid, while in the model attachment was neglected and the influent was assumed to contain no bacterial species. Alternatively, the populations of Period A could have been acclimated to the conditions in Period B, which also can result in changed parameter values. Furthermore, as calibrated parameters such as the affinity constants may describe apparent features, lumping other phenomena such as diffusion (Arnaldos *et al.* 2015), these phenomena may have been changing over the experimental period.

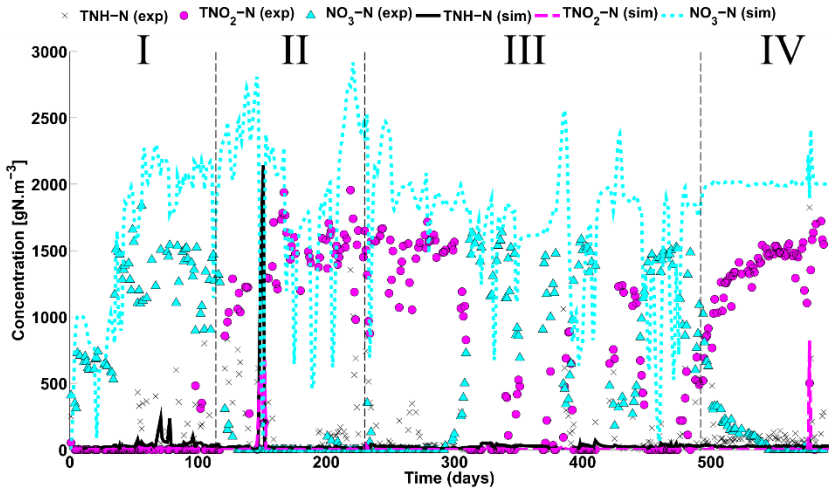


Figure 5.8 Simulation of the bulk output of the reactor using the calibrated 1-dimensional biofilm model considering the growth and decay of 2 AOB and 2 NOB species (Approach 3), besides heterotrophs. Exp: experimental data and sim: simulated data. The roman numbers denote the different periods distinguished (Table 5.6).

5.6 Conclusions

Using a correlation analysis and a simulation study, the influence of process dynamics on the nitrifying microbial community in a nitrifying inverse turbulent bed reactor, controlled for nitrite accumulation, was analysed.

From the correlation analysis of the physical and chemical data, it can be concluded that temperature, bulk liquid oxygen concentration and nitrogen loading rate, besides pH had a large influence on the bulk liquid concentration of the different nitrogen compounds and thus constituted suitable control handles for process operation.

In order to be able to reflect the experimental observations, a 1-dimensional biofilm model with FA and FNA inhibition, considering growth and decay of 1 AOB population, 1 NOB population and 1 heterotrophic population, each characterized by lumped parameter values reflecting the mean behaviour of their functional guild, had to be calibrated during two periods. These periods corresponded with a previously observed AOB population shift. The difference of calibrated microbial parameters of the AOB and NOB in the two calibrated periods indicates that besides a previously observed AOB population shift, also

the NOB guild was changed due to an increased nitrogen loading rate resulting in a drop of the bulk liquid oxygen concentration.

The diversity of the total bacterial community resembled the diversity of the NOB, while the diversity of the AOB was much lower. A large number of small, subdominant NOB populations was presumably present in the biofilm. The calibrated AOB parameter values for the two different periods correspond probably with two different AOB species (*Nitrosomonas halophila* and *Nitrosomonas europaea*), while the NOB parameters represent two different NOB guilds.

Although CE-SSCP analysis indicated that the two considered control strategies for nitrite accumulation (temperature control and fuzzy-logic control of the liquid flow rate) may have influenced the microbial diversity, the bulk liquid ammonium, nitrite and nitrate concentration was shown not to be influenced by these control strategies using the developed biofilm model. However, it should be noted that unnoticed changes in diversity can influence the reactor performance and process stability in the long term.

5.7 Appendix 5A: Literature review on FA and FNA inhibition of nitrifiers

The results of the literature review on the FA and FNA inhibition of AOB and NOB are summarized in Table A.5.1.

Table A.5.1 Values of the FA and FNA inhibition constants for AOB and NOB found in literature. Growth type: S = suspended growth and A = attached growth. Publication type: E = experimental determination, C = calibration of model based on experimental results and L = other literature values. It should be noted that FA inhibition of AOB and FNA inhibition of NOB is generally described by a Haldane term, while FNA inhibition of AOB and FA inhibition of NOB is described with a non-competitive inhibition term.

	AOB		NOB		Growth type	Publication type	Publication
	K_{FA}^{AOB} g FA-N.m ⁻³	K_{FNA}^{AOB} g FNA-N.m ⁻³	K_{FA}^{NOB} g FA-N.m ⁻³	K_{FNA}^{NOB} g FNA-N.m ⁻³			
1	95.53	0.18	0.43	0.019	S	L	Baquerizo <i>et al.</i> (2005)
2				0.19	S	E	Boon and Laudelout (1962)
3		0.245			S	E	Brouwer (1995)
4	11.4			0.018	S	E/C	Carrera <i>et al.</i> (2004)
5	48.09			0.105	A	E/C	Carrera <i>et al.</i> (2004)
6	51.9			0.1	A	E	Carvalho <i>et al.</i> (2002)
7			1.13		S	E/C	Chandran and Smets (2000)
8	605.48	0.49			S	E	Ganigue <i>et al.</i> (2007)
9		0.2			S	E	Hellinga <i>et al.</i> (1998)
10		0.21		0.27	S	L	Hellinga <i>et al.</i> (1999)
11				0.13	S	E/C	Jubany <i>et al.</i> (2005)
12	5.8	0.16	0.78	0.018	S	E	Jubany <i>et al.</i> (2008)
13	76.6	0.16			S	E	Jubany <i>et al.</i> (2009)
14		0.203			S	E	Lochtman (1995)
15	24.9	0.44	14.18	2.31	S	E/C	Magri <i>et al.</i> (2007)
16	241	0.053	3.9 or 11.1		S	E/C	Pambrun <i>et al.</i> (2006)
17	13.23	0.168	0.644	0.0595	S	E/C	Park and Bae (2009)
18		0.57			S	E/C	Vadivelu <i>et al.</i> (2006a)
19		2.04			S	E	Van Hulle <i>et al.</i> (2007)
20	3000	2.8	20	2.8	S	L	Wett and Rauch (2003)
21	540			0.26	S	E	Wiesmann (1994)
$\mu \pm SD$	392.83±846.68	0.57±0.81	6.19±8.64	0.52±0.96			

6

Conclusions & perspectives

The overall goal of this PhD research was to study the interaction between microbial community structure, process performance and operational conditions in biofilm reactors for biological nitrogen removal from wastewater.

Conclusions on the incorporation of microbial diversity and competition in 1-dimensional biofilm models, the influence of microbial diversity on steady state and dynamic behaviour of nitrifying biofilms and biofilm reactors and the influence of process conditions and microbial characteristics on microbial competition are given below. These conclusions are supplemented with perspectives and suggestions for future research.

6.1 Modelling microbial diversity in nitrifying biofilms

6.1.1 Rationale behind the inclusion of microbial diversity

Conventional nitrifying biofilms models only make a distinction between the functional guilds, i.e., ammonium oxidation by AOB and nitrite oxidation by NOB, although a large variety of microbial parameter values for nitrifiers (maximum growth rate, affinity and yield) is reported in literature (Chapter 2). This variety is especially a consequence of the large microbial biodiversity detected in nitrifying biofilm systems. Depending on the aims of a study, it can be important to implement this observed nitrifying diversity in mathematical biofilm models.

In this thesis, it was shown that multispecies models including microbial diversity are useful tools to investigate the individual influence of various microbial characteristics on microbial population dynamics (Chapter 2). Nitrifying biofilm models including the growth of several species performing the same function not only demonstrate that a constant effluent composition may be hiding major microbial community shifts (Chapter 3), but can also be used to investigate experimentally observed microbial population shifts resulting in a different nitrifying performance (Chapter 4).

It is likely a general rule that the inclusion of microbial diversity in models, which results in an increased model complexity, will be more useful when the

focus is on understanding microbial competition and coexistence or for research addressing fundamental ecological questions on microbial competition and niche partitioning, see for example Chapter 2 and 3. In Chapter 2, the factors influencing microbial competition and coexistence at steady state were analysed. In Chapter 3, the change of a nitrifying community in a biofilm was modelled over time until steady state on both the bulk and the microbial composition of the biofilm were at steady state. In Chapter 3, the functional redundancy of a nitrifying community, i.e., the possibility of a changed nitrifying community to function equally as the original one, upon an increased nitrogen loading rate, was also verified. Moreover, in Chapter 2 and 3, the hypothesis that in biofilms ecophysiologicaly different species, both from the same or a different functional guild, can coexist due to the creation of different niches by diffusional substrate gradients, was tested.

When the focus is on substrate removal rates and optimal bulk conditions, the consideration of microbial diversity is clearly not always necessary. Eberl *et al.* (2006) emphasize the value of identifying model features that can be omitted without decreasing the utility of the model for its intended purpose, as summarized in their “golden rule” of modelling: “a model should be as simple as possible, and only as complex as needed.” However, additional model features such as within-guild diversity can be critically informative for bulk reactor behaviour prediction or understanding, for example if molecular data indicates changes in the species composition of the biofilm and these shifts are correlated with changes in the process performance, as demonstrated in Chapter 4. Also under specific conditions, for example upon environmental or operational changes such as an increased nitrogen loading rate, gaining insights on how the microbial community is affected, based on models including diversity, can be very informative (see Chapter 3). Furthermore, if the bulk liquid output of the reactor has changed, but no molecular data is available, models considering different guilds and different species per guild could help to identify possible microbial population shifts governing the changes in process performance.

Mathematical models considering within-guild diversity have important roles to play in the view of synthetic ecology, which is the design and construction of microbial communities with desirable properties (Fredrickson 2015) and the management of available microbial resources in open systems where the dynamics of microbial ecology are dominant, e.g., for research on wastewater treatment population optimization (Yuan & Blackall 2002) and on microbial resource management (Verstraete *et al.* 2007). These models could help in finding the answers on the questions of who is there, who is doing what with whom and how can one adjust, control and/or steer these mixed cultures and communities.

In conclusion, one should consider to implement diversity in models when the research topic is microbial ecology and competition. Also, when bulk composition is shown to be influenced by microbial community dynamics and microbial community information (such as fingerprinting information and/or metagenomics) is available, implementation of within-guild diversity in models could be very rewarding, especially if the aim is to develop control strategies for microbial population optimization.

6.1.2 Strategies to implement microbial diversity

In this thesis, different species performing the same function were represented by different kinetic parameter sets. As microbial properties cannot be defined with certainty, two different stochastic methods were used in this thesis to implement the reported diversity of microbial characteristics in mathematical models. Both methods were based on the extensive literature review on reported ranges for maximum growth rate, affinity for electron donor and acceptor and yield from Chapter 2. The different species in the model can be given similar initial concentrations or, if the aim is to investigate the inoculum effect, the initial concentrations of each species can be given different values. Although the models used in this thesis were non-linear and initial conditions can influence the steady state outcome, the initial concentrations of the species did not determine the competition outcome at steady state unless the dominant species were removed from the biofilm (Chapter 2).

6.1.2.1 *The species classes method*

In Chapter 2, the growth and decay of 60 species of AOB and NOB were implemented in a biofilm model. The ranges of maximum growth rate, affinity for electron donor and oxygen, besides yield, reported in literature (Chapter 2) were represented as boxplots. Twelve species classes, with 1 competitive advantage, e.g., a high growth rate, 1 competitive disadvantage, e.g., a low oxygen affinity, and two neutral characteristics were proposed. For each species per species class, values were taken from the following ranges: low values from the range between minimum and the first quartile of the respective boxplot, neutral values from the range between the first and third quartile and high values between the third quartile and the maximum. This approach was used to reflect trade-offs, and thus niche differentiation (Kneitel & Chase 2004) among species of the same functional guild by assuming that 1 competitive advantage comes at the cost of 1 competitive disadvantage, as advantageous traits often have side effects (Futuyma 2005). It should be noted that (1) niche differentiation is a priori supposed using this method and (2) that minimum 1 species per species class should be constructed, resulting in 12 different species. In this thesis, 5 species per class were constructed using the *rand* function in Matlab. Although the obtained numbers were rounded to two digits to the right of the decimal point, the *rand* function provides uniformly distributed random numbers with an accuracy of $1 \cdot 10^{-4}$. It could be possible to test whether closeness of parameter values results in more species coexisting at steady state by constructing many species that are only different in 1 microbial parameter such as the maximum growth rate and varying its value between randomly generated numbers with an accuracy of $1 \cdot 10^{-4}$.

6.1.2.2 *The bimodal distribution method*

For the models used in Chapter 3, the ranges of values for maximum growth rate, affinities for electron donor and oxygen and yield were also based on the literature review described in Chapter 2. However, for each microbial parameter, a normal bimodal distribution was now constructed as in Ramirez *et al.* (2009), who based this distribution on a curve fitting process using experimental data. The eight bimodal distributions were each typified by two

means ($\mu_1 = 0.6 \cdot k$; $\mu_2 = 1.4 \cdot k$) and standard deviations of $\sigma_{1,2} = 0.125 \cdot k$, with k the average value of the range of the corresponding parameter reported in literature (Chapter 2). Alternatively, k could also be the median value of this range, which could be a better choice, as the median is less influenced by outliers. A certain number of species (>2) can then be constructed by randomly picking values from each bimodal distribution. In this thesis, 10 species per type were constructed, by randomly selecting 10 values for maximum growth rate, affinity for electron donor and acceptor, besides yield for AOB and NOB using the Matlab function *randsample*. Considering this method, one should note that, based on the definition of the bimodal distribution, parameters with a larger average or median value (k), such as the maximum growth rate and affinity constants, will differ more between species of the same functional type than parameters such as yield with a smaller average or median value. However, as shown in Chapter 2, the maximum growth rate and affinity constants are the most important parameters influencing the competition outcome. Furthermore, a stoichiometric relationship exists between the amount of electron donor removed and biomass yield, therefore, yield should not differ too much between different species of 1 functional type. Similarly as for the species classes method, the bimodal distribution method could be used to generate a larger number of species to verify if more species can coexist at steady state when their parameter values become closer.

6.1.2.3 Parameter estimation

The microbial parameters representing different species can also be estimated by calibration of the model using experimental information on the bulk liquid composition. In Chapter 4, the microbial parameter values for the two considered AOB species were already calibrated in a previous study based on a 0-dimensional biofilm model (Volcke *et al.* 2008).

By calibrating the (lumped) microbial parameters of the (nitrifying) community over different time periods, using experimental data on the bulk liquid composition, it can be verified whether or not the community changed over these periods. For example, in Chapter 5, the total experimental period was split in two periods based on an observed AOB population shift (detected

by the combination of SSCP and DNA cloning). The nitrifying community was calibrated for these two periods by numerical minimizing the sum of the squares of the weighted difference between actual measurements of the bulk liquid composition and the corresponding simulated results (χ^2) using the secant method in Aquasim. The parameters were calibrated within the constraints of the parameter ranges given in Chapter 2 (maximum growth rate, decay rate and affinity constants) and Chapter 5 (inhibition constants for free ammonia and free nitrous acid). As the parameter values of both the AOB and the NOB changed over the two calibrated periods, it was concluded that besides the observed AOB population shift, also a shift in the NOB guild had taken place.

A model without inclusion of within-guild diversity, can thus be calibrated to get a snapshot in time of the microbial community. It should be noted that in this thesis, the focus was on the microbial diversity in nitrifying biofilms. Therefore, in Chapter 5, no sensitivity analysis was performed but instead it was verified whether or not the simplest model possible was able to simulate the overall reactor behaviour (nitrite versus nitrate accumulation) when only the microbial parameters were calibrated. By checking the total χ^2 -value and visual verification of the fit of the simulation results with the observed overall reactor behaviour, it was found that maximum growth rate, affinity constants for electron donor and acceptor, decay rate and inhibition constants for FA and FNA of both the AOB and the NOB guild needed to be calibrated for two different periods in order to be able to simulate the overall reactor behaviour using a model including 1 AOB population, 1 NOB population and 1 heterotrophic population.

6.1.3 Biological interpretation of the taxa

The rise of next-generation sequencing (NGS) techniques provides us with large datasets on microbial community composition of different ecosystems (Jansson & Prosser 2013; Prosser 2015). However, this large volumes of nucleotide sequences from a variety of strains, species, genera, etc., should be classified and ranked with maximum biological sense (Bertrand *et al.* 2011), although among the different microbiological disciplines there is an important

degree of disagreement on the definition of a microbial species (Rossello-Mora & Amann 2015). Microbes are currently assigned to a common species if their reciprocal, pairwise DNA re-association values are greater than or equal to 70% in DNA–DNA hybridization experiments under standardized conditions and their melting temperature ΔT_m , i.e., the temperature at which half of the DNA in a solution is dissociated into single strands (Lawrence 2005), is less than or equal to 5°C (Stackebrandt *et al.* 2002). Alternatively, strains that are more than 3% divergent in 16S rRNA are nearly always members of different species, as determined by DNA-DNA hybridization (Cohan 2002; Achtman & Wagner 2008; Rossello-Mora & Amann 2015). These definitions lack a true biological basis, in contrast to the biological species concept for eukaryotes, given by Mayr (1942).

The taxa in the models of this study, represented by a specific set of microbial parameters, may correspond to different species by the definition handled by microbial taxonomists. For example, in Chapter 4, the two considered AOB species are representing *Nitrosomonas europaea* (K-strategist) and *Nitrosomonas* sp. (r-strategist) observed by Volcke *et al.* (2008) using molecular data (SSCP in combination with DNA cloning). Coexisting species could also belong to different genera. For example, the NOB species shown to coexist in Chapter 2 and 3 could belong to the genera *Nitrobacter* and *Nitrospira*, similar to the coexisting NOB experimentally observed by (Downing & Nerenberg 2008).

The taxa implemented in the models in this thesis can also represent genetically different populations (strains) of 1 species detected by molecular data or even 1 species acclimated to new conditions. Lydmark *et al.* (2006) observed the coexistence of two genetically different populations of *Nitrosomonas oligotropha* with niche differentiation in a biofilm. The kinetic parameters describing microbial growth and substrate utilization of a species depend also on the adaptation to different operational conditions (Grady *et al.* 1996; Kim 2013). In other words, 1 species can, depending on the environmental conditions, be represented by different microbial parameters in mathematical models.

It is assumed that including a larger (>100) number of species in mathematical models could increase the total number of coexisting species at steady state as the differences in values for maximum growth rate and affinity constants would become smaller. If the total number of species included in mathematical models increases, it is important to consider the biological meaning of the species included in the model. If more and more species would be included per functional guild in mathematical models, the discussion of what is a microbial species could extend to the field of mathematical modelling and environmental engineering.

Furthermore, as discussed in Chapter 5, a set of microbial parameters can also represent a whole guild, made up by 1 or more species performing the same function, if within-guild diversity is not included in the model. In Chapter 5, it was demonstrated that the calibrated microbial parameters of the AOB guild, typified by a very low diversity, for two periods of reactor operation corresponded probably to two AOB species: *Nitrosomonas europaea* (Period A) and *Nitrosomonas halophila* (Period B). Using molecular data, it was shown that the NOB diversity was much higher than the AOB diversity, probably due to the presence of a high number of subdominant NOB species. Therefore, the calibrated microbial parameters of the NOB guild per period were most likely lumped values representing more than 1 NOB species.

6.1.4 Determination of microbial parameters

The large variety in parameter values observed in literature could not only be a consequence of microbial diversity, but also of the different conditions under which the parameters are determined and the large number of different analysis techniques used (Chapter 2).

A large range of different techniques is used for the determination of maximum growth rate and yield (Blackburne *et al.* 2007a) and substrate affinity constants (Riefler *et al.* 1998; Carvallo *et al.* 2002; Guisasola *et al.* 2005), whether or not combined with the calibration of a mathematical model (Munz *et al.* 2012). For aerobic systems, many of the applied methods for determination of kinetic parameters are based on the indirect determination of the substrate uptake

profile by the associated oxygen uptake profile (Riefler *et al.* 1998). However, the operational conditions for parameter determination, for example reactor configuration, pH and temperature can differ substantially. Some incentives were given to standardize the determination of parameters, e.g., Spanjers and Vanrolleghem (1995) and Vanrolleghem *et al.* (1999). In order to make the comparison of parameter values more straightforward and to attribute observed parameter value differences to the applied determination techniques versus the intrinsic microbial characteristics, the use of these standardized analysis techniques is advised.

Also a large microbial diversity of the nitrifying community can give rise to a large variety of parameter values. Therefore, microbial community information should be monitored together with the determination of parameter values. For example, the use of different mixed-culture inocula (Terada *et al.* 2010) versus pure (axenic) cultures (Hunik *et al.* 1992, 1993; Hunik *et al.* 1994) can have a major influence on the microbial species composition of the investigated system and thus the resulting parameter values. Determination of parameter values in combination with culture-independent molecular techniques (Table 1.2) and the next generation sequencing techniques (Table 1.3), could allow the association of the determined parameter values with specific species or even genes and enzymes. The latter would allow the development of trait based models, as done by Allison (2012), who developed a model that links microbial community composition with physiological and enzymatic traits to predict litter decomposition rates. If parameter values differ for the same species, operational conditions may have influenced the microbial characteristics, e.g., one similar microbial community was acclimated to new operational conditions (Kim 2013) or different strains of a species had different metabolic characteristics (Lydmark *et al.* 2006). The combination with genomics and transcriptomics would allow to test whether the acclimated community for example expresses different genes, and which enzymes are active in populations under stress. The interaction between modellers and microbiologists is therefore encouraged in order to keep track of microbial diversity in mathematical modelling.

This interaction is further encouraged by the fact that mathematical models implementing metagenomic data could allow testing central theories in microbial ecology associated with growth rates and other kinetic microbial parameters (Vieira-Silva & Rocha 2010). In metagenomics, attention is often paid on genes that are involved in the conversion of substrates into products, but metagenomics provides little information on quantitative physiological characteristics such as maximum specific growth rate and affinity constants (Prosser 2015). Attempts to determine the genetic and/or genomic basis of these characteristics are in their infancy, although it was shown already that the maximum growth rate can be predicted from sequence alone (Vieira-Silva & Rocha 2010) and in combination with biochemical models the actual growth rate could be predicted (Ibarra *et al.* 2002).

Synthetic microbial ecology has gained a lot of interest in the last few years. Because of their reduced complexity and increased controllability, synthetic communities are often preferred over complex communities to examine ecological theories. Synthetic microbial communities limit the factors that influence the microbial community to a minimum, allowing their management and identifying specific community responses (De Roy *et al.* 2014). These synthetic communities would be of great interest to determine microbial parameter values for modelling, as their microbial composition is known a priori. This would, in combination with metagenomics, proteomics and transcriptomics allow researchers to check gene expression and metabolic pathways of the community under different environmental conditions. Furthermore, further research could be done on the linking of microbial parameters such as affinity constants with certain genes or even enzymes.

In this thesis apparent affinity constants were used, which consider the effect of mixing (advection), substrate limitation (biological limitation) and diffusion (floc characteristics) in flocs (Arnaldos *et al.* 2015) although in biofilm models, the true coefficients corresponding to the kinetics of suspended cells should be used (Pérez *et al.* 2005). This choice was made as the determination of affinity constants on axenic cultures of suspended cells is limited. Furthermore, the focus of this thesis was on the modelling of microbial diversity and its effect

on the overall reactor behaviour, not on the exact prediction of bulk liquid concentrations. Novel modelling strategies that could be followed to alleviate the limitations of the half-saturation index have been presented by Arnaldos *et al.* (2015). One approach could be the integration of models describing transport phenomena with biokinetic models. Although in the models of this thesis, perfect mixing of the bulk liquid is assumed, diffusion and advection of dissolved substances are considered in the biofilm. Therefore, models presented in this thesis could provide a valuable tool for distinguishing diffusion and substrate limitation effects if affinity constants determined on axenic cultures of suspended cells are applied.

6.1.5 Alternative approaches for the modelling of diversity

The modelling in this thesis was performed using the Aquasim software (Reichert 1994), supplemented with Matlab (MathWorks) for data analysis and the construction of plots. The Aquasim software allowed the construction of 1-dimensional biofilm models, considering microbial diversity, in a straightforward way. However, the implementation of a large number of species (> 60 species per type) can be tricky. Furthermore, the interface is quite robust and does not allow to change the underlying differential equations. Possible alternative computational tools for Aquasim are Matlab and Comsol. Comsol Multiphysics (Stockholm, Sweden) gives the users more freedom in the development of the multispecies biofilm model and presents the advantage of a total flexibility in choosing model structure, model equations and domain meshing, a modern graphical user interface and state-of-the-art numerical methods for the model solution (Sierra *et al.* 2014).

It should be noted that, when models including diversity would be used for the prediction of reactor behaviour based on experimental data different from the calibration data set, which was beyond the scope of the current study, uncertainty analysis (Klepper 1997) should be performed in order to assess the uncertainty of the model predictions and output, originating from the uncertainties of the modelling process: (1) epistemic uncertainty, i.e., uncertainty coming from lacking knowledge and (2) stochastic uncertainty, i.e., inherent variability (Oberkampf *et al.* 2004). Some possible

methodologies for uncertainty assessment are (1) Monte Carlo analysis, which traces out the structure of the distributions of the model output based on the probability functions of all the inputs and parameters and (2) error propagation equations (Refsgaard *et al.* 2007).

Concerning microbial diversity, further simulation studies based on multispecies nitrification biofilm models are required to investigate the individual role of various microbial characteristics and operation conditions on microbial competition. Besides, there is increasing interest in explicitly incorporating our rapidly expanding understanding of microbial community structure and dynamics via molecular tools into predictive process models. Seshan *et al.* (2014) present an example of this via a support vector regression model using microbial community diversity indices derived from DNA fingerprinting (T-RFLP) to predict reactor removal performance for COD, ammonia, nitrate, and 3-chloroaniline. Wastewater treatment modellers would also be well served by adapting emerging techniques in this direction in biogeochemical modelling. For example, Reed *et al.* (2014) provide a gene-based framework for incorporating environmental genomics data into a model of nitrogen cycling in the Arabian Sea oxygen minimum zone. A similar approach may be possible in bioprocess modelling to refine our understanding of the role of microbial diversity and community dynamics on the bulk composition and microbial biofilm composition in biofilm reactors. Furthermore, in the view of the development of genomics, proteomics and transcriptomics, metabolic pathway models, e.g., Heijnen and Verheijen (2013) and Baroukh *et al.* (2014) could be linked to models including diversity, for example to connect biochemical processes to certain metabolic pathways (Larsen *et al.* 2012; Song *et al.* 2014).

The modelling of microbial diversity and analysis of microbial competition could also be introduced in individual based biofilm models, allowing simulations based on the global consequences of local interactions of members of a population, e.g., single cells. Individual based 2- or 3-dimensional biofilm models were already developed (Picioreanu *et al.* 1998; Kreft *et al.* 2001; Picioreanu *et al.* 2004). These models could be used to verify if a higher steady

state microbial diversity is observed than in 1-dimensional models as substrate concentration gradients are expected to differ spatially due to different biofilm thicknesses. Such a model was already used by Lardon *et al.* (2011), to investigate the metabolic switching of denitrifying bacteria triggered by external oxygen concentrations in chemostats and biofilms. It was found that chemostats show competitive exclusion but biofilms maintain a diverse community, and that this diversity is highest under fluctuating conditions.

Insights in microbial competition may also be achieved by using an individual-based cellular automata approach. Cellular automata models are characterized by a discrete lattice of cells, homogeneity, as all cells are equivalent, discrete states, local interactions and discrete dynamics (Ilachinski 2001). For example, cellular automata were used to verify and reformulate the competitive exclusion principle, postulating that species competing for the same limiting resource in one homogeneous habitat cannot coexist, contradicting with the observed biodiversity in reality (Kalmykov & Kalmykov 2013). Although mostly used for modelling events that occur at discrete time points, cellular automata models are also used to model biological processes that take place continuously, for example to predict interspecific competition outcome (Mancy *et al.* 2013) and to analyze the impact of initial evenness, i.e., the relative distribution of the species present in the microbial community, on the preservation of biodiversity (Daly *et al.* 2015).

In some cases it can be interesting to analyse models of observed population shifts as such without the need for simulation. Volcke *et al.* (2008) demonstrated the applicability of the criteria developed by Hsu *et al.* (1977) and Hsu (1980) for continuous cultures to predict steady state interspecies outcome for 0-dimensional biofilm models, in which a homogenous distribution of solubles and overall biomass throughout the biofilm is assumed. As elaborated in Chapter 4, this strategy is not applicable with 1-dimensional biofilm models. Steady state coexistence of two species performing the same function, as observed in 1-dimensional biofilm models (Chapter 2, Chapter 3 and Chapter 4) is not possible in 0-dimensional models (Tilman 1994) and can thus not be predicted. Furthermore, the criterion used by Volcke *et al.* (2008), to predict

the competition outcome between two AOB species, following the r- and K-strategy related to oxygen, could not be used for 1-dimensional biofilm models when the mean SRT for the coexisting species, instead of the overall SRT, was used. Furthermore, it should also be noted that the simulations with the 1-dimensional model first need to be performed to calculate the SRT regardless of the SRT definition applied. Therefore, when the focus is on biomass distribution in the biofilm and/or microbial coexistence at steady state, 1-dimensional biofilm models should be chosen over 0-dimensional biofilm models, while the latter provide a less computational intensive solution for determining competition outcome when the biofilm thickness is very thin and diffusional substrate gradients can be neglected, as for example observed for the biofilms considered in Chapter 4 ($LF_{SS} = 9.6 \cdot 10^{-6}$ m).

6.2 Influence of microbial diversity on steady state and dynamic reactor behaviour

In this thesis, the influence of microbial diversity on the overall process performance (in terms of bulk liquid composition) was verified. The models developed were used to verify the microbial dynamics and the effects on the overall process performance and bulk liquid composition, not to predict bulk liquid composition based on microbial community information, as done by Seshan *et al.* (2014) or to predict reactor behaviour based on experimental data different from the calibration dataset. Therefore, uncertainty analysis of the simulation results (Klepper 1997) was assumed to be beyond the scope of this study.

Furthermore, apparent affinity constants, considering both diffusion and substrate limitation, were used in biofilm models, resulting in possible too low estimation of the affinity of the considered organisms. This may result in small changes of the bulk liquid composition compared to what in reality can be expected. In Chapter 4 and Chapter 5, the microbial parameters were estimated to experimental data, but there again, the main purpose was to intertwine the microbial community dynamics and not the to predict the bulk liquid composition in future experiments with the same reactor type (ITBR).

Furthermore, in Chapter 2 and 3, the bulk liquid oxygen concentration and temperature were set at a fixed value. As became clear from the dataset used in Chapter 5, this could be seen as an oversimplification. Indeed, more temporal variability in operational conditions (pH, bulk liquid oxygen concentration, temperature) could increase the diversity in reactors, see for example also Hsu (1980), who proposed the coexistence of two species in a chemostat due to seasonal variation in a numerical study.

In this thesis, the mathematical modelling of microbial diversity revealed possible unnoticed, i.e., without effect on the effluent composition, changes in the biofilm microbial composition. For example, in Chapter 2, the influence of nitrogen loading rate and bulk liquid oxygen concentration on the microbial community was verified, using a biofilm model including the growth and decay of 60 AOB and 60 NOB species. It was shown that for different combinations of nitrogen loading rate and bulk liquid oxygen concentration, the steady state microbial composition of biofilms could differ significantly even if the bulk liquid output was very similar. Furthermore, in Chapter 3, it was shown that a steady state effluent composition not necessarily reflects steady state conditions in the biofilm (in terms of biofilm thickness and microbial composition). In Chapter 5, the possibility to simulate the bulk liquid composition of a biofilm reactor in a period with two different control strategies for nitrite accumulation, using a model considering the growth of 1 AOB population and 1 NOB population, besides heterotrophs, indicates that in this case no diversity needed to be included in the model to explain the bulk output of the reactor and that the control strategies for nitrite accumulation were influencing the microbial community mainly on the level of guilds (AOB and NOB). This implies that, although changes in microbial diversity or population shifts in were possible, they did not influence the reactor behaviour.

Although all this may indicate that one could neglect microbial diversity easily, as it seems that process performance is not influenced by the microbial diversity, it should be noted that these unnoticed changes in microbial composition and diversity of the (nitrifying) community may have important effects on the reactor performance and process stability on the long term, e.g.,

when facing disturbances (Daims *et al.* 2001b; Egli *et al.* 2003; Ramirez *et al.* 2009) or when the decision is taken to go back from nitrite accumulation to complete nitrification (Bougard *et al.* 2006a). Indeed, diverse systems have a greater pool of physiological and genetic traits, which provide them the capacity to change and sustain function under varying environmental conditions (Bellucci *et al.* 2015). This was confirmed in Chapter 3, where the functional redundancy of a nitrifying biofilm upon an increased nitrogen loading rate assured almost complete ammonium conversion to nitrate within 8 months after the shift of operational conditions. The constant nitrifying performance was possible due to a population shift in the NOB guild; without the changes of the biofilm composition, the increased nitrogen loading rate would have resulted in nitrite accumulation.

In this thesis, also cases in which observed population shifts do influence the bulk liquid composition were described. In Chapter 4, the influence of an experimentally observed AOB population shift on the nitrifying performance was investigated. In a nitrite accumulating inverse turbulent bed reactor (ITBR), a lowered nitrogen loading rate resulted in nitrate accumulation due to the appearance of NOB, while *Nitrosomonas* sp. started to grow at the expense of *Nitrosomonas europaea* (Bernet *et al.* 2004; Volcke *et al.* 2008). Dynamic simulations with a biofilm model, including the growth and endogenous respiration of 2 AOB and 1 NOB species, confirmed the influence of the increase in bulk liquid oxygen concentration, following the lowering of the nitrogen loading rate, on the changes observed in bulk liquid and biofilm composition.

In Chapter 2, the suggestion of Terada *et al.* (2010), that the AOB and NOB population compositions of the inoculum may determine the dominant species in the biofilm, which in turn affects the nitrifying performance, was confirmed. Steady state simulations with a different initial species composition of the biofilm were shown to result in a different steady state composition of effluent and biofilm.

6.3 Factors influencing microbial competition and coexistence

In this thesis, both biofilm and microbial characteristics as well as operation parameters and variables were shown to influence the microbial biofilm composition. These factors are described in detail below.

As the focus of this study was on the microbial diversity, no sensitivity analysis was performed, as this is beyond the scope of the study. In models for the prediction of bulk liquid composition, not all the parameters considered in this thesis would be equally important determinants of bulk liquid composition, see for example Brockmann and Morgenroth (2007), Brockmann and Morgenroth (2010), and Brockmann *et al.* (2008). However, considering 60 AOB species and 60 NOB species varying maximum growth rate, affinity constants and yield (Chapter 2) could actually be seen as an inherent sensitivity analysis. In further studies, it is recommended to specifically determine the sensitivity of the models for the different microbial parameters, especially if it is the aim to calibrate and validate the model to experimental data and use the model for bulk liquid composition prediction.

6.3.1 Biofilm characteristics

6.3.1.1 Internal and external mass transfer limitation

Biofilms increase the possibility of coexistence of species due to spatial heterogeneity, i.e., different niches are created by the diffusional substrate concentration gradients (Costerton *et al.* 1994; Nicolella *et al.* 2000; Stewart 2003). In this thesis, the simulated biomass distribution profiles in the biofilm were indeed shown to reflect the ecological niches created by substrate gradients in the biofilms (Chapter 2 and 3).

The 1-dimensional biofilm multispecies models including microbial diversity in this thesis were able to simulate steady state microbial coexistence of species performing the same function (Chapter 2-4). Considering oxygen and nitrogen limitation, a maximum of 3 dominant species in the nitrifying community, with two species performing the same function (ammonium oxidation or nitrite

oxidation) coexisting at steady state was observed. This contrasts with the behaviour of continuous cultures of microorganisms competing for 1 limiting nutrient, in which only 1 species is able to survive at steady state (Hsu *et al.* 1977; Tilman 1977; Hsu 1980). Similarly, when describing microbial competition in biofilms using 0-dimensional model or other non-spatial models, no more consumer species can coexist at steady state than there are limiting resources (Tilman 1994).

Internal mass transfer limitation was also shown to determine the thickness of the active layer (Chapter 2). In this thesis, most modelled biofilms showed the typical structure of a nitrifying biofilm with inert particles at the bottom, NOB dominant in the middle and AOB dominant at the surface of the biofilm. The active layer (active, viable biomass of AOB and NOB) corresponded to the oxygen penetration depth (oxygen limited biofilm), or, if oxygen was available in sufficient concentrations, the penetration of ammonium and nitrite (nitrogen limited biofilm), as only the aerobic AOB and NOB guild were considered. If also other guilds, such as denitrifying heterotrophs or anammox would be considered, the active layer would be much thicker.

The 1-dimensional models developed in this thesis assume that the variation of the state variables is restricted to a single direction perpendicular to the surface of the solid carrier and spatial heterogeneity parallel to the carrier surface was neglected. When modelling biofilm structures with highly irregular surface, it is expected that the substrate concentration gradients will differ spatially due to different biofilm thicknesses. Therefore, a higher steady state microbial diversity is expected when considering 2- or 3-dimensional biofilm models instead of 1-dimensional ones. As proposed by Vannecke *et al.* (2015), spatial heterogeneity could also be considered when mathematical models would be developed including both within-guild diversity and mesoscale heterogeneity (flocs and granules): granular biomass could be modelled considering mass transfer limitations for soluble substrate and stratified biomass corresponding to local growth conditions, while flocs could be assumed as not mass transport limited (Hubaux *et al.* 2015).

In this thesis, it was shown that besides internal mass transfer limitation, creating diffusional substrate concentration gradients in the biofilm, also external mass transfer limitations (boundary layer) affects the competition between AOB and NOB and the bulk liquid composition in terms of nitrite and/or nitrate accumulation (Chapter 4), by determining the concentration of (limiting) substrates such as ammonium, nitrite and oxygen in the biofilm.

6.3.1.2 Initial species composition of the biofilm

Simulations from Chapter 2 confirm the suggestion of Terada *et al.* (2010), that the AOB and NOB population compositions of the inoculum may determine the dominant species in the biofilm, which in turn affects the overall reactor behaviour. The inoculum effect on the AOB communities of parallel sequential batch reactors was also demonstrated experimentally by Wittebolle *et al.* (2009). However, it should be noted that the observation on initial species composition in Chapter 2 only holds for systems operated with synthetic wastewater lacking microorganisms in the feed, as the systems in this thesis. The result may be different for reactors operated with real wastewater, where microorganisms are continuously fed to the reactor and microorganisms from the bulk liquid could attach to the biofilm.

6.3.1.3 Biofilm detachment

In the models of this thesis, biofilm detachment was considered to take place at the surface, with a velocity equalling the advective velocity of the biofilm at the surface when the steady state biofilm thickness is reached. Species growing at the surface, mainly the AOB, need to cope more with detachment than species growing deeper into the biofilm. This is one of the possible reasons why in Chapter 2 and Chapter 3, the NOB:AOB ratio was elevated.

6.3.2 Microbial characteristics

6.3.2.1 Maximum growth rate and affinity

Species coexisting in a biofilm are mostly assumed to have a different niche (Schilthuizen 2008), even if they belong to the same functional guild. Therefore, they must have interspecific trade-offs (Tilman 1994; Escalante *et*

al. 2015). Without niche differentiation or specialization and concomitant fitness trade-offs, as advantageous traits often have side effects (Futuyma 2005), stable coexistence of genotypes is generally not possible (Rainey et al. 2000). Furthermore, the specialist-generalist paradigm predicts that specialists should have a local advantage over generalists and thus be more abundant, as confirmed by Mariadassou et al. (2015).

In this thesis, it was demonstrated (Chapter 2) that coexisting species of the same functional guild are typified by a trade-off between their maximum growth rate and their affinity for the most limiting nutrient (nitrogen or oxygen). If two species performing the same function coexisted in a biofilm, they were likely to be an r-strategist with a high growth rate but relatively low affinity for the most limiting nutrient and a K-strategist, characterized by a low growth rate but a higher affinity, according to the r-K selection theory (Andrews & Harris 1986). The most limiting nutrient can be determined by calculating the ratio of the bulk liquid oxygen and ammonium concentrations ($O_2:NH_4^+$), as was done in Chapter 2 or by checking the ammonium conversion in the bulk liquid and the substrate concentration profiles in the biofilm. Typically, the r-strategist was dominant at the outside of the biofilm while the K-strategist was dominant deeper in the biofilm (Chapter 2). However, this cannot be seen as a proof that confirms the niche theory in contrast to the neutral theory. First of all, the species were constructed by considering niche differentiation a priori, as trade-offs between maximum growth rate, affinity and yield were implemented in the models. Furthermore, the considered biofilm systems were small scale, i.e., the focus was on a biofilm in a reactor on 1 point in 1 dimension (perpendicular on the substratum), and immigration was not considered in the models, as attachment of biomass from the bulk liquid was neglected in this thesis. As neutral community models were proposed to be the foundation of any description of open biological systems (Ofițeru *et al.* 2010), it could be interesting to use 1-dimensional biofilm models in Aquasim, considering within-guild diversity, that also consider attachment of biomass from the bulk into a diffusive biofilm (considering diffusion of particulate components) and particulate components in the pores

of the biofilm (Wanner & Reichert 1996). These models could be used to test the niche versus neutral theory in biofilm systems.

Although it can be certainly concluded that both maximum growth rate and affinity determine competition outcome and position in the biofilm, it should be noted that in this study apparent affinity constants were used (Pérez *et al.* 2005; Arnaldos *et al.* 2015). Therefore, the affinity of the organisms could be estimated too low. However, the species were given a value for the affinity constants based on a broad range from literature (Chapter 2) and it is especially the difference in their values instead of the exact values that determine whether or not a species survives in the biofilm at steady state. In future studies, the contribution of different resistances to the affinity constants should be considered carefully.

In Chapter 3, it was shown that the r-K selection theory also can be used to explain major population shifts in time, due to temporal heterogeneity: r-strategists can grow rapidly on the prevailing conditions but get replaced by K-strategists as soon as a substrate becomes limiting.

While this thesis focusses mainly on steady state behaviour, it is clear that there is an even higher chance of coexistence of species from the same functional guild during dynamic reactor operation (Gieseke *et al.* 2003), as temporal heterogeneity can result in stable coexistence of two genotypes on a single resource (Rainey *et al.* 2000). A higher steady state diversity is also expected when taking into account the diversity of affinity for additional limiting nutrients (besides oxygen and nitrogen) such as carbon dioxide.

6.3.2.2 *Endogenous respiration or decay rate*

In this study, endogenous respiration (Chapter 3 and 4) or decay (Chapter 2 and 5) was used to simulate the formation of inerts from active biomass. Endogenous respiration is the use of stored reserve polymers in absence of external substrate for growth and maintenance processes while decay depicts the transition of living cells in organic substrate for heterotrophs and inerts (van Loosdrecht & Henze 1999). It should be noted that decay could be included in biofilm models instead of endogenous respiration when (1) a lot of

species per functional guild are included in the models (Chapter 2), to reduce the number of necessary equations and (2) when the growth of heterotrophs is included in the model, as these can use the organic substrate originating from biomass decay. The latter can be important to verify if the growth of heterotrophs on decayed biomass is significant or not (Mozumder *et al.* 2014).

As little is known on the diversity of the values of the endogenous respiration or decay rates, three methods were applied to determine the endogenous respiration or decay rate: (1) species were given a fixed value (Chapter 4), (2) the values were calculated from the maximum growth rate, assuming the endogenous respiration rate or decay rate was 5% of the maximum growth rate (Chapter 2-4) and (3) the decay rates were calibrated to reflect the experimentally observed reactor behaviour (Chapter 5). The chosen value for endogenous or decay rate has important consequences for the microbial competition outcome, as pointed out in Chapter 4. Species with a low growth rate, and thus a lower endogenous respiration rate, were shown to win the competition from faster growing species (high endogenous respiration rate) in a larger range of bulk liquid oxygen concentrations than when endogenous respiration was neglected (Chapter 4). This is also a possible reason why in Chapter 2 and 3 an elevated NOB:AOB ratio was found, as the AOB have a higher growth rate and thus a higher endogenous respiration rate than NOB. Furthermore, as NOB live deeper in the biofilm, endogenous respiration using oxygen as electron acceptor (described with a Monod term for oxygen: $\frac{S_{O_2}}{S_{O_2}+K_{O_2}}$) is lower for the NOB than the AOB, also resulting in an elevated NOB:AOB ratio.

6.3.2.3 Inhibition constants for FA and FNA

In Chapter 5, free ammonia and free nitrous acid inhibition of AOB and NOB were implemented. Without implementation of inhibition, the model was not able to reflect the bulk liquid composition observed experimentally. The observed bulk liquid concentrations of FA and FNA were equal to, or even higher than the median value of the reported FA inhibition constants for NOB and FNA inhibition constants for AOB and NOB in literature, indicating

possible inhibition of the NOB by FA and the AOB and NOB by FNA. By calibrating the microbial characteristics of AOB and NOB to the available experimental data this was further confirmed.

In this thesis, the diversity observed in inhibition constants, originating from differences between species but also acclimation of species to operational conditions (Grady *et al.* 1996), was not included in the used mathematical models. A higher steady state diversity is expected when taking into account the diversity of inhibition constants for free ammonia (FA), nitric acid (FNA) or even other inhibitors.

6.3.2.4 Yield

Although the diversity of the yield was implemented in the models used in this thesis, no clear influence on reactor behaviour was observed (Chapter 2-3). This indicates that in the considered model, kinetic parameters were more important than stoichiometric ones for the steady state results. In this study, this is most likely due to the fact that the ranges of considered values for yield were rather small compared to the ranges considered for maximum growth rate and affinity constants: Y_{AOB} : 0.09-0.41 g COD.(g N)⁻¹ and Y_{NOB} : 0.02-0.20 g COD.(g N)⁻¹. This results from the fact that yield is determined mainly on the basis of the energy yielded from catabolic reactions. Also Hsu *et al.* (1977), who developed a mathematical model, based on Michaelis-Menten kinetics, for one substrate and n competing species concluded that the species will survive whose Michaelis-Menten constant (affinity constant) is smallest in comparison with its intrinsic rate of natural increase and that it is irrelevant how abundant the competitors are at the start, or how efficiently the species convert the nutrient into cell growth (yield). In real systems, due to the trade-off between growth rate and yield (Pfeiffer & Bonhoeffer 2002), yield besides kinetic parameters as growth rate could indeed play an important role in biofilm competition, for example when yet another limiting substrate for the autotrophs, carbon dioxide (Guisasola *et al.* 2007), their carbon source for biomass production, would be considered in mathematical models. For example, species with a high yield but lower growth rate, using their resources

economically, could promote altruism in spatially structured environments, such as biofilms (Kreft 2004).

Furthermore, considering competition between different guilds, yield can play an important role, i.e., AOB obtain more energy from the oxidation of ammonium to nitrite than NOB from the oxidation of nitrite to nitrate.

6.3.2.5 *Considered microbial guilds*

It should be noted that in this thesis the focus was on the diversity within the nitrifying community, i.e., ammonia-oxidizing bacteria and nitrite-oxidizing bacteria. Future research could be directed on the influence of diversity in other microbial guilds than AOB and NOB, for example heterotrophs and anammox. Furthermore, also predation by eukaryotic microorganisms could be considered, as it is expected to shape the microbial community in biofilms (Saur *et al.* 2014), e.g., selective predation pressure can favour or suppress particular bacterial species (Pernthaler 2005).

6.3.3 Operational parameters and variables

6.3.3.1 *NLR and DO*

In Chapter 2, it was shown that the nitrogen loading rate and the bulk liquid oxygen concentration influence the microbial composition of the biofilm, besides the effluent composition. The nitrogen loading rate determines the concentration of major nitrogen substrates and inhibitors in the bulk liquid, i.e., total ammonium and free ammonia, and after biological conversion also total nitrite and free nitrous acid. Furthermore, as the nitrogen loading rate determines the concentration of these substrates, it also affects the bulk liquid oxygen concentration by its effect on the biological activity of the AOB and NOB when the aeration is fixed, i.e., when the flow rate of air to the reactor is constant (Chapter 5).

In Chapter 4 and Chapter 5, based on experimental data, and Chapter 3, based on dynamic simulations, it was shown that changes in the nitrogen loading rate of nitrifying biofilm reactors can govern major population shifts in the nitrifying community besides possible changes in the nitrifying performance.

In Chapter 4 and 5, the change in bulk liquid oxygen concentration following an increase of the nitrogen loading rate (the aeration was assumed to be fixed), was identified as the key variable governing the population shifts.

6.3.3.2 *Temperature and pH*

Temperature and pH were shown in this thesis to be important factors influencing microbial competition and the resulting effluent composition (Chapter 5).

Temperature influences the maximum growth rate of microorganisms: the maximum growth rate increases with increasing temperatures, until an optimum is reached (Madigan & Martinko 2006), and at temperatures higher than 30 °C, the maximum growth rate of AOB is higher than the one of NOB (Wiesmann 1994).

The fraction of FA:TNH and FNA:TNO₂ depends on temperature and pH. The fraction of FA increases with increasing temperature and pH, while the fraction of FNA decreases with increasing temperature and pH (Anthonisen *et al.* 1976). Therefore, both pH and temperature can have an influence on the inhibition of AOB and NOB by FA and FNA (Chapter 5). Even small changes in reactor pH, for example small deviations from the control set-point, can influence FA and FNA inhibition.

Finally, temperature also influences the diffusion of oxygen, ammonium, nitrite and nitrate in the biofilm, determining the concentration of limiting nutrients in the biofilm, besides the thickness of the active layer.

6.4 Outlook

In this work, 1-dimensional nitrifying biofilm models including microbial diversity were shown to be useful tools to investigate microbial competition and coexistence in nitrifying biofilms and allowed the study of the influence of the microbial community on steady state and dynamic biofilm reactor behaviour. It is hoped that this thesis will stimulate further research in the field of mathematical modelling of microbial diversity. The concepts developed in this thesis could be easily extended to other processes important in wastewater treatment such as denitrification, anammox and biological phosphorus removal. The developed models could be seen as a bridge for the collaboration of microbiologists, wastewater engineers and modellers to transform knowledge from microbial ecology into optimized or novel technical implementations for sustainable wastewater treatment. Indeed, wastewater treatment engineering and ecology have complementary goals and need to interact much more closely. Wastewater engineers should use the fundamentals of ecological theory to help guide future system design and ecologists should view engineered biosystems as valuable new platforms for ecological research (Graham & Smith 2004; Daims *et al.* 2006). Mathematical models including diversity could be an excellent platform for this.

Possible use of these models in combination with information from metagenomics in hypothesis generation, testing, experimental design and data mining is summarized in Figure 6.1. Rapid DNA sequencing and other molecular analysis technologies can provide large-scale data on the combined genomes of a microbial community, potentially revealing unanticipated community members or activities (Jansson & Prosser 2013). However, hypotheses generated by descriptive studies should be tested by experiments. In combination with experiments using pure (axenic) cultures and/or synthetic microbial ecosystems (De Roy *et al.* 2014), mechanistic models can be of great interest for (1) the testing or proposal of ecological hypotheses, (2) the development of control strategies for microbial population optimization and (3) the prediction of reactor performance based on microbial community data.

Synthetic communities are of utmost importance for the calibration and validation of models including diversity, because their microbial composition is known a priori. The models can help in the design of new experiments with synthetic microbial ecosystems and can benefit from the determination of microbial parameters from cultures with well-known microbial community composition. In this way, using microbial community information provided by metagenomics, bacterial diversity could be modelled at both the very large and the very small scales at which microbial systems interact with their environments and the models could help to connect biogeochemical processes to specific microbial metabolic pathways (Larsen *et al.* 2012; Song *et al.* 2014).

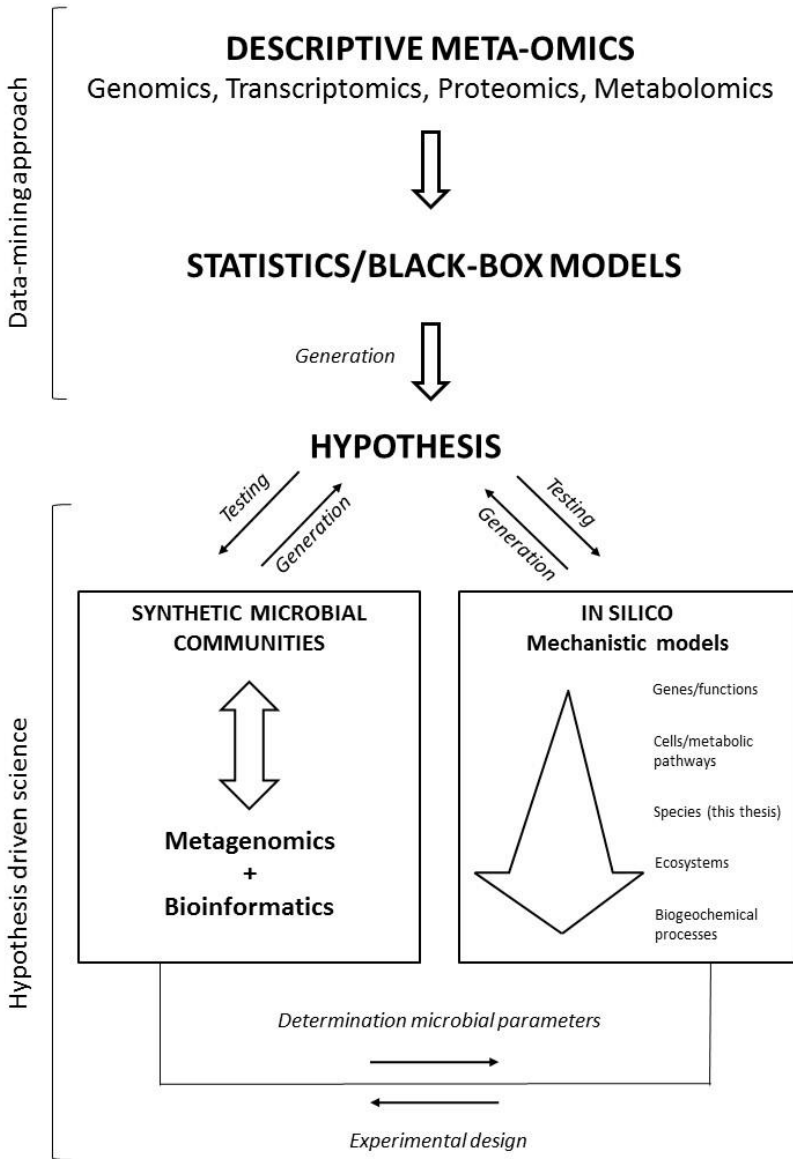


Figure 6.1 Possible use of mathematical models including within-guild diversity and information from metagenomics in hypothesis generation, testing, experimental design and data mining. Loosely based on Jansson and Prosser (2013).

References

- Achtman, M. and Wagner, M. (2008). Microbial diversity and the genetic nature of microbial species. *Nature Reviews Microbiology* 6(6), 431-440.
- Allison, S.D. and Martiny, J.B. (2008). Colloquium paper: resistance, resilience, and redundancy in microbial communities. *Proceedings of the National Academy of Sciences of the United States of America* 105 Suppl 1, 11512-11519.
- Allison, S.D. (2012). A trait-based approach for modelling microbial litter decomposition. *Ecology Letters* 15(9), 1058-1070.
- Almstrand, R., Lydmark, P., Lindgren, P.E., Sörensson, F. and Hermansson, M. (2013). Dynamics of specific ammonia-oxidizing bacterial populations and nitrification in response to controlled shifts of ammonium concentrations in wastewater. *Applied Microbiology and Biotechnology* 97(5), 2183-2191.
- Alpkvist, E., Picioreanu, C., van Loosdrecht, M.C. and Heyden, A. (2006). Three-dimensional biofilm model with individual cells and continuum EPS matrix. *Biotechnology and Bioengineering* 94(5), 961-979.
- Altmann, D., Stief, P., Amann, R., De Beer, D. and Schramm, A. (2003). In situ distribution and activity of nitrifying bacteria in freshwater sediment. *Environmental Microbiology* 5(9), 798-803.
- Andrén, O. and Balandreau, J. (1999). Biodiversity and soil functioning—from black box to can of worms? *Applied Soil Ecology* 13(2), 105-108.
- Andrews, J.H. and Harris, R.F. (1986). R-selection and K-selection and microbial ecology. *Advances in Microbial Ecology* 9, 99-147.
- Anthonisen, A.C., Loehr, R.C., Prakasam, T.B.S. and Srinath, E.G. (1976). Inhibition of nitrification by ammonia and nitrous acid. *Journal Water Pollution Control Federation* 48(5), 835-852.
- Arnaldos, M., Amerlinck, Y., Rehman, U., Maere, T., Van Hoey, S., Naessens, W. and Nopens, I. (2015). From the affinity constant to the half-saturation index: Understanding conventional modeling concepts in novel wastewater treatment processes. *Water Research* 70, 458-470.
- Bae, W. and Rittmann, B.E. (1996). A structured model of dual-limitation kinetics. *Biotechnology and Bioengineering* 49(6), 683-689.
- Baquerizo, G., Maestre, J.P., Sakuma, T., Deshusses, M.A., Gamsans, X., Gabriel, D. and Lafuente, J. (2005). A detailed model of a biofilter for ammonia removal: model parameters analysis and model validation. *Chemical Engineering Journal* 113(2), 205-214.
- Baroukh, C., Muñoz-Tamayo, R., Steyer, J.-P. and Bernard, O. (2014). DRUM: a new framework for metabolic modeling under non-balanced growth. Application to the carbon metabolism of unicellular microalgae. *PloS one* 9(8), 1-15.
- Bellucci, M., Ofiteru, I.D., Beneduce, L., Graham, D.W., Head, I.M. and Curtis, T.P. (2015). A preliminary and qualitative study of resource ratio theory to nitrifying lab-scale bioreactors. *Microbial Biotechnology* 8(3), 590-603.
- Beltrame, P., Beltrame, P. and Carniti, P. (1980). Use of the haldane equation for steady - state substrate inhibition in biodegradation kinetics. *Biotechnology and Bioengineering* 22(11), 2405-2409.

- Beneduce, L., Spano, G., Lamacchia, F., Bellucci, M., Consiglio, F. and Head, I. (2014). Correlation of seasonal nitrification failure and ammonia-oxidizing community dynamics in a wastewater treatment plant treating water from a saline thermal spa. *Annals of Microbiology*, 1-12.
- Bernet, N., Dangcong, P., Delgenès, J. and Moletta, R. (2001). Nitrification at low oxygen concentration in biofilm reactor. *Journal of Environmental Engineering* 127(3), 266-271.
- Bernet, N., Sanchez, O., Dabert, P., Olaizola, A., Godon, J.J. and Delgenes, J.P. (2004). Effect of solid hold-up on nitrite accumulation in a biofilm reactor - molecular characterization of nitrifying communities. *Water Science and Technology* 49(11-12), 123-130.
- Bernet, N., Sanchez, O., Cesbron, D., Steyer, J.P. and Delgenes, J.P. (2005). Modeling and control of nitrite accumulation in a nitrifying biofilm reactor. *Biochemical Engineering Journal* 24(2), 173-183.
- Bertrand, J.-C., Caumette, P., Lebaron, P., Matheron, R., Normand, P. and Sime-Ngando, T. (2011). *Environmental microbiology: Fundamentals and applications*. Springer, 933 pages.
- Bisswanger, H. (2008). *Enzyme Kinetics: Principles and Methods*. Wiley, 256 pages.
- Blackburne, R., Vadivelu, V.M., Yuan, Z. and Keller, J. (2007a). Determination of growth rate and yield of nitrifying bacteria by measuring carbon dioxide uptake rate. *Water Environment Research* 79(12), 2437-2445.
- Blackburne, R., Vadivelu, V.M., Yuan, Z.G. and Keller, J. (2007b). Kinetic characterisation of an enriched *Nitrospira* culture with comparison to *Nitrobacter*. *Water Research* 41(14), 3033-3042.
- Bohmann, K., Evans, A., Gilbert, M.T.P., Carvalho, G.R., Creer, S., Knapp, M., Douglas, W.Y. and de Bruyn, M. (2014). Environmental DNA for wildlife biology and biodiversity monitoring. *Trends in Ecology & Evolution* 29(6), 358-367.
- Boon, B. and Laudelout, H. (1962). Kinetics of nitrite oxidation by *Nitrobacter winogradskyi*. *Biochemical Journal* 85(3), 440.
- Boon, N., De Windt, W., Verstraete, W. and Top, E.M. (2002). Evaluation of nested PCR-DGGE (denaturing gradient gel electrophoresis) with group-specific 16S rRNA primers for the analysis of bacterial communities from different wastewater treatment plants. *FEMS Microbiology Ecology* 39(2), 101-112.
- Bothe, H., Jost, G., Schlöter, M., Ward, B.B. and Witzel, K.P. (2000). Molecular analysis of ammonia oxidation and denitrification in natural environments. *FEMS Microbiology Reviews* 24(5), 673-690.
- Bougard, D. (2004). *Traitement biologique d'effluents azotés avec arrêt de la nitrification au stade nitrite*. PhD thesis, L'école nationale supérieure agronomique de Montpellier, Montpellier, 234 pages.
- Bougard, D., Bernet, N., Dabert, P., Delgenes, J.P. and Steyer, J.P. (2006a). Influence of closed loop control on microbial diversity in a nitrification process. *Water Science and Technology* 53(4-5), 85-93.
- Bougard, D., Bernet, N., Cheneby, D. and Delgenes, J.P. (2006b). Nitrification of a high-strength wastewater in an inverse turbulent bed reactor: Effect of temperature on nitrite accumulation. *Process Biochemistry* 41(1), 106-113.

- Braun, F., Hamelin, J., Bonnafous, A., Delgenès, N., Steyer, J.-P. and Patureau, D. (2015). Similar PAH fate in anaerobic digesters inoculated with three microbial communities accumulating either volatile fatty acids or methane. *PLoS one* 10(4).
- Brockmann, D. and Morgenroth, E. (2007). Comparing global sensitivity analysis for a biofilm model for two-step nitrification using the qualitative screening method of Morris or the quantitative variance-based Fourier Amplitude Sensitivity. *Water Science and Technology* 56(8), 85-94.
- Brockmann, D., Rosenwinkel, K.H. and Morgenroth, E. (2008). Practical identifiability of biokinetic parameters of a model describing two - step nitrification in biofilms. *Biotechnology and Bioengineering* 101(3), 497-514.
- Brockmann, D. and Morgenroth, E. (2010). Evaluating operating conditions for outcompeting nitrite oxidizers and maintaining partial nitrification in biofilm systems using biofilm modeling and Monte Carlo filtering. *Water Research* 44(6), 1995-2009.
- Brockmann, D., Caylet, A., Escudé, R., Steyer, J.P. and Bernet, N. (2013). Biofilm model calibration and microbial diversity study using Monte Carlo simulations. *Biotechnology and Bioengineering* 110(5), 1323-1332.
- Brouwer, M. (1995). Biologische stikstofverwijdering op Sluisjesdijk met het SHARON proces, TU Delft, Delft, The Netherlands.
- Brown, M.N., Briones, A., Diana, J. and Raskin, L. (2013). Ammonia-oxidizing archaea and nitrite-oxidizing nitrospiras in the biofilter of a shrimp recirculating aquaculture system. *FEMS Microbiology Ecology* 83(1), 17-25.
- Buffiere, P., Bergeon, J.P. and Moletta, R. (2000). The inverse turbulent bed: a novel bioreactor for anaerobic treatment. *Water Research* 34(2), 673-677.
- Buffière, P. and Moletta, R. (1999). Some hydrodynamic characteristics of inverse three phase fluidized-bed reactors. *Chemical Engineering Science* 54(9), 1233-1242.
- Buffière, P. and Moletta, R. (2000). Collision frequency and collisional particle pressure in three-phase fluidized beds. *Chemical Engineering Science* 55(22), 5555-5563.
- Carrera, J., Jubany, I., Carvallo, L., Chamy, R. and Lafuente, J. (2004). Kinetic models for nitrification inhibition by ammonium and nitrite in a suspended and an immobilised biomass systems. *Process Biochemistry* 39(9), 1159-1165.
- Carvallo, L., Carrera, J. and Chamy, R. (2002). Nitrifying activity monitoring and kinetic parameters determination in a biofilm airlift reactor by respirometry. *Biotechnology Letters* 24(24), 2063-2066.
- Chandran, K. and Smets, B.F. (2000). Single - step nitrification models erroneously describe batch ammonia oxidation profiles when nitrite oxidation becomes rate limiting. *Biotechnology and Bioengineering* 68(4), 396-406.
- Chen, K. and Pachter, L. (2005). Bioinformatics for whole-genome shotgun sequencing of microbial communities. *PLoS Computational Biology* 1(2), 106-112.

- Ciudad, G., Werner, A., Bornhardt, C., Munoz, C. and Antileo, C. (2006). Differential kinetics of ammonia- and nitrite-oxidizing bacteria: A simple kinetic study based on oxygen affinity and proton release during nitrification. *Process Biochemistry* 41(8), 1764-1772.
- Cohan, F.M. (2002). What are bacterial species? *Annual Review of Microbiology* 56(1), 457-487.
- Cole, J.A. and Brown, C.M. (1980). Nitrite reduction to ammonia by fermentative bacteria: A short circuit in the biological nitrogen cycle. *FEMS Microbiology Letters* 7(2), 65-72.
- Copp, J.B. and Murphy, K.L. (1995). Estimation of the active nitrifying biomass in activated sludge. *Water Research* 29(8), 1855-1862.
- Costerton, J.W., Lewandowski, Z., Debeer, D., Caldwell, D., Korber, D. and James, G. (1994). Biofilms, the customized microniche. *Journal of Bacteriology* 176(8), 2137-2142.
- Daims, H., Nielsen, J.L., Nielsen, P.H., Schleifer, K.-H. and Wagner, M. (2001a). In situ characterization of nitrospira-like nitrite-oxidizing bacteria active in wastewater treatment plants. *Applied and Environmental Microbiology* 67(11), 5273-5284.
- Daims, H., Purkhold, U., Bjerrum, L., Arnold, E., Wilderer, P.A. and Wagner, M. (2001b). Nitrification in sequencing biofilm batch reactors: lessons from molecular approaches. *Water Science and Technology* 43(3), 9-18.
- Daims, H., Taylor, M.W. and Wagner, M. (2006). Wastewater treatment: a model system for microbial ecology. *Trends in Biotechnology* 24(11), 483-489.
- Daly, A.J., Baetens, J.M. and De Baets, B. (2015). The impact of initial evenness on the preservation of biodiversity for in silico bacterial communities: a stochastic, spatial, individual-based model. *Communications in Agricultural and Applied Biological Sciences* 80(1), 17-22.
- de Kreuk, M.K., Heijnen, J.J. and van Loosdrecht, M.C. (2005). Simultaneous COD, nitrogen, and phosphate removal by aerobic granular sludge. *Biotechnology and Bioengineering* 90(6), 761-769.
- de Kreuk, M.K., Picioreanu, C., Hosseini, M., Xavier, J.B. and van Loosdrecht, M.C.M. (2007). Kinetic model of a granular sludge SBR: Influences on nutrient removal. *Biotechnology and Bioengineering* 97(4), 801-815.
- De Roy, K., Clement, L., Thas, O., Wang, Y. and Boon, N. (2012). Flow cytometry for fast microbial community fingerprinting. *Water Research* 46(3), 907-919.
- De Roy, K., Marzorati, M., Van den Abbeele, P., Van de Wiele, T. and Boon, N. (2014). Synthetic microbial ecosystems: an exciting tool to understand and apply microbial communities. *Environmental Microbiology* 16(6), 1472-1481.
- Downing, L.S. and Nerenberg, R. (2008). Effect of oxygen gradients on the activity and microbial community structure of a nitrifying, membrane-aerated biofilm. *Biotechnology and Bioengineering* 101(6), 1193-1204.
- Eberl, H., Morgenroth, E., Noguera, D.R., Picioreanu, C., Rittmann, B.E., van Loosdrecht, M. and Wanner, O. (2006). *Mathematical modeling of biofilms*, IWA Publishing, London, UK.

- Egli, K., Langer, C., Siegrist, H.-R., Zehnder, A.J.B., Wagner, M. and van der Meer, J.R. (2003). Community analysis of ammonia and nitrite oxidizers during start-up of nitrification reactors. *Applied and Environmental Microbiology* 69(6), 3213-3222.
- Eisen, J.A. (2007). Environmental shotgun sequencing: its potential and challenges for studying the hidden world of microbes. *PLoS Biology* 5(3), 384-388.
- Elawwad, A., Sandner, H., Kappelmeyer, U. and Koeser, H. (2013). Long-term starvation and subsequent recovery of nitrifiers in aerated submerged fixed-bed biofilm reactors. *Environmental Technology* 34(8), 945-959.
- Erguder, T.H., Boon, N., Wittebolle, L., Marzorati, M. and Verstraete, W. (2009). Environmental factors shaping the ecological niches of ammonia-oxidizing archaea. *FEMS Microbiology Reviews* 33(5), 855-869.
- Escalante, A.E., Rebolledo-Gómez, M., Benítez, M. and Trivisano, M. (2015). Ecological perspectives on synthetic biology: insights from microbial population biology. *Frontiers in Microbiology* 6.
- Fang, F., Ni, B.J., Li, X.Y., Sheng, G.P. and Yu, H.Q. (2009). Kinetic analysis on the two-step processes of AOB and NOB in aerobic nitrifying granules. *Applied Microbiology and Biotechnology* 83(6), 1159-1169.
- Flora, E., Suidan, M.T., Flora, J.R.V. and Kim, B.J. (1999). Speciation and chemical interactions in nitrifying biofilms. I: Model development. *Journal of Environmental Engineering* 125(9), 871-877.
- Foesel, B.U., Gieseke, A., Schwermer, C., Stief, P., Koch, L., Cytryn, E., de la Torre, J.R., van Rijn, J., Minz, D., Drake, H.L. and Schramm, A. (2008). *Nitrosomonas* Nm143-like ammonia oxidizers and *Nitrospira marina*-like nitrite oxidizers dominate the nitrifier community in a marine aquaculture biofilm. *FEMS Microbiology Ecology* 63(2), 192-204.
- Fredrickson, J.K. (2015). Ecological communities by design. *Science* 348(6242), 1425-1427.
- Freitag, A., Rudert, M. and Bock, E. (1987). Growth of *Nitrobacter* by dissimilatory nitrate reduction. *FEMS Microbiology Letters* 48(1-2), 105-109.
- Futuyma, D.J. (2005). *Evolution*. Sinauer Associates, Sunderland, Mass., 603 pages.
- Ganigue, R., Lopez, H., Balaguer, M.D. and Colprim, J. (2007). Partial ammonium oxidation to nitrite of high ammonium content urban landfill leachates. *Water Research* 41(15), 3317-3326.
- Garrido, J.M., van Benthum, W.A.J., van Loosdrecht, M.C.M. and Heijnen, J.J. (1997). Influence of dissolved oxygen concentration on nitrite accumulation in a biofilm airlift suspension reactor. *Biotechnology and Bioengineering* 53(2), 168-178.
- Gear, C.W. (1971). The automatic integration of ordinary differential equations. *Communications of the ACM* 14(3), 176-179.
- Gee, C.S., Suidan, M.T. and Pfeffer, J.T. (1990). Modeling of nitrification under substrate-inhibiting conditions. *Journal of Environmental Engineering* 116(1), 18-31.
- Gentry, T., Wickham, G., Schadt, C., He, Z. and Zhou, J. (2006). Microarray applications in microbial ecology research. *Microbial Ecology* 52(2), 159-175.

- Gieseke, A., Purkhold, U., Wagner, M., Amann, R. and Schramm, A. (2001). Community structure and activity dynamics of nitrifying bacteria in a phosphate-removing biofilm. *Applied and Environmental Microbiology* 67(3), 1351-1362.
- Gieseke, A., Bjerrum, L., Wagner, M. and Amann, R. (2003). Structure and activity of multiple nitrifying bacterial populations co-existing in a biofilm. *Environmental Microbiology* 5(5), 355-369.
- Gilbert, E.M., Agrawal, S., Karst, S.M., Horn, H., Nielsen, P.H. and Lackner, S. (2014). Low temperature partial nitrification/anammox in a moving bed biofilm reactor treating low strength wastewater. *Environmental Science and Technology* 48(15), 8784-8792.
- Gill, P.E., Murray, W. and Wright, M.H. (1981). *Practical optimization*. Academic Press, London pages.
- Glover, H.E. (1985). The relationship between inorganic nitrogen oxidation and organic-carbon production in batch and chemostat cultures of marine nitrifying bacteria. *Archives of Microbiology* 142(1), 45-50.
- Grada, A. and Weinbrecht, K. (2013). Next-generation sequencing: Methodology and application. *J Invest Dermatol* 133(8), e11.
- Grady, C.P.L., Smets, B.F. and Barbeau, D.S. (1996). Variability in kinetic parameter estimates: a review of possible causes and a proposed terminology. *Water Research* 30(3), 742-748.
- Graham, D.W. and Smith, V.H. (2004). Designed ecosystem services: application of ecological principles in wastewater treatment engineering. *Frontiers in Ecology and the Environment* 2(4), 199-206.
- Graham, D.W., Knapp, C.W., Van Vleck, E.S., Bloor, K., Lane, T.B. and Graham, C.E. (2007). Experimental demonstration of chaotic instability in biological nitrification. *The ISME journal* 1(5), 385-393.
- Griffiths, A.J.F., Wessler, S.R., Lewontin, R.C. and Carroll, S.B. (2008). *Introduction to genetic analysis*. W.H. Freeman and Company, 837 pages.
- Guisasola, A., Jubany, I., Baeza, J.A., Carrera, J. and Lafuente, J. (2005). Respirometric estimation of the oxygen affinity constants for biological ammonium and nitrite oxidation. *Journal of Chemical Technology and Biotechnology* 80(4), 388-396.
- Guisasola, A., Petzet, S., Baeza, J.A., Carrera, J. and Lafuente, J. (2007). Inorganic carbon limitations on nitrification: Experimental assessment and modelling. *Water Research* 41(2), 277-286.
- Haegeman, B. and Loreau, M. (2011). A mathematical synthesis of niche and neutral theories in community ecology. *Journal of Theoretical Biology* 269(1), 150-165.
- Hammes, F., Berney, M., Wang, Y., Vital, M., Köster, O. and Egli, T. (2008). Flow-cytometric total bacterial cell counts as a descriptive microbiological parameter for drinking water treatment processes. *Water Research* 42(1), 269-277.
- Handelsman, J. (2004). Metagenomics: Application of genomics to uncultured microorganisms. *Microbiology and Molecular Biology Reviews* 68(4), 669-685.
- Hao, X.D., Heijnen, J.J. and Van Loosdrecht, M.C.M. (2002a). Model-based evaluation of temperature and inflow variations on a partial nitrification-ANAMMOX biofilm process. *Water Research* 36(19), 4839-4849.

- Hao, X.D., Heijnen, J.J. and van Loosdrecht, M.C.M. (2002b). Sensitivity analysis of a biofilm model describing a one-stage completely autotrophic nitrogen removal (CANON) process. *Biotechnology and Bioengineering* 77(3), 266-277.
- Hao, X.D. and van Loosdrecht, M.C. (2004). Model-based evaluation of COD influence on a partial nitrification-Anammox biofilm (CANON) process. *Water Science and Technology* 49(11-12), 83-90.
- Hawkes, C.V. and Keitt, T.H. (2015). Resilience vs. historical contingency in microbial responses to environmental change. *Ecology Letters* 18(7), 612-625.
- Heijnen, J.J. and Verheijen, P.J. (2013). Parameter identification of in vivo kinetic models: Limitations and challenges. *Biotechnology journal* 8(7), 768-775.
- Hellinga, C., Schellen, A.A.J.C., Mulder, J.W., van Loosdrecht, M.C.M. and Heijnen, J.J. (1998). The SHARON process: An innovative method for nitrogen removal from ammonium-rich waste water. *Water Science and Technology* 37(9), 135-142.
- Hellinga, C., Van Loosdrecht, M.C.M. and Heijnen, J.J. (1999). Model based design of a novel process for nitrogen removal from concentrated flows. *Mathematical and Computer Modelling of Dynamical Systems* 5(4), 351-371.
- Henze, M., Gujer, W., Mino, T. and Van Loosdrecht, M.C.M. (2000). *Activated sludge models ASM1, ASM2, ASM2d and ASM3*, IWA Publishing, London.
- Hermansson, A. and Lindgren, P.-E. (2001). Quantification of ammonia-oxidizing bacteria in arable soil by real-time PCR. *Applied and Environmental Microbiology* 67(2), 972-976.
- Hill, M.O. (1973). Diversity and evenness: a unifying notation and its consequences. *Ecology* 54(2), 427-432.
- Hill, T.C.J., Walsh, K.A., Harris, J.A. and Moffett, B.F. (2003). Using ecological diversity measures with bacterial communities. *FEMS Microbiology Ecology* 43(1), 1-11.
- Hogeweg, P. (2011). The roots of bioinformatics in theoretical biology. *PLoS Computational Biology* 7(3), 1-5.
- Holt, R.D. (2009). Bringing the Hutchinsonian niche into the 21st century: Ecological and evolutionary perspectives. *Proceedings of the National Academy of Sciences* 106(Supplement 2), 19659-19665.
- Hsu, S.B., Hubbell, S. and Waltman, P. (1977). A mathematical theory for single-nutrient competition in continuous cultures of micro-organisms. *Siam Journal on Applied Mathematics* 32(2), 366-383.
- Hsu, S.B. (1980). A competition model for a seasonally fluctuating nutrient. *Journal of Mathematical Biology* 9(2), 115-132.
- Hubaux, N., Wells, G. and Morgenroth, E. (2015). Impact of coexistence of flocs and biofilm on performance of combined nitrification-anammox granular sludge reactors. *Water Research* 68, 127-139.
- Hubbell, S.P. (2001). *The unified neutral theory of biodiversity and biogeography*. Princeton University Press, 375 pages.

- Huber, J.A., Mark Welch, D.B., Morrison, H.G., Huse, S.M., Neal, P.R., Butterfield, D.A. and Sogin, M.L. (2007). Microbial Population Structures in the Deep Marine Biosphere. *Science* 318(5847), 97-100.
- Hunik, J.H., Meijer, H.J.G. and Tramper, J. (1992). Kinetics of *Nitrosomonas europaea* at extreme substrate, product and salt concentrations. *Applied Microbiology and Biotechnology* 37(6), 802-807.
- Hunik, J.H., Meijer, H.J.G. and Tramper, J. (1993). Kinetics of *Nitrobacter agilis* at extreme substrate, product and salt concentrations. *Applied Microbiology and Biotechnology* 40(2-3), 442-448.
- Hunik, J.H., Bos, C.G., Vandenhooogen, M.P., Degooijer, C.D. and Tramper, J. (1994). Co-immobilized *Nitrosomonas europaea* and *Nitrobacter agilis* cells - Validation of a dynamic model for simultaneous substrate conversion and growth in kappa-carrageenan gel beads. *Biotechnology and Bioengineering* 43(11), 1153-1163.
- Hutchinson, G.E. (1957). Concluding remarks. *Cold Spring Harbor Symposia on Quantitative Biology* 22, 415-427.
- Ibarra, R.U., Edwards, J.S. and Palsson, B.O. (2002). *Escherichia coli* K-12 undergoes adaptive evolution to achieve in silico predicted optimal growth. *Nature* 420(6912), 186-189.
- Ilchinski, A. (2001). *Cellular automata: a discrete universe*. World Scientific Publishing, Singapore, 808 pages.
- Jansson, J.K. and Prosser, J.I. (2013). Microbiology: The life beneath our feet. *Nature* 494(7435), 40-41.
- Jayamohan, S., Ohgaki, S. and Hanaki, K. (1988). Effect of DO on kinetics of nitrification. *Water Supply* 6(3), 141-150.
- Johnson, D.R., Lee, T.K., Park, J., Fenner, K. and Helbling, D.E. (2014). The functional and taxonomic richness of wastewater treatment plant microbial communities are associated with each other and with ambient nitrogen and carbon availability. *Environmental Microbiology*, 1-10.
- Jones, R., Dold, P., Takács, I., Chapman, K., Wett, B., Murthy, S. and Shaughnessy, M. (2007). Simulation for operation and control of reject water treatment processes. *Proceedings of the Water Environment Federation* 2007(14), 4357-4372.
- Jubany, I., Baeza, J.A., Carrera, J. and Lafuente, J. (2005). Respiriometric calibration and validation of a biological nitrite oxidation model including biomass growth and substrate inhibition. *Water Research* 39(18), 4574-4584.
- Jubany, I. (2007). Operation, modelling and automatic control of complete and partial nitrification of highly concentrated ammonium wastewater. PhD thesis, Universitat Autònoma de Barcelona, Barcelona, Spain, 286 pages.
- Jubany, I., Carrera, J., Lafuente, J. and Baeza, J.A. (2008). Start-up of a nitrification system with automatic control to treat highly concentrated ammonium wastewater: Experimental results and modeling. *Chemical Engineering Journal* 144(3), 407-419.
- Jubany, I., Lafuente, J., Baeza, J.A. and Carrera, J. (2009). Total and stable washout of nitrite oxidizing bacteria from a nitrifying continuous activated sludge system using automatic control based on Oxygen Uptake Rate measurements. *Water Research* 43(11), 2761-2772.

- Kaelin, D., Manser, R., Rieger, L., Eugster, J., Rottermann, K. and Siegrist, H. (2009). Extension of ASM3 for two-step nitrification and denitrification and its calibration and validation with batch tests and pilot scale data. *Water Research* 43(6), 1680-1692.
- Kalff, J. (2002). *Limnology: Inland water ecosystems*. Prentice Hall, 592 pages.
- Kalmykov, L.V. and Kalmykov, V.L. (2013). Verification and reformulation of the competitive exclusion principle. *Chaos, Solitons & Fractals* 56, 124-131.
- Kalmykov, L.V. and Kalmykov, V.L. (2015). A white-box model of S-shaped and double S-shaped single-species population growth. *PeerJ* 3, 1-16.
- Kampschreur, M.J., Picioreanu, C., Tan, N., Kleerebezem, R., Jetten, M.S. and van Loosdrecht, M. (2007). Unraveling the source of nitric oxide emission during nitrification. *Proceedings of the Water Environment Federation* 2007(2), 843-860.
- Keen, G.A. and Prosser, J.I. (1987). Steady state and transient growth of autotrophic nitrifying bacteria. *Archives of Microbiology* 147(1), 73-79.
- Kim, Y.M. (2013). Acclimatization of communities of ammonia oxidizing bacteria to seasonal changes in optimal conditions in a coke wastewater treatment plant. *Bioresource Technology* 147(0), 627-631.
- Klepper, O. (1997). Multivariate aspects of model uncertainty analysis: tools for sensitivity analysis and calibration. *Ecological Modelling* 101(1), 1-13.
- Kneitel, J.M. and Chase, J.M. (2004). Trade-offs in community ecology: linking spatial scales and species coexistence. *Ecology Letters* 7(1), 69-80.
- Koch, G., Kuhni, M., Gujer, W. and Siegrist, H. (2000a). Calibration and validation of Activated Sludge Model No. 3 for Swiss municipal wastewater. *Water Research* 34(14), 3580-3590.
- Koch, G., Egli, K., Van der Meer, J.R. and Siegrist, H. (2000b). Mathematical modeling of autotrophic denitrification in a nitrifying biofilm of a rotating biological contactor. *Water Science and Technology* 41(4-5), 191-198.
- Kovács, E., Wirth, R., Maróti, G., Bagi, Z., Rákhely, G. and Kovács, K.L. (2013). Biogas production from protein-rich biomass: fed-batch anaerobic fermentation of casein and of pig blood and associated changes in microbial community composition. *PloS one* 8(10), 1-18.
- Kowalchuk, G.A., Stephen, J.R., De Boer, W., Prosser, J.I., Embley, T.M. and Woldendorp, J.W. (1997). Analysis of ammonia-oxidizing bacteria of the beta subdivision of the class Proteobacteria in coastal sand dunes by denaturing gradient gel electrophoresis and sequencing of PCR-amplified 16S ribosomal DNA fragments. *Applied and Environmental Microbiology* 63(4), 1489-1497.
- Kraft, B., Strous, M. and Tegetmeyer, H.E. (2011). Microbial nitrate respiration – Genes, enzymes and environmental distribution. *Journal of Biotechnology* 155(1), 104-117.
- Kreft, J.-U. (2004). Biofilms promote altruism. *Microbiology* 150(8), 2751-2760.
- Kreft, J.U., Picioreanu, C., Wimpenny, J.W. and van Loosdrecht, M.C. (2001). Individual-based modelling of biofilms. *Microbiology* 147(Pt 11), 2897-2912.

- Kruse, M., Keuter, S., Bakker, E., Spieck, E., Eggers, T. and Lipski, A. (2013). Relevance and diversity of *Nitrospira* populations in biofilters of brackish RAS. *PLoS one* 8(5).
- Laanbroek, H.J. and Gerards, S. (1993). Competition for limiting amounts of oxygen between *Nitrosomonas europaea* and *Nitrobacter winogradskyi* grown in mixed continuous cultures. *Archives of Microbiology* 159(5), 453-459.
- Lackner, S., Terada, A. and Smets, B.F. (2008). Heterotrophic activity compromises autotrophic nitrogen removal in membrane-aerated biofilms: Results of a modeling study. *Water Research* 42(4-5), 1102-1112.
- Lackner, S., Terada, A., Horn, H., Henze, M. and Smets, B.F. (2010). Nitrification performance in membrane-aerated biofilm reactors differs from conventional biofilm systems. *Water Research* 44(20), 6073-6084.
- Landau, S. and Everitt, B.S. (2004). *A Handbook of Statistical Analyses Using SPSS*. Taylor & Francis, 339 pages.
- Lardon, L.A., Merkey, B.V., Martins, S., Dotsch, A., Picioreanu, C., Kreft, J.U. and Smets, B.F. (2011). iDynoMiCS: next-generation individual-based modelling of biofilms. *Environmental Microbiology* 13(9), 2416-2434.
- Larsen, P.E., Gibbons, S.M. and Gilbert, J.A. (2012). Modeling microbial community structure and functional diversity across time and space. *FEMS Microbiology Letters* 332(2), 91-98.
- Lawrence, E. (2005). *Henderson's Dictionary of Biology*. Pearson/Prentice Hall, 748 pages.
- Lettinga, G., Vanvelsen, A.F.M., Hobma, S.W., Dezeew, W. and Klapwijk, A. (1980). Use of the Upflow Sludge Blanket (USB) Reactor concept for biological wastewater treatment, especially for anaerobic treatment. *Biotechnology and Bioengineering* 22(4), 699-734.
- Li, D. and Ganczarczyk, J. (1991). Size distribution of activated sludge flocs. *Research Journal of the Water Pollution Control Federation* 63(5), 806-814.
- Lochtman, S.F.W. (1995). *Proceskeuze en -optimalisatie van het SHARON proces voor slibverwerkingsbedrijf Sluisjesdijk* (Process choice and optimisation of the SHARON process for the sludge treatment plant Sluisjesdijk), TU Delft, BODL report.
- Loisel, P., Haegeman, B., Hamelin, J., Harmand, J. and Godon, J.-J. (2008). A method for measuring the biological diversity of a sample. In: *HAL Archives ouvertes.fr*, France.
- Lopez-Fiuza, J., Buys, B., Mosquera-Corral, A., Omil, F. and Mendez, R. (2002). Toxic effects exerted on methanogenic, nitrifying and denitrifying bacteria by chemicals used in a milk analysis laboratory. *Enzyme and Microbial Technology* 31(7), 976-985.
- Lotti, T., Kleerebezem, R., Hu, Z., Kartal, B., Jetten, M.S.M. and van Loosdrecht, M.C.M. (2014). Simultaneous partial nitrification and anammox at low temperature with granular sludge. *Water Research* 66, 111-121.

- Lücker, S., Wagner, M., Maixner, F., Pelletier, E., Koch, H., Vacherie, B., Rattei, T., Damsté, J.S.S., Spieck, E., Le Paslier, D. and Daims, H. (2010). A *Nitrospira* metagenome illuminates the physiology and evolution of globally important nitrite-oxidizing bacteria. *Proceedings of the National Academy of Sciences* 107(30), 13479-13484.
- Lydmark, P., Lind, M., Sorensson, F. and Hermansson, M. (2006). Vertical distribution of nitrifying populations in bacterial biofilms from a full-scale nitrifying trickling filter. *Environmental Microbiology* 8(11), 2036-2049.
- Madigan, M.T. and Martinko, J.M. (2006). *Brock biology of microorganisms*. Pearson Prentice Hall, Upper Saddle River, NJ, 992 pages.
- Magri, A., Corominas, L., Lopez, H., Campos, E., Balaguer, M., Colprim, J. and Flotats, X. (2007). A model for the simulation of the SHARON process: pH as a key factor. *Environmental Technology* 28(3), 255-265.
- Mancy, R., Prosser, P. and Rogers, S. (2013). Discrete and continuous time simulations of spatial ecological processes predict different final population sizes and interspecific competition outcomes. *Ecological Modelling* 259, 50-61.
- Manser, R., Gujer, W. and Siegrist, H. (2005). Consequences of mass transfer effects on the kinetics of nitrifiers. *Water Research* 39(19), 4633-4642.
- Manser, R., Gujer, W. and Siegrist, H. (2006). Decay processes of nitrifying bacteria in biological wastewater treatment systems. *Water Research* 40(12), 2416-2426.
- Mardis, E.R. (2008). The impact of next-generation sequencing technology on genetics. *Trends in Genetics* 24(3), 133-141.
- Mariadassou, M., Pichon, S. and Ebert, D. (2015). Microbial ecosystems are dominated by specialist taxa. *Ecology Letters* 18(9), 974-982.
- Mayr, E. (1942). *Systematics and the origin of species, from the viewpoint of a zoologist*. Harvard University Press, 334 pages.
- McMahon, S.M., Harrison, S.P., Armbruster, W.S., Bartlein, P.J., Beale, C.M., Edwards, M.E., Kattge, J., Midgley, G., Morin, X. and Prentice, I.C. (2011). Improving assessment and modelling of climate change impacts on global terrestrial biodiversity. *Trends in Ecology & Evolution* 26(5), 249-259.
- Michelland, R.J., Dejean, S., Combes, S., Fortun-Lamothe, L. and Cauquil, L. (2009). StatFingerprints: a friendly graphical interface program for processing and analysis of microbial fingerprint profiles. *Molecular Ecology Resources* 9(5), 1359-1363.
- Monod, J. (1949). The growth of bacterial cultures. *Annual Review of Microbiology* 3, 371-394.
- Monràs Boet, A. (2009). *Mathematical modelling and molecular analysis of a nitrifying packed bed biofilm reactor*. PhD thesis, Universitat Autònoma de Barcelona pages.
- Moussa, M.S., Hooijmans, C.M., Lubberding, H.J., Gijzen, H.J. and van Loosdrecht, M.C.M. (2005). Modelling nitrification, heterotrophic growth and predation in activated sludge. *Water Research* 39(20), 5080-5098.
- Mozumder, M.S.I., Picioreanu, C., van Loosdrecht, M.C.M. and Volcke, E.I.P. (2014). Effect of heterotrophic growth on autotrophic nitrogen removal in a granular sludge reactor. *Environmental Technology* 35(8), 1027-1037.

- Mulder, A., Vandegraaf, A.A., Robertson, L.A. and Kuenen, J.G. (1995). Anaerobic ammonium oxidation discovered in a denitrifying fluidized-bed reactor. *FEMS Microbiology Ecology* 16(3), 177-183.
- Muller, A., Wentzel, M.C., Loewenthal, R.E. and Ekama, G.A. (2003). Heterotroph anoxic yield in anoxic aerobic activated sludge systems treating municipal wastewater. *Water Research* 37(10), 2435-2441.
- Munz, G., Mori, G., Vannini, C. and Lubello, C. (2010). Kinetic parameters and inhibition response of ammonia - and nitrite - oxidizing bacteria in membrane bioreactors and conventional activated sludge processes. *Environmental Technology* 31(14), 1557-1564.
- Munz, G., Lubello, C. and Oleszkiewicz, J.A. (2011a). Factors affecting the growth rates of ammonium and nitrite oxidizing bacteria. *Chemosphere* 83(5), 720-725.
- Munz, G., Lubello, C. and Oleszkiewicz, J.A. (2011b). Modeling the decay of ammonium oxidizing bacteria. *Water Research* 45(2), 557-564.
- Munz, G., Szoke, N. and Oleszkiewicz, J.A. (2012). Effect of ammonia oxidizing bacteria (AOB) kinetics on bioaugmentation. *Bioresource Technology* 125, 88-96.
- Muyzer, G. (1999). DGGE/TGGE a method for identifying genes from natural ecosystems. *Current Opinion in Microbiology* 2(3), 317-322.
- Nash, J. and Sutcliffe, J.V. (1970). River flow forecasting through conceptual models part I—A discussion of principles. *Journal of hydrology* 10(3), 282-290.
- Nelson, E., Mendoza, G., Regetz, J., Polasky, S., Tallis, H., Cameron, D., Chan, K.M.A., Daily, G.C., Goldstein, J., Kareiva, P.M., Lonsdorf, E., Naidoo, R., Ricketts, T.H. and Shaw, M. (2009). Modeling multiple ecosystem services, biodiversity conservation, commodity production, and tradeoffs at landscape scales. *Frontiers in Ecology and the Environment* 7(1), 4-11.
- Nicolella, C., van Loosdrecht, M.C.M. and Heijnen, J.J. (2000). Wastewater treatment with particulate biofilm reactors. *Journal of Biotechnology* 80(1), 1-33.
- Nielsen, P.H., Mielczarek, A.T., Kragelund, C., Nielsen, J.L., Saunders, A.M., Kong, Y.H., Hansen, A.A. and Vollertsen, J. (2010). A conceptual ecosystem model of microbial communities in enhanced biological phosphorus removal plants. *Water Research* 44(17), 5070-5088.
- Norton, J.M., Alzerreca, J.J., Suwa, Y. and Klotz, M.G. (2002). Diversity of ammonia monooxygenase operon in autotrophic ammonia-oxidizing bacteria. *Archives of Microbiology* 177(2), 139-149.
- Nowak, O., Svardal, K. and Schweighofer, P. (1995). The dynamic behavior of nitrifying activated sludge systems influenced by inhibiting wastewater compounds. *Water Science and Technology* 31(2), 115-124.
- Oberkampf, W.L., Helton, J.C., Joslyn, C.A., Wojtkiewicz, S.F. and Ferson, S. (2004). Challenge problems: uncertainty in system response given uncertain parameters. *Reliability Engineering & System Safety* 85(1-3), 11-19.

- Ofițeru, I.D., Lunn, M., Curtis, T.P., Wells, G.F., Criddle, C.S., Francis, C.A. and Sloan, W.T. (2010). Combined niche and neutral effects in a microbial wastewater treatment community. *Proceedings of the National Academy of Sciences* 107(35), 15345-15350.
- Okabe, S., Kindaichi, T., Ito, T. and Satoh, H. (2004). Analysis of size distribution and areal cell density of ammonia-oxidizing bacterial microcolonies in relation to substrate microprofiles in biofilms. *Biotechnology and Bioengineering* 85(1), 86-95.
- Osborn, A.M., Moore, E.R.B. and Timmis, K.N. (2000). An evaluation of terminal-restriction fragment length polymorphism (T-RFLP) analysis for the study of microbial community structure and dynamics. *Environmental Microbiology* 2(1), 39-50.
- Otawa, K., Asano, R., Ohba, Y., Sasaki, T., Kawamura, E., Koyama, F., Nakamura, S. and Nakai, Y. (2006). Molecular analysis of ammonia-oxidizing bacteria community in intermittent aeration sequencing batch reactors used for animal wastewater treatment. *Environmental Microbiology* 8(11), 1985-1996.
- Pambrun, V., Paul, E. and Sperandio, M. (2006). Modeling the partial nitrification in sequencing batch reactor for biomass adapted to high ammonia concentrations. *Biotechnology and Bioengineering* 95(1), 120-131.
- Park, H.-D., Wells, G.F., Bae, H., Criddle, C.S. and Francis, C.A. (2006). Occurrence of ammonia-oxidizing archaea in wastewater treatment plant bioreactors. *Applied and Environmental Microbiology* 72(8), 5643-5647.
- Park, H., Sundar, S., Ma, Y. and Chandran, K. (2015). Differentiation in the microbial ecology and activity of suspended and attached bacteria in a nitrification-anammox process. *Biotechnology and Bioengineering* 112(2), 272-279.
- Park, S. and Bae, W. (2009). Modeling kinetics of ammonium oxidation and nitrite oxidation under simultaneous inhibition by free ammonia and free nitrous acid. *Process Biochemistry* 44(6), 631-640.
- Parks, D.H. and Beiko, R.G. (2010). Identifying biologically relevant differences between metagenomic communities. *Bioinformatics* 26(6), 715-721.
- Peng, Y.Z. and Zhu, G. (2006). Biological nitrogen removal with nitrification and denitrification via nitrite pathway. *Applied Microbiology and Biotechnology* 73(1), 15-26.
- Pérez, J., Picioreanu, C. and van Loosdrecht, M. (2005). Modeling biofilm and floc diffusion processes based on analytical solution of reaction-diffusion equations. *Water Research* 39(7), 1311-1323.
- Pernthaler, J. (2005). Predation on prokaryotes in the water column and its ecological implications. *Nature Reviews Microbiology* 3(7), 537-546.
- Petzold, L.R. (1982). A description of DASSL: A differential/algebraic system solver. In: *Proc. IMACS World Congress*, pp. 430-432.
- Pfeiffer, T. and Bonhoeffer, S. (2002). Evolutionary consequences of tradeoffs between yield and rate of ATP production. *Zeitschrift für Physikalische Chemie International journal of research in physical chemistry and chemical physics* 216(1/2002), 51.

- Picioreanu, C., van Loosdrecht, M.C.M. and Heijnen, J.J. (1997). Modelling the effect of oxygen concentration on nitrite accumulation in a biofilm airlift suspension reactor. *Water Science and Technology* 36(1), 147-156.
- Picioreanu, C., van Loosdrecht, M.C. and Heijnen, J.J. (1998). Mathematical modeling of biofilm structure with a hybrid differential-discrete cellular automaton approach. *Biotechnology and Bioengineering* 58(1), 101-116.
- Picioreanu, C., Kreft, J.-U. and van Loosdrecht, M.C. (2004). Particle-based multidimensional multispecies biofilm model. *Applied and Environmental Microbiology* 70(5), 3024-3040.
- Poduska, R.A. and Andrews, J.F. (1975). Dynamics of nitrification in the activated sludge process. *Journal of the Water Pollution Control Federation* 47(11), 2599-2619.
- Poly, F., Wertz, S., Brothier, E. and Degrange, V. (2008). First exploration of *Nitrobacter* diversity in soils by a PCR cloning-sequencing approach targeting functional gene *nxrA*. *FEMS Microbiology Ecology* 63(1), 132-140.
- Prosser, J.I., Bohannon, B.J., Curtis, T.P., Ellis, R.J., Firestone, M.K., Freckleton, R.P., Green, J.L., Green, L.E., Killham, K. and Lennon, J.J. (2007). The role of ecological theory in microbial ecology. *Nature Reviews Microbiology* 5(5), 384-392.
- Prosser, J.I. (2015). Dispersing misconceptions and identifying opportunities for the use of 'omics' in soil microbial ecology. *Nature Reviews Microbiology* 13(7), 439-446.
- Purvis, A. and Hector, A. (2000). Getting the measure of biodiversity. *Nature* 405(6783), 212-219.
- Pynaert, K., Smets, B.F., Wyffels, S., Beheydt, D., Siciliano, S.D. and Verstraete, W. (2003). Characterization of an autotrophic nitrogen-removing biofilm from a highly loaded lab-scale rotating biological contactor. *Applied and Environmental Microbiology* 69(6), 3626-3635.
- Quick, J., Quinlan, A.R. and Loman, N.J. (2014). A reference bacterial genome dataset generated on the MinION™ portable single-molecule nanopore sequencer. *GigaScience* 3(1), 22.
- Rainey, P.B., Buckling, A., Kassen, R. and Travisano, M. (2000). The emergence and maintenance of diversity: insights from experimental bacterial populations. *Trends in Ecology and Evolution* 15(6), 243-247.
- Ralston, M.L. and Jennrich, R.I. (1978). DUD, A derivative-free algorithm for nonlinear least squares. *Technometrics* 20(1), 7-14.
- Ramirez, I., Volcke, E.I.P., Rajinikanth, R. and Steyer, J.P. (2009). Modeling microbial diversity in anaerobic digestion through an extended ADM1 model. *Water Research* 43(11), 2787-2800.
- Ras, M., Lefebvre, D., Derlon, N., Paul, E. and Girbal-Neuhauser, E. (2011). Extracellular polymeric substances diversity of biofilms grown under contrasted environmental conditions. *Water Research* 45(4), 1529-1538.
- Reed, D.C., Algar, C.K., Huber, J.A. and Dick, G.J. (2014). Gene-centric approach to integrating environmental genomics and biogeochemical models. *Proceedings of the National Academy of Sciences*.
- Refsgaard, J.C., van der Sluijs, J.P., Højberg, A.L. and Vanrolleghem, P.A. (2007). Uncertainty in the environmental modelling process—a framework and guidance. *Environmental Modelling & Software* 22(11), 1543-1556.

- Reichert, P. (1994). Aquasim - a tool for simulation and data-analysis of aquatic systems. *Water Science and Technology* 30(2), 21-30.
- Reichert, P., von Schulthess, R. and Wild, D. (1995). The use of AQUASIM for estimating parameters of activated sludge models. *Water Science and Technology* 31(2), 135-147.
- Reichert, P. and Wanner, O. (1997). Movement of solids in biofilms: Significance of liquid phase transport. *Water Science and Technology* 36(1), 321-328.
- Reichert, P. (1998). AQUASIM 2.0—user manual. Swiss Federal Institute for Environmental Science and Technology. Dübendorf, Switzerland.
- Riefler, R.G., Ahlfeld, D.P. and Smets, B.F. (1998). Respirometric assay for biofilm kinetics estimation: parameter identifiability and retrievability. *Biotechnology and Bioengineering* 57(1), 35-45.
- Riefler, R.G. and Smets, B.F. (2003). Comparison of a type curve and a least-squared errors method to estimate biofilm kinetic parameters. *Water Research* 37(13), 3279-3285.
- Riesenfeld, C.S., Schloss, P.D. and Handelsman, J. (2004). Metagenomics: genomic analysis of microbial communities. *Annual Review of Genetics* 38, 525-552.
- Rondon, M.R., August, P.R., Bettermann, A.D., Brady, S.F., Grossman, T.H., Liles, M.R., Loiacono, K.A., Lynch, B.A., MacNeil, I.A. and Minor, C. (2000). Cloning the soil metagenome: a strategy for accessing the genetic and functional diversity of uncultured microorganisms. *Applied and Environmental Microbiology* 66(6), 2541-2547.
- Rongsayamanont, C., Limpiyakorn, T., Law, B. and Khan, E. (2010). Relationship between respirometric activity and community of entrapped nitrifying bacteria: Implications for partial nitrification. *Enzyme and Microbial Technology* 46(3-4), 229-236.
- Rosenzweig, M.L. (1995). *Species diversity in space and time*. Cambridge University Press, 436 pages.
- Rossello-Mora, R. and Amann, R. (2015). Past and future species definitions for Bacteria and Archaea. *Systematic and Applied Microbiology* 38(4), 209-216.
- Sanapareddy, N., Hamp, T.J., Gonzalez, L.C., Hilger, H.A., Fodor, A.A. and Clinton, S.M. (2009). Molecular diversity of a north carolina wastewater treatment plant as revealed by pyrosequencing. *Applied and Environmental Microbiology* 75(6), 1688-1696.
- Sánchez, O., Martí, M.C., Aspe, E. and Roeckel, M. (2001). Nitrification rates in a saline medium at different dissolved oxygen concentrations. *Biotechnology Letters* 23(19), 1597-1602.
- Sánchez, O., Bernet, N. and Delgenès, J.P. (2003). Ammonia and nitrite oxidation rates in the inverse turbulent bed reactor determined by respirometric assay. In: IWA Biofilm Conference.
- Sánchez, O., Michaud, S., Escudie, R., Delgenes, J.P. and Bernet, N. (2005a). Liquid mixing and gas-liquid mass transfer in a three-phase inverse turbulent bed reactor. *Chemical Engineering Journal* 114(1-3), 1-7.
- Sánchez, O., Aspé, E., Martí, M.C. and Roeckel, M. (2005b). Rate of ammonia oxidation in a synthetic saline wastewater by a nitrifying mixed-culture. *Journal of Chemical Technology and Biotechnology* 80(11), 1261-1267.

- Saur, T., Milferstedt, K., Bernet, N. and Escudie, R. (2014). An automated method for the quantification of moving predators such as rotifers in biofilms by image analysis. *Journal of Microbiological Methods* 103, 40-43.
- Schilthuizen, M. (2008). *The loom of life: unravelling ecosystems*. Springer, Springer-Verlag Berlin Heidelberg, 167 pages.
- Schmeisser, C., Steele, H. and Streit, W.R. (2007). Metagenomics, biotechnology with non-culturable microbes. *Applied Microbiology and Biotechnology* 75(5), 955-962.
- Scholz, M.B., Lo, C.-C. and Chain, P.S. (2012). Next generation sequencing and bioinformatic bottlenecks: the current state of metagenomic data analysis. *Current Opinion in Biotechnology* 23(1), 9-15.
- Schramm, A., Larsen, L.H., Revsbech, N.P., Ramsing, N.B., Amann, R. and Schleifer, K.-H. (1996). Structure and function of a nitrifying biofilm as determined by in situ hybridization and the use of microelectrodes. *Applied and Environmental Microbiology* 62(12), 4641-4647.
- Schramm, A., de Beer, D., Wagner, M. and Amann, R. (1998). Identification and activities in situ of *Nitrosospira* and *Nitrospira* spp. as dominant populations in a nitrifying fluidized bed reactor. *Applied and Environmental Microbiology* 64(9), 3480-3485.
- Schramm, A., de Beer, D., van den Heuvel, J.C., Ottengraf, S. and Amann, R. (1999). Microscale distribution of populations and activities of *Nitrosospira* and *Nitrospira* spp. along a macroscale gradient in a nitrifying bioreactor: Quantification by in situ hybridization and the use of microsensors. *Applied and Environmental Microbiology* 65(8), 3690-3696.
- Schramm, A., De Beer, D., Gieseke, A. and Amann, R. (2000). Microenvironments and distribution of nitrifying bacteria in a membrane-bound biofilm. *Environmental Microbiology* 2(6), 680-686.
- Sebat, J.L., Colwell, F.S. and Crawford, R.L. (2003). Metagenomic profiling: Microarray analysis of an environmental genomic library. *Applied and Environmental Microbiology* 69(8), 4927-4934.
- Seshan, H., Goyal, M.K., Falk, M.W. and Wuertz, S. (2014). Support vector regression model of wastewater bioreactor performance using microbial community diversity indices: Effect of stress and bioaugmentation. *Water Research* 53(0), 282-296.
- Shaw, L.J., Nicol, G.W., Smith, Z., Fear, J., Prosser, J.I. and Baggs, E.M. (2006). *Nitrosospira* spp. can produce nitrous oxide via a nitrifier denitrification pathway. *Environmental Microbiology* 8(2), 214-222.
- Sheintuch, M., Tartakovsky, B., Narkis, N. and Rebhun, M. (1995). Substrate inhibition and multiple states in a continuous nitrification process. *Water Research* 29(3), 953-963.
- Shi, S. and Tao, W. (2013). Numerical modeling of nitrogen removal processes in biofilters with simultaneous nitrification and anammox. *Water Science and Technology* 67(3), 549-556.
- Sierra, J.M., Picioreanu, C. and van Loosdrecht, M. (2014). Modeling phototrophic biofilms in a plug-flow reactor. *Water Science and Technology* 70(7), 1261-1270.

- Simberloff, D. and Dayan, T. (1991). The guild concept and the structure of ecological communities. *Annual Review of Ecology and Systematics* 22(1), 115-143.
- Sin, G., Kaelin, D., Kampschreur, M., Takacs, I., Wett, B., Gernaey, K., Rieger, L., Siegrist, H. and van Loosdrecht, M. (2008). Modelling nitrite in wastewater treatment systems: a discussion of different modelling concepts. *Water Science and Technology* 58(6), 1155-1171.
- Siripong, S. and Rittmann, B.E. (2007). Diversity study of nitrifying bacteria in full-scale municipal wastewater treatment plants. *Water Research* 41(5), 1110-1120.
- Slikkers, A.O., Haaijer, S.C.M., Stafsnes, M.H., Kuenen, J.G. and Jetten, M.S.M. (2005). Competition and coexistence of aerobic ammonium- and nitrite-oxidizing bacteria at low oxygen concentrations. *Applied Microbiology and Biotechnology* 68(6), 808-817.
- Solli, L., Håvelsrud, O.E., Horn, S.J. and Rike, A.G. (2014). A metagenomic study of the microbial communities in four parallel biogas reactors. *Biotechnology for biofuels* 7(1), 1-15.
- Song, H.-S., Cannon, W.R., Beliaev, A.S. and Konopka, A. (2014). Mathematical modeling of microbial community dynamics: A methodological review. *Processes* 2(4), 711-752.
- Spanjers, H. and Vanrolleghem, P. (1995). Respirometry as a tool for rapid characterization of wastewater and activated sludge. *Water Science and Technology* 31(2), 105-114.
- Spieck, E. and Bock, E. (2005). The lithoautotrophic nitrite-oxidizing bacteria. In: *Bergey's Manual® of Systematic Bacteriology*, Springer, pp. 149-153.
- Stackebrandt, E., Frederiksen, W., Garrity, G.M., Grimont, P.A., Kämpfer, P., Maiden, M.C., Nesme, X., Rosselló-Mora, R., Swings, J. and Trüper, H.G. (2002). Report of the ad hoc committee for the re-evaluation of the species definition in bacteriology. *International Journal of Systematic and Evolutionary Microbiology* 52(3), 1043-1047.
- Stenstrom, M.K. and Poduska, R.A. (1980). The effect of dissolved oxygen concentration on nitrification. *Water Research* 14(6), 643-649.
- Stewart, P.S. (2003). Diffusion in biofilms. *Journal of Bacteriology* 185(5), 1485-1491.
- Stirling, G. and Wilsey, B. (2001). Empirical relationships between species richness, evenness, and proportional diversity. *The American Naturalist* 158(3), 286-299.
- Stoddard, S.F., Smith, B.J., Hein, R., Roller, B.R.K. and Schmidt, T.M. (2015). rrnDB: improved tools for interpreting rRNA gene abundance in bacteria and archaea and a new foundation for future development. *Nucleic Acids Research* 43(D1), D593-D598.
- Streit, W.R. and Schmitz, R.A. (2004). Metagenomics—the key to the uncultured microbes. *Current Opinion in Microbiology* 7(5), 492-498.
- Suzuki, I., Dular, U. and Kwok, S. (1974). Ammonia or ammonium ion as substrate for oxidation by *Nitrosomonas europaea* cells and extracts. *Journal of Bacteriology* 120(1), 556-558.

- Swayne, D.A., Yang, W., Rizzoli, A. and Filatova, T. (2010). Parameter optimization and Bayesian inference in an estuarine eutrophication model of intermediate complexity. In: International Congress on Environmental Modelling and Software, Ottawa, Ontario, Canada.
- Tchobanoglous, G., Burton, F. and Stensel, H. (2003). Wastewater Engineering Treatment and Reuse. Inc. McGraw-Hill Company, 1848 pages.
- Terada, A., Lackner, S., Kristensen, K. and Smets, B.F. (2010). Inoculum effects on community composition and nitrification performance of autotrophic nitrifying biofilm reactors with counter-diffusion geometry. *Environmental Microbiology* 12(10), 2858-2872.
- Terada, A., Sugawara, S., Yamamoto, T., Zhou, S., Koba, K. and Hosomi, M. (2013). Physiological characteristics of predominant ammonia-oxidizing bacteria enriched from bioreactors with different influent supply regimes. *Biochemical Engineering Journal* 79, 153-161.
- Tiedje, J., Sexstone, A., Myrold, D. and Robinson, J. (1983). Denitrification: ecological niches, competition and survival. *Antonie Van Leeuwenhoek* 48(6), 569-583.
- Tilman, D. (1977). Resource competition between plankton algae: an experimental and theoretical approach. *Ecology* 58(2), 338-348.
- Tilman, D. (1994). Competition and biodiversity in spatially structured habitats. *Ecology* 75(1), 2-16.
- Toze, S. (1999). PCR and the detection of microbial pathogens in water and wastewater. *Water Research* 33(17), 3545-3556.
- Tringe, S.G. and Rubin, E.M. (2005). Metagenomics: DNA sequencing of environmental samples. *Nature reviews genetics* 6(11), 805-814.
- Turk, O. and Mavinic, D. (1986). Preliminary assessment of a shortcut in nitrogen removal from wastewater. *Canadian Journal of Civil Engineering* 13(6), 600-605.
- Vadivelu, V.M., Keller, J. and Yuan, Z.G. (2006a). Effect of free ammonia and free nitrous acid concentration on the anabolic and catabolic processes of an enriched *Nitrosomonas* culture. *Biotechnology and Bioengineering* 95(5), 830-839.
- Vadivelu, V.M., Yuan, Z.G., Fux, C. and Keller, J. (2006b). Stoichiometric and kinetic characterisation of *Nitrobacter* in mixed culture by decoupling the growth and energy generation processes. *Biotechnology and Bioengineering* 94(6), 1176-1188.
- Vadivelu, V.M., Keller, J. and Yuan, Z.G. (2006c). Stoichiometric and kinetic characterisation of *Nitrosomonas* sp. in mixed culture by decoupling the growth and energy generation processes. *Journal of Biotechnology* 126(3), 342-356.
- van Benthum, W.A.J., van Loosdrecht, M.C.M., Tjihuis, L. and Heijnen, J.J. (1995). Solids retention time in heterotrophic and nitrifying biofilms in a biofilm airlift suspension reactor. *Water Science and Technology* 32(8), 53-60.
- Van Hulle, S.W.H., Volcke, E.I.P., Teruel, J.L., Donckels, B., van Loosdrecht, M.C.M. and Vanrolleghem, P.A. (2007). Influence of temperature and pH on the kinetics of the Sharon nitrification process. *Journal of Chemical Technology & Biotechnology* 82(5), 471-480.

- van Loosdrecht, M.C.M. and Henze, M. (1999). Maintenance, endogenous respiration, lysis, decay and predation. *Water Science and Technology* 39(1), 107-117.
- Vannecke, T.P.W., Bernet, N., Steyer, J.P. and Volcke, E.I.P. (2014). Modelling ammonium-oxidizing population shifts in a biofilm reactor. *Water Science and Technology* 69(1), 208-216.
- Vannecke, T.P.W., Wells, G., Hubaux, N., Morgenroth, E. and Volcke, E.I.P. (2015). Considering microbial and aggregate heterogeneity in biofilm reactor models: How far do we need to go? *Water Science and Technology* 72(10), 1692-1699.
- Vannecke, T.P.W. and Volcke, E.I.P. (2015). Modelling microbial competition in nitrifying biofilm reactors. *Biotechnology and Bioengineering* 112(12), 2550-2561.
- Vanrolleghem, P.A., Spanjers, H., Petersen, B., Ginestet, P. and Takacs, I. (1999). Estimating (combinations of) Activated Sludge Model No. 1 parameters and components by respirometry. *Water Science and Technology* 39(1), 195-214.
- Velten, K. (2009). *Mathematical modeling and simulation: introduction for scientists and engineers*. John Wiley & Sons, Weinheim, 348 pages.
- Verstraete, W. and Philips, S. (1998). Nitrification-denitrification processes and technologies in new contexts. *Environmental Pollution* 102(1), 717-726.
- Verstraete, W., Wittelbolle, L., Heylen, K., Vanparys, B., de Vos, P., van de Wiele, T. and Boon, N. (2007). *Microbial resource management: The road to go for environmental biotechnology*. *Engineering in Life Sciences* 7(2), 117-126.
- Vieira-Silva, S. and Rocha, E. (2010). The systemic imprint of growth and its uses in ecological (meta) genomics. *PLoS Genetics* 6(1), e1000808.
- Volcke, E.I.P., Sanchez, O., Steyer, J.P., Dabert, P. and Bernet, N. (2008). Microbial population dynamics in nitrifying reactors: Experimental evidence explained by a simple model including interspecies competition. *Process Biochemistry* 43(12), 1398-1406.
- Volcke, E.I.P., Picioreanu, C., De Baets, B. and Van Loosdrecht, M.C.M. (2010). Effect of granule size on autotrophic nitrogen removal in a granular sludge reactor. *Environmental Technology* 31(11), 1271-1280.
- Wang, Y., Hammes, F., De Roy, K., Verstraete, W. and Boon, N. (2010). Past, present and future applications of flow cytometry in aquatic microbiology. *Trends in Biotechnology* 28(8), 416-424.
- Wang, Z., Zhang, X.-X., Lu, X., Liu, B., Li, Y., Long, C. and Li, A. (2014). Abundance and diversity of bacterial nitrifiers and denitrifiers and their functional genes in tannery wastewater treatment plants revealed by high-throughput sequencing. *PloS one* 9(11), 1-19.
- Wanner, O. and Gujer, W. (1986). A multispecies biofilm model. *Biotechnology and Bioengineering* 28(3), 314-328.
- Wanner, O. and Reichert, P. (1996). Mathematical modeling of mixed - culture biofilms. *Biotechnology and Bioengineering* 49(2), 172-184.
- Wanner, O. and Morgenroth, E. (2004). Biofilm modeling with AQUASIM. *Water Science & Technology* 49(11-12), 137-144.

- Washington, H. (1984). Diversity, biotic and similarity indices: a review with special relevance to aquatic ecosystems. *Water Research* 18(6), 653-694.
- Wertz, S., Poly, F., Le Roux, X. and Degrange, V. (2008). Development and application of a PCR-denaturing gradient gel electrophoresis tool to study the diversity of Nitrobacter-like nxrA sequences in soil. *FEMS Microbiology Ecology* 63(2), 261-271.
- Wett, B. and Rauch, W. (2003). The role of inorganic carbon limitation in biological nitrogen removal of extremely ammonia concentrated wastewater. *Water Research* 37(5), 1100-1110.
- Wett, B., Jimenez, J.A., Takacs, I., Murthy, S., Bratby, J.R., Holm, N.C. and Ronner-Holm, S.G.E. (2011). Models for nitrification process design: one or two AOB populations. *Water Science and Technology* 64(3), 568-578.
- Whiteley, A.S., Jenkins, S., Waite, I., Kresoje, N., Payne, H., Mullan, B., Allcock, R. and O'Donnell, A. (2012). Microbial 16S rRNA Ion Tag and community metagenome sequencing using the Ion Torrent (PGM) Platform. *Journal of Microbiological Methods* 91(1), 80-88.
- Wiesmann, U. (1994). Biological nitrogen removal from wastewater. In: *Advances in Biochemical Engineering/Biotechnology* Fiechter A (ed.), Springer-Verlag Berlin Heidelberg, Berlin, pp. 113-154.
- Wijffels, R.H., Englund, G., Hunik, J.H., Leenen, E.J.T.M., Bakketun, A., Gunther, A., Decastro, J.M.O. and Tramper, J. (1995). Effects of diffusion limitation on immobilized nitrifying microorganisms at low temperatures. *Biotechnology and Bioengineering* 45(1), 1-9.
- Wik, T. and Breitholtz, C. (1996). Steady-state solution of a two-species biofilm problem. *Biotechnology and Bioengineering* 50(6), 675-686.
- Williamson, K. and McCarty, P.L. (1976). Verification studies of the biofilm model for bacterial substrate utilization. *Journal of the Water Pollution Control Federation* 48(2), 281-296.
- Wilson, J.B. (1999). Guilds, functional types and ecological groups. *Oikos* 86(3), 507-522.
- Winkler, M.-K.H., Le, Q.H. and Volcke, E.I.P. (2015). Influence of partial denitrification and mixotrophic growth of nob on microbial distribution in aerobic granular sludge. *Environmental Science & Technology* 49(18), 11003-11010.
- Winkler, M.K., Bassin, J.P., Kleerebezem, R., Sorokin, D.Y. and van Loosdrecht, M.C. (2012). Unravelling the reasons for disproportion in the ratio of AOB and NOB in aerobic granular sludge. *Applied Microbiology and Biotechnology* 94(6), 1657-1666.
- Winkler, M.K., Kleerebezem, R., de Bruin, L.M.M., Verheijen, P.J.T., Abbas, B., Habermacher, J. and van Loosdrecht, M.C.M. (2013). Microbial diversity differences within aerobic granular sludge and activated sludge flocs. *Applied Microbiology and Biotechnology* 97(16), 7447-7458.
- Wittebolle, L., Boon, N., Vanparys, B., Heylen, K., De Vos, P. and Verstraete, W. (2005). Failure of the ammonia oxidation process in two pharmaceutical wastewater treatment plants is linked to shifts in the bacterial communities. *Journal of Applied Microbiology* 99(5), 997-1006.
- Wittebolle, L., Vervaeren, H., Verstraete, W. and Boon, N. (2008). Quantifying community dynamics of nitrifiers in functionally stable reactors. *Applied and Environmental Microbiology* 74(1), 286-293.

- Wittebolle, L., Verstraete, W. and Boon, N. (2009). The inoculum effect on the ammonia-oxidizing bacterial communities in parallel sequential batch reactors. *Water Research* 43(17), 4149-4158.
- Wyffels, S., Van Hulle, S.W., Boeckx, P., Volcke, E.I., Cleemput, O.V., Vanrolleghem, P.A. and Verstraete, W. (2004). Modeling and simulation of oxygen - limited partial nitrification in a membrane - assisted bioreactor (MBR). *Biotechnology and Bioengineering* 86(5), 531-542.
- Xiuheng, W., Zhang, K., Nanqi, R., Nan, L. and Lijiao, R. (2009). Monitoring microbial community structure and succession of an A/O SBR during start-up period using PCR-DGGE. *Journal of Environmental Sciences* 21(2), 223-228.
- Xu, H., Wang, C., Liang, Z., He, L. and Wu, W. (2015). The structure and component characteristics of partial nitrification biofilms under autotrophic and heterotrophic conditions. *Applied Microbiology and Biotechnology* 99(8), 3673-3683.
- Xu, J. (2006). Microbial ecology in the age of genomics and metagenomics: concepts, tools, and recent advances. *Molecular Ecology* 15(7), 1713-1731.
- Ye, L., Hu, S.H., Poussade, Y., Keller, J. and Yuan, Z.G. (2012a). Evaluating a strategy for maintaining nitrifier activity during long-term starvation in a moving bed biofilm reactor (MBBR) treating reverse osmosis concentrate. *Water Science and Technology* 66(4), 837-842.
- Ye, L., Zhang, T., Wang, T. and Fang, Z. (2012b). Microbial structures, functions, and metabolic pathways in wastewater treatment bioreactors revealed using high-throughput sequencing. *Environmental Science & Technology* 46(24), 13244-13252.
- Yilmaz, G., Lemaire, R., Keller, J. and Yuan, Z. (2008). Simultaneous nitrification, denitrification, and phosphorus removal from nutrient-rich industrial wastewater using granular sludge. *Biotechnology and Bioengineering* 100(3), 529-541.
- Yoshioka, T., Terai, H. and Saijo, Y. (1982). Growth kinetic studies of nitrifying bacteria by the immunofluorescent counting method. *Journal of General and Applied Microbiology* 28(2), 169-180.
- Yuan, Z. and Blackall, L.L. (2002). Sludge population optimisation: a new dimension for the control of biological wastewater treatment systems. *Water Research* 36(2), 482-490.

Curriculum vitae

Personal particulars

Thomas Pieter Willem Vannecke

Oostende, 8 June 1987

thomasvannecke@gmail.com

Belgian

married to Annelies De Groot (on 29 August 2014)

Basic education

2005 – 2008

Faculty of Sciences, Ghent University

Bachelor of Science in Biology

graduated on 3 July 2008, Magna cum laude

2008 – 2010

Faculty of Sciences, Ghent University

Master of Science in Biology

graduated on 30 June 2010, Summa cum laude

2010 – 2011

Faculty of Bioscience Engineering, Ghent University

Master of Science in Environmental Sanitation and Management

graduated on 8 July 2011, Magna cum laude

Extra training

UGent Doctoral Training Programme (Doctoral School of Bioscience Engineering)

6th Advanced Biofilm Course, TU Delft, 3 – 8 October 2011

Advanced Course on Environmental Biotechnology, TU Delft, 12 – 22 June 2012

Employment

From 1 October 2011

Ghent University, Department of Biosystems Engineering

FWO PhD Fellowship (Research Foundation Flanders):

- Research in view of obtaining a PhD degree:
‘Controlling microbial populations for sustainable wastewater treatment’
Supervisor: Prof. dr. ir. Eveline Volcke
- Supervision of master dissertation students (6)

Research stays abroad

23 April 2012 – 2 June 2012

Laboratory of Environmental Biotechnology (LBE) of the French National Institute for Agricultural Research (INRA), Narbonne, France.

Funding obtained through Scientific Research Committee (CWO) of the Faculty of Bioscience Engineering of Ghent University

29 November 2014 – 12 December 2014

Laboratory of Environmental Biotechnology (LBE) of the French National Institute for Agricultural Research (INRA), Narbonne, France.

This research stay was funded by the Tournesol Project T2013.03

Publications

Papers in international journals with reading committee

Vannecke, T.P.W., Wells, G., Hubaux, N., Morgenroth, E. & Volcke, E.I.P. (2015). Considering microbial and aggregate heterogeneity in biofilm reactor models: How far do we need to go? *Water Science and Technology*, 72(10), 1692-1699. doi:10.2166/wst.2015.389 (IF 2014: 1.106)

Vannecke, T.P.W. & Volcke, E.I.P. (2015). Modelling microbial competition in nitrifying biofilm reactors. *Biotechnology and Bioengineering*, 112(12), 2550-2561. doi: 10.1002/bit.25680 (IF 2014: 4.126)

Winkler, M.-K.H., Ettwig, K.F., **Vannecke, T.P.W.**, Stultiens, K., Bogdan, A., Kartal, B., Volcke, E.I.P. (2015). Modelling simultaneous anaerobic methane and ammonium removal in a granular sludge reactor. *Water Research*, 73, 323–331. doi: 10.1016/j.watres.2015.01.039 (IF 2014: 5.528)

Vannecke, T.P.W., Lampens, D.R.A., Ekama, G.A. & Volcke, E.I.P. (2015). Evaluation of the 5 and 8 pH point titration methods for monitoring anaerobic digesters treating solid waste. *Environmental Technology*, 36(7), 861-869. doi: 10.1080/09593330.2014.964334 (IF 2014: 1.560)

Vannecke, T.P.W., Bernet, N., Steyer, J.-P. & Volcke, E.I.P. (2014). Modelling ammonium oxidizing population shifts in a biofilm reactor. *Water Science and Technology*, 69(1), 208-215. doi: 10.2166/wst.2013.701 (IF 2014: 1.106)

Oral presentations at conferences

Vannecke, T.P.W. & Volcke, E.I.P. (2015). Modelling microbial competition in nitrifying biofilm reactors. In: Proceedings of the IWA Nutrient Removal and Recovery conference 2015: moving innovation into practice (NRR2015), Gdansk, Poland, 18-21 May 2015, p. 260-266.

Vannecke, T.P.W., & Volcke, E.I.P. (2014). Modelling microbial competition in biofilms. In: Book of abstracts of the 9th European Nitrogen Cycle Meeting, Ghent, Belgium, 10 – 12 September 2014, p. 37.

Wells, G., **Vannecke, T.P.W.**, Hubaux, N., Morgenroth, E. & Volcke, E.I.P. (2014). Increasing complexity in biofilm reactor models: How far do we need to go? In: Proceedings of the 4th IWA/WEF Wastewater treatment modelling seminar (WWTmod2014), Spa, Belgium, 30 March - 2 April 2014, p. 63-76.

Vannecke, T.P.W., & Volcke, E.I.P. (2014). Modelling microbial community dynamics in a nitrifying biofilm: effect of the nitrogen loading rate. *Communications in Agricultural and Applied Biological Sciences* 79, 21–26. In: Proceedings of the 19th National symposium on Applied Biological Sciences, Gembloux, Belgium, 7 February 2014.

Vannecke, T.P.W., Bernet, N., Steyer, J.-P. & Volcke, E.I.P. (2013). Modelling population shifts in a nitrifying biofilm reactor. In: Proceedings of the 9th International Conference on Biofilm Reactors (IWA), Paris, France, 28-31 May 2013.

Other conference contributions

Vannecke, T.P.W. & Volcke, E.I.P. (2015). Modelling microbial competition in biofilm reactors. 20th National symposium on Applied Biological Sciences, Louvain-la-Neuve, Belgium, 30 January 2015. Poster presentation.

Vannecke, T.P.W. & Volcke, E.I.P. (2014). Modelling microbial competition in biofilm reactors. IWA World Water Congress & Exhibition 2014, Lisbon, Portugal, 21-26 September 2014. Poster presentation presented by Volcke, E.I.P.

Winkler, M.-K.H., **Vannecke, T.P.W.**, Bogdan, A. & Volcke, E.I.P. (2014). Modelling simultaneous anaerobic methane and ammonium removal in a granular sludge reactor. 4th IWA/WEF Wastewater treatment modelling seminar (WWTmod2014), Spa, Belgium, 30 March - 2 April 2014. Poster presentation presented by Winkler, M.-K.H.

Copot, D., Ionescu, C.-M., **Vannecke, T.P.W.**, Volcke, E.I.P., & De Keyser, R. (2013). An approach towards multivariable control of anaerobic digestion using the EPASAC predictive control strategy. 11th IWA Instrumentation

Control and Automation, Narbonne, France, 18-20 September 2013. Poster presentation presented by Copot, D.

Vannecke, T.P.W., Bernet, N., Steyer, J.-P. & Volcke, E.I.P. (2013). Modelling population shifts in a nitrifying biofilm reactor. 18th National symposium on Applied Biological Sciences, Ghent, Belgium, 8 February 2013. Poster presentation.

Ordace, A., Ionescu, C.-M., **Vannecke, T.P.W.**, Volcke, E.I.P., Nascu, I., & De Keyser, R. (2012). Predictive control of anaerobic digestion of wastewater sludge: a feasibility study. In: Proceedings of the 16th International Conference on System Theory, Control and Computing, Sinaia, Romania, 12-14 October 2012. Oral presentation presented by Ordace, A.

MSc theses

Vannecke, T.P.W. (2011). Anaerobe vergisting van waterzuiveringsslib: simulatiestudie op basis van praktijkgegevens. Vakgroep Biosysteemtechniek, Universiteit Gent (in collaboration with Aquafin).

Promotor: Prof. dr. ir. Eveline Volcke

Vannecke, T.P.W. (2010). De invloed van nutriëntenbeschikbaarheid op de fotosynthetische efficiëntie en allocatie van fotosyntheseproducten in *Phaeodactylum tricornutum* Bohlin. Onderzoeksgroep Protistologie en Aquatische ecologie, Universiteit Gent.

Promotor: Prof. dr. Wim Vyverman

BSc thesis

Vannecke, T.P.W. (2008). Kartering van intertidale biofilms in ‘de IJzermondig’ aan de hand van remote sensing beelden. Onderzoeksgroep Protistologie en Aquatische Ecologie, Universiteit Gent.

Promotor: Prof. dr. Koen Sabbe

Supervision of thesis students

2011-2012, Anamaria Ordace

Bachelor of Applied Science Automation Engineer Technology/Technician,
University of Cluj-Napoca, Cluj, Romania

Title: Predictive control of anaerobic digestion of wastewater sludge: a feasibility study

2011-2012, Michael Catrysse

MSc in Bioscience Engineering: Environmental Technology, UGent

Title: Optimization of the nitrification process in a Sequencing Batch Biofilm Reactor

2012-2013, Dieter Lampens

MSc in de bio-ingenieurswetenschappen: Chemie en Bioprocestechnologie,
UGent

Title (Dutch): Monitoring van anaerobe vergistingsprocessen

2012-2013, Aleksandra Bogdan

Master student of the Erasmus Mundus Programme "Erasmus Mundus
International Master of Science in Environmental Technology and
Engineering"

Title: Modelling and simulation of anaerobic ammonium and methane
oxidation in granular sludge reactors

2013-2014, Md. Mohibul Alam

MSc in Environmental Sanitation, UGent

Title: Simulation study on the anaerobic digestion of manure

2014-2015, Veronica del Rosario Diaz Soza

Master student of the Erasmus Mundus Programme "Erasmus Mundus
International Master of Science in Environmental Technology and
Engineering"

Title: Autotrophic nitrogen removal from tannery industry wastewater in
biofilm reactors